UNIVERSITY OF MINNESOTA
SPACE SCIENCE CENTER

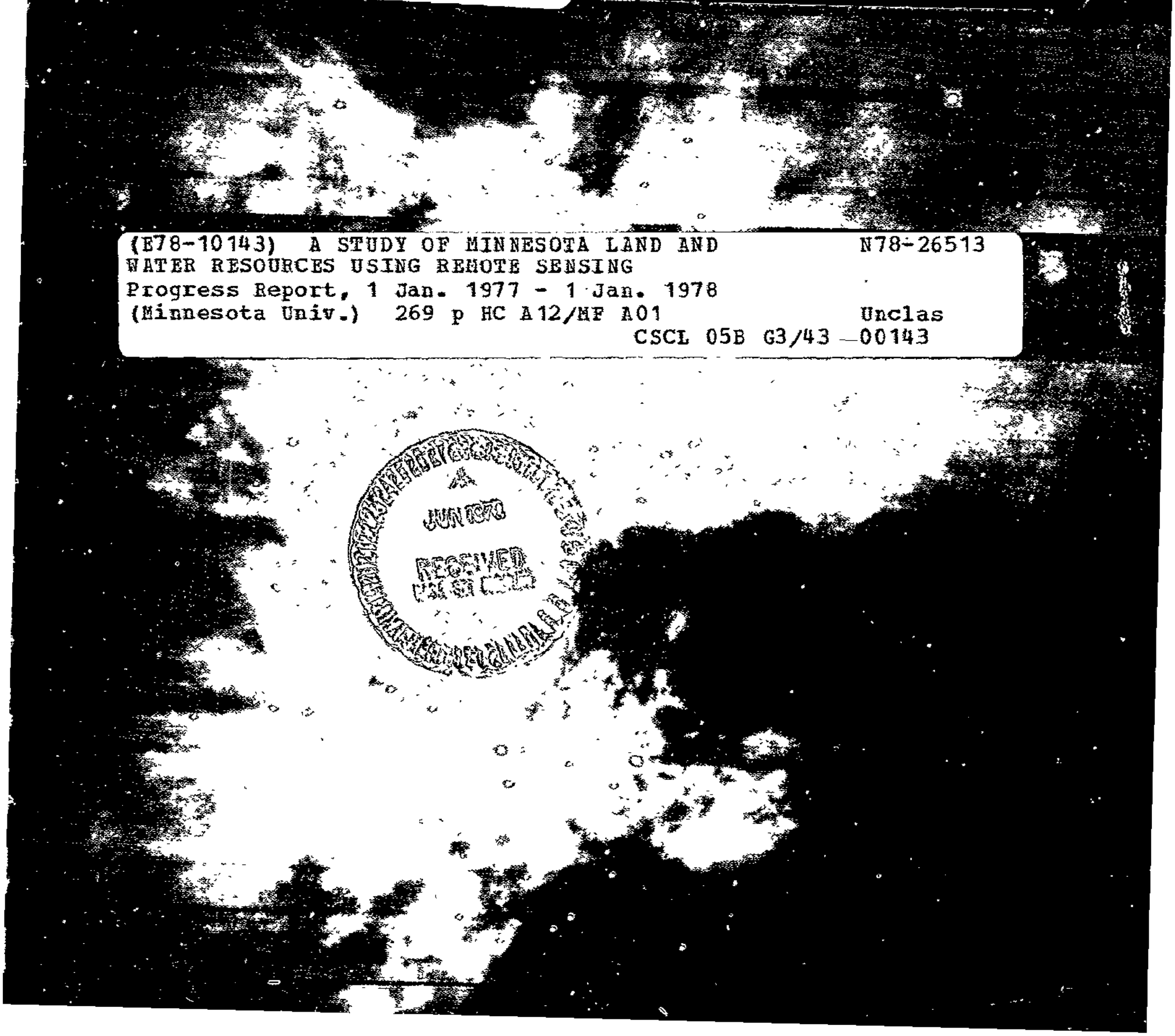

(E78-10143) A STUDY OF MINNESOTA LAND AND WATER RESOURCES USING REMOTE SENSING Progress Report, 1 Jan. 1977 - 1 Jan. 1978 (Minnesota Univ.) 269 p HC A12/MF A01 CSCL 05B

N78-26513

Unclas
G3/43 00143

[redacted]

ON THE COVER — The area of the heavens around the Orion Constellation, shown in the cover photograph made through the 120-inch telescope of the Lick observatory, is also the region of observations with an infrared telescope developed by University of Minnesota astro-physicists. The infrared sensory equipment reveals stellar bodies that could not be studied by conventional telescopes, and it is expected to provide data on the birth of stars.

A STUDY OF
MINNESOTA LAND AND WATER
RESOURCES USING REMOTE SENSING

December 31, 1977

NASA GRANT 24-005-263 VOL. XI

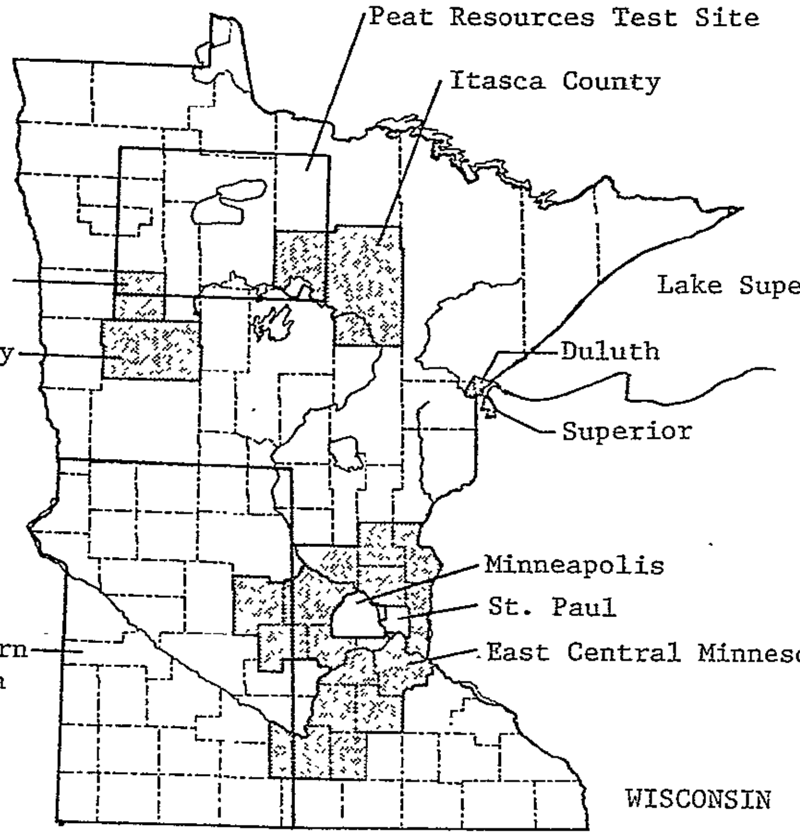

SPACE SCIENCE CENTER

University of Minnesota

Minneapolis, Minnesota 55455

A STUDY OF MINNESOTA LAND AND WATER RESOURCES USING REMOTE SENSING

PROGRESS REPORT

January 1, 1978

Supported by:

NASA GRANT NGL 24-005-263

Submitted to:

NATIONAL AERONAUTICS AND SPACE ADMINISTRATION

Washington, D.C. 20546

TABLE OF CONTENTS

SPACE SCIENCE CENTER

PROGRESS REPORT

JANUARY 1978

INTRODUCTION

This report covers research at the University of Minnesota during the twelve month interval from January 1, 1977 to December 31, 1977.

Section A is a final report by Robert A. Warrick entitled "Evaluation of Four Methods for Using LANDSAT Data to Analyze Lake Condition in Minnesota." This report represents a thesis submitted to the Geography Department of the University of Minnesota in partial fulfillment of the requirements for a Master of Science degree in Geography. The work was done under the immediate supervision of Professors Dwight Brown and Richard Skaggs and was supported by NASA Grant NGL 24-005-263 during earlier years. The report is a study of the utility of LANDSAT data for the evaluation of lake condition. In order to test the use of LANDSAT data for this purpose 81 lakes in East Central Minnesota were investigated. Extensive ground truth information is available for many of these lakes which made possible a comparison of the classifications arising from the LANDSAT evaluations with the known qualities of the lakes. The first part of the report describes the optical properties of natural water and the factors influencing the reflectance. The second part of the report is devoted to the analysis of the LANDSAT data for the lakes under study. After finding the Bendix System expensive and not applicable to this type of basin study, Mr. Warrick attempted to use density slicing and a micro-densitometer for black and white film transparencies but found that the results were not reproducible. He then turned to computer compatible tapes and having chosen appropriate sample sites used a 20 pixel (22 acres) sample to obtain reflectance data.

Data obtained in this way were then subjected to two types of analysis; cluster analysis and discriminate analysis. The cluster analysis technique which is described resulted in the identification of ten classes or lake groups. However, these groupings are not entirely distinct and the method inherently involves certain ambiguities. It has the advantage that it does identify the inherent grouping tendencies that exist in the data.

Discriminate analysis cannot identify inherent grouping tendencies but requires a prespecification of the groups, or classes, between which discrimination is desired. The discriminant analysis in Warrick's study was based on groups defined by the results of the cluster analysis, ground truth and subjective estimation of the condition of selected lakes in the study area. Ten types of water conditions representative of those in the study area were identified and thirty-seven lakes were used to statistically describe these ten classes. These training lakes provided the basis for the discriminant analysis of 104 observations into ten classes. Warrick describes the possible errors in the classification methods and the probability of misclassification between adjacent classes.

Also included in Section A is a second report entitled "Reconnaissance Analysis of Lake Condition in East Central Minnesota", which was written by Dwight Brown, Robert Warrick and Richard Skaggs. This report to the Minnesota State Planning Agency was partially supported by NASA Contract 20985 to the above agency. It represents an application of the methods of analysis developed by Robert Warrick. It extended the earlier study to an expanded area which included 1,000 lakes larger than 50 acres. The study was limited to lakes over 100 acres in size, resulting in 619 observations for 421 lakes. Ground data for 81 lakes were used to define six classes into which the lakes were classified. This report emphasizes what its title suggests: that the use of the LANDSAT data in this way provides a reconnaissance tool and cannot be depended upon for detailed information on water quality. The reconnaissance should be an important tool in guiding ground based studies and management of lakes.

Section B is a report by Michael Sydor of his continuing study of Lake Superior. In previous work reported in the December 31, 1976 report on NGL 24-005-263 Sydor demonstrated the ability to identify three major contaminants in Lake Superior using LANDSAT observations. In this section, the earlier investigation has been extended and a linear transformation developed to provide a relationship between the residual LANDSAT intensities and concentrations of the three contaminants quantified by correlation of remote sensing data with in situ measurements. From the inverse transformation the concentrations of the particulates can be obtained from the multi-spectral signal intensities. These analytical methods can be extended to other regions of the Lake subject to limiting factors discussed in the report.

As an appendix to Section B a paper entitled "Use of Remote Sensing in Determination of Chemical Loading of Lake Superior Due to Spring Runoff" by G. J. Oman and M. Sydor is included. This report's work was supported under an E.P.A. grant, but was dependent on techniques which were developed under NASA Grant NGL 24-005-263.

Section C is a final report on work carried on by M. R. Nash, M. P. Meyer and D. W. French entitled "Detection of Dutch Elm Disease Using Oblique 35mm Aerial Photography." This represents results obtained with support from NASA Grant NGL 24-005-263 in the 1976-1977 funding period. In our report for the period January 1, 1976 to December 31, 1976 French and Meyer had reported earlier aerial photographic detection results on the identification of trees infected with Dutch Elm Disease. Those data were obtained with vertical stereoscopic color infrared. The results were disappointing with only 47-50% of the diseased elms detected by any one of the interpreters. It was suspected that a major problem arises from confusion of the tree crown with the background below the tree when photographed vertically.

The present study employed oblique 35mm aerial photography. The conditions of the photograph and the scene analysis are described. The results are substantially better than those achieved in previous studies by individual interpreters ranging up to 78% correct detection for the most experienced observer depending on the scale and type of film.

Although the authors feel that even with the 35mm oblique photography the success in detecting Dutch Elm Disease is less than satisfactory, the technique still can be a valuable tool in the speedy location of diseased trees permitting prompt response in sanitation control.

An appendix to their report is a paper titled " Field Evolution of Small Scale Forest Resource Aerial Photography which is a follow up study funded by the McIntire - Stennis Cooperative Forestry Research Program and the University of Minnesota Agricultural Experimental Station.

Section D is a report by Joseph E. Goebel and Matt Walton entitled "Use of LANDSAT Imagery for the Statewide Mapping and Classification of Peat Resources." As the authors point out, peat is an important resource in the State of Minnesota as a possible source of energy. Approximately 50% of the peat of the contiguous United States is found in Minnesota, three times as much as any other state. It is estimated at 13 billion tons dry weight and equivalent in energy to 7 billion tons of bituminous coal. Its extent and condition is not easily determined from the ground because of its occurrence in bogs. It becomes a natural target for an investigation of the utility of LANDSAT observations in determining its location and character.

Goebel and Walton undertook an investigation of the information in LANDSAT imagery. For this purpose they made use of three seasonal bands and three black and white film transparencies of bands 5, 6 and 7. They examined the utility of each of these representations individually and in various combinations to determine which provided the most accurate information on the drainageways and artificially disturbed areas relative to the total peatland. These results are reported. The authors conclude that LANDSAT imagery used in accordance with optimum procedures identified from this study, in conjunction with ground truth, provide an efficient, economical method for developing a regional inventory.

Section E is a status report on a research project "Assessment of Ice Coverage of Selected Lakes and Streams in Minnesota and Relationship to Meteorological, Hydraulic, and Man-Made Conditions." This project was funded for one year under NASA Grant NGL-24-005-263. The purpose of the investigation was to determine whether LANDSAT imagery could be used to provide information on the times of freeze-over and ice disappearance on lakes and streams. Such data would be used to test predictive relationships involving the factors controlling the heat budget of the bodies of water of interest. The LANDSAT imagery was found to be useful in providing the information desired and also revealed anomalies which appear to be related to thermal inputs from non atmospheric sources.

It appears that the ice disappearance is controlled primarily by an ice surface-atmospheric heat exchange and thermal input from streams and essentially independent of the mean depth of the lake.

The studies reported have demonstrated that LANDSAT observations can provide information of the type needed. Since a Minnesota State agency is interested and apparently willing to support a continuation of the program, support from NGL-24-005-263 has been discontinued.

Section F is a report entitled "Evaluation of Soil Moisture Stress in Western and Southwestern Minnesota" by R. H. Rust and Pierre Robert. These agricultural areas of Minnesota are unusually susceptible and sensitive to drouth conditions. The purpose of the study was to determine the utility of LANDSAT and low altitude color infrared photographic information in detecting moisture stress through crop signatures. Additional objectives include the detection of stress from other causes and the location of droughty and poorly drained soils. The end objective is the development of a forecasting ability for seasonal crop management. The years 1975 and 1976 had been drouth years in the areas under study. Fortunately for the farmers but unfortunately for this study the rainfall pattern for 1977 was such that soil water content was always adequate or eventually in excess.

The report describes the steps undertaken to establish a ground truth network in the area under study which would provide information on leaf and soil moisture, precipitation events and crop signatures to be correlated with remote sensing information. In addition to the field data, greenhouse studies were undertaken to provide data on plant water stress under controllable conditions. Useful information has been obtained and will be correlated with LANDSAT CCT information for summer 1977 when this becomes available.

SECTION A

EVALUATION OF FOUR METHODS FOR USING LANDSAT DATA TO ANALYZE LAKE CONDITION IN MINNESOTA

Robert A. Warwick
Drs. Dwight Brown and Richard Skaggs
Department of Geology
Minneapolis, Minnesota

INDEX

APPENDIX A - CONDITION OF SELECTED EAST-CENTRAL MINNESOTA LAKES

Dwight Brown, Richard Skaggs

INTRODUCTION

About 15,000 lakes larger than 10 acres are located in Minnesota. The creation and maintenance of an inventory of the state's water resources is difficult because of the dynamic nature of lakes and the effects of the cultural activities. The present methods of assessing the condition of a lake require on site analysis, which cannot be done on a regular basis for even a large minority of lakes in Minnesota. The synoptic scale and repetitive nature of LANDSAT coverage make it useful in a continuous program of monitoring the status of Minnesota's lakes.

LANDSAT (formerly the Earth Resources Technology Satellite, ERTS) data have been employed successfully for both lake inventories and investigations of their water conditions. The absorption of near infrared light by water is the basis for LANDSAT lake inventories. Visual interpretation of LANDSAT images have been used to monitor Minnesota lakes (Brown, et al., 1974; 1977) and the extent of 1973 flooding in the Mississippi River Valley (Rango and Anderson, 1974; Deutsch and Ruggles, 1974). Automated procedures for lake indentification and mapping from LANDSAT digital data have been developed and achieve very high accuracy (the DAMS package, 1974; Boland, 1974; Work and Gilmer, 1976).

Investigations of the condition rather than existence of natural waters are based on the reflectance of light, rather than its absorption. In river and reservoir systems, relationships between suspended solids and reflectance have been examined (e.g., Yarger and McCauley, 1975; Kritikos, Yorkins and Smith, 1974; Klemas, 1973).

The relationships between reflectance and a variety of water quality parameters have been investigated for lakes located in northern states (Boland, 1974; Scherz, and Van Domelen, 1975; Scherz et al., 1975; Rogers, et al., 1975; Scherz, 1977).

Lakes inventories are relatively simple applications of LANDSAT data. An area either is or is not water. Investigation of water condition is more complex. Classification of lakes requires knowledge of the ecological characteristics of lakes, the optical properties of natural water, and the non-water sources of reflection included in the total signal which is recorded by the satellite scanner.

This study reports an investigation of how LANDSAT data can be used to evaluate the water conditions of Minnesota lakes. The first section considers the nature of lakes and their "life cycle". The second covers the causes of the reflection of light from natural waters. The final section outlines several techniques for employing LANDSAT data in surveys of Minnesota lakes and provides the results of a classification of a sample of 81 lakes in East Central Minnesota. The development of the techniques reported here were applied to a larger sample of lakes and the results of this classification are reported elsewhere (Brown, Warwick and Skaggs, 1977).

LAKE SYSTEMS

In his Treatise on Limnology, G.E. Hutchinson remarked:

> "Lakes seem, on the scale of years, or human life spans, permanent features of landscapes, but they are geogolically transitory, usually born of catastrophes, to mature and die quickly and imperceptibly " (1957, p. 348).

Trophic state classification, based on the nutrient status and primary productivity of lakes, reflects the 'state of life' view of lake systems evident in Hutchinson's remark. Young lakes have rugged basins and low nutrient levels, especially phosphorus. These oligotrophic (literally 'few foods') lakes are very transparent because they support only limited numbers of phytoplankton. Over time sediment is deposited, changing basin morphology and supplying nutrients to the water. Lakes become mesotrophic, or mature, and support moderate plant life. Eutrophic lakes, with abundant nutrients and high productivity, are smaller and shallower because of sedimentation. This sucessional process continues as a lake becomes for example, a marsh, meadow, and eventually a forest or a prairie. The rate of a lake's progression through this cycle depends on the availability of sunlight, nutrients, and the sedimentation rate.

Two additional lake types exist which follow modified pathways to terrestrial systems: bog dystrophic and hardwater marl lakes. The first type receives large quantities of "relatively resistant humic substances of largely terrestrial plant origin" (Wetzel, 1975, p. 648) from the lake's drainage basin. These compounds contain nutrients which are not available to biota and which stain lake water a yellow or brown color. The phytoplanktonic productivity of these lakes is normally low to moderate, with the metabolism of the lakes dominated by the littoral vegetation (Wetzel, 1975, p. 648).

Hardwater marl lakes are characterized by low productivity because of low nutrient availability under extremely buffered conditions. High input of carbonates into these lakes result in the sedimentation, and loss, of phosphorus.

Differences in lake types often are reflected by the rates of supply of organic materials to the lake. Dystrophic lakes receive large amounts of organic material from their drainage area (allochthonous matter) and produce little internally (autochthonous matter). Autochthonous organic materials dominate in eutrophic lakes (Figure 1).

Fig. I

Classical Model of Lake Eutrophication

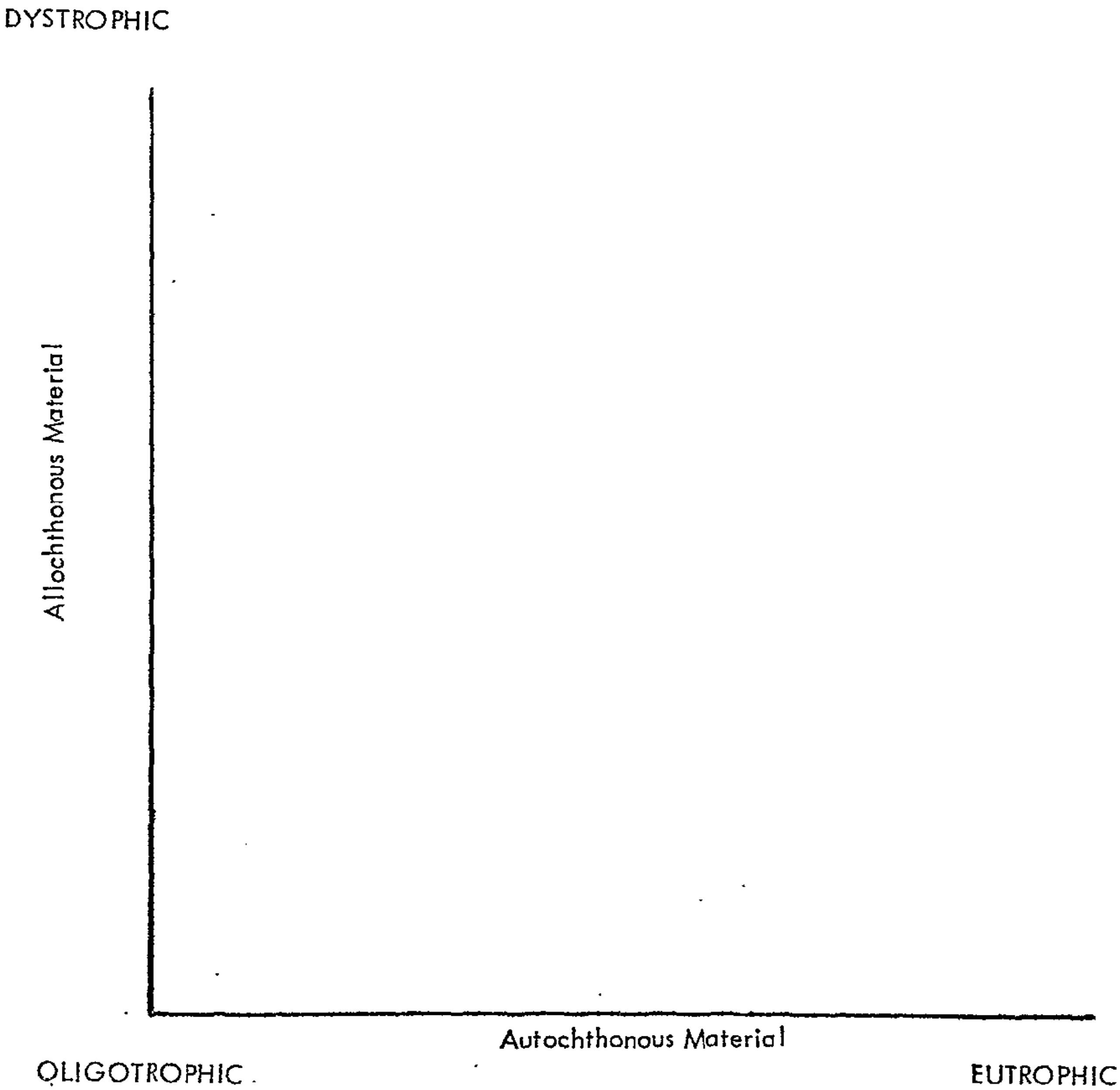

Source: Watzel, 1975.

Changes in lake water conditions, particularly the eutrophication process, are often viewed as resulting from man's disruptive activities. Unfortunately this point is often well taken, as the cultural practices of man frequently cause an increased rate of lake succession by making available nutrients without a corresponding increase in the rate of sedimentation. Lakes with mesotrophic basin characteristics, for example, then exhibit the high productivity of eutrophic lakes.

The succession or evolution of lakes depend on the cycling of the inorganic and organic materials which regulate a lake's productivity. An assessment of trophic state should incorporate a variety of measurements because of the variety of interactions which occur under different conditions. Trophic state indicators include morphometric, chemical, and biological parameters (Table 1). Single indicators used for the sake of simplicity, have shortcomings, and a multivariate method of estimation is preferrable. Boland (1974, p. 47) suggested several possible reasons for the lack of studies which employ multivariate methods, viz., unfamiliarity with the necessary techniques, lack of the necessary computer hard- and soft-ware, the lack of the comparable data for many lakes.

The goal of a lake monitoring program should be to identify those lakes which are undergoing relatively rapid eutrophication. If the high nutrient inputs to these lakes are stopped, the eutrophication process can be reversed or at least slowed (Edmondson, 1969, p. 127).

OPTICAL PROPERTIES OF NATURAL WATER

Solar radiation is a significant factor for lakes. With the partial exception of wind and stream generated currents, "probably all the events within a lake are directly or indirectly determined by the radiation which that lake receives" (Hutchinson, 1957, p. 366). Even

TABLE 1

Trophic Indicators and Their Response to Increased Eutrophication

Physical	Chemical	Biological
Transparency (d) (Secchi disk reading)	Nutrient concentrations (i) (e.g., at spring maximum)	Algal bloom frequency (i)
Morphometry (d) (mean depth)	Chlorophyll *a* (i)	Algal species diversity (d)
	Conductivity (i)	Littoral vegetation (i)
	Dissolved Solids (i)	Zooplankton (i)
	Hypolimnetic oxygen deficit (i)	Fish (i)
	Epilimnetic oxygen supersaturation (i)	Bottom fauna (i)
	Sediment type	Bottom fauna diversity (d)
		Primary production (i)

An (i) after an indicator signifies the value increases with eutrophication; a (d) signifies the value decreases with eutrophication. The biological indicators all have associated qualitative charges (i.e., species changes occur as well as quantitative (biomass) changes as eutrophication proceeds).

Source: Boland, 1974, p. 45

the currents "reflect the thermal structure and so the previous optical history of a lake" (Hutchinson, 1957, p. 366). The attenuation of solar radiation in lakes has been studied by limnologists and ecologists because sunlight provides the energy that heats a lake and that makes photosynthesis posssible.

Investigations of lake water condition with satellite data, however, is based on the energy reflected from a lake. LANDSAT measures the reflected energy in four spectral bands: Green (Band 4), 0.5 - 0.6 μm; Red (Band 5), 0.6 - 0.7 μm; IR1 (Band 6), 0.7 - 0.8 μm; and IR2 (Band 7), 0.8 - 1.1 μm. The Green and Red bands include light visible to the human eye, while the near infrared bands do not. Objects reflect differentially across the solar spectrum. Photosynthetic plants, for example, reflect highly in the Green and infrared bands. Sand or snow reflect highly in all four bands. Applications of LANDSAT data are based on the identification of the spectral signatures of different objects.

LANDSAT data are available either as images or digital data on computer compatable tapes (CCT). The photographic images are easily examined, but the information they contain has been compressed, relative to the digital data. The CCT's contain so much data that they are difficult to analyze.

Tonal variations within and between lakes are evident on LANDSAT images of Minnesota. The tones on an image result from different amounts of reflected energy reaching the sensor system from the lake. The total reflectance monitored by the satellite, however, has several components, not all of which are due to the lake (Figure 2). The total signal is a function of atmospheric scattering, which affects both the energy incident on the lake and the energy reflected by the lake; the surface conditions of the lake; the lake itself (volume reflectance); and the lake bottom.

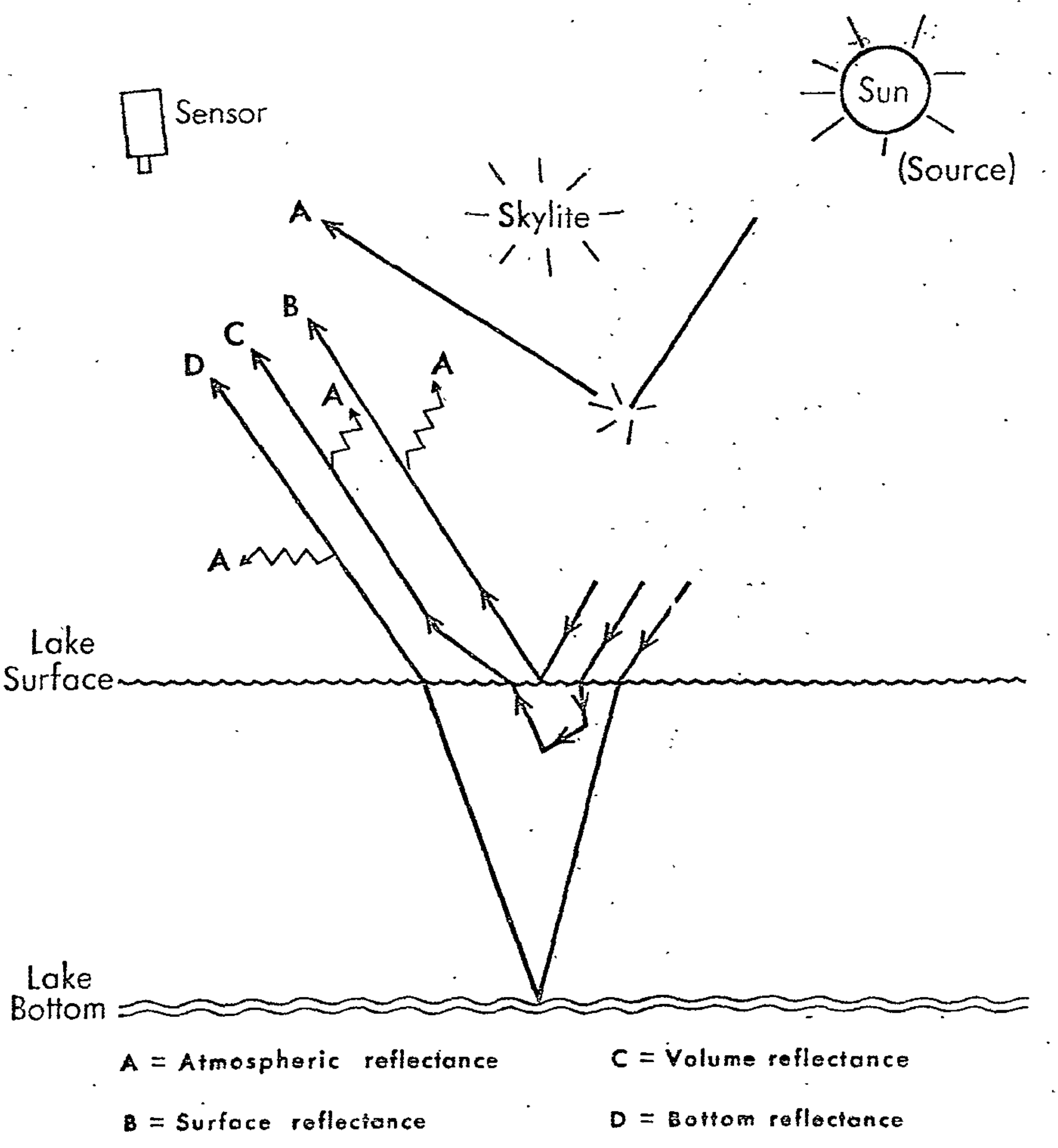

Sensor
Sun
(Source)
Skylite
A
B
C
D
A
A
A
Lake
Surface
Lake
Bottom
A = Atmospheric reflectance
B = Surface reflectance
C = Volume reflectance
D = Bottom reflectance

Fig. 2

The volume component of the reflectance signal should indicate the type and concentration of the material present in the water, and is the most important part of the total signal in determining lake conditions. The other components modify the volume signal and are quantitatively more importnat (Scherz, et al., 1975, p. 15). The analysis of satellite data is based on the total signal, the interpretation is based on the portion of the signal due to material in the water.

The Volume Component of Total Reflectance

The reduction of the intensity of a particular wavelength of light with increasing water depth is due to the selective absorption and the selective and non-selective scattering of that wavelength by the water, suspended particles, and by dissolved organic matter (stain or color). This can be expressed as:

$$I_z = I_o e^{-n z} \qquad (1)$$

where I_z = The intensity of depth z,

I_o = the intensity of depth o (usually one meter),

e = base of the natural log,

n = the extinction coefficient for a particular wavelength.

As the extinction coefficient increases, less light will be transmitted through the water. The extinction coefficient (n) can be broken into the action of water, color, and suspended particles:

$$n'_t = n'_w + n'_{pc} + \frac{s_t}{2} \qquad (2)$$ (Hutchinson, 1957, p.406)

where n'_t = Total extinction coefficient,

n'_w = the absorption of light by water,

n'_{pc} = the absorption of light by particulate matter and color,

s_t = the total amount of light scattered.

The effects of each of these on light will be described.

Water acts very selectively on light, approaching the qualities of a black body. The slight deviation (4%) from a black body results from surface reflection. The amount of light scattered by distilled water is zero (Hutchinson, 1957, p. 377). Light, then, is either transmitted through or absorbed by pure water. The absorption of light by water itself is highly selective. (Table 2) Long wavelengths are absorbed more than short wavelengths, which are transmitted through the water. Over 90% of the light of wavelength greater than 0.75 µm. is absorbed by the first meter of water, and less than one per cent remains at a depth of two meters (Figure 3). Light at 0.48 µm is the most highly transmitted, i.e., the LANDSAT green band. In lakes, the effect of water on reflectance is a constant factor. Variations in the absorption and reflection of light are due to other factors.

It is difficult to separate the effects which stain and suspended particles have on light because their effects vary with their concentration. Stain in lakes results from the presence of dissolved organic acids. While this type of material reflects little, if any, light, it selectively absorbs shorter wavelengths. The amount of stain varies between lakes, but within a single lake it is a fairly constant quantity (Birge and Juday, 1932, p. 526). The absorptive effects of stain is negligible at very low concentrations. In colored, but not deeply stained lakes, yellow light (approx. 0.58 µm) is transmitted to the greatest degree, with shorter wavelengths being absorbed, and longer wavelengths are affected little. With increasing color, yellow light is also absorbed and red light (approx. 0.64 µm) becomes the most transmissive (Birge and Juday, 1932, p.555). In deeply stained lakes the combined action of color/stain and water results in a change in the composition of the transmitted light as those wavelengths unaffected by the stain are acted on by water itself. The total intensity of all light present at a given depth decreases with increasing stain (Figure 4 The selective absorption of the shorter wavelengths by color/stain can

TABLE 2 Optical properties of water (room temperature)

		Wave Length, A.		Extinction Coefficient	Percentile Absorption 1 meter depth
LANDSAT range		8200	(infrared)	2.42	91.1
		8000		2.24	89.4
	IR1 band	7800		2.31	90.1
		7600		2.45	91.4
		7400		2.16	88.5
		7200		1.04	64.5
		7000		0.598	45.0
	Red band	6800	(red)	0.455	36.6
		6600		0.370	31.0
		6400		0.310	26.6
		6200	(orange)	0.273	23.5
		6000		0.210	19.0
	Green band	5800	(yellow)	0.078	7.0
		5600		0.040	3.9
		5400		0.030	3.0
		5200	(green)	0.016	1.6
		5000		0.0075	0.77
		4800		0.0050	0.52
		4600	(blue)	0.0054	0.52
		4400		0.0078	0.70
		4200		0.0088	0.92
		4000	(violet)	0.0134	1.63
		3800		0.0255	2.10

Source: Hutchinson, 1957, p. 382

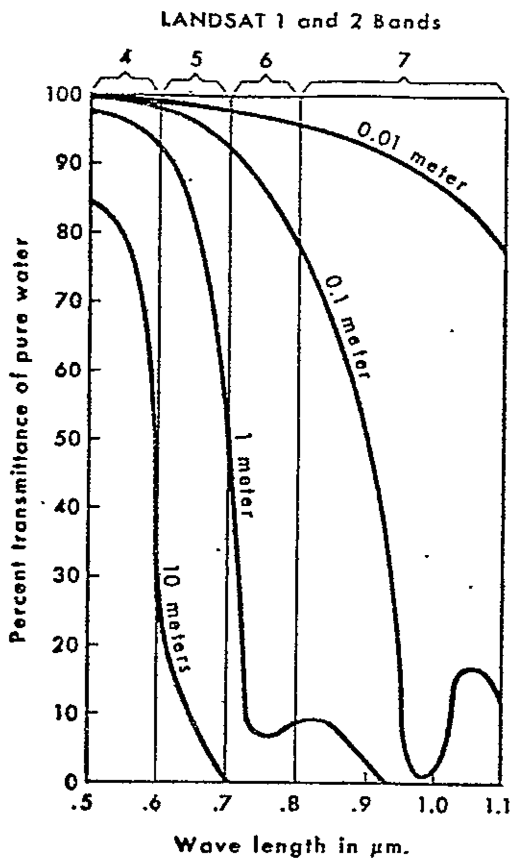

Fig. 3

Spectral transmittance of pure water, for different path lengths.

Source: Modified from Work and Gilmer, 1976.

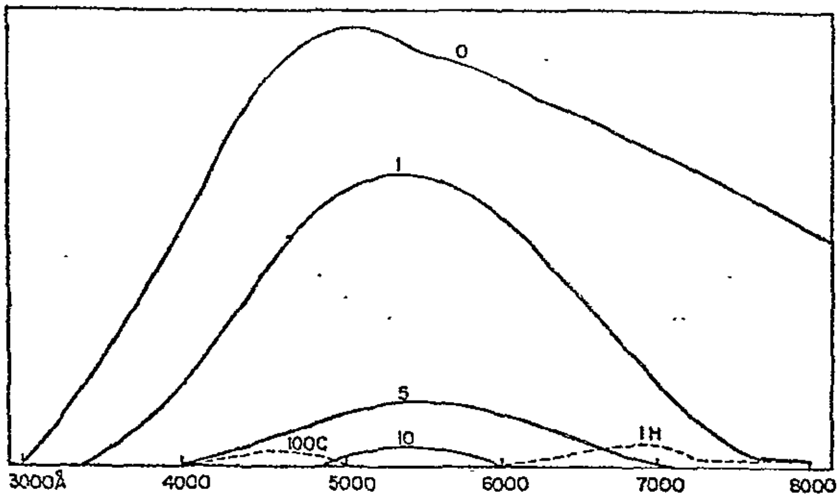

Fig. 4

Variation in spectral composition
of light with depth.

The outer curve, 0, gives an approximate standard spectral energy distribution for sunlight; solid lines (1, 5, and 10), energy distribution at 1, 5, and 10 meters in the Lunzer Untersee, Austria, calculated from 0 and the data of Sauberer; 1H (broken), the same at 1 meter in Helmet Lake, Wisconsin; 100C (broken), the same at 100 meters in Crater Lake, Oregon. Crater Lake is unstained, Lunzer Untersee contains low amounts of stain, and Helmet Lake is highly stained. All are somewhat approximate.

Source: Hutchinson, 1957.

interfere with photosynthesis, as the primary absorption bands of chlorophyll is in the shorter wavelengths (Ghassemi and Christman, 1969, p. 583).

While both color and water act selectively and, for the most part, uniformly within an individual lake, particulate matter generally acts non-selectively on light and varies both temporally and spatially within a lake (Birge and Juday, 1929, p. 525; 1932, p. 526). All sizes and colors of suspended particles can be found within lakes, and these are the attributes which affect light. Particles scatter light either selectively or non-selectively. Selective scattering results either from a correspondence between the wavelength of light and the size of the particles (Rayleigh scattering) or from the molecular structure of the particles (Mie scattering). Rayleigh scattering is important when particles are microscopic, while Mie scattering is due to the absorption of most wavelengths.

Turbidity, the general term for suspended particles, includes both organic and inorganic particles. In Minnesota lakes turbidity generally results from phytoplankton. Silt may be present, but its effects on light will be less than that of algae. There are two reasons for this state of affairs. First, the incidence of silt in lakes is associated with the seasonality of vegetative land cover. In both spring and fall, when cover is minimal, lakes undergo de-stratification, or turn-over, and nutrients within the lake are cycled. The increase in available nutrients results in an increase in primary production. Increases in the concentrations of wind-blown silt will generally be exceeded by concentrations of organic matter. When the source of the silt is erosion, which also implies a lack of vegetation, there will be a corresponding increase in the nutrient loading of the lake from the run-off, which will stimulate production. In both cases the algae should have an effect greater than the silt. Exceptions will exist, but in several cases where local residents have attributed the turbidity to silt, subsequent limnological investigations showed algae present in high concentrations and the primary cause of turbidity

(Megard; personal communication). Effluent discharges could alter this general conculsion but such cases are rare. The dominance of algae over other causes of turbidity is particularly true for eutrophic lakes, where the action of algae on light not only dominates the effect of silt, but also the effect of stain, unless the stain is present in very high concentrations (Birge and Juday, 1929, p. 525).

Turbidity can be estimated with a Secchi disk, a white disk normally 20 cm (8 inches) in diameter. The average of the depths of disappearance and subsequent reappearence of the disk upon being lowered into the water and then raised again is the Secchi transparency. Turbidity is inversely related to the Secchi transparency, in the absence of high concentrations of color/stain (Juday and Birge, 1933, p. 212), and measures the depth of light penetration. The Secchi depth is equal to the depth of penetration of about five percent of incident light (Odum, 1971, p. 297; Hutchinson, 1957, p. 403), and can be used to estimate compensation point or the depth to which one percent of incident light penetrates. The compensation point, where photosynthesis just balances respiration, is approximately 1.2 times the Secchi transparency (Hutchinson, 1957, p. 620).

The presence of color, however, decreases the transmission of light to a degree greater than transparency decreases. A more stained, less transmissive, less turbid lake will have a higher transparency than a less stained, more transmissive and turbid lake (Wetzel, 1975, p. 64; Hutchinson, 1957, p. 402). Two lakes with equal concentrations of algae, but unequal concentrations of stain, will have different transparencies, and exhibit different reflective characteristics. The general relationship between the transparency and turbidity breaks down when lakes in an area vary greatly in color.

When there is little variation in the concentration of color, however, the general correlation between transparency and turbidity can be specified with respect to the dominant suspensoid. Thus, in streams and reservoirs, transparency is generally correlated with total suspensoids, while in lakes, the relation is normally expressed as a function of productivity, usually chlorophyll concentrations (Table 3). These secondary correlations assume knowledge of the specific conditions which dominate the lakes of an area.

Secchi transparency ranges from a few centimers in very eutrophic lakes to over forty meters in a few very clear lakes, e.g. Crater Lake, Oregon. Seasonal variations in transparency occur in most lakes, and in Minnesota are generally related to variations in the lake's productivity. (Figures 5 and 6).

When a Secchi disk is lowered into the water, the color of the white disk will be modified by the action of the stain and particules suspended in the water. This is the apparent color of the lake, which includes the effects of both the true color (i.e., stain) and those of suspensoids. Apparent color ranges from clear through blue, green, yellow, and brown to black, in very highly stained lakes. By noting the apparent color of the water, the cause of the turbidity, and thus of the reflection of light, can be inferred. A green color usually indicates algae, for example, and algae is identified easily. A reddish-brown color, however, can be caused by stain, suspended clay or silt, or soluble iron compounds. When a combination of substances are present, it is impossible to tell from the Secchi transparency how much of the attenuation or reflection of light is attributable to each factor. For lakes with similar qualities, however, the reflective characteristics will be similar (Hutchinson, 1957, p. 402). The relationships between light reflectance can be specified by examining representative lakes.

While this description of the optical properties of lakes has been necessarily biased toward the attenuation, rather than the reflection, of light, some generalized relationships between materials found in lakes and the spectral bands monitored by LANDSAT can be formulated. The addition of a single type of material to a very clear lake will change the transparency of that lake, and also its reflective characteristics. The concentration of the material present

TABLE 3

Generalized Relationship between Transparency, Chlorophyll and Phosphorus

	Constant blooms	Pea Soup Green		Occassional blooms and odors	Underwater visibility restricted	Water begins to be greenish	
Chlorophyll (mg/m^3)	100	80	60	40	20	10	0
Transparency (ft.)	1.5	2	2.5	3	4.5	7	∞
Total Phosphorus (ug/l.)	165	135	105	75	45	30	0

$\longleftarrow$

Eutrophication

Source: Barr Engineering, 1976

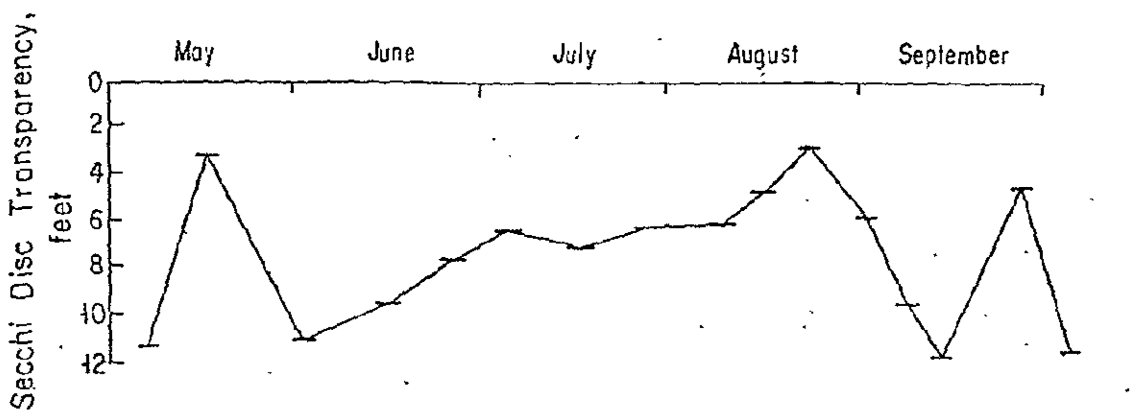

Fig. 5

Graph of Secchi disk measurements.

Source: Lundquist, 1975.

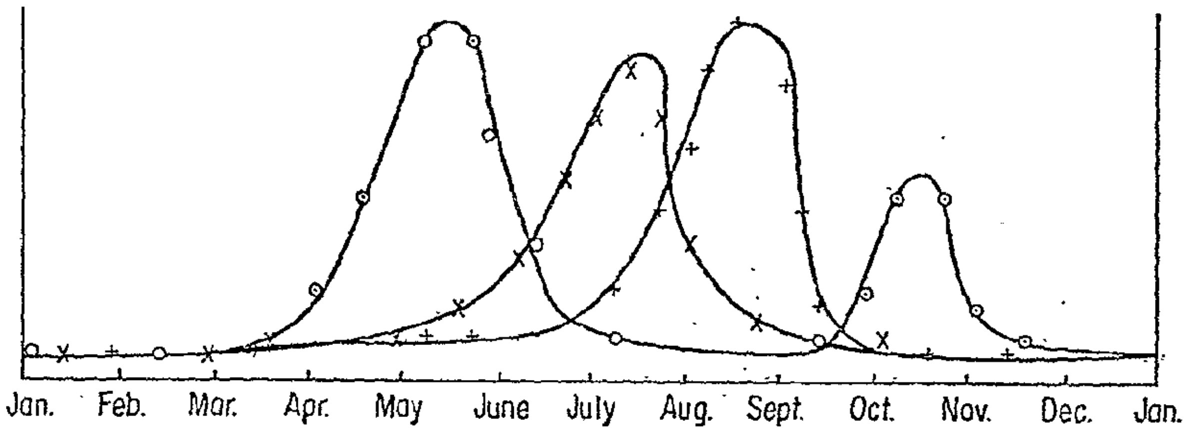

Fig. 6

Seasonal fluctuations of phytoplankton populations.

o = diatoms
x = green algae
+ = blue-green algae

This is an idealized record for temperate climate lakes, but by no means does it apply to all of them.

Source: Lundquist, 1975.

will be best predicted by the LANDSAT spectral band which penetrates clear water to the depth of that lake's transparency and no deeper.

Oligotrophic lakes, characterized by high transparency and low concentrations of suspended materials will transmit or absorb all wavelengths of light. Low algal concentrations will generally be distributed uniformly throughout the water column (Wetzel, 1975, p. 286). Because light of the LANDSAT Green band penetrates the water most deeply, it will encounter more particles and its reflection will show an increase greater than the other bands. When medium algal concentrations are present in a lake, causing lower transparency, the Red band will best indicate the water conditions. In hypereutrophic lakes, the very near surface concentrations of algae will cause the reflectance in the IR1 and IR2 bands, which is normally low due to absorption by water, to increase.

Intuitively it might be expected that the absorption of the 0.63 μm spectral region by chloroplasts would supress reflectance in the Red band when high concentrations of algae are present. The photosynthetic efficiency of aquatic plants, however, is considerably less than their terestrial counterparts, because they utilize less than one percent of incident light (Wetzel, 1975, p. 287). The combination of low efficiency and the small portion of the Red band involved indicates that this effect is negligible. However, more of the shorter wavelengths (i.e., Green band energy) which are scattered in the water volume will reach the water surface, and therefore the satellite scanner, because of differences in the refractive patterns of the different wavelengths (Wetzel, 1975, p. 50). The intensity of reflectance in the Green band should exceed that in the Red band.

Non-Water Sources of Reflection

The signal recorded by the LANDSAT sensor includes reflection from the atmosphere, the water surface and, if visible, the lake bottom (Figure 2). Reflection from these sources does not contribute to the identification of the type of materials in a lake, and their affects must be understood to use LANDSAT data for investigating water conditions.

Atmospheric Effects

Light in the atmosphere, as in water, is either transmitted, scattered, or absorbed. Ultraviolet light, 0.004 - 0.4 μm, is absorbed, while scattering primarily affects blue light, 0.4 - 0.5 μm. Longer wavelengths are transmitted through the atmosphere to a greater degree than are shorter wavelengths. Of the spectral bands monitored by LANDSAT, the Green band is most affected by the atmosphere. Backscattering of incident light increases the signal recorded by the satellite, and is noise, while the scattering of the light reflected by a lake results in the loss of information. LANDSAT investigators normally assume atmospheric effects to be constant across a scene for analysis purposes, and such is the case for this study.

Surface Reflection

It was noted above that the optical properties of water approached the characteristics of a black body, differing slightly because of surface reflection, which is a function of the angle of incidence, for both sunlight and diffuse skylight. Under windless conditions, with a sun angle less than 40°, the total amount of reflected sunlight is small (Figure 7).

Fig. 7

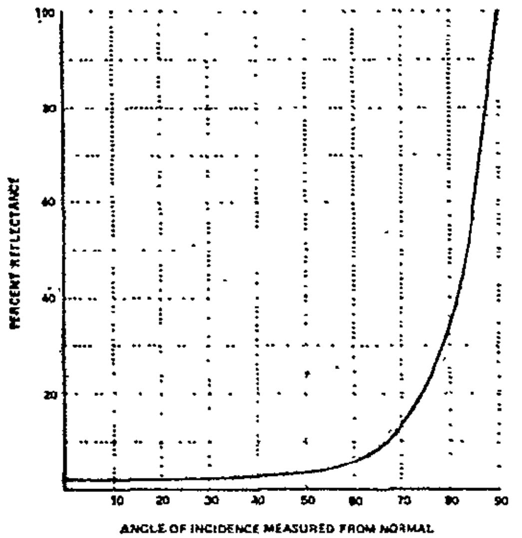

Percent reflectance of the air-water interface as a function of the angle of incidence (measured from the normal direction). These values are for unpolarized light only.

Source: Piech and Walker, 1972

The LANDSAT scanner will not view the resultant reflectance because the field of view of the sensor system "is limited to near vertical observations" (Work and Gilmer, 1976, p. 686). In order that light reflected by the water surface reach the sensor, it must originate near the zenith location. While this is true for diffuse skylight, the angle of incidence is then close to zero, so the surface reflection of skylight will also be low. Surface reflection, on calm lakes, can therefore be considered constant.

Wind, however, can cause an increase in reflection that does not allow simplifying assumptions to be made. The primary effect of the wind is the creation of waves, but several secondary processes also affect the reflective properties of water. Wind driven water forms waves, whose size varies with wind speed, fetch, and water depth. Unless large portions of an individual lake are very shallow (less than 1 meter) and exposed to the wind, water depth is of minimal importance. If the wind speed and direction are constant across a LANDSAT scene, the size of the waves depends upon the orientation of individual lake basins to the wind. The surface presented to incident light is no longer uniform, as under calm conditions. Strumpf and Strong (1974, p. 87) found that diffuse glitter from ocean waves contaminated LANDSAT imagery when the sun elevations are greater than 55^{o}. Work and Gilmer (1976) found no evidence of sun glitter in their study of North Dakota praire lakes. They pointed out that the surface conditions of inland lakes are calm relative to those of the oceans, and that the critical sun elevation angle is exceeded for only "a limited period of time centered on 22 June". (p. 686) However, Work and Gilmer were not examining the water condition of the North Dakota lakes, but doing an inventory primarily using the LANDSAT IR2 spectral band, which may not be as sensitive to sun glitter as the other bands because of the absorption of infrared light by water.

Wetzel (1975, p. 48) has suggested that the presence of waves would decrease reflection, as a more nearly perpendicular surface is presented to incident light. This decrease is probably important only when the sun elevation angle is low because of the naturally low reflective characteristics of water. A systematic evaluation of the effects of waves themselves must include not only the effects of sun angle, but also wind speed and direction with respect to the sun angle. These factors have not been adequately examined to isolate their effect on the satellite signal, either here or elsewhere. In addition to causing waves, the wind also moves the material in and on the water. Algae and surface debris will be found in higher concentrations to the windward. The volume reflectance will also increase, indicating the more turbid conditions. Care must be taken in interpreting a down wind increase in reflection as due solely to turbidity. Reflection may also increase because of bubbles and surface foam caused by breaking waves. As concentrations of both suspended materials and surface foam would increase down wind, their effects are additive and difficult to separate.

Unlike atmospheric scattering, surface reflection cannot be assumed to be constant across a LANDSAT scene when winds are present. The effect of the wind will vary with the size, shape and orientation of a lake basin to the wind. Variations within a lake will also exist between areas exposed to and protected from the wind. Simplifying assumptions concerning the effects of wind on the reflection of light will not indicate the complexities exhibited in real situations.

Bottom Reflection

When a lake's transparency exceeds the water depth, the lake bottom will alter the signal recorded by the satellite. A light colored bottom, e.g., sand or marl, will increase the signal. A dark colored bottom will decrease reflection because the transmitted light will be absorbed. In either case the bottom effect will vary with water depth, decreasing in deeper water and increasing in shallower water. The composition of the signal will also change with depth. The effect of the bottom will be greatest on the Green band because the light of the shorter wavelengths are transmitted to a greater degree than the other bands. Conversely, the minimum effect will occur on the IR2 band because that light is absorbed near the surface. The effect of bottom is not entirely noise, but indicates the morphology of the lake basin.

SUMMARY

The signal recorded by the LANDSAT scanner system is composed of reflectance from the water volume of a lake, the surface of the lake, the atmosphere, and possibly the lake bottom. Assessments of lake water conditions are based on the portion of the signal which results from the water volume. Because pure, or distilled, water reflects little light, the addition of stain, algae, or other suspended particles will alter the volume reflectance of a lake. The intensity of the change will indicate the concentration of the material present while the relative strengths on the four LANDSAT bands will indicate the type of material.

Atmospheric scattering and surface reflection cause the signal monitored by the satellite to increase. The effects of both the atmosphere and the water surface can vary across a LANDSAT scene, but in the absence of ground information, have been assumed to be constant.

The effects of bottom reflection on the satellite signal vary from lake to lake, and where present, contain information on the depth of the lake. Because the intensity of bottom reflection depends on water depth, the presence of bottom reflection in the signal may not be identifiable.

ANALYSIS

Water qulaity investigations using LANDSAT data included multivariate analysis of water transparency relationships with both LANDSAT image density measurements and digital data from CCTs. Two methods of image density evaluation were explored, density-slicing techniques and microdensitometry; but neither method yielded consistent results. The analysis of the digital data appears useful for classification of lakes.

Image Density Evaluation

The analysis of LANDSAT imagery was undertaken because of the low technological and cost requirements relative to the use of digital data (CCTs). The four transparencies (Green, Red, IR1, and IR2) necessary to analyze a scene cost $20 while a CCT costs $200. The development cost of requisite software for analysis of the CCTs is also high compared to the relatively simple procedures necessary for analysis of imagery.

Tonal differences are visible to the unaided eye both within and between lakes on LANDSAT imagery of Minnesota. Since these gross variations existed, further analysis of LANDSAT imagery appeared to be potentially rewarding. Although the data contained on LANDSAT imagery are compressed relative to those contained on the CCTs, significant results have been obtained by other investigators (e.g., Yarger and McCauley, 1975).

The image densities for several scenes of East Central Minnesota were analyzed using a VP-8 density slicer, coupled with a Sony Video camera. Transmission voltage readings for selected lakes with areas greater than 100 acres were taken on each of the four LANDSAT black and white 9-inch positive transparencies. The readings were standardize to the fifteen step calibration scale on the transparencies. Because variation of lake quality between scenes was not being examined, a standard calibration wedge, as suggested by Ashley and Rea (1975, p. 714) was not used.

Secchi transparency readings were available for all the lakes analyzed. Step-wise regression analysis was used to examine the relationship between the image densities and the transparency readings. Multiple correlation coefficients (R) obtained ranged from 0.38 to 0.89, with the Red band generally being the best single predictor of transparency. The results of an analysis of a July 3, 1973 scene of east Central Minnesota (Scene number 1579-16275) are summarized in Table 4.

TABLE 4

SUMMARY OF LAKE WATER QUALITY MULTIPLE REGRESSION ANALYSIS

Step	Variable entered	B coefficient	Std. error B	Multiple r	r^2
1.	Band 5	-0.08785	0.02035	.566	.32
2.	Band 6	0.02975	0.01286	.658	.433
	(constant)	2.30432	0.387		

Dependent variable: Secchi Disk Transparency N=29

Source: calculated by author

These findings, although consistent with those reported by other researchers with regard to both the range of the correlation coefficients and the importance of the Red band (Boland, 1974; Yarger and McCauley, 1975), were not replicable. The primary cause of variation in the correlation coefficients was variation in the response of the VP-8 and video camera.

As it was equipment which caused the inconclusive results, further investigations of the image density-water transparency relationship seemed warranted. A microdensitometer, made available by the Space Science Center of the University of Minnesota, was to continue this research. The ERTS Data User's Handbook suggests that only macrodensitometry work be done with the 9 inch transparencies. The recommended 3mm aperture encompasses an area of approximately 700 acres on a 9 inch transparency. Few Minnesota lakes have size and shape such that 700 acres of water could be examined with so large an aperture. A 0.4mm aperture, corresponding to an area of approximately 20 acres was used because Ashley and Rea (1975), in examining vegetation cover, found that such an aperture size provided excellent correspondence with the suggested 3mm size.

Yarger and McCauley (1975) reported good correspondence between the reflectence values found on the CCTs and image density values calibrated to the grey wedge, as the grey wedge is linearly related to the digital radiance values (DN counts). They did not, however, report the aperture size of the densitometer employed, although they mentioned that it was macrodensitometric work.

In this study several LANDSAT scenes of East Central Minnesota were analyzed, yielding multiple coefficients of determination (r^2) ranging from 0.45 to 0.72. In addition to the calibrated density values, band ratios were used to control for unequal scene illumination and to eliminate the common brightness component of the reflectance, as suggested by Vincent (1972), and employed by Yarger and McCauley (1975) and Boland (1974).

The major portion of the variation in the correlation coefficients resulted form machine variation. Comparison of two sets of readings for 34 lakes on an August 20, 1974 scene (1758-16171) shows that the data were not replicated with high accuracy (Table 5). Further investigations using the equipment were halted.

TABLE 5

Comparison of Two Sets of Densitometric Readings

Lake	ID NR.	BAND 7		BAND 6		BAND 5		BAND 4	
		Set 1	Set 2	Set 1	Set 2	Set 1	Set 2	Set 1	Set 2
Otter	02-003	82.0	86.5	83.0	76.0	92.0	89.5	73.5	75.5
Crystal	19-026	77.0	83.5	73.5	71.0	85.0	91.0	64.0	59.5
Silver	62-001	71.0	77.5	69.5	72.5	89.5	81.0	67.5	59.0
Bald Eagle	62-002	91.0	88.5	90.5	94.5	94.0	96.5	71.5	81.0
Kohlman	62-006	69.5	74.5	66.0	61.0	87.0	81.0	66.0	69.5
Gervais	62-007	81.0	72.0	79.0	83.5	90.5	93.0	65.0	63.0
Keller	62-010	67.0	61.0	63.5	51.0	86.5	90.0	56.0	62.0
Wakefield	62-011	58.5	53.5	46.0	54.5	81.5	74.5	47.0	41.0
Phalen	62-013	80.0	84.5	76.0	67.0	92.0	80.5	69.0	58.0
Birch	62-024	72.5	67.0	74.0	79.0	92.0	81.0	70.0	78.0
Gillfillan	62-027	67.0	69.5	68.0	60.5	94.5	96.5	66.0	56.5
McCarron	62-054	70.0	75.0	68.0	75.0	88.0	92.0	53.5	65.5
Como	62-055	68.5	64.0	62.5	68.5	83.5	88.5	50.5	55.0
Owasso	62-056	84.0	88.0	79.5	82.0	89.0	89.5	60.0	52.0
Josephine	62-057	72.0	70.5	67.5	73.0	82.5	86.0	55.0	62.5
Turtle	62-061	87.0	83.0	85.5	89.5	92.5	87.0	69.0	81.0
Round	62-070	54.0	58.0	47.5	42.0	59.0	66.0	27.0	41.5
Snail	62-073	72.5	81.5	78.0	78.0	91.0	83.0	72.0	65.0
Johanna	62-078	75.5	71.5	72.0	75.0	85.5	81.5	60.0	56.0
Wabasso	62-082	72.0	64.0	69.0	71.5	88.0	90.5	64.0	71.0
Cannon	66-008	91.0	94.0	86.5	88.0	91.5	87.5	77.0	75.0
Dudley	66-014	48.0	56.0	55.0	50.5	91.5	88.0	66.0	70.5
Kelly	66-015	52.5	63.0	65.0	68.5	94.0	83.5	68.0	61.5
Roberds	66-018	78.0	74.0	78.5	82.5	94.5	96.0	67.5	72.5
Circle	66-027	75.0	71.0	75.0	82.5	91.0	89.0	70.5	63.5
Fox	66-029	72.0	79.0	77.0	83.0	93.0	84.0	70.0	73.0
French	66-038	86.5	76.5	82.5	78.0	89.5	92.0	64.0	56.0
Mazaska	66-039	82.5	78.5	76.0	72.0	91.0	85.5	65.0	72.0
Cedar	66-052	81.0	85.5	79.5	75.0	88.0	92.0	63.5	71.5
St. Croix	82-001	92.0	88.5	90.0	94.0	93.5	96.0	72.5	81.5
Square	82-046	77.0	84.0	85.0	87.0	98.0	91.0	76.0	70.5
Big Marine	82-052	97.0	98.5	98.5	95.0	96.5	99.0	79.0	86.0
Jane	82-104	77.5	73.0	78.0	66.0	92.5	84.0	69.0	57.0
White Bear	82-167	98.5	96.5	97.0	99.0	97.0	94.0	78.0	83.0
r		.87		.905		.664		.764	
r^2		.757		.819		.441		.581	
mean		75.9	76.2	74.8	74.9	89.6	87.7	65.1	65.9
s.d.		11.8	11.5	12.0	13.4	6.7	6.8	10.1	11.4

LANDSAT scene: August 20, 1974, 1758-16171

Source: Calculated by author

ORIGINAL PAGE IS
OF POOR QUALITY

Problems encountered in the analysis of image densities result from scale compression, variations in the equipment used and chemical adjacency effects. The low reflection of water targets means that small actual density variations exist between lakes, and these become smaller when the scale is compressed. Much of the variation in the readings appears to have been due to the equipment. Subsequent comparison of the readings obtained by microdensitometry with the digital data recorded on CCTs showed a low correspondence. The densitometer readings also exhibit variations which correlate with lake size. When examining small lakes with an instrument with a relatively large aperture the area surrounding the lake will influence the density of the image, especially in high contrast situations. This problem stems from photographic technology and is inherent in the use of film imagery, and cannot be overcome by including a measure of lake size in the analysis, because transparency generally shows a positive correlation with lake size. The effects of chemical adjacency and actual differences in lake quality cannot be statistically separated. This still allows for the analysis of large lakes, the number and importance of small (less than 500 acres) lakes in Minnesota makes the technique incompatible with the goals of our investigation.

Image density analysis proved not feasible given the equipment available. This does not prove that other methods and equipment would not yield adequate results, particularly in light of the work of Yarger and McCauley (1974). Results here support Boland's conclusion that the evaluation of image density in water quality studies is of limited applicibility (1974, p. 76).

Computer Compatible Tapes Analysis

The use of CCT's for the study of water quality, while more expensive than image data extraction, has several significant advantages. The data on the tapes are the actual picture element (pixel) reflectance values recorded by the satellite. The data analyzed are from a first generation product, as opposed to the image, a fourth generation product. As Boland (1974, p. 79) pointed out, "Investigators can avoid the numerous uncertainties introduced when the original MSS data are coded by an electron beam recorder (EBR) into photographic forms and then re-quantified through microdensitometry."

With relatively sophisticated programming methods, and hardware, the CCT's can be used to produce enhanced photographic products. The use of CCT's, however, necessitates computing facilities and relatively large amounts of computer time. The type of programs and analysis used will determine the cost. The analysis methods used by Boland (1974), Scherz and his associates (1974, 1975, 1976), Rogers, et al. (1975) are quite sophisticated. Our efforts are more modest, attempting to show the applicability of the LANDSAT data to water quality studies, rather than develop an integrated package of both computer programs and the associated program of ground information collection.

Our method was influenced by the previous work on northern latitude lakes by Boland (1974) and by Scherz and his associates (1977). Their work differs in a number of ways. Boland used the mean reflectance value of an entire lake to predict that lake's trophic state. He first isolated lakes using a binary masking technique on the IR2 band and then calculated descriptive statistics for each LANDSAT band. The trophic state classification was based on a multivariate analysis of data collected on the individual lakes by the National Eutrophication Survey (NES) of the EPA, in 1972. The use of the mean reflectance value of the entire lake in the prediction of the lake's trophic state follows from Boland's method of identification and isolation of the individual lakes. Because an entire lake is the unit of management, or study, this appears sound. However the mean reflectance values of an individual lake may not represent the variety of conditions present in the basin, especially when the basin is complex.

Scherz and his associates have attempted to overcome this problem by classifying lakes on a pixel by pixel basis; that is, each pixel is identified and classified by its similarity to predefined classes which encompass the entire range of water conditions encountered in a scene. In order to define the types and range of conditions, they employed both low level aerial surveys of the study area and a heuristic device for eliminating the effects of atmosphere and surface. While Boland used band ratioing to eliminate common scene brightness, thus leaving the water volume information, Scherz employed a method he termed residual signal analysis. A very deep clear lake is first identified by ground analysis. The reflective properties of this lake should approximate those of very pure water, i.e., the volume reflectance should approach zero and the LANDSAT signal will be composed of reflection common to all lakes in the area. Using the signal of this lake as a base for all other lakes on the scene yields satellite residual signals for those lakes. These then represent not only the volume component of the lake, but form families of characteristic signals or curves, which correspond to the various types and concentrations of materials in the waters of lakes (Figs. 8-11). When the nature of a selected group of 'pure' types is known through ground analysis, and verified by the characteristic curve, they can be used to define the groups for the computer classification of lakes by their pixels. Thus, lakes which would be classified by Boland's mean reflectance value as some mean trophic state, are represented in their variety when classified on a pixel by pixel basis.

The ideal type of method would be similar to that employed by Scherz, but including the number of pixels of each water type found in individual lake basins. A pixel by pixel classification scheme, however, requires specialized software that was not available. A more simplistic method incorporating elements found in the methods of both Boland and Scherz was used for this analysis. The CCT of

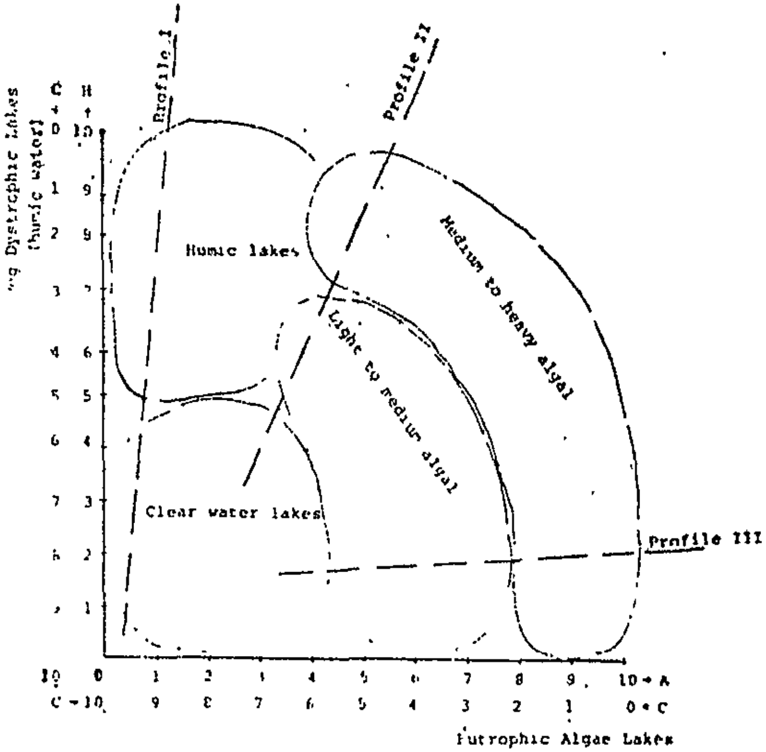

Fig. 8

Scheme used to classify lakes from LANDSAT data. Satellite residual fingerprints along profiles I, II, and III are shown in Fig. 7, 8, and 9.

Source: Scherz, 1977.

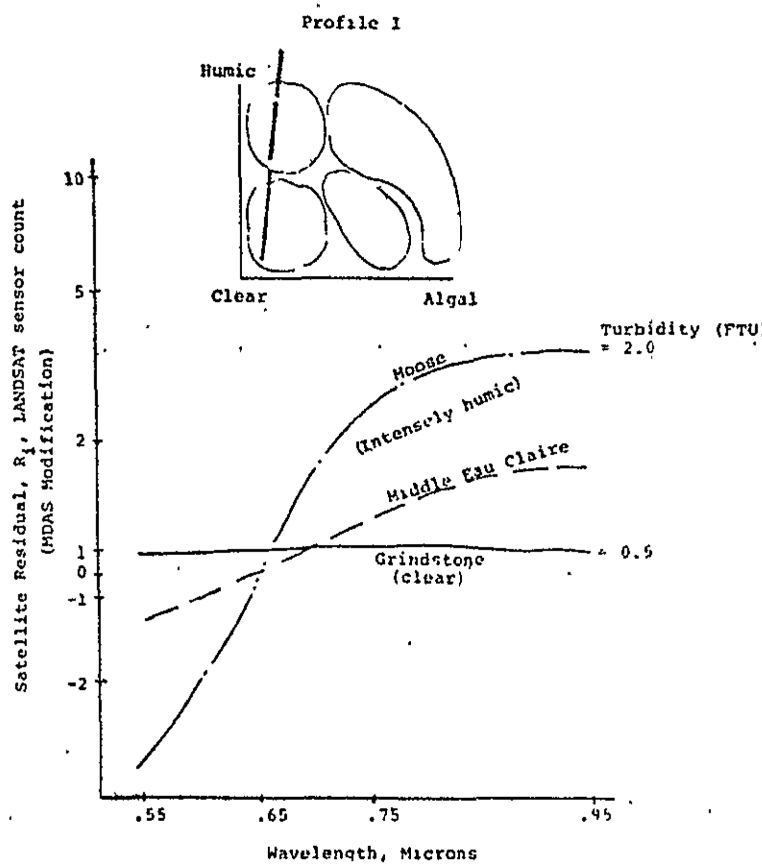

Fig. 9

Satellite residual fingerprints for clear, moderate, and intensely stained lakes. (profile I in Fig. 6.)

Source: Scherz, 1977.

Note: The M-DAS modification of LANDSAT reflectance value increases the DN counts on the Green, Red and IR1 bands by a factor of two and on the IR2 band by a factor of four. This applies to Figs. 9, 10, and 11.

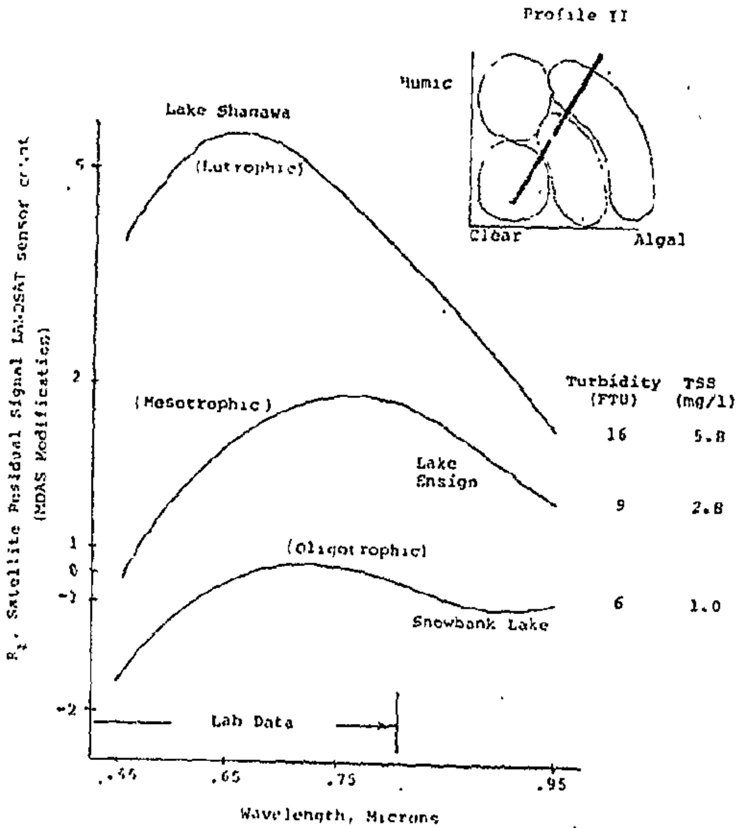

Fig. 10

Satellite residual fingerprints for moderately stained lakes containing various amounts of algae. (profile II in Fig. 6.) TSS = total suspended solids.

Source: Scherz, 1977.

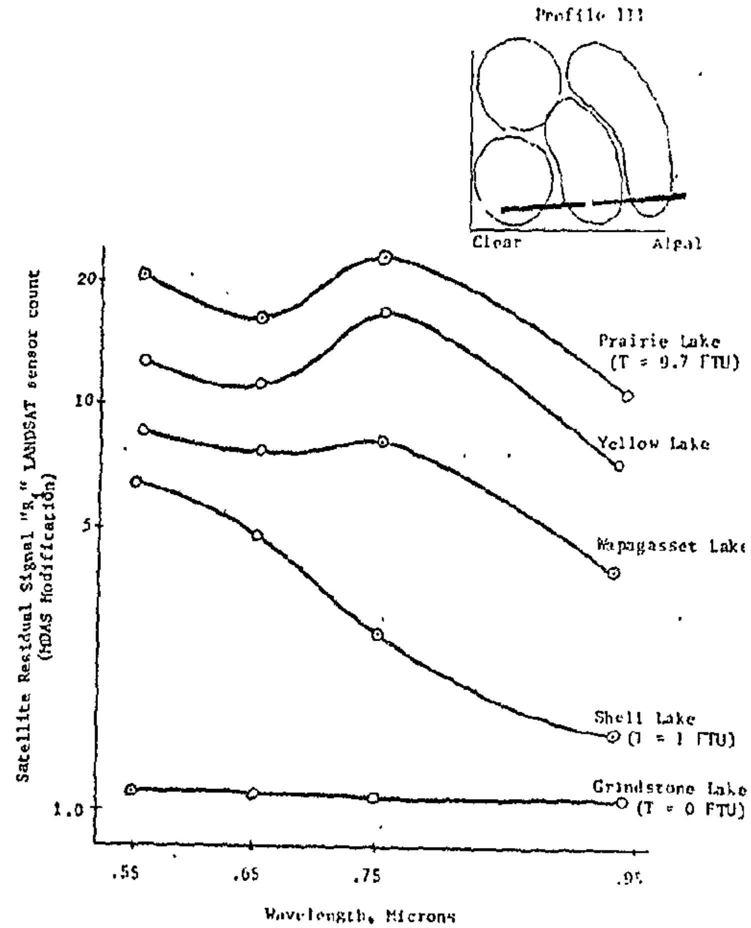

Fig. 11

Satellite residual fingerprints for unstained lakes, containing various amounts of algae. (profile III in Fig. 6.) T = turbidity.

Source: Scherz, 1977.

an August 7, 1975 scene (2197-16201) was reformatted into the Environmental Planning Programming Language (EPPL4) and a grid system imposed on the reformatted tapes. The area surrounding a lake larger than 100 acres was printed. The prints showed the actual reflectance values recorded by the satellite. Individual lakes were identified from the IR2 band printouts by comparing them with Bull. 25, An Inventory of Minnesota Lakes. The lakes were identified both by number and name, which may not be consistent with those found on USGS topographic maps. From each individual lake a sample site was selected. Usually a twenty pixel (22 acres) area was sampled, a site four elements by five scan lines. The primary orientation of the sites was normal to the satellite ground track, and the sample sites were located to minimize any effects of the sixth scan line degradation noticable on some imagery. The IR2 print, with the sample site(s) located was traced onto the other three printouts. The mean reflectance value of each LANDSAT band was calculated for each sample site. In large lakes, or those with complex basins, multiple sites were sampled.

Statistical Analysis

The effective application of a statistical technique depends, in a non-statistical sense, on the required input data, the desired output, and the theory, or causal linkages, which mediate between them. Statistically the data must fulfill certain assumptions and the requisite computer hard- and software must be available. Three techniques which meet these requirements are regression, cluster analysis, and discriminant analysis. Each has different types of theoretical and statistical assumptions, which result in different types of classification and prediction.

Each of these techniques classify, or predict the conditions, or quality, of a lake according to the reflective characteristics of the water. The reflectance values, or input data, are constant for each type of analysis. The type and use of ground truth information in the creation or calibration of each statistical model varies from one to another. Regression analysis requires interval level ground truth information, while both cluster and discriminant analyses are less stringent requiring ordinal level data. While discriminant analysis was used in the final classification of lakes in the study area, both regression and cluster analysis might provide useful insights for other investigators. The usefulness of these techniques rests on the type of water conditions present and the amount and type of information available on them.

The ground truth data requirements for each type of analysis become more important when consideration is given to the cost and effectiveness of their collection. A variety of chemical, biological, and morphological parameters normally are measured when examining an individual lake basin. Not all of these are directly related to the reflective properties of water; however, they are necessary to evaluate water conditions. In order that LANDSAT data be used correctly, the full range of lake types must be included in the ground monitoring. Complete analysis of a large number of lakes is both expensive and difficult to accomplish in conjunction with LANDSAT overflight. The nature of lakes is such that extreme changes may occur over short time periods, so the collection of ground truth and image acquisition must be coordinated. This increases the cost of ground truth collection, as multiple teams are necessary.

This requirement can be circumvented in two ways. First, if a complete assay of individual lakes is desired, the monitoring of the more stable lakes can be temporally divergent from over pass. A hypereutrophic lake, for example, will exhibit little change from late June to mid September. The same is true of oligotrophic lakes.

The second method is to forgo a complete analysis of lake conditions and examine transparency. This can be done by untrained, but interested citizens thereby decentralizing data acquisition. This is the method used by the Limnological Research Center (LRC) in their transparency study of Minnesota lakes. From a theoretical point of view, transparency has several advantages over other quality parameters. Because Secchi transparency measures the attenuation of light, it indicates the amount of light reflected, which is in turn monitored by LANDSAT. Additionally, most chemical and biological assays are done on water samples from the surface or near surface of a lake's ("grab samples"). The surface conditions may not adequately represent the conditions throughout the entire illuminated zone and errors will result when the results of such analysis are manipulated statistically with the reflectance values which are indicative of the entire zone of illumination.

In order that complete chemical and biological surveys do indicate conditions throughout the entire water column, multiple samples from a site must be taken at various depths, as was done by the NES, which data were employed by Boland (1974).

During the summer months of 1975, approximately 120 lakes in the study were surveyed. Only transparency data were available for about 60 of these lakes, while chemical and biological data existed on the others. The use of the ground information for about 20 lakes was limited because of the date of data collection.

Regression Analysis

The primary attractiveness of regression analysis for examining the relationship between reflectance and a quality parameter, in this case transparency, is that the resulting predictions of that parameter will be interval level. Lakes are not easily classified into discrete types, particularly on the basis of a single measure of their quality. They represent a variety of distinct types and gradations between these types. This continuum of lake types or water conditions can be seen for lakes which fall between oligotrophic and hypereutrophic. In the absence of high concentrations of silt or stain, transparency is linearly related to primary productivity, and available nutrients. The use of reflectance data for prediction of transparency of lakes of unknown quality would be useful.

In areas where dystrophic lakes occur, regression analysis cannot be used to predict the transparency of lakes when the amount of stain/color present in them is unknown. The model can be used to explore the relationship between reflectance and both the transparency and color of known lakes, through analysis of covariation. But the extension of the model to lakes which have unknown qualities is not possible.

Cluster Analysis

Cluster analysis groups observations (lakes) on the basis of their reflective characteristics alone, and assumes that there is good correspondence between the reflectance of lakes and the water conditions. Goodness of fit is defined by the data and inferred from analysis of the resulting groups or clusters. The ground truth information is used to verify the goodness of the groups, not to define them. The coordination of ground truth information collection with satellite overpass is not required for cluster analysis. The general state of lakes throughout the season is a guide to the interpretation of the resulting groups. Ground truth collected earlier or later in the summer is a good indication of the general conditions which prevail in a given lake and can be used to interpret the clusters. The technique is attractive because its use lowers the cost of ground truth information collection.

An average linkage clustering algorithim was used to group the lakes according to their standardized reflectance values (z-scores). The routine calculates a similarity coefficient for each pair of lakes which is the Euclidean distance separating them, i.e.,

$$S_{ij} = \left((W_i - W_j)^2 + (X_i - X_j)^2 + (Y_i - Y_j)^2 + (Z_i - Z_j)^2 \right)^{1/2}$$

where W, X, Y, and Z are the standardized reflectance values of the four LANDSAT bands, and S_{ij} is the similarity coefficient for observations i and j. The routine identifies the two points with the smallest similarity coefficient (i.e., the closest points in four dimension Euclidean space) and groups them. These two observations become a single observation, or group, with two members and a location equal to the mean values of the two observations. Similarity coefficients are once again calculated, with n-1 observations, and the two closest points grouped. The clustering procedure continues until all observations are grouped together. The routine begins with complete individuality (n groups, each with one member) and ends with complete generalization (one group, with n members).

Ninety-nine observations on eighty lakes for which transparency were available, were clustered and the results analyzed. The process of generalization is summarized by a dendrogram (Fig. 12). Two major groups and seven to twelve smaller groups can be readily discerned in the dendrogram. The major groups are lakes with relatively high transparency and quality, and those with lower transparency and quality. There are, in addition, several lakes which are dissimilar to these two large groups and join groups only when forced.

The smaller groups were identified subjectively. Analysis of variance is commonly used to analytically differentiate groups with cluster analysis. Statistical rigor was considered less important than the identification of the range of water conditions, as deduced from an analysis of the satellite residual signal and ground truth information available on the clustered lakes. The smaller classes are also indicated on the dendrogram. Comparison of the mean reflectance values and transparency reading for each of these classes (Table 6) shows that lakes with similar transparencies have different reflectance values and vice versa. The interpretation of the classes reflect these differences.

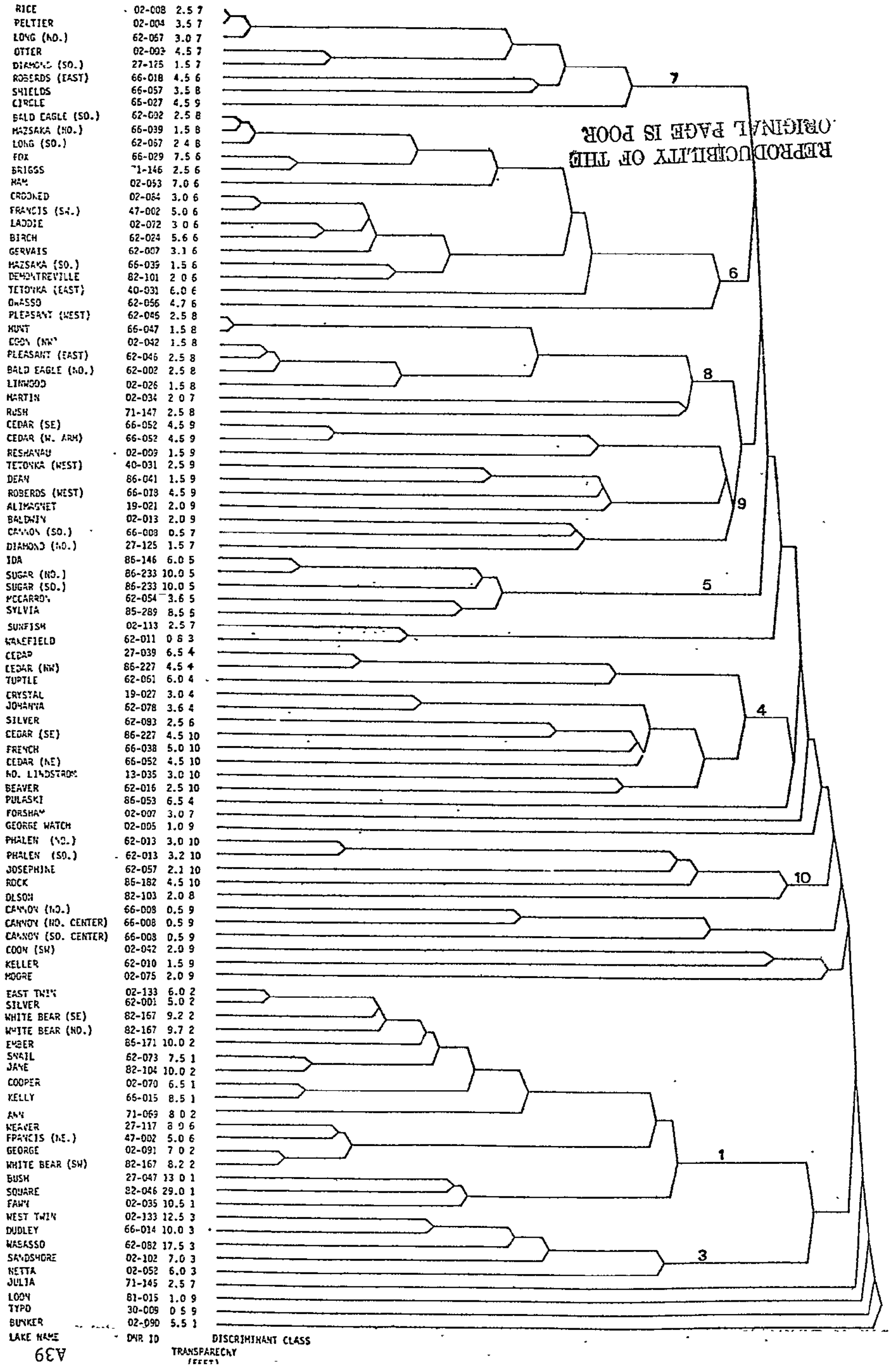

Results of the Clustering Routine

Fig. 12

TABLE 6.

DESCRIPTIVE STATISTICS FOR GROUPS IDENTIFIED THROUGH CLUSTER ANALYSIS

Class Nr.	n	IR1		IR2		Green		Red		Transparency (feet)	
		mean	s.d.	mean	s.d.	mean	s.d.	mean	s.d.	mean	s.d.
1	17	2.168	0.153	9.07	0.516	11.518	0.742	14.288	0.742	9.476	3.44
3	5	3.021	0.192	10.99	0.366	11.37	0.749	13.47	0.417	10.2	3.91
4	11	2.377	0.243	11.391	1.562	12.518	0.661	18.386	0.317	4.15	1.36
5	5	1.83	0.148	8.97	0.431	12.27	0.189	17.03	0.462	7.62	2.78
6	15	2.347	0.245	10.75	0.667	14.037	0.496	16.7	0.349	3.82	1.98
7	8	2.725	0.225	12.58	0.686	14.006	0.601	15.738	0.524	3.41	1.06
8	8	2.644	0.268	12.406	.41	15.1	0.384	16.912	0.38	2.06	0.495
9	10	3.046	0.172	13.99	.767	14.965	0.707	16.93	0.752	2.5	1.472
10	5	2.6	0.194	12.34	.345	16.94	0.698	19.63	0.74	2.96	1.01
Unclassified	15	3.82	1.748	15.94	4.384	16.473	2.702	17.597	2.084	2.02	1.826
Total	99	2.687	0.893	11.93	2.885	14.127	2.121	16.587	1.809	4.773	4.04

Description of Water Conditions

1. Clear Water.
3. Stained, algae free water, or clear, small lakes with littoral vegetation included in the sample site.
5. Clear surface water with macrophytes or algae deep in the euphotic zone.
4. Same as class 5, with more algae.
6. Light to medium algal concentrations.
7. Stained water with medium algal concentrations. Includes some shallow lakes with visible bottoms.
8. Medium algal concentrations.
9. Same as class 7, with higher algal concentrations.
10. Medium to heavy algae.

Unclassified lakes are primarily characterized by heavy to very heavy algal concentrations.

Source: calculated by author

The dissimilarities which exist between groups (in their reflectance and transparency values) again points out the problems which can be expected if regression analysis is used to predict the transparency of lakes.

Care must be taken when the classes are interpreted on the basis of the transparency readings. As mentioned above, the time of collection of the ground truth may not be temporally concordant with satellite overpass, and the individual lakes may be undergoing rapid phytoplanktonic growth. Weekly transparency readings for several lakes, e.g., Peltier (02-004), Cedar (27-039), and Tetonka (40-031) indicate that rapid growth occurred between August 1 and August 14. In addition to the temporal aspect of ground truth acquisition, and satellite overpass, there can be spatial variations in the distribution of material, especially algae, within a single lake. For most lakes with available ground information the exact location of the ground sampling point was not known. Thus any correspondence between the site sampled from the LANDSAT tapes and that monitored on the ground is coincidental. This problem then is related to basin size and complexity and is compounded by the sampling method. Because those lakes which are large or complex were expected to exhibit greater variations in algal concentrations, multiple sites were extracted from the LANDSAT tapes. When only a single transparency reading was available, and its location unknown, it was used as a guide to conditions for all sample sites on that lake, and may not be indicative of conditions for any of these sites.

Examination of the results of the cluster procedure showed that few deeply stained, clear lakes were present in the study area. The lakes which do contain appreciable amounts of stain also support algal populations (Classes 9 and 7, Table 6) and exhibit reflective characteristics similar to those of shallow lakes with muck bottoms. Scherz has also noted this problem in regard to rice lakes in Wisconsin (personal communication).

Cluster analysis appeared to yield groups and to indicate the relative differences between them rather well. The procedure has several faults however. When average linkage Euclidean distance algorithim is used to cluster the lakes (or any set of data), the location of a group is given as the mean of that group's members. The location of the entire group 'moves' as members are added. Because of this there is no assurance that, given three points such that "a" is closer to "b" than it is to "c", that "a" will become a member of the same group as "b", rather than "c" (A discussion of this problem, termed chaining and a mathematical description of cluster analysis can be found in Cooley and Lohnes (1962).). The second problem with the cluster routine is that once an observation has joined a group, it cannot be removed. No optimal clusters can be formed because of this.

A second problem with cluster analysis is that a single lake, or observation, can be but slightly closer to one group than another. It can join only one of these (i.e., the closer of the two). Knowledge that a lake is similar to more than a single class may be as important as the class to which it is most similar. A classification scheme for lakes should reflect the continuous nature of lake and water conditions. While this continuum can be inferred from the results of the cluster algorithim, discriminant analysis accomplishes this explicitly.

A third problem stems from the use of equally weighted variables, such as the standardized reflectance values used here, to cluster the lakes. A single LANDSAT band may be relatively more important than the other bands for the differentiation of two types of water conditions. The similarity coefficient does not indicate the contributions of the individual bands to the total distance between observations. The reflective characteristics of Groups 4 and 5 (Table 6) are similar to the clear water group on the IR1 and IR2 bands and similar to lakes containing medium to heavy algae (Groups 6 and 10) on the visible bands. Lakes of Groups 4 and 5 have relatively high transparencies, but were clustered together with the groups of poorer quality. It is not necessary that cluster analysis yeild coherent groups, although it appears that in this analysis it has.

Discriminant Analysis

Discriminant analysis, like cluster analysis, classifies, or groups, lakes on the basis of their reflective characteristics. Unlike clustering, it cannot identify the inherent grouping tendencies that exist for a set of data, so the groups, or classes, between which discrimination is desired must be prespecified. In this, the use of discriminant analysis for estimating water conditions is similar to the use of regression analysis, for the liklihood of correct classification is determined by the correct specification of a sample of lakes into classes.

Discrimination between prespecified groups is based on linear combinations of the reflectance values. These combinations, or linear discriminant functions, are independent of each other (orthogonal) and maximize the difference between the groups. These functions are expressed as

$$D_i = d_{i1}X_1 + d_{i2}X_2 + d_{i3}X_3 + d_{i4}X_4 + a$$

where D_i is the score on discriminant function I, the d's are weighting coefficients, a is a constant, and the X's are the values of the discriminating variables used in the analysis (Nie, et al., 1970, p. 435). The maximum number of discriminant functions which can be derived is either one less than the number of groups specified, or equal to the number of discriminating variables. Using LANDSAT reflectance bands as discriminating variables limits the number of functions to four. The number of groups which can be discriminated between is in this case limited by the number of functions which can be derived. The maximum number of groups is 2^p, where p is the number of discriminating variables. Thus using LANDSAT data, with four spectral bands, a maximum of 16 groups can be used with four functions, 8 groups with three functions, and 4 groups with two functions.

While a full mathematical description of the derivation of the functions is beyond the scope of this paper, it should be mentioned that the solution required solving the eigenvector problem $WA = \lambda Ba$, and that the discriminant functions can be interpreted in the same manner as principle components (For a mathematical description, see either King, 1969, or Cooley and Lohnes, 1971).

Identification and Specification of Original Group Membership

Discriminant analysis classifies lakes by comparing their scores on the discriminant functions to those of the prespecified groups. The analysis assumes that any given lake is a member of one of the prespecified groups, that is, that all lakes are from the same population. The resulting classification is only as good as the specification of the members of the original groups. The results of the cluster analysis, ground truth and subjective estimation of the condition of selected lakes in the study area were used to specify the original groups. The greatest weight was placed on the results of the cluster procedure, as this showed the range and inherent grouping tendencies of the reflectance data.

Ideally the ground truth information should be given the greatest emphasis. Without doing so, it can be argued, the methodology is circular. Because the lakes group or cluster according to their reflective characteristics, they can be further classified according to those characteristics. The model is calibrated according to the hypothesis that there is a good correspondence between reflectance and water conditions, rather than showing that such correspondence exists by calibrating the model with ground collected information. Such argumentation is correct. However, adequate ground truth coincidental with the date of LANDSAT data acquisition does not exist for the entire range of lakes within the study area. Second, the work of Scherz and his associates in the field and the laboratory has shown excellent correspondence with the LANDSAT data. Finally, the results of the classification can be evaluated independently of the satellite data by studying the lakes. If the classification appears good, the hypothesis is confirmed, at least pragmatically.

From the results of the cluster analysis and examination of the residual signals of the lakes of known transparency, ten types of water conditions representative of those in the entire study area were identified. The use of residual signal analysis, in addition to the cluster results, insured that the specified groups were spectrally uniform. While the ground truth information was used as a guide in groups specification, it does not provide information on the depth, bottom conditions and concentrations of stain present in lakes adequate for complete group identification.

The range of water conditions of the lakes of known transparency fall dominantly along an algal continuum. Few lakes show satellite signals characteristic of clear lakes with high concentrations of stain, but a large number show reflectance curves which indicate the presence of stain or bottom effects in addition to algae. Ignoring those lakes where the depth is less than the transparency, the lakes of the area can be classified according to their combination of stain and algae (Fig. 13). Because the effect of muck (i.e., dark colored bottom sediments) bottoms on light of the visible bands (Green and Red) is similar to the effects of stain on those same bands, the vertical axis actually represents both stain and an inverse measure of lake depth. Both bottom effects and stain may be present in the same lake.

Thirty-seven lakes were used to statistically describe these ten classes. The discriminant functions derived to differentiate between the training lakes were then used to classify the remainder of the lakes for which transparency readings were available. This included the ninety-nine observations clustered, plus five observations for Lake Minnetonka (27-133) which were not included in the cluster analysis. The classes are those nine identified from the clustering routine, with the clear water class (Class 1) subdivided into a very clear

Fig. 13. Trophic State Relationships Between Classes

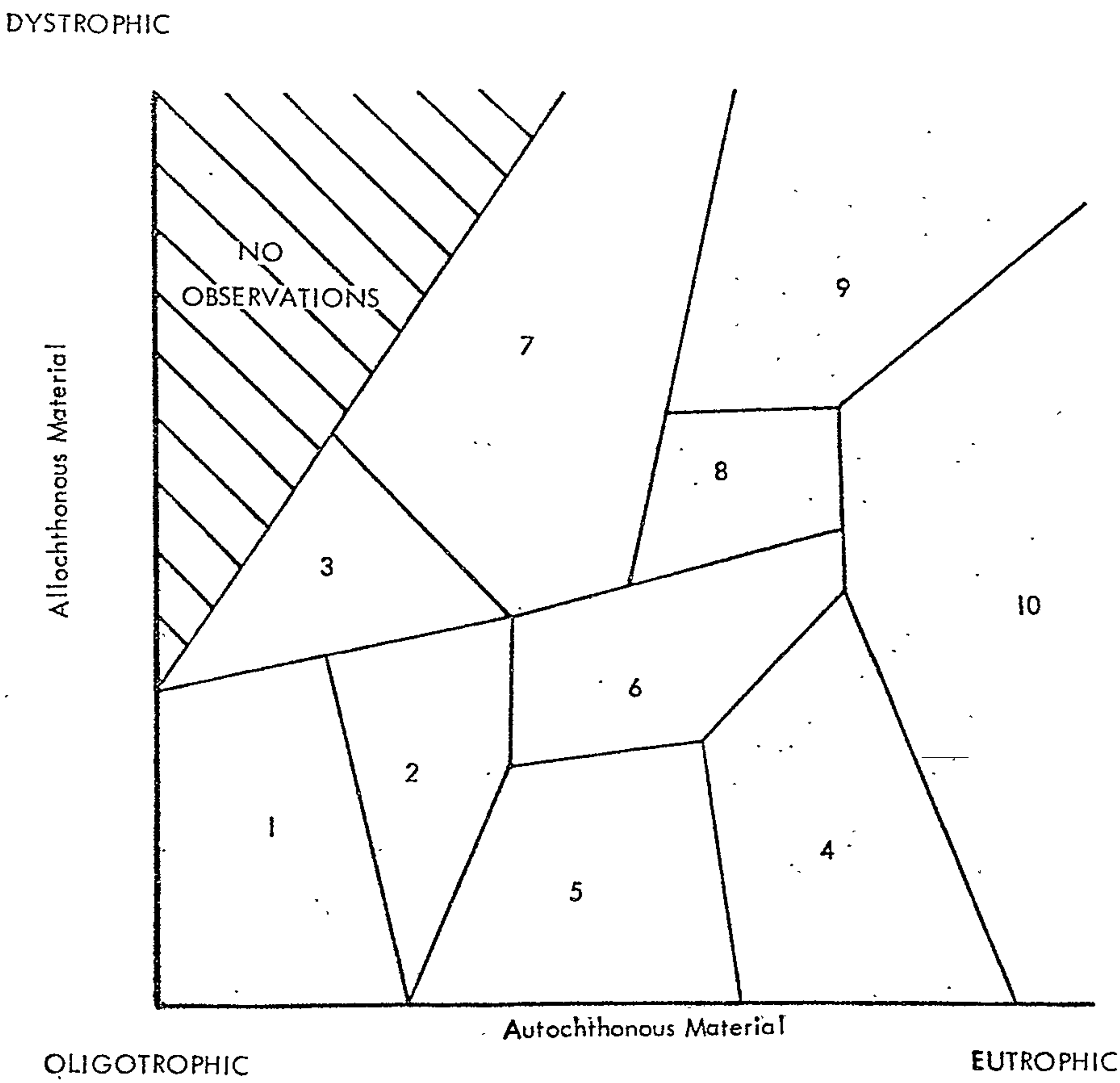

The vertical and horizontal axes can also be interpreted as corresponding to increasing reflectance on the IRI and visible bands, respectively.

(Class 1) and clear (Class 2) classes. Class descriptions and the classification results are found in Fig. 16 and the listing in Appendix I.

A comparison of the discriminant classification and the results of the clustering procedure can be found in the dendrogram (Fig. 12), which includes the class number from both techniques. The inadequacy of the ground truth information precludes a more detailed comparison of the two techniques, but because of the problems which can occur when using the clustering method, the result of the discriminant analysis should be the more reliable of the two.

Two types of errors exist in the classification based on the discriminant analysis, those which are a result of the sampling method and those due to the classification procedure. While both types of error may be present in some cases, they can be described as if they are mutually exclusive.

The lakes were classified on the basis on the mean reflectance values of a twenty pixel site. If this sample site is not representative of the lake, it will be misclassified. Spatial variations in depth, algal concentrations, submergent and emergent macrophytes and composition of bottom sediments are common in lakes, and will be present in the LANDSAT data. The variations in the reflectance values for individual lakes were, therefore, examined prior to the sample site selection. This procedure, admittedly subjective, was intended to minimize misclassification errors. Multiple samples were extracted for lakes which showed considerable variations, or when a basin was large or of complex shape. In small lakes, sampling error can also result because the sample size can be large for the size of the lake, thus including shallow water pixels in an otherwise clear water lake. Inclusion of several non-representative pixels alters the mean reflectance values, especially on the IR1 band. Several small, very transparent lakes were misclassified because of this type of error. Wabasso (62-082), for example, had a transparency of 17.5 feet, but was classified with stained and shallow lakes containing algae, with transparency of 3 to 5 feet.

There are two types of errors which can result from the classification procedure. First, the original groups can be specified incorrectly, and the subsequent classification will be biased. Second, the correspondence between the reflectance of lakes of unknown conditions and the specified groups will not be good for every unknown lake, but these lakes will be classified. Specification error is a greater problem than the second type, which is expected when attempting to create discrete classes from observations of a continuous nature. In either case an error will mean that the group description is not appropriate for an individual lake.

Specification error results from including lakes in the training groups which contain combinations of materials which alter the reflectance values subtly from those of the material(s) expected or desired. The existence or extent of this type of error is impossible to evaluate because of the lack of ground information.

There are three ways in which a lake of unknown conditions can differ from the description of its assigned class: 1) an individual lake's reflectance values can fall within the decision space between two or more groups; 2) an individual lake's reflectance values can fall outside of the decision space of all groups; and 3) different combinations of materials can yield similar reflectance values. Each of these classification problems yields an inaccurate description of the lake; but the first and second types effectively define new classes which indicate the continuous nature of both the reflectance data and the water conditions found in lakes. These can be identified from the statistics which accompany the classification results in Appendix I. The third type is true error and is impossible to identify from the statistics. These problems are not mutually exclusive. The interpretation of the statistics is an additional guide to the classification results. The best device for examining the conditions of an individual lake is residual signal analysis.

Because the combinations and concentrations of materials in lakes are found in continuous, rather than discrete, quantities, the reflectance values of some lakes will be similar to more than one of the specified classes. The statistics associated with the classifying functions indicate this by identifying both the most similar class and the likelihood of membership in a second class. Twenty-two of the sites classified have a probability greater than 10% of multiple group membership (Table 7). Twelve of these have a probability greater than 30% (Table 8). Individual lakes which fall between two groups usually have water conditions similar to each of the two. The extent of these combinations of conditions can be found by examining pairs of cross-over classes. The major transition zones occur between classes 1 and 2, and 6 and 8. These two boundaries account for about 57% of the total number of cases which have greater than a 30% probability of multiple group membership. The water conditions of each of the classes can be expected to grade into the one other, and the statistics identify these intergrades.

Lakes characterized by extreme types of water conditions (e.g., very heavy algae or weeds) will fall outside of the decision space of all the specified groups. Errors of this type can be identified by examining the distance which separates the observation from the centroid of the nearest group (D^2 in Appendix I) and the probability that a number of that group would be found in that distance (P(X/G) in Appendix I). Most lakes which are dissimilar to the specified groups have been classified as containing heavy algae in stained water (Class 9). Generally, these lakes are hypereutrophic, and are themselves a new, distinct group.

Errors resulting from an individual lake falling between or outside of the decision space of the specified groups cannot be avoided. Although new groups could be specified, the effect would be a lowering of the distance necessary for a lake to become a marginal member of one or more of those specified. Specification of a large number of groups

TABLE 7

Number of Cases with Probability Greater than 10%
of Multiple Group Membership, by Class

Likelihood of 2nd Class membership greater than 10%	Most Likely Class 1	2	3	4	5	6	7	8	9	10	Total
1	(1)	3	0	0	0	0	0	0	0	0	3
2	4	–	0	0	0	1	0	0	0	0	5
3	0	0	–	0	0	0	2	0	0	0	2
4	0	0	0	(1)	0	0	0	0	0	0	0
5	0	0	0	0	–	1	0	0	0	0	1
6	0	0	0	0	0	–	0	1	0	0	1
7	0	0	1	0	0	0	(2)	1	0	0	2
8	0	0	0	0	0	3	2	–	1	0	6
9	0	0	0	0	0	0	0	0	(9)	0	0
10	0	0	0	1	0	1	0	0	0	(1)	2
Total	4	3	1	1	0	6	4	2	1	0	22
Proportion of cases with greater than 10% probability of multiple group membership	57%	33%	17%	10%	0%	38%	36%	17%	6%	0%	21%
Class n	7	9	6	10	5	16	11	12	18	10	104

(Numbers on the diagonal indicate the number of cases which fall outside of the decision space for the class indicated.)

Source: Calculated by author

ORIGINAL PAGE IS
OF POOR QUALITY

TABLE 8

Number of Cases With Probability Greater Than 30% of Multiple Group Membership, by Class

Most Likely Class

Likelihood of 2nd Class Membership greater than 30%	1	2	3	4	5	6	7	8	9	10	Total
1	–	1	0	0	0	0	0	0	0	0	1
2	2	–	0	0	0	1	0	0	0	0	3
3	0	0	–	0	0	0	0	0	0	0	0
4	0	0	0	–	0	0	0	0	0	0	0
5	0	0	0	0	–	1	0	0	0	0	1
6	0	0	0	0	0	–	0	1	0	0	1
7	0	0	1	0	0	0	–	0	0	0	1
8	0	0	0	0	0	3	1	–	0	0	4
9	0	0	0	0	0	0	0	0	–	0	0
10	0	0	0	0	0	1	0	0	0	–	1
Total	2	1	1	0	0	6	1	1	0	0	12
Proportion of cases with greater than 30% probability of multiple group membership	29%	11%	17%	0%	0%	38%	9%	8%	0%	0%	12%
Class n	7	9	6	10	5	16	11	12	18	10	104

Source: Calculated by author

would significantly lower the number of marginal members of the groups. However the number of groups is limited by the number of input variables, and there are only sixteen groups possible using LANDSAT data. These two types of errors will exist for most any classification of observations of a continuous nature.

The third type of error in the classification occurs as a result of different combinations of materials reflecting light similarly. The reflectance signal of stained water is similar to that of shallow water with a dark bottom and macrophytes. Red clay can be confused with a combination of stain and algae. Scherz has suggested using late May and late August images together in order to identify stained and shallow lakes (personal communication). Aquatic macrophytes and algal concentrations are usually very low in late May and peak in late August. The transparency of an individual lake will be at maximum in late May, and the reflectance signal monitored by LANDSAT will indicate the presence of stain, silt or bottom in the euphotic zone. Because these materials can then be assumed present in late August, special classes can be identified, minimizing classification error.

Another method of decreasing this type error would be to include ground collected information on basin shape, depth and the presence and concentration of stain in lakes being examined in addition to the analysis of LANDSAT data. It would not be necessary to monitor these parameters annually as they change little over periods of years. Either ordinal or interval level measurement of these variables would identify errors in the classification of lakes based on the reflectance of light.

WIND EFFECTS

On August 7, 1975 an 18 mph wind from the south-south-east was measured at the Minneapolis-Saint Paul International Airport. The effect of this relatively strong wind on the reflection of light from lakes was examined for several lakes in Anoka, Ramsey, Hennepin and Washington Counties. Because wave formation is a function of wind speed and fetch, its effects cannot be constant across the scene for lakes of different sizes and orientations to the wind. The examination of a large clear lake should show the extent of increased reflection caused by surface foam and near surface air bubbles. The raw LANDSAT data for White Bear Lake (82-167) were visually studied, and also analyzed statistically. Statistical analysis was done with the Bendix Multispectral Data Analysis System (M-DAS), which classifies LANDSAT data in a pixel by pixel fashion. The variations within a single lake can be visually examined. No increase in the reflection was found within the open water zone of the lake (Fig. 14). On the north-northwest shore area, however, a considerable increase was noted. It seems reasonable to assume that this shore area was washed by high waves, and that debris from the land-water boundary was suspended in the water. The increase in reflection then indicates these more turbid conditions. A similar examination and analysis of Lake Minnetonka (27-144), which has higher algal concentrations than White Bear, showed a pattern of increasing reflection downwind (Fig. 15). This was interpreted as an indication of increased concentrations of algae. While a more rigorous examination of the effects of wind is necessary prior to making definite assertions on wind effects, from this analysis it appears that wind and waves add little noise to the LANDSAT data, and that down wind increases in reflectance are due to increased turbidity.

SUMMARY

The purpose of this research was to show the usefulness of LANDSAT data to surveys of the water conditions of Minnesota lakes. The use of both LANDSAT imagery and digital data were investigated. Initial consideration was given to analysis of LANDSAT image densities because of the low technologic and cost requirements. The techniques employed, however, yielded inconsistent and unreplicable results and further research halted.

Fig. 14
White Bear Lake
82-167

Fig. 15
Lake Minnetonka
27-133

Legend for Figs. 14 and 15

Dark blue	Very clear water
Blue	Clear water
Light blue	Light algal concentrations
Light green	Light to medium algal concentrations
Ocher	Medium to heavy algal concentrations
Dark green	Heavy algal concentrations
Black	Unclassified (i.e., non-water pixels)

LANDSAT digital data for a sample of 81 lakes in East Central Minnesota were used to develop techniques for the classification of lakes. Regression analysis could not be used effectively because the ground truth data available were not necessarily syncronous with LANDSAT data acquisition and stain is present in some of the sample lakes.

Cluster analysis and discriminant analysis were both used to group the sample lakes. The ground truth requirements for these techniques are not as stringent as those for regression analysis. An average linkage algorithim was used to cluster the mean reflectance values of a 20 pixel sample from each of the lakes. The results provided useful groupings and pointed out the clustering tendencies inherent in the reflectance data.

While the clustering technique was a useful exploratory method, discriminant analysis allowed the reflectance data to be better represented by indicating the probability of group membership. Using discriminant analysis a ten group classification scheme of lake types was developed, and 104 observations on 81 lakes were classified.

An evaluation of the classification results should be included here, but because of the lack of uniform ground collected information, a rigorous evaluation is not possible. However several suggestions for future investigations can be made.

In order that classification of lake conditions be fully evaluated, ground collected information must be available for a large number of lakes. Lakes of known qualities were used to specify the original groups and cannot provide an independent assessment of the results. There is also a problem with the synchronity and uniformity of the data. Evaluation and specification require that the ground information be collected near the time of image acquisition, and this is not the case for a majority of the available data.

Variations in the data for individual lakes from different sources are also evident. The transparency of Wabasso (62-882) in early July, 1975, for example, was reported as 15.5' by a participant in the LRC transparency study, 8' by a consulting firm (Hickok, 1975, p. 78), and 10' by the DNR (unpublished data). The Secchi transparency measure is perhaps the simplest procedure required by any quality parameter.

Another method of evaluation would be a comparison of the results with a previous investigation based on different data. No other studies of this type have been done for the study area.

Future investigations of water conditions using LANDSAT data can increase the accuracy of classification by integrating analysis with a program of ground surveys. Lakes in the study area should be stratified according to depth and, if possible, concentration of stain. Ground surveys of lakes representative of the various combinations of depth, and stain should be accomplished synchronously with LANDSAT overpass. Finally the method of sampling should reflect the intended use of the resulting classification. A pixel by pixel classification of lakes shows variations in algal concentrations and would be useful for location sources of nutrient inputs (Scherz, 1977). The type of sampling method used for this study is useful in studies concerned with the dominant conditions in the open water zone.

ORIGINAL PAGE IS
OF POOR QUALITY

Acknowledgements

I would like to express my appreciation to Dr. Richard H. Skaggs and Dr. Dwight A. Brown for providing the opportunity and encouragement which permitted the pursuit of this topic. Les Maki of the Minnesota State Planning Agency and personnel of the Minnesota Land Management Information System developed computer programs for extraction of the LANDSAT digital data. Jim Kenna, Martin Roller, Letitia Cavalier and Dwight Wilcox aided in data extraction and preparation. Dr. Eric Sheppard and Dr. Tony Lea provided statistical first aid.

The Space Science Center and Mr. Roland Mohr are acknowledged for permitting the use of a microdensitometer.

Dr. James Scherz, University of Wisconsin, provided much assistence, both through critical comments and his written work. Dr. Robert H. Rogers, Aerospace division of the Bendix Corporation, contributed time and effort in order that I might better understand techniques of digital image processing.

I profited greatly from conversations concerning lakes with Dr. Robert Megard and Dr. Joseph Shapiro of the University of Minnesota.

This research was supported under National Aeronautics and Space Administration (NASA) Contract Number NGL 24-005-263. Computer time was provided by the University of Minnesota Computer Center (UCC).

I greatly appreciate the efforts of Jean Hamann and Dawn Drilling in the preparation of this manuscript.

Literature Cited

Ashley, M.D., and J. Rea. 1975. Seasonal Vegetation Differences from ERTS Imagery. Photogrammetric Engineering and Remote Sensing. 41:713-719.

Barr Engineering. 1976. 1975 Water Quality Inventory Riley - Purgatory Creek Watershed District. (mimeo) Minneapolis, Minnesota.

Birge, A.E., and C. Juday. 1929. Transmission of Solar Radiation by the Waters of Inland Lakes. Transactions of the Wisconsin Academy of Sciences, Arts, and Letters. 24:504-580.

------ 1932. Solar Radiation and Inland Lakes. Fourth Report. Observations of 1931. Transactions of the Wisconsin Academy of Sciences, Arts, and Letters. 27:523-562.

Boland, D.H.P. 1974. An Evaluation of the Earth Resources Technology Satellite (ERTS-1) Multispectral Scanner as a Tool for the Determination of Lacustrine Trophic State. Ph.D. Thesis. Oregon State University: Corvallis.

Brown, D., R. Skaggs, J. Smiley, and E. Stern. 1975. Monitoring Surface Water Dynamics in Minnesota. Minnesota Land Management Information System Report Nr. 5014. Center for Urban and Regional Affairs, University of Minnesota: Minneapolis.

Brown, D., R. Warwick, L. Cavalier, and M. Roller. 1977. The Persistence and Condition of Douglas County, Minnesota Lakes. Minnesota Land Management Information System Report Nr. 5021. Center for Urban and Regional Affairs, University of Minnesota: Minneapolis.

Brown, D., R. Warwick, and R. Skaggs. 1977. Reconnaissance Analysis of Lake Conditions in East Central Minnesota. Minnesota Land Management Information System Report Nr. 5022. Center for Urban and Regional Affairs, University of Minnesota: Minneapolis.

Cooley, W.W., and P.R. Lohnes. 1962. Multivariate Procedures for the Behavioral Sciences. New York: John Wiley and Sons, Inc.

------. 1971. Multivariate Data Analysis. New York: John Wiley and Sons, Inc.

Deutsch, M., and F.H. Ruggles, 1974. Optical Data Processing and Projected Applications of the ERTS-1 Imagery Covering the 1973 Mississippi River Valley Floods. Proceedings, Third Earth Resources Technology Satellite-1 Symposium. Vol. 1 (Section B) NASA (Goodard Space Flight Center): Greenbelt, Maryland. 1167-1188.

Edmondson, W.T. 1969. Eutrophication in North America. In Eutrophication: Causes, Consequences, Correctives, Proceedings of a Symposium. National Academy of Sciences: Washington, D.C. 124-149.

Ghassemi, M., and R.F. Christman. 1969. Properties of the Yellow Organic Acids of Natural Waters. Limnology and Oceanography. 13: 583-597.

Hickok, E.A., and Associates. 1975. An Investigation of Selected Lakes, Ramsey County, 1975. (mimeo) Wayzata, Minnesota.

Hutchinson, G.E. 1957. A Treatise on Limnology. Volume I. Geography, Physics, and Chemistry. New York: John Wiley and Sons, Inc.

Juday, C., and E.A. Birge. 1933. The Transparency, the Color and the Specific Conductance of the Lake Waters of Northwestern Wisconsin. Transactions of the Wisconsin Academy of Sciences, Arts, and Letters. 28: 205-259.

King, L.J. 1969. Statistical Analysis in Geography. Englewood Cliffs, New Jersey: Prentice-Hall, Inc.

Klemas, V. 1973. Applicability of ERTS-1 Imagery to the Study of Suspended Sediment and Aquatic Fronts. Symposium on Significant Results Obtained from Earth Resources Technology Satellite - 1. Vol. 1 (Section B). NASA (Goodard Space Flight Center): Greenbelt, Maryland. 1275-1290.

Kritikos, H., L. Yorinks, and H. Smith. 1974. Suspended Solids Analyses using ERTS-1 data. Remote Sensing of the Environment. 3: 69-78.

Lundquist, H.B. 1975. A Primer on Limnology: Public Report Series, No. 1. Water Resources Research Center, University of Minnesota: Minneapolis.

Minnesota Department of Conservation. 1968. An Inventory of Minnesota Lakes. Bulletin Number 25. Division of Waters, Soils, and Minerals: St. Paul.

National Aeronautics and Space Administration. 1971. ERTS Data Users Handbook. Goodard Space Flight Center: Greenbelt, Maryland.

------. 1973. Development of a Computer Aided Procedure for the National Program of Inspection of Dams. Science and Application Directorate (Lyndon B. Johnson Space Center): Houston, Texas.

Nie, N.H., C.H. Hull, J.G. Jenkins, K. Steinbrenner, and D.H. Bent. 1975. SPSS: Statistical Package for the Social Sciences. (Second Ed.) New York: McGraw-Hill, Inc.

Odum, E.P. 1971. Fundamentals of Ecology. (Third Ed.) Philadelphia: W.B. Saunders Company.

Piech, K.R., and J.E. Walker. 1972. Thematic Mapping of Flooded Acreage. Photogrammetric Engineering. 38:1081-1090.

Rango, A., and A.T. Anderson. 1974. ERTS-1 Flood Hazard Studies in the Mississippi River Basin. Proceedings, Third ERTS-1 Symposium. Vol. 1 (Section B). NASA (Goodard Space Flgiht Center): Greenbelt, Maryland. 1127-1166.

Rogers, R.H., N.J. Shah, J.B. McKeon, C. Wilson, and L. Reed. 1975. Application of LANDSAT to the Surveillance and Control of Eutrophication in Saginaw Bay. Presented at the Tenth International Symposium on Remote Sensing of Environment. October 6-10, 1975. Ann Arbor, Michigan.

Scherz, J.P. 1977. Lake Water Quality Mapping from LANDSAT. Presented at the Eleventh International Symposium on Remote Sensing of Environment. April 25-29, 1977. Ann Arbor, Michigan.

Scherz, J.P., D.R. Crane, and R. Rogers. 1975. Classifying and Monitoring Water Quality by Use of Satellite Imagery. Proceedings, American Society of Photogrammetry--American Congress of Surveying and Mapping. Fall Convention. Phoenix, Arixona. 320-343.

Scherz, J.P., and J.F. Van Domelen. 1975. Water Quality Indication Obtainable from Aircraft and LANDSAT Images and Their Use in Classifying Lakes. Proceedings, Tenth International Symposium on Remote Sensing of Environment. Ann Arbor, Michigan. 447-460.

Strumpf, H.G., and A.E. Strong. 1974. ERTS-1 Views an Oil Slick? Remote Sensing of the Environment. 3: 87-90.

Vincent, R.K. 1972. An ERTS Multispectral Scanner Experiment for Mapping Iron Compounds. Proceedings, Eighth International Symposium on Remote Sensing of Environment. Ann Arbor, Michigan. 1239-1243.

Wetzel, R.G. 1975. Limnology. Philadelphia: W.B. Saunders Company.

Work, E.A., and D.S. Gilmer. 1976. Utilization of Satellite Data for Inventorying Prairie Ponds and Lakes. Photogrammetric Engineering and Remote Sensing. 42: 685-694.

Yarger, H.L., and J.R. McCauley. 1975. Quantitative Water Quality with LANDSAT and SKYLAB. Proceedings, NASA Earth Resources Survey Symposium. NASA (Goodard Space Flight Center): Greenbelt, Maryland. 347-370.

Appendix I

Classification of lakes

The 104 observations were classified according to their statistical similarity to ten specified groups. The resulting classification follows the residual signals of these groups (Fig. 16), where

D^2 is the distance between the observation and the most probable group's centroid,

(P(X/G)) is the probability that the observation would be located at distance D^2 from that group's centroid, and

(P(G/X)) is the probability that the observation is a member of that group.

Notice that Bunker Lake (02-090) is unclassified, with a probability of zero for group membership. Pixels which included heavy emergent vegetation were included in the sample and the reflectance on the infrared bands is very high.

Fig. 16

Satellite Residual Signals for Training Groups

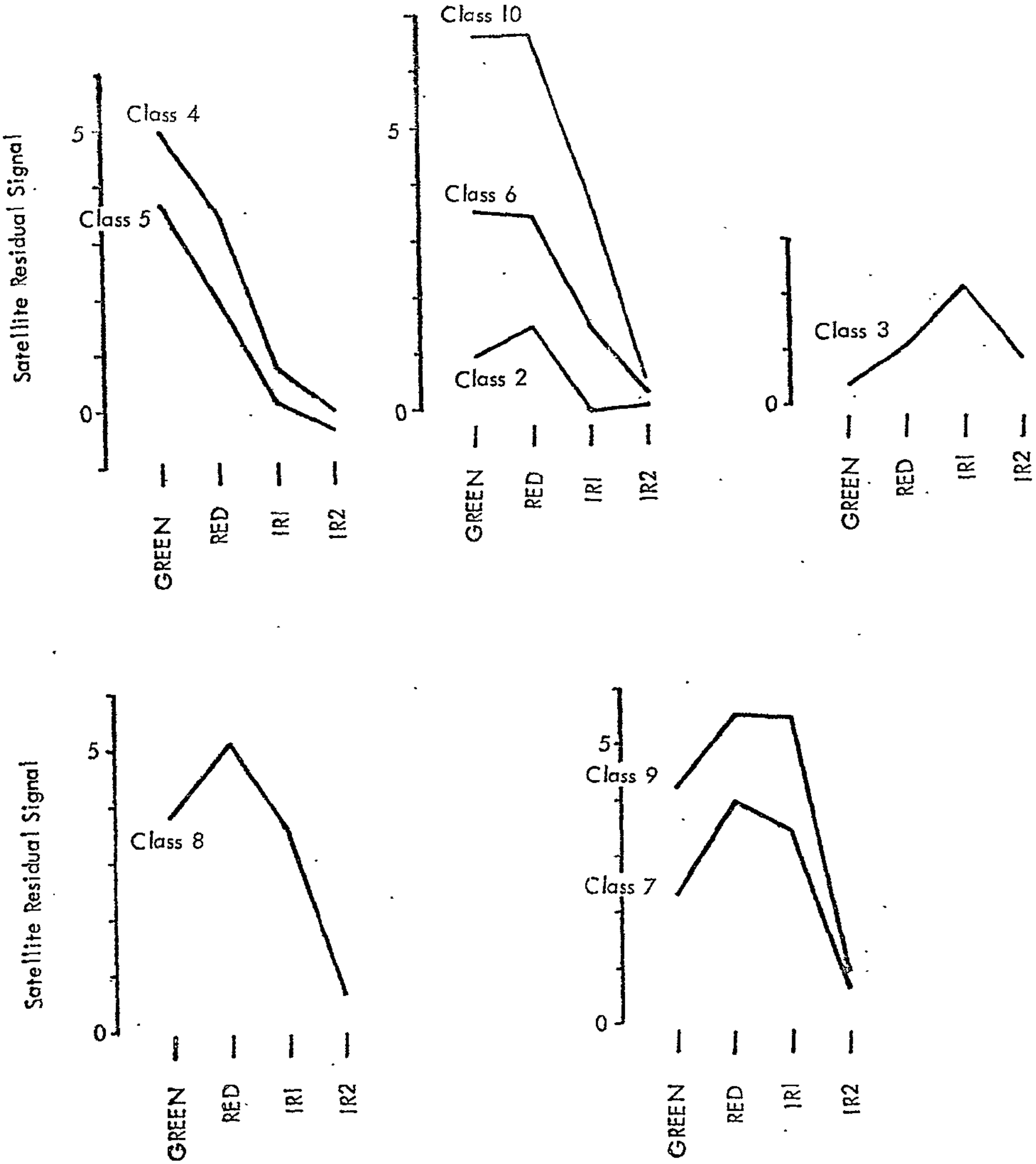

Source: Calculated by author.

LAKE NAME	DNR ID	TRANSPARENCY	MOST PROBABLE GROUP	D^2	(P(X/G))	(P(G/X))	SECOND GROUP	(P(G/X))
OTTER	02-003	4.5	7	2.601	.627	.754	8	.246
PELTIER	02-004	3.5	7	.993	.911	1.000		
GEORGE WATCH	02-005	1.0	9	62.245	.000	1.000		
FORSHAM	02-007	3.0	7	87.236	.000	.871	3	.126
RICE	02-008	2.5	7	.705	.951	1.000		
RESHANAU	02-009	1.5	9	14.065	.007	.909	7	.090
BALDWIN	02-013	2.0	9	2.677	.613	1.000		
LINWOOD	02-026	1.5	8	2.596	.627	.967	7	.033
MARTIN	02-034	2.0	7	12.673	.013	.608	8	.378
FAWN	02-035	10.5	1	2.665	.615	.978	2	.022
COON (NW)	02-042	1.5	8	.261	.992	.996	9	.003
COON (SW)	02-042	2.0	9	39.547	.000	1.000		
NETTA	02-052	6.0	3	4.668	.323	.999	7	.001
HAM	02-053	7.0	6	14.235	.007	.603	8	.379
COOPER	02-070	6.5	1	4.394	.355	.778	2	.214
LADDIE	02-072	3.0	6	4.470	.346	.996	8	.004
MOORE	02-075	2.0	9	130.355	0	1.000		
CROOKED	02-084	3.0	6	.682	.953	1.000		
BUNKER	02-090	5.5	1	*	0	0		
GEORGE	02-091	7.0	2	5.330	.255	.927	6	.071
SANDSHORE	02-102	7.0	3	3.284	.511	.999		
SUNFISH	02-113	2.5	7	36.644	.000	.730	3	.269
WEST TWIN	02-133	12.5	3	3.029	.553	1.000		
EAST TWIN	02-133	6.0	2	1.780	.776	.965	1	.035
NO. LINDSTROM	13-035	3.0	10	10.178	.038	1.000		
ALIMAGNET	19-021	2.0	9	16.094	.003	.988	8	.010
CRYSTAL	19-027	3.0	4	11.681	.020	.874	10	.125
CEDAR	27-039	6.5	4	2.442	.655	.998	5	.002
BUSH	27-047	13.0	1	1.330	.856	.805	2	.195
WEAVER	27-117	8.0	6	9.117	.058	.673	2	.324
DIAMOND (NO.)	27-125	1.5	7	.529	.971	.999	8	.001
DIAMOND (SO.)	27-125	1.5	7	14.918	.005	1.000		
MINNETONKA:	27-133							
LOWER LAKE		4.0	4	6.754	.149	.999	5	.001
WAYZATA BAY		4.3	4	7.242	.124	.999	10	.001
ECHO BAY		3.7	4	6.007	.199	.909	5	.091
WEST ARM		2.1	10	20.274	.000	1.000		
CRANE ISLAND		2.9	4	16.535	.002	.994	10	.006
TYPO	30-009	0.5	9	470.666	0	.000		
TETONKA (EAST)	40-031	6.0	6	6.421	.170	.999		
TETONKA (WEST)	40-031	2.5	9	4.757	.313	.999	8	.001
FRANCIS (NE.)	47-002	5.0	6	8.630	.071	.935	2	.064
FRANCIS (SW.)	47-002	5.0	6	2.043	.728	1.000		
SILVER	62-001	5.0	2	2.722	.605	.872	1	.128
BALD EAGLE (NO.)	62-002	2.5	8	1.510	.825	.999	9	.001
BALD EAGLE (SO.)	62-002	2.5	8	5.276	.260	.952	6	.038
GERVAIS	62-007	3.1	6	3.055	.549	1.000		
KELLER	62-010	1.5	9	58.724	.000	1.000		
WAKEFIELD	62-011	0.8	3	30.876	.000	.534	7	.464
PHALEN (NO.)	62-013	3.0	10	8.280	.082	1.000		
PHALEN (SO.)	62-013	3.2	10	5.887	.208	1.000		
BEAVER	62-016	2.5	10	12.764	.012	1.000		
BIRCH	62-024	5.6	6	3.091	.543	1.000		
PLEASANT (EAST)	62-046	2.5	8	1.472	.832	.939	9	.061
PLEASANT (WEST)	62-046	2.5	8	4.349	.361	.992	7	.005
MCCARRON	62-054	3.6	5	3.149	.533	.996	4	.004
OWASSO	62-056	4.7	6	15.355	.004	.856	5	.142
JOSEPHINE	62-057	2.1	10	4.664	.321	1.000		
TURTLE	62-061	6.0	4	.893	.926	1.000		

LONG (NO.)	62-067	3.0	7	1.137	.888	1.000		
LONG (SO.)	62-067	2.4	8	6.675	.154	.504	6	.495
SNAIL	62-073	7.5	1	4.475	.346	.540	2	.460
JOHANNA	62-078	3.6	4	3.922	.417	1.000		
WABASSO	62-082	17.5	3	2.086	.720	1.000		
SILVER	62-083	2.5	6	16.567	.002	.364	10	.320
CANNON (NO.)	66-008	0.5	9	35.043	.000	1.000		
CANNON (NO. CENTER)	66-008	0.5	9	12.772	.012	1.000		
CANNON (SO. CENTER)	66-008	0.5	9	23.995	.000	.987	7	.011
CANNON (SO.)	66-008	0.5	7	13.250	.010	.994	9	.006
DUDLEY	66-014	10.0	3	1.900	.754	1.000		
KELLY	66-015	8.5	1	4.720	.317	.546	2	.453
ROBERDS (EAST)	66-018	4.5	6	16.694	.002	.588	6	.397
ROBERDS (WEST)	66-018	4.5	9	10.173	.038	1.000		
CIRCLE	66-027	4.5	9	16.490	.002	.561	8	.436
FOX	66-029	7.5	6	7.166	.127	.980	8	.020
FRENCH	66-038	5.0	10	5.959	.202	.997	8	.003
MAZSAKA (SO.)	66-039	1.5	6	4.148	.386	.999	8	.001
MAZSAKA (NO.)	66-039	1.5	8	5.591	.232	.959	6	.034
HUNT	66-047	1.5	8	2.418	.659	.994	7	.006
CEDAR (SE)	66-052	4.5	9	2.461	.652	.947	8	.053
CEDAR (W. ARM)	66-052	4.5	9	.867	.929	.990	8	.010
CEDAR (NE)	66-052	4.5	10	10.112	.039	.996	8	.004
SHIELDS	66-057	3.5	8	7.496	.112	.716	7	.282
ANN	71-069	8.0	2	10.892	.028	.752	1	.248
JULIA	71-145	2.5	7	272.817	0	.000		
BRIGGS	71-146	2.5	6	13.611	.009	.567	8	.433
RUSH	71-147	2.5	8	15.589	.004	.995	7	.005
LOON	81-015	1.0	9	178.272	0	.000		
SQUARE	82-046	29.0	1	1.338	.655	.987	2	.013
DEMONTREVILLE	82-101	2.0	6	8.193	.085	.991	8	.009
OLSON	82-103	2.0	8	16.871	.002	.999	9	.001
JANE	82-104	10.0	2	.163	.997	.971	1	.029
WHITE BEAR (NO.)	82-167	9.7	2	4.401	.354	.982	1	.018
WHITE BEAR (SE)	82-167	9.2	2	7.027	.134	.662	1	.338
WHITE BEAR (SW)	82-167	8.2	2	4.257	.372	.994	6	.006
DEAN	86-041	1.5	9	10.366	.035	.807	8	.193
PULASKI	86-053	6.5	4	25.840	.000	1.000		
IDA	86-146	6.0	5	4.261	.372	.996	6	.004
EMBER	86-171	10.0	2	6.755	.149	.942	1	.053
ROCK	86-182	4.5	10	9.390	.052	1.000		
CEDAR (SE)	86-227	4.5	10	12.202	.016	.761	8	.144
CEDAR (NW)	86-227	4.5	4	5.501	.240	.964	5	.036
SUGAR (NO.)	86-233	10.0	5	1.055	.901	.999	4	.001
SUGAR (SO.)	86-233	10.0	5	2.099	.718	.930	4	.069
SYLVIA	85-289	8.5	5	4.472	.346	.995	4	.005

Appendix A

CONDITION OF SELECTED EAST-CENTRAL MINNESOTA LAKES

Investigators: Dr. Dwight Brown
Dr. Richard Skaggs
Center for Urban and
Regional Affairs
State Planning Agency
Minneapolis, Minnesota

ABSTRACT

The condition of East Central Minnesota Lakes is examined using LANDSAT digital data on lake reflectance for August 7, 1975. Lakes are grouped into condition classes by multiple discrimanant function analysis, which groups lakes of unkown condition around lakes of known condition, according to the satellite measured reflectance. The centroids of these classes are selected to maximize differences in condition. The data extraction methods are described and the classification is discussed and presented in map form. Problems of cell size of analysis and wind effects are described along with the limitations imposed by single time period analysis.

LANDSAT measured lake reflectance seems to provide a valuable means of extending secchi disc transparency measurements, which provide the necessary basis for reconnaissance analysis of lake condition using LANDSAT data.

INTRODUCTION

This paper attemps a reconnaissance analysis of lake conditions in East Central Minnesota based on the interaction between incident light and the materials contained in lakes, which results in selective absorption, transmission, reflection, and scattering of the spectral components of incident light. The reflectance spectra resulting from incident solar energy - lake material interactions, as collected by the LANDSAT satellite, are employed to evaluate lake condition.

This report will briefly describe the basis for using reflectance of solar energy to monitor the condition of lakes, review the study area, and provide the background of LANDSAT data applications to problems of lake condition. The analytical procedures will then be outlined, the results evaluated, and finally conclusions drawn about lake conditions and the problems and prospects of performing reconnaissance analysis of Minnesota Lake conditions with LANDSAT data. The term "reconnaissance analysis" implies that the results should be a first look at lake conditions to guide detailed ground based analysis and not as the final word on condition. It is hoped that the map will give water resource planners, managers, policy formulators, and limnologists some idea about the locations and numbers of lakes in general condition classes.

BACKGROUND

The interaction of solar radiation with the water, the material it contains, and lake bottom materials are fundamental to the application of satellite collected data to a reconnaissance analysis of lake conditions (Figure 1). The LANDSAT scanner system detects the intensities of reflected green light (.5-.6 m, band 4), red light (.6-.7 m, band 5) and two spectral bands of reflected near infrared radiation (.7-.8 m,

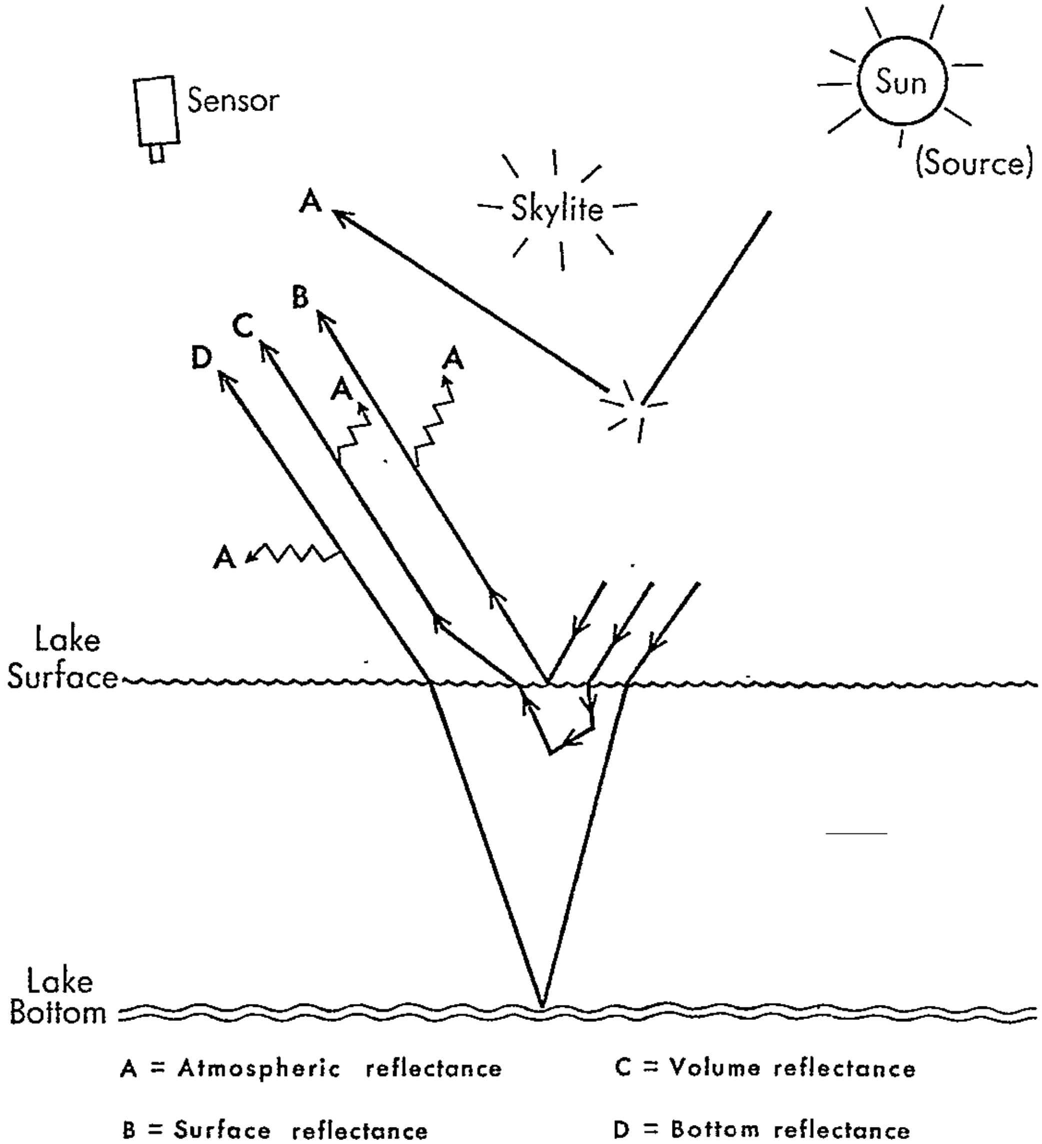

FIGURE 1. Reflected solar energy flows for a lake.

band 6; and .8-1.1 m, band 7). Unlike true or thermal infrared, bands 6 and 7 do not detect thermal differences but do respond much like the visible bands to wet, black plowed fields and to bright white snow or clouds. The important difference comes in the way the near infrared bands respond to growing plants and to water. While plants are actively photosynthesizing they reflect very high portions of the near infrared radiation. When plants die or become dormant the infrared reflectance falls off dramatically, even though they remain green. Most of the near infrared radiation is absorbed by the first meter of pure water while over 95% of green and almost 80% of the red spectral bands penetrate the top meter of water (Figure 2). The differential water transmittance of green and near infrared radiation can be used to infer that aquatic vegetation is at or near the surface if both the green and the near infrared bands show strong signals, if only the green reflectance is high, the aquatic vegetation is probably a meter or more below the surface.

Bottom conditions of shallow lakes create considerable difficulty for interpretation of lake condition. Shallow, clean lakes with muck bottoms produce a reflectance spectrum that is very similar to that for a deep, clear lake with heavily tannin stained water. Further complications arise where lake bottoms are visible only to green light. Under these conditions a 50% cover of bottom vegetation over muck would appear as a much lower reflectance than over a light colored bottom. When the lake is shallow enough for red light to be reflected from the bottom, it can show a response only to the light colored sediments, and bottom sediments can be differentiated from vegetation.

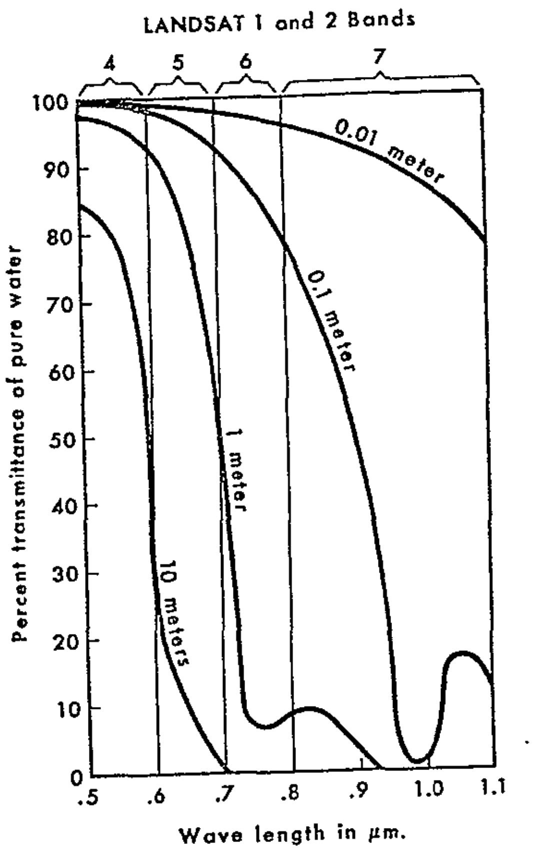

FIGURE 2. Spectral transmittance of pure water for different path lengths (Adapted from Work and Gilmer, 1976).

Where algae produced a high green reflectance the relative depths of algal concentrations may sometimes be inferred from the differences between the amount of reflection detected by band 6 and band 7. Band 7 reflectance increases with algae in the first half meter of the water column. The response to suspended mineral sediments also can be detected; but, the spectral response depends on sediment color. In some instances it may be necessary to use spatial patterns to separate the signal of suspended mineral sediments from algal concentrations.

STUDY AREA

The area included in this applications study incorporates a variety of lakes, mostly natural and of late Wisconsin glacial origin. The lakes are water filled depressions on glacial till and outwash with a few reservoirs on major streams. Three major groups of lakes lying northeast, northwest, and south-southwest of the Mississippi and Minnesota Rivers junction are included. The surrounding land cover grades from urban metropolitan, surrounding the rivers' junction, to forest, marsh, grass, and modest agricultural crops to the northeast, to agricultural crops, marsh, and some forest to the northwest. Agricultural crops dominate to the south-southwest. Over 1000 lakes larger than 20 hectares (50 acres) are included in the area that covers all or parts of 18 east central Minnesota counties.

The area was selected because it contained the highest concentration of lakes with existing current information on lake transparency and because of the recreational importance of lakes in the most populous region of the state. LANDSAT reflectance data from 81 lakes with known transparency formed the basis for classifying and describing lakes of unknown condition. From this lake inventory 421 of the larger lakes were selected for study.

METHODOLOGY

A number of studies have developed a variety of methodologies and procedures that use LANDSAT data and the solar energy flux for lakes to interpret lake conditions (Boland, 1974; Scherz, 1975; Rogers et al., 1975; and Warwick, 1977). The techniques have been further applied to specific problems or areas by Scherz (1977) and by Brown et al., (1977). Most of these researchers used LANDSAT digital tape data and differ primarily in the ways that data are extracted, size of the study unit, method of classifications, and degree of automation. Warwick (1977), who studied the use of both digital tape data and less expensive black-and-white film transparencies, found the latter produced different results on several data extraction trials with both a density slicer and a micro-densitometer. Scherz (1977) used a Bendix interactive system to classify individual ground resolution cells (pixels). Warwick also used the system in a brief experiment. Although such a system has time and certain other advantages, it was not employed in this study.

Non-automated data extraction from digital tapes was selected over the Bendix or similar interactive systems because it was considered more important to classify whole lakes or bays rather than pixels because the former are normally the management units. Additionally, variations among the LANDSAT 1 detector elements were considered to create problems; especially in band 7, where small variations created important classification changes in sample studies by Warwick (1977). Brown et al. (1977) attempted to minimize the effect of detector element differences on classification by averaging multiple pixel data for polygons including data from several detectors.

Although multiple date classification is not attempted in this classification it was used by Brown et al. (1977) and could be done, given adequate LANDSAT data, with the methods employed in this study. The cost of using multiple dates in an automated system that classifies individual pixels would multiply rapidly because of the need to preregister multiple date scenes, making data input costs climb from approximately \$200 per ground scene to about \$2000.

DATA EXTRACTION

The data for lake classification in this study were extracted from LANDSAT 1 digital tapes for August 7, 1975. The tapes were reformatted using programs developed by Minnesota Land Management Information Systems personnel. These programs produced reformatted tapes in the Environmental Planning Programming Language (EPPL4) and imposed a grid system on the reformatted tapes. Other programs were used to print the reflectance data for the area surrounding each lake or group of lakes included in the study at a 1:31,000 scale. The study was limited to major lakes, including most lakes over 40 hectares (100 acres). Some smaller lakes were included to help define the lake classes if ground based information was available.

A computer printout map was produced for the reflectance values of each of the four LANDSAT multispectral scanner (MSS) bands. The previously mentioned need to classify whole lakes or bays and the need to avoid the bias of a single detector made it desirable to extract an average response taken from several scan lines in a polygon that, if possible, avoided edge and shallow water effects. These polygons of generally 20 pixels (9 hectares or 22 acres) were identified and outlined on band 7 computer printout. The band 7 printout was then successively registered on the other three bands on a light table, the polygons outlined, and the values recorded and averaged by hand. In some larger lakes multiple samples were taken; e.g., 22 sites in Lake Minnetonka were sampled. In all a total of 619 observations for 421 lakes were classified with LANDSAT data. Ground collected data for 81 lakes were used to define and describe the classes of lake-condition.

CLASSIFICATION

The classification procedure employed multivariate discriminant analysis to assign each of the 619 observations to one of 10 classes. A discriminant function routine was selected as opposed to the cluster analysis used by Brown et al. (1977) because the large number of samples to be classified would be much more costly with cluster routines and would necessitate modifying available programs. The ground data for 81 lakes was used to identify the classes necessary for discriminant analysis, which groups the lakes of unknown condition according to their reflective similarities to the pre-defined groups. Forty-four lakes with ground data were used to specify 10 groups, and the remainder of the lakes with ground data were grouped in the same manner as those with no ground data. These lakes of known condition were used in developing class desriptions. Use of cluster analysis would not identify the probability that a lake is similar to more than a single class of water condition, which is useful information because of the intergrades that exist between the artificially discrete classes.

Table 1 shows the number of observations which were statistically similar to more than one class, with .30 - .49 and .10 - .49 probabilities of being members of a second class. Six classes were aggregated from the original ten classes to simplify the map. Table 1 illustrates the near border relationships between the water condition of a number of observations in each class. The percentage of observations in each class with a less than .10 and less than .30 probability of being in a second class gives an idea about the clustering of observations around the class cores. It also provides insight into the degree of confusion among the classes.

The lakes were mapped according to the dominant class identified from the discriminant analysis (Map inside back cover). Most lakes have been classified as a unit although multiple observations from some of the larger lakes were treated independently in the discriminant analysis. Where the classification of the multiple observations differed

TABLE 1. — NUMBER OF OBSERVATIONS WITH MODERATE OR HIGH PROBABILITY OF A SECOND CLASS MEMBERSHIP BY FIRST AND SECOND MOST PROBABLE CLASS OF MEMBERSHIP

Class Assignment	Second Most Probable Class														% with Probability of Second Class Assignment of:		Total in Class
	.30-.49 Probability of Second Class Assignment							.10-.49 Probability of Second Class Assignment									
	1	2	3	4	5	6	Sub-Total	1	2	3	4	5	6	Sub-Total	.10	.30	
1	-	0	2	3	0	0	5	-	1	8	6	0	0	15	83	94	88
2	0	-	3	0	1	0	4	0	-	12	0	2	0	14	75	93	55
3	1	1	-	3	0	0	5	5	5	-	10	9	0	29	68	94	90
4	8	0	6	-	3	1	18	12	0	15	-	13	4	44	78	91	204
5	0	1	3	1	-	0	5	0	2	6	8	-	0	16	79	93	76
6	0	0	0	3	0	-	3	0	0	0	7	0	-	7	93	97	106

within a lake, possible bottom effect classes were ignored and the resulting classification represents the best conditions found in the lake except where relatively discrete bays are classified differently. Lake Minnetonka, because of its many distinct bays, was treated differently. Samples of 22 areas were used to assign various parts of the lake to different classes.

The descriptions of the six mapped classes were interpreted from the 81 ground based transparency observations that were included in this study. The range in conditions of the ground data sub-set is not as great as for the entire group of study lakes. This is to be expected because ground data are collected from lakes of greater public importance, which is selective and biased toward larger, deeper, better quality lakes. This bias created problems for separation of shallow lakes with visible dark bottoms.

Differences in the reflectance spectra for the different lake classes can be seen more easily when the reflectance from a very clear lake, in this instance the average of Square and Christmas lakes, is subtracted from the mean spectra of the centroid around which lakes of unknown condition are assigned. These residual curves are shown in Figure 3.

Where two residual curves are shown in Figure 3, two different groups of lakes were used in the statistical classification procedure and later combined for mapping purposes. The general characteristics of these combined classes are similar, but they differ in the concentrations of material in the water. The within class variations are controlled by the degree to which the training set incorporates the full

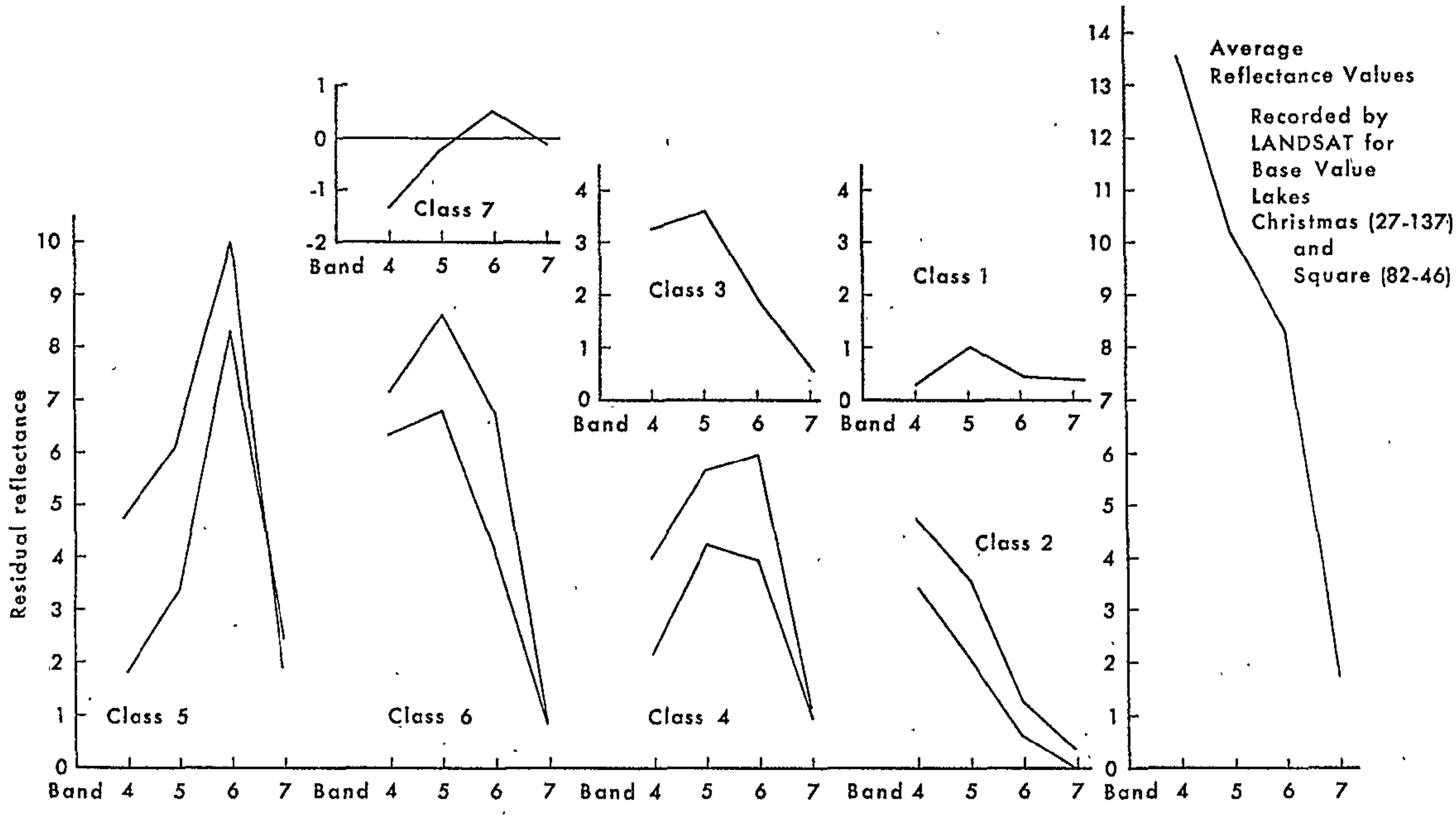

FIGURE 3. Residual reflectance for centroids of classes around which lakes of unknown condition were assigned by discriminant analysis. Residual values are the difference between the reflectance of lakes and the reflectance of a clear deep lake. The average for Christmas and Square Lakes was used here as the clear lake base. Class 7 is an extreme example of the clear, shallow lakes separated from class 1 because they were known to be shallower than the minimum transparency of 240 cm for class 1.

range of lake conditions. Class 7 is the prime illustration of this problem. In the discriminant analysis these shallow lakes were grouped in class 1. Sixty percent of these lakes are transitional between classes 1 and 3 or 1 and 4. The remaining 40% have generally lower residuals on bands 4 and 5 and slightly higher residuals on band 6 than the class 1 centroid. If a clear shallow lake with a visible dark colored bottom had been included in the training set along with similar lakes with some algae and weeds, the post classification separation of class 7 might not have been necessary.

Lakes in class 1 as mapped generally have clear water and are tightly clustered. Class 2 lakes are relatively clear in the top meter, with weeds or algal concentrations in the lower illuminated zone. Class 3 lakes have higher algal concentrations and lower transparencies than class 2 lakes. Lakes in class 4 are either shallow with dark bottom sediments or have tannin stains. In either case, algae and possible bottom weeds are present in sufficient quantity to produce a transparency range of 70-170 cm.

Conditions in class 5 lakes are similar to class 4 but algal concentrations are higher, resulting in lower transparency. Class 6 lakes are dominated by medium to heavy populations of algae, and have transparencies of 15-100 cm. Class 7 lakes are shallow, with some algae and weeds, but transparency generally exceeds depth.

The degree to which the classes intergrade into one another can be seen by analyzing the relative frequency of high probability of secondary class membership (Table 1). About 22% of the class 2 members have a probability of .10 or greater of class 3 membership. Few lakes in other classes have strong secondary probabilities of a class 2 assignment.

Class 3 has considerable transitional problems with 4 and 5 and to a lesser degree with 1 and 2. Class 4 is modestly confused with classes 3 and 5. The complex combination of conditions that are found in this group indicate how numerous possible combinations of condition can produce similar reflectance spectra. Class 5 shows modest confusion with class 3 while class 6 shows very little confusion with any other classes.

The spatial pattern of the classes shown on the map (inside back cover) is difficult to analyze in terms of other resource information such as general land cover, soils, or geomorphology. About all that could be said is that there is a higher probability of a lake being in the better condition classes (1, 2, or 3) in the northeastern part of the study area where somewhat more land remains in forest cover and less under cultivation or pasture. The most obvious conclusion that can be drawn from the map is that lake condition is strongly related to local morphologic, drainage, and land cover conditions.

EVALUATIONS AND CONCLUSIONS

The only true evaluation of this reconnaissance analysis can come from scientists who study lakes and those with lake resource responsibilities. If it aids their work by guiding their ground based detailed studies effectively, it is successful; if not, it has failed to meet its objective. However, several technical evaluations related to problems of analysis and classification can be pointed out.

Alleviation of three problems encountered in this study might improve the results. First is the size of sample area of reflectance taken from each lake. The efforts to average reflectance over too large an area resulted in reduced homogeneity. This means that some sample pixels of deep, clear water may be averaged with pixels covering shallow areas or ones with emergent vegetation. The classification that results may be unsatisfying if compared with ground observations. Lake Wabasso (82) in Ramsey County illustrates this case. It was classified as Class 4 when 20 pixels were included. By subtracting 7 pixels around the edge showing shallow-emergent vegetation, classification was changed to class 1 with reflectance values almost as low as the two clear lakes used as a base. The lake had several recorded transparency observations from late summer ranging from 3.5 to 5.5 meters, suggesting that the original classification was misleading.

The second problem is wind effect. On the morning of the LANDSAT overpass of August 30, 1975 the wind at Minneapolis – St. Paul Airport was southeast at 29 KM/hour (18 mph). This had some impact on the classification of pixels for some larger lakes. Lake Minnetonka and Bald Eagle both showed remarkably good conditions very near the windward shore of the lake and considerably higher concentration of algae on the down wind side (Warwick, 1977). Wind may be a partial factor in the dual classification of Lakes Waconia and Minnetonka. Either image dates should be selected to minimize wind or researchers should be aware of wind effects and sample lakes in a way that avoids a wind induced bias to the classification.

The third problem that should be avoided, if possible, is the limitation imposed by using only one date of LANDSAT coverage. Seasonal changes provide some insight into the biological calendar of lakes. Defining these seasonal trends should allow separation of lake condition problems by degree of severity. Differences in the seasonal dynamics of lakes that display similar spectral reflectance in August have been observed in western Minnesota Lakes (Brown et al., 1977), and may indicate variations in the thermal and nutrient regime. However, the validity of these inferences must still be substantiated by ground observations.

Cursory investigation of the results of reflectance spectral analysis without thoroughly knowing what on-the-ground observations might yield may lead to the conclusion that the procedures used here could substitute for on site studies. That is not the case. While LANDSAT reflectance data may extend the usefulness of secchi disc transparency data, it is also absolutely dependent on an abundance of ground-based transparency information to yield believable results. It should be kept in mind that this technique, which seems to the authors to be successful, extends a reconnaissance analysis and draws no conclusions about detailed lake water quality.

ACKNOWLEDGEMENTS

This work was partially supported by NASA contract #20985 to the Minnesota State Planning Agency and carried out under a contract with the Center for Urban and Regional Affairs, the University of Minnesota. The University of Minnesota Computer Center also provided grants for partial subvention of computing costs. The methods of analysis used were developed under NASA grant NGL 24-005-263 to the Space Science Center, University of Minnesota.

Thanks are due to Jeannie Hamann, Minnesota Land Management Information System; Les Maki, Minnesota State Planning Agency; Margaret Rasmussen and Sandra Haas, Geography Department, University of Minnesota; the Printing Department, University of Minnesota; and Dwight Wilcox, Martin Roller, Letitia Cavalier for their assistance in production.

Special thanks are also due professors Joseph Shapiro and Robert Megard, Limnological Research Center, University of Minnesota and James Scherz, University of Wisconsin for ground based data used to interpret satellite reflectance signals and the guidance they have freely given the authors.

LITERATURE CITED

Boland, D.H.P., An evaluation of the Earth Resources Technology Satellite (ERTS-1) Multispectral scanner as a tool for the determination of lacustrine trophic state: Ph.D. Thesis, Oregon State University: Corvallis, Oregon, 1974.

Brown, D.A., Warwick, R., Cavalier, L., and Roller, M., The Persistence and Condition of Douglas County, Minnesota Lakes: Minnesota Land Management Information System Report #5021, Center for Urban Regional Affairs, University of Minnesota, Minneapolis, Minnesota, 1977.

Rogers, R.H., Shah, N.J., McKeon, J.B., Wilson, C., and Reed, L., Applications of LANDSAT to the Surveillance and Control of Eutrophication in Saginaw Bay: a paper presented at the Tenth International Symposium on Remote Sensing of Environment, Ann Arbor, Michigan, October, 1975.

Scherz, J.P., Lake Water Quality Mapping from LANDSAT: presented at the Eleventh International Symposium on Remote Sensing of Environment, Ann Arbor, Michigan, April, 1977.

Scherz, J.P., Crane, D.R., And Rogers, R., Classifying and Monitoring Water Quality By Use of Satellite Imagery: Proceedings of the American Society of Photogrammetry - American Congress of Surveying and Mapping, Fall convention, pp. 320-43, 1975.

Work, E.A., and Gilmer, D.S., Utilization of Satellite Data for Inventorying Prairie Ponds and Lakes: Photogrammetric Engineering and Remote Sensing, V42, pp. 685-94, 1976.

Warwick, R., Evaluation of Four Methods for Using LANDSAT Data To Analyze Lake Condition in Minnesota, a report submitted to the Space Science Center, University of Minnesota, Minneapolis, Minnesota, June, 1977

MAP

CONDITION OF SELECTED
EAST-CENTRAL MINNESOTA LAKES

ABOUT THE MAP
CONDITION OF SELECTED EAST-CENTRAL MINNESOTA LAKES

Purpose and Limitations

The map was made as an experiment to see if an analysis of reflected sunlight as measured by the Landsat satellite, could be used to allow us to take information from a group of well-known lakes and apply it to find out about a much larger number of lakes. Specifically, we would like to find out if the satellite can tell us about several different lake characteristics: the kind and amount of vegetation -- microscopic algae, floating or submerged plants -- in the water, the presence or absence of organic staining or suspended mud and other materials, the approximate depth of the water and the type of bottom if the bottom is visible.

The map is intended to assist people who are studying lakes by providing information on the distribution of lakes that appear similar. The classification scheme is a comparative one and is based on comparisons with Christmas Lake in Hennepin County and Square Lake in Washington County, two very clear and deep lakes.

The map is based on only one time period, August 7, 1975, and the conditions at that time should not be assumed to be the same at other seasons or in other years at the same season. On that date a strong southeast wind was blowing, and it appears to have moved some of the plants and suspended material in some larger lakes, and this may be responsible for the fact that some large lakes appear to have different characteristics in different parts of their basin areas.

How It Was Made

Lakes were classified according to the way green, red, and two bands of near infrared energy were reflected by the lakes, as measured the Landsat satellite. Different kinds of material in the water of a lake will reflect these four kinds of energy in different ways, and these apparent differences can be detected by the satellite, which measures the amount of reflected sunlight for each of the four types of light it monitors.

The classification was based around lakes whose condition was known when the satellite went over them; other lakes were included in a particular condition class if their reflectance pattern is close enough to the one for the "known" lakes that were used to define the class. The description of condition for each class was also aided by additional information about the transparency for some of the lakes that make up the class. Class 7 lakes are an exception. They were grouped by supplemental ground information on depth. It is possible that some members of class 1 belong in class 7 but could not be so assigned because of lack of depth information.

For additional technical information refer to Minnesota Land Management Information Report 5022 or contact Dwight Brown, Department of Geography, University of Minnesota, Minneapolis, MN 55455; phone, (612) 373-5372.

2.

SECTION B

ANALYSIS OF SUSPENDED SOLIDS IN LAKES USING LANDSAT MULTISPECTRAL DATA

Dr. Michael Sydor
Department of Physics
University of Minnesota, Duluth
Duluth, Minnesota

INDEX

ANALYSIS OF SUSPENDED SOLIDS IN LAKES USING LANDSAT MULTISPECTRAL DATA

Investigator: Dr. Michae_ _,___
Department of Physics
University Of Minnesota, Duluth
Duluth, Minnesota

ABSTRACT

A set of criteria are given for using LANDSAT data in identification of three categories of particulate contaminants in Lake Superior. A linear transformation giving the relationship between the residual LANDSAT intensities and concentrations of the three contaminants was obtained from correlation of remote sensing data with insitu measurements. The inverse transformation gives the concentration of particulates in terms of the multispectral signal intensities. The paper discusses the dependence of the volume reflectance on the contaminant concentrations and presents the rudiments for selection of the optical signatures for identification of suspended solids in lakes.

INTRODUCTION

To use multispectral satellite data for contaminant identification and determination of contaminant concentrations in lakes, it is necessary to pick out broad spectral characteristics (McNeil and Thompson[1]) of contaminants by using lake reflectance measurements in a few spectral regions. LANDSAT data provides reflectance measurements over four broad bands: .5 - .6 μm, .6 - .7 μm, .7 - .8 μm, and .8 - 1.1 μm. Only the first three bands are directly useful in water quality work. The selection of the available bands limits the usefulness of the satellite data to identification of a maximum of only three major contaminants for any given area of a lake. Furthermore, because the reflectivity for particulates in water is generally low the noise to signal ratio limits the usefulness of the satellite data to the areas of the lake where relatively high concentrations of particulates are present. The limiting concentration for identifying particulate contaminants in Lake Superior was 5 mg/ℓ in poor quality water characterized by secchi transparency on the order of 1 m, and 2 mg/ℓ in clear lake water. For very clean lakes such as Lake Baikal, and the central portion of Lake Superior, a single category of particulates or mixtures of two particulate contaminants can be detected and identified down to 1 mg/ℓ concentration, provided the atmospheric scattering is low and uniform.

To examine how LANDSAT data can be used to develop a set of criteria for identification of suspended solids in lakes and how the reflected light measurements can be used to determine the concentrations of particulates, we examine some properties of the volume reflectance of suspended solids. Volume reflectance from suspended particulates oriented over all angles can be approximated by an expression derived by Kortüm[2]. For isotropic scatterers and infinitely thick medium the reflectance R is given by:

$$1) \qquad R = \frac{S}{S+K+\sqrt{K(K+2S)}}$$

S = two times the reflectivity coefficient

K = two times the absorption coefficient

The reflectance is a single valued function of the photon scattering length and the photon absorption length. For suspended solids in lakes, the scattered signal is generally limited by the absorption of the carrying medium. For a single type of particulate contaminant, the reflected light intensity in any spectral band can be correlated directly with the particulate concentration. The reflected signal is a reasonably linear function of the particulate concentrations provided the concentrations are low enough to neglect cross-section overlap. This condition is generally satisfied for the range of suspended solids normally encountered outside of the immediate offshore areas of lakes. An example of the behavior of reflectance as a function of absorption and scattering length for Lake Superior is shown in Figure 1. An example of the printout format and the range of reflected signal for a large high density turbidity plume with a single contaminant type is shown for Lake Superior in Figure 2. The plume in Figure 2 is typical of red clay plumes resulting from erosion and resuspension in western Lake Superior. The concentration of suspended solids in the plume ranged from .5 - 25 mg/ℓ. Figure 2 was obtained from LANDSAT digital data in Band 5 (.6 - .7 μm). Since one type of particulate contaminant predominated in the plume it is possible to correlate the reflected signal in Band 5 directly to the red clay concentrations. Often, however, turbidity plumes arise from a mixture of sources, each contributing a separate category of particulate matter. For a mixture of particulate types, the reflected signal in one band cannot be directly related to the suspended solids concentrations, thus the spectral character of the reflectance must be considered.

Lake Superior has three major particulate contaminants, the red clay from erosion and resuspension occurring along the Wisconsin shore, an iron ore tailings discharge at Silver Bay, Minnesota, and a highly organic tannin water originating from runoff of the St. Louis River (including Duluth-Superior Harbor), the Nemadji River, and the Amnicon River. The locations of the major contaminant sources are shown in Figure 3. When more than one contaminant is present in any given area of the Lake, as is usually the case during spring runoff, the reflected signal in any band will depend on the ratio of the contaminant concentrations as well as the spectral dependence of the reflectivity of each contaminant. The dependence of volume reflectance of the Lake on suspended solids composition can be found by considering first the dependence of the multispectral signals on the volume reflectance for individual contaminants near their sources of origin. Subsequently a linear transformation approximating the relationship between the suspended load composition and the multispectral signal intensities can be developed from a linear superposition of the responses due to individual contaminants. To be able to separate the contributions to the reflected signal due to each category of particulate, the spectral distribution of the reflectance for each category of particulates must be distinct and reasonably repeatable.

The spectral dependence of reflectivities for the three particulate contaminants in Lake Superior are shown in Figure 4. Also shown is the transmission of tannin water for a 10 cm cell.

The differential scattering for the two major particulates is shown in Figure 5. The data shown in this figure are the result of laser illumination of samples where the incident beam is either vertically or horizontally polarized and the detector is arranged to detect scattered light polarized in the incident direction. The detector angle is the angle between the direction of the incident beam the the direction from which the detector receives the scattered radiation. The insolation from the sun is unpolarized so that the scattering for each of the two particulates will be represented by the sum of the two components. The insolation, of course, consists of a continuum of wavelengths and the differential scattering is a function of wavelength. Laser data were obtained for both red and green light and fortunately the combination of the data in the neighborhood of the scattering angle around $\theta = 130°$ approximates well to the solar illumination. The differential scattering for suspended solids found in the Lake looks much like light scattering from particulates in the micron size range Kerker[3]. In the case of satellite observations of particulates in lakes the contribution to the observed reflected signal comes largely from the scattering region around $\theta = 130°$. Since this region is not flat, the observed signal is a weak function of seasonal variation in the sun angle. Figure 4 shows that the reflectivities for the three categories of contaminants in Lake Superior have substantially different spectral shapes; thus the corresponding behavior of the satellite signal for each contaminant in pure form, say near the contaminant source, can be readily determined, and the satellite identification criteria for a single contaminant can be devised on the basis of spectral shape independently of particulate concentration. The spectral shape of the reflectivity for a single contaminate can be obtained from the ratios of signals in the three LANDSAT bands, provided the multispectral signals are above the threshold levels. For an individual contaminant the ratios of multispectral signals would be independent of concentration if the reflected signal intensity above background behaved linearly with the concentration. This is not the case, but the nonlinearity can be compensated somewhat by taking for any point on an image the residual signal in a given band in reference to the signal in an adjacent band; that is, by considering the ratio of the differences of signals in various bands. An example of this behavior is shown in Figure 6, where it can be seen that the red clay plume whose intensity levels ranged over 11 digital steps above background, (Figure 2) shows up mainly in the compensated signal ratio range $-1.00 \pm .25$. Similar relationships exist for other band combinations and other contaminants. The distinct character of spectral reflectance provided by relative LANDSAT signal intensities and signal ratios can be used to establish a set of selection criteria for identification of particulates in the Lake. Laboratory measurements of the spectral distribution of the total reflectivity for each contaminant provide the information necessary for selection of the initial set of band combinations used in development of the identification criteria. The initial combinations picked on the basis of total reflectance measurements are first tested by statistical correlations of the combinations with contaminant identity at sampling stations. The criteria are further refined by narrowing the cutoff limits on each band ratio combination for the respective contaminant types. The band combinations, and the values of signal ratio cutoff limits, serve as the final LANDSAT signatures for identification of the particulates in the Lake. The optical signatures produced in this manner do not, however, provide information on the concentration of the individual contaminants since only the information on the relative reflected signal intensities is used in the development of the signatures. However, the concentration of contaminants in any area can be estimated separately from a linear combination of the direct relationships between the individual contaminant concentration and the multispectral signal intensity levels.

In using LANDSAT data in the above procedure for analysis of lake turbidity, it is necessary to extract the signal intensities above the background for any area of the lake, and to account for atmospheric conditions such as haze and fog. The background signal level for the three bands used directly in water quality measurements can be generally established from the baseline digital reading over the central portions of the Lake well away from the turbidity plumes. Band 7, ranging from .8 μm to 1.1 μm, is a high absorption region for water; thus, its use in water quality measurements is limited. However, Band 7 can be used as an indicator of scattering by haze and fog. Intensity structures over lakes with readings in excess of 1 above the background in Band 7 were regarded as atmospheric phonomena due to fog or heavy haze; such sections of the Lake were not considered in the contaminant identification. An additional criterion on light haze, demanding that $B_5 \leq 6$ and $B_7 \geq 1$, was also imposed in determination of the contaminant concentrations to exclude areas of light haze. Light haze may not obscure contaminant identity, but it does affect the calculation of contaminant concentration. Band 7 was also useful in distinguishing land from the highly turbid water near the erosion bank.

RESULTS

Lake Superior, having clear waters and three physically separated turbidity sources with distinct optical properties, is an ideal study area for the use of remote sensing in contaminant identification. Using the spectral properties of particulates, Figure 4, and the Landsat data in correlation with sampling measurements for 6 overflights, a set of criteria was obtained for the identification of particulates in the western Lake Superior. The signatures are given in Table I. The criteria listed in Table I work well for identifying the individual particulate contaminants in the Lake. The criteria also work in identifying a combination of contaminants for the regions where high concentration of two or three contaminants are present. For instance, Allouez Bay, (Figure 3) always shows a mixture of red clay and tannin water with the respective signatures in Table I appearing together in Allouez Bay on all images.

Table I.

Contaminant	Band Combinations
Red Clay (LANDSAT 1)	$(B_4-B_5) < 0$ $(B_5-B_6) > 1$
	$(B_4-B_6)/(B_5-B_6) < 1$
(LANDSAT 2)	$(B_4-B_5) \leq 1$ $(B_5-B_6) > 1$
	$(B_4-B_6)/(B_5-B_6) \leq 1.2$
Tailings	$(B_4-B_5) > 0$ $(B_4/B_5) \geq 1.5$
	$(B_4-B_5)/(B_5-B_6) \geq 1.5$
Tannin	$(B_4-B_5) \leq -2$ $(B_4-B_6) \leq -2$
	$(B_4-B_5) \leq 0.6$

The bay normally has a concentration of red clay and tannin particulates well in excess of the threshold detectability levels. Similarly, in the relatively opaque tannin water of the Duluth-Superior Harbor and the St. Louis River, the signatures for red clay show up for concentrations of red clay in excess of 5 mg/ℓ. Thus, during the spring runoff, sources of red clay are identifiable in the St. Louis River. Figure 7 shows an example of the results of applying the above signatures to LANDSAT 2 data for June 14, 1975. The image shows a turbidity plume caused by rain runoff from the Nemadji River. A band of turbidity due to erosion from the red clay bank is evident along the Wisconsin shore, and an upwelling patch of tailings appears along the Minnesota shore, and the periphery of a deep trough where the tailings are deposited. A region of mixed contaminants appears where the zones affected by runoff and erosion overlap along the Wisconsin shore and near the mouth of the Nemadji River. The Allouez Bay, as mentioned before, also shows a mixture of tannin and red clay. A tongue of haze north of Allouez Bay (shown symbolically same as the land) is evident from excessive Band 7 readings over parts of Superior Bay and the Lake area east of the Minnesota Point. The more stringent criterion on haze will show later that light haze actually obscures a more extensive area east of the Duluth harbor and a large area of the Lake northeast of Silver Bay. Light haze does not interfere with contaminant identification; however, it will produce false estimates for the concentration of tannin.

To consider the use of remote sensing data in measurement of contaminant concentrations, we examine the relationship between the LANDSAT signal above background and a median concentration of contaminant about which other contaminant concentration values can be approximated from a linear fit. The median concentration for each category of particulates was based on the average concentration of the contaminant determined from samples taken in the observed plumes. For red clay this concentration was 4 mg/ℓ while for the tailings the reference concentration was 1 mg/ℓ. Such levels of particulates are detectable in the satellite data and represent concentrations of fine particulates found generally over wide regions of the Lake. For tannin, characterized by high absorption, the total dissolved solids concentration rather than the suspended solids is used as the reference concentration parameter. The concentration of dissolved solids in the harbor averages at 130 mg/ℓ and is generally associated with an average suspended concentration of undissolved particlates, other than red clay, of 4 mg/ℓ. Thus, in our discussion of the composition of turbidity in Lake Superior, the contribution to the suspended solids from tannin is given in terms of the nominal 4 mg/ℓ reference value.

For an individual contaminant it was possible to develop, over a reasonable range in suspended solids concentrations, a linear approximation between the contaminant concentration and the LANDSAT intensities. When more than one major contaminnat was present the relationship took on a linear transformation form. If we denote the residual band intensities by B_4, B_5, and B_6, and the concentrations of red clay, tailings, and tannin partiuclates as α, β, γ respectively, we obtain a relationship giving the residual (LANDSAT 1 and 2 respectively) band intensities in terms of the reference concentrations of particulates.

$$2)\quad \begin{bmatrix} B_4 \\ B_5 \\ B_6 \end{bmatrix} = \begin{bmatrix} 2.4 & 3 & 0 \\ 3.5 & 1.7 & 1.5 \\ 1.3 & 1 & 3 \end{bmatrix} \begin{bmatrix} \alpha \\ \beta \\ \gamma \end{bmatrix} \qquad \begin{bmatrix} B_4 \\ B_5 \\ B_6 \end{bmatrix} = \begin{bmatrix} 3.4 & 5 & 0 \\ 3.3 & 1.7 & 2 \\ 1.3 & 1 & 3 \end{bmatrix} \begin{bmatrix} \alpha \\ \beta \\ \gamma \end{bmatrix}$$

The coefficients in the transformation were obtained from least-square fits to sampling data. When β and γ are zero, relationship 2) yields

LANDSAT intensities as a function of the red clay concentration expressed as a multiple of the 4 mg/ℓ reference value. From the inverse relationship we obtain:

$$3)\quad \begin{bmatrix}\alpha\\ \beta\\ \gamma\end{bmatrix} = \begin{bmatrix}-.21 & .53 & -.26\\ .5 & -.42 & .26\\ -.08 & -.09 & .38\end{bmatrix}\begin{bmatrix}B_4\\ B_5\\ B_6\end{bmatrix} \qquad \begin{bmatrix}\alpha\\ \beta\\ \gamma\end{bmatrix} = \begin{bmatrix}-.12 & .6 & -.4\\ .28 & -.4 & .27\\ .04 & -.12 & .42\end{bmatrix}\begin{bmatrix}B_4\\ B_5\\ B_6\end{bmatrix}$$

Relationship 3) gives the concentration of each contaminant for any area of the lake in terms of the LANDSAT signal levels above background. The results for June 14, 1975, and April 6, 1976, are shown in Figures 8 and 9. The columns of three numbers printed over the lake give the concentrations of red clay, tailings, and tannin particulates in mg/ℓ for each section of the lake. Notice that the harbor and parts of the lake north of Silver Bay in Figure 8 now show additional areas affected by haze marked by (H). The April 6 image, Figure 9, taken at the time of spring runoff, shows concentrations of red clay in the harbor and the St. Louis River. A more detailed printout of the April 6 image pinpoints the red clay sources in the St. Louis River. The concentrations of particulate shown in Figures 8 and 9 agree well with the experimental results (Sydor and Oman 1978[4]). Equation 3) could also be used for contaminant identification work, however, the criteria in Table I are better for this purpose since the criteria are independent of the assumption of linearity, linear superposition, and are not susceptible errors due to light haze. The digital nature of the multispectral scanner signal, low Band 6 intensity levels, and the possible time dependent character of tannin particulates, do not allow for detection of low concentrations of tannin. The lowest detectable concentration of tannin in the lake is 20% of the average concentration of tannin particulates in the harbor. The lowest detectable concentrations of red clay and tailings is 1 mg/ℓ for Lake water with secchi transparency exceeding 3 m. For the harbor water where secchi transparency averages 0.5 m, the detectable threshold for red clay is 5 mg/ℓ. The detectability threshold for any individual day also depends on the atmospheric and surface affects and is theoretically limited by the concentration of contaminant necessary to produce a signal level a half a digital step above background over an array of pixels constituting the lowest resolution area in the print-out format for the scene. Generally it was found that LANDSAT data could be used in identification of major particulate contaminants for suspended loads above 1 mg/ℓ. The technique is particularly useful in separation of runoff plumes from the usually accompanying turbidity background arising from erosion and resuspension.

ACKNOWLEDGMENTS

I wish to thank Kirby Stortz for work on data reduction. My sincere thanks to Dr. Robert Bukata (Canada Center for Inland Waters) and Andrew Watson (IJC) for stimulating and helpful discussions.

LITERATURE CITED

McNeil, W.R., and Thompson, P.B.: Remote Sensing of Earth Resources, 3, 147 (1974). (Univ. of Tennessee Space Institute Publication.)

Kortum, G.: "Reflectance Spectroscopy," Springer-Verlagd, New York, (1969).

Kerker, M: "The Scattering of Light," Academic Press, (1969).

Sydor M., and Oman, G.J.: "The Effects of Spring Runoff from Nemadji River on Lake Superior." Final Report E.P.A. Contract on work for PLUARG, R005286011 (1978).

FIGURE CAPTIONS

Figure 1. Reflectance as a function of absorption and reflectivity coefficients in .5 - .6 μm region.

Figure 2. Red clay turbidity plume April 11, 1975, produced from computer printout of LANDSAT Band 5 intensity above background averaged over 50 pixels. The intensity levels range over 11 digital steps.

Figure 3. Location of the major turbidity sources for western Lake Superior.

Figure 4. Spectral dependence of total reflectivities for particulates in western Lake Superior. Curve 1 - transmission of tannin water for 10 cm cell, Curve 2 - red clay, Curve 3 - tannin, and Curve 4 - tailings.

Figure 5. Laboratory determined optical reflectivity for two particulates as a function of the scattering angle θ relative to the incident direction for a horizontally and vertically polarized beam and with the detector arranged to receive light of that polarization.

Figure 6. Printout of the ratio of LANDSAT intensities referenced to adjacent bands (for April 11, 1975). Notice the red clay plume ranging in intensity levels over 11 digital steps, falls distinctly in the -1.00 ±.25 ratio, and is separated from the clear water where the ratio is 0.25.

Figure 7. Identification of particulates in Lake Superior using LANDSAT 2 data (June 14, 1975). The mixtures of red clay and tannin are shown as crosses. Red Clay (.), Tailings (/), Tannin (-).

Figure 8. Concentration of particulates in Lake Superior using LANDSAT 2 data for June 14, 1975. The columns give red clay, tailings, and tannin in mg/ℓ. Haze criterion is shown by letter H. Notice even though the harbor waters were identified in Figure 7 as tannin, the concentrations of particulates can not be determined in the St. Louis River because of light haze.

Figure 9. Concentration of particulates in Lake Superior using LANDSAT 1 data for April 6, 1976. (Red clay, tailings, tannin) in mg/ℓ.

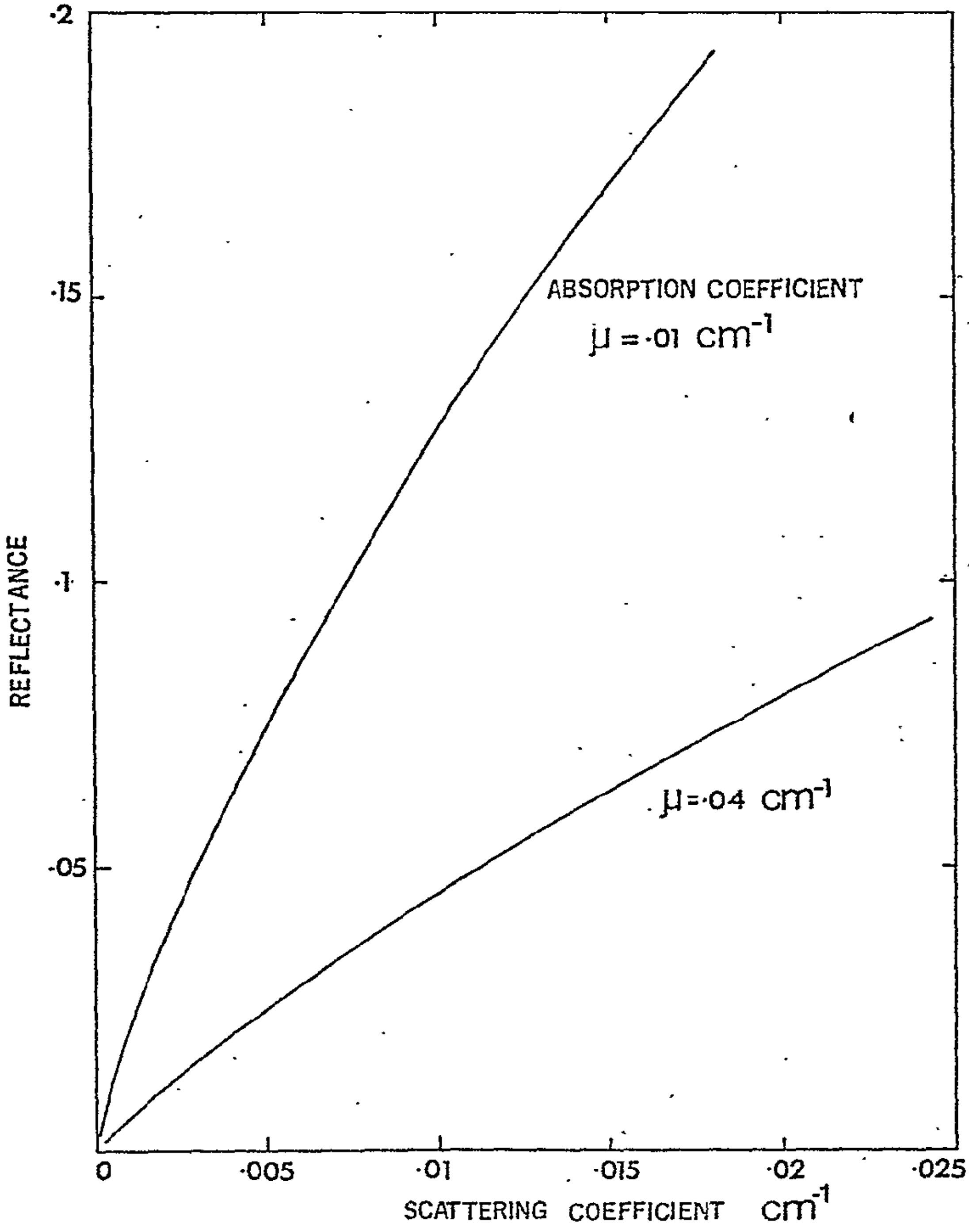

·2
·15
·1
·05
REFLECTANCE
0
·005
·01
·015
·02
·025
SCATTERING COEFFICIENT cm^{-1}
ABSORPTION COEFFICIENT
μ = ·01 cm^{-1}
μ = ·04 cm^{-1}

Figure 1.

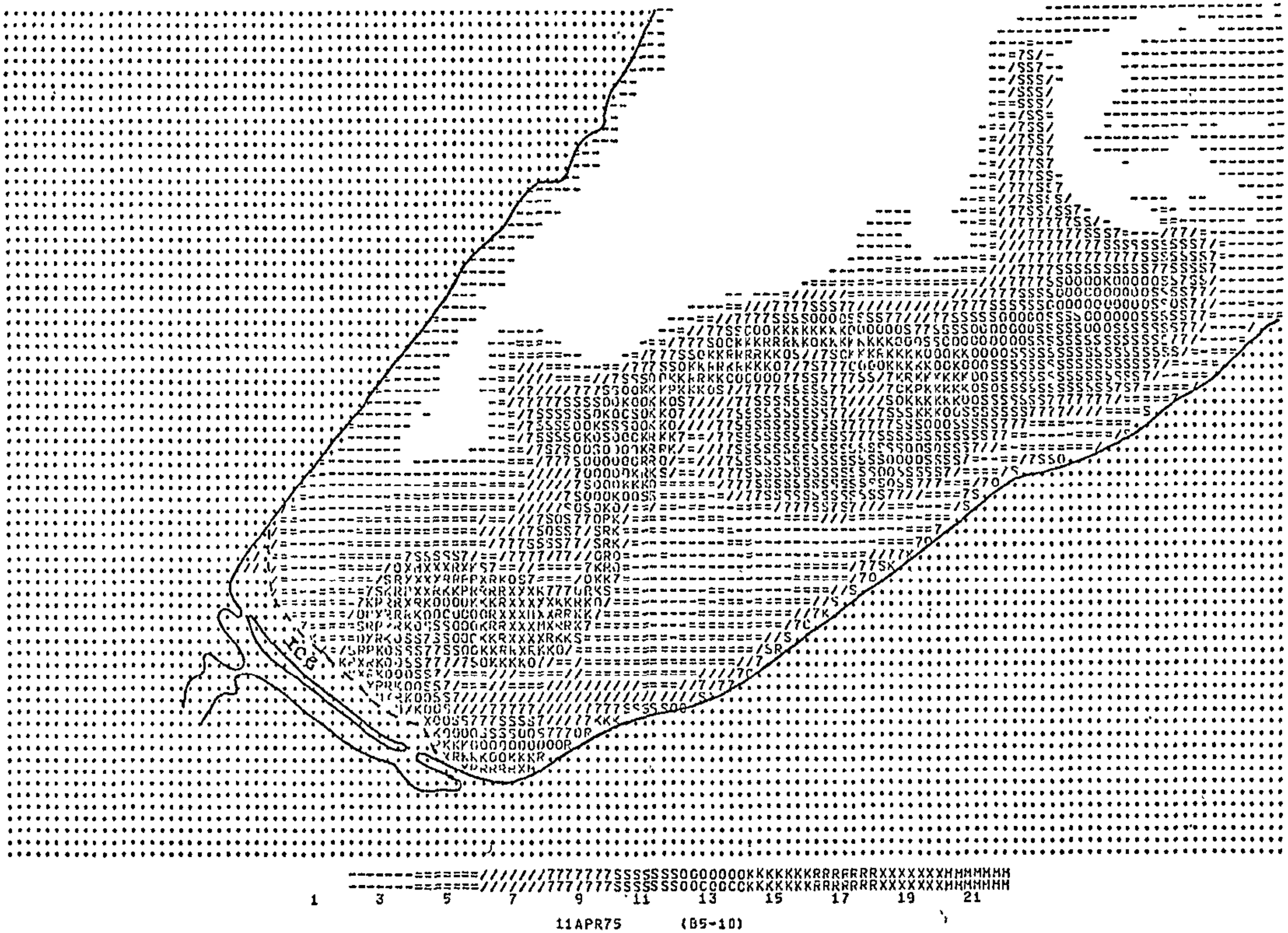

Figure 2.

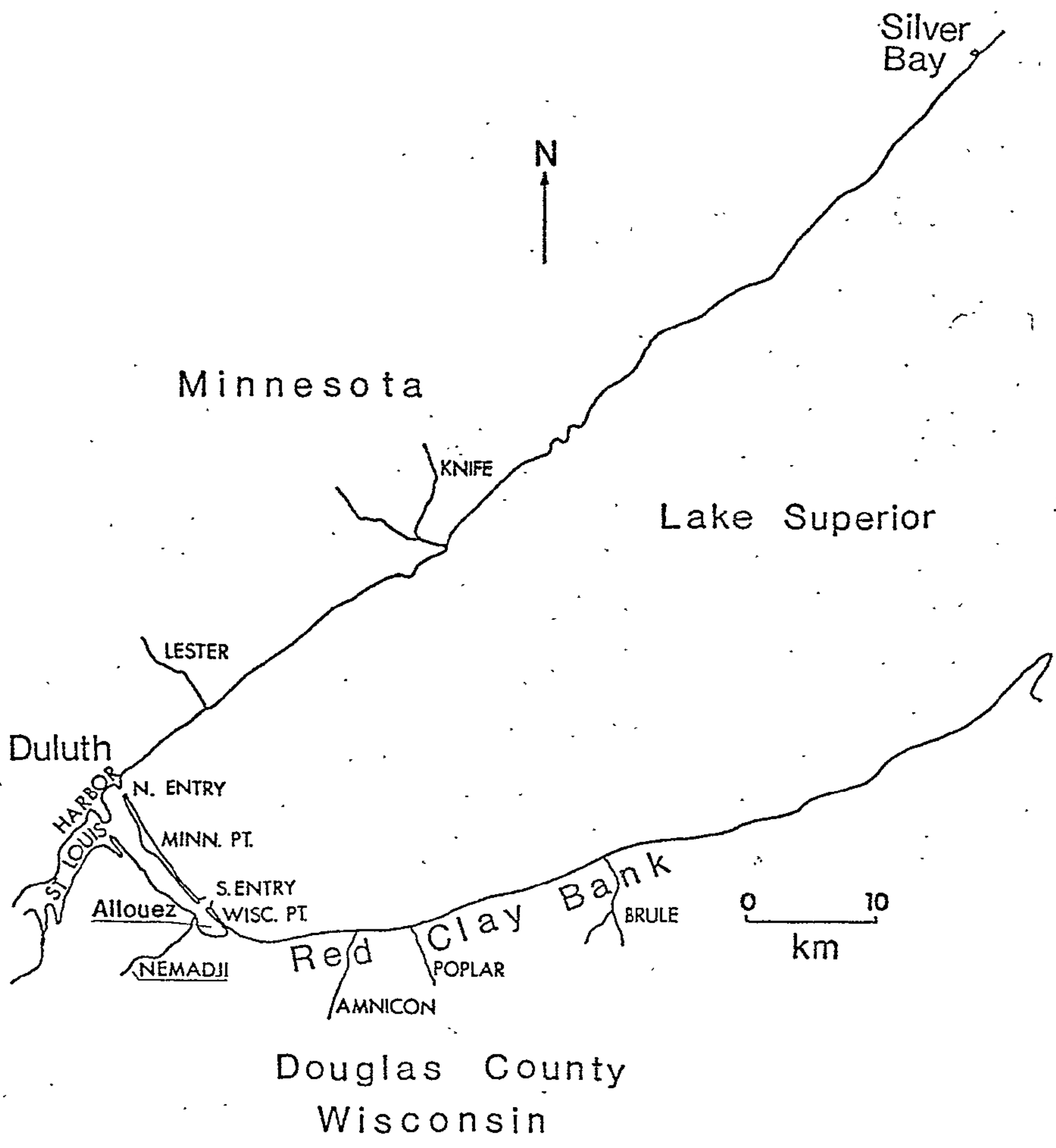

Silver Bay
N
Minnesota
KNIFE
Lake Superior
LESTER
Duluth
HARBOR
N. ENTRY
ST LOUIS
MINN. PT.
S. ENTRY
Allouez
WISC. PT.
NEMADJI
Red Clay Bank
BRULE
0 10
km
AMNICON
POPLAR
Douglas County
Wisconsin

Figure 3.

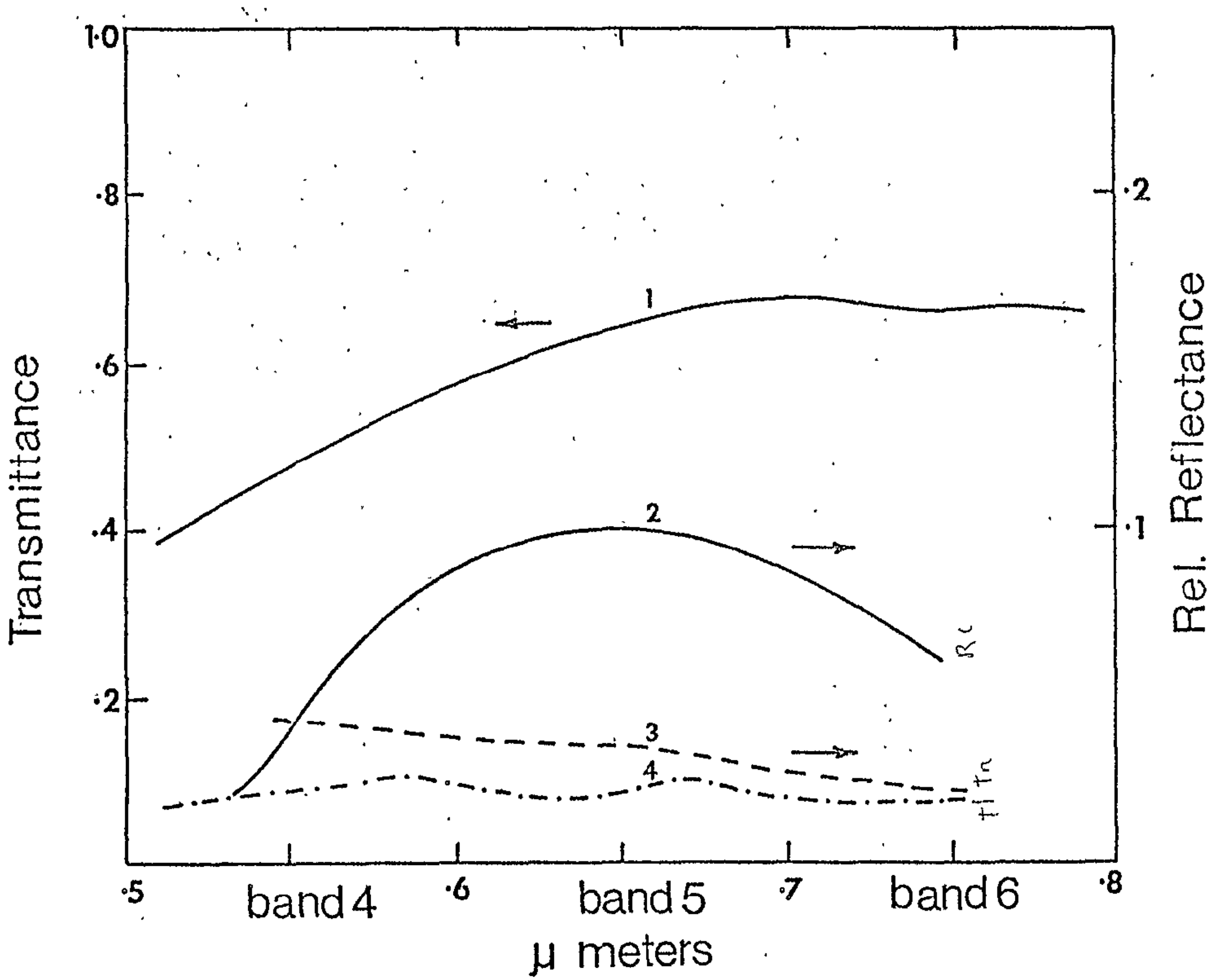
1·0
·8
·6
·4
·2
Transmittance
·2
·1
Rel. Reflectance
1
2
3
4
·5
band 4
·6
band 5
·7
band 6
·8
μ meters

Figure 4.

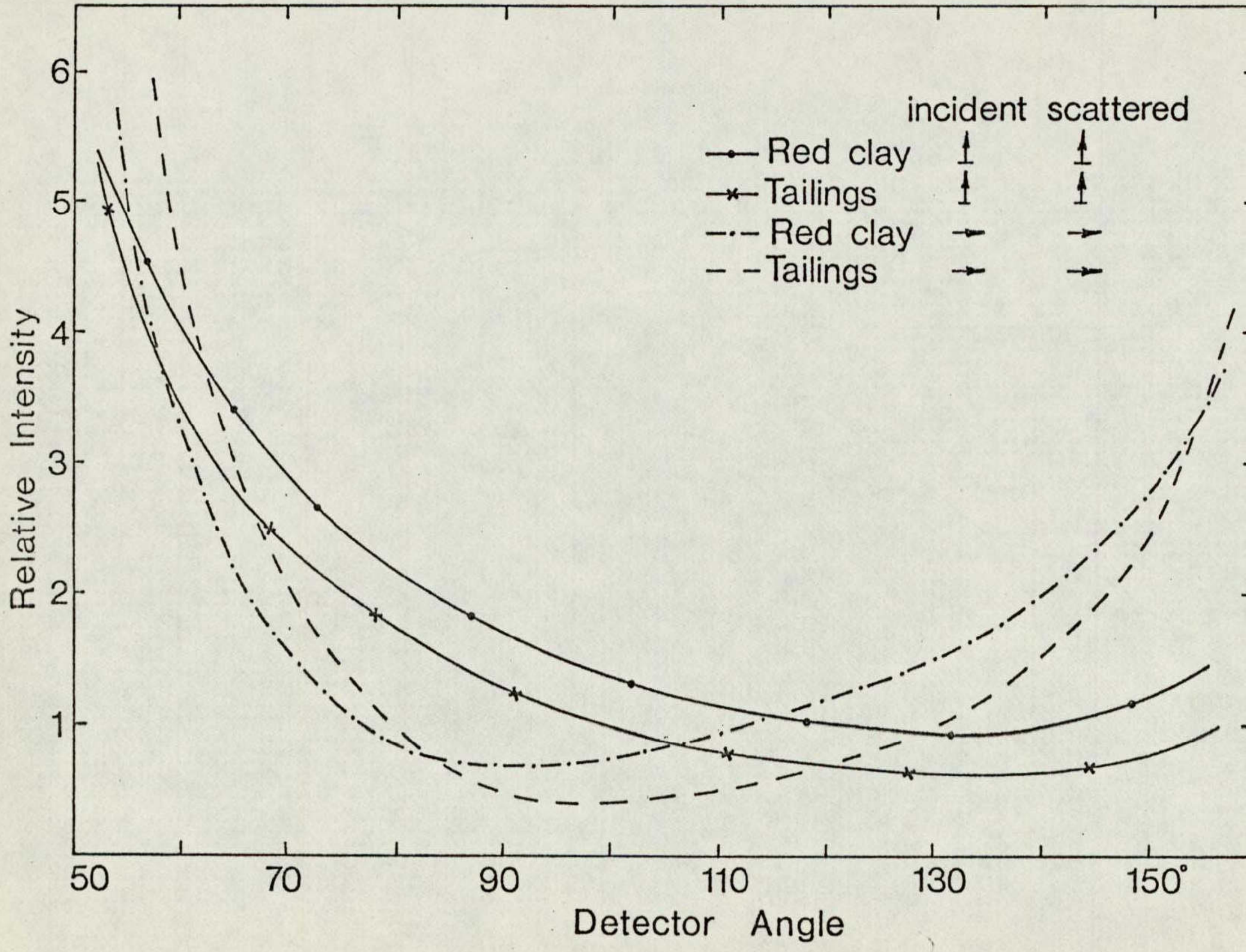
incident scattered
Red clay
Tailings
Red clay
Tailings
Relative Intensity
1
2
3
4
5
6
50
70
90
110
130
150°
Detector Angle

Figure 5.

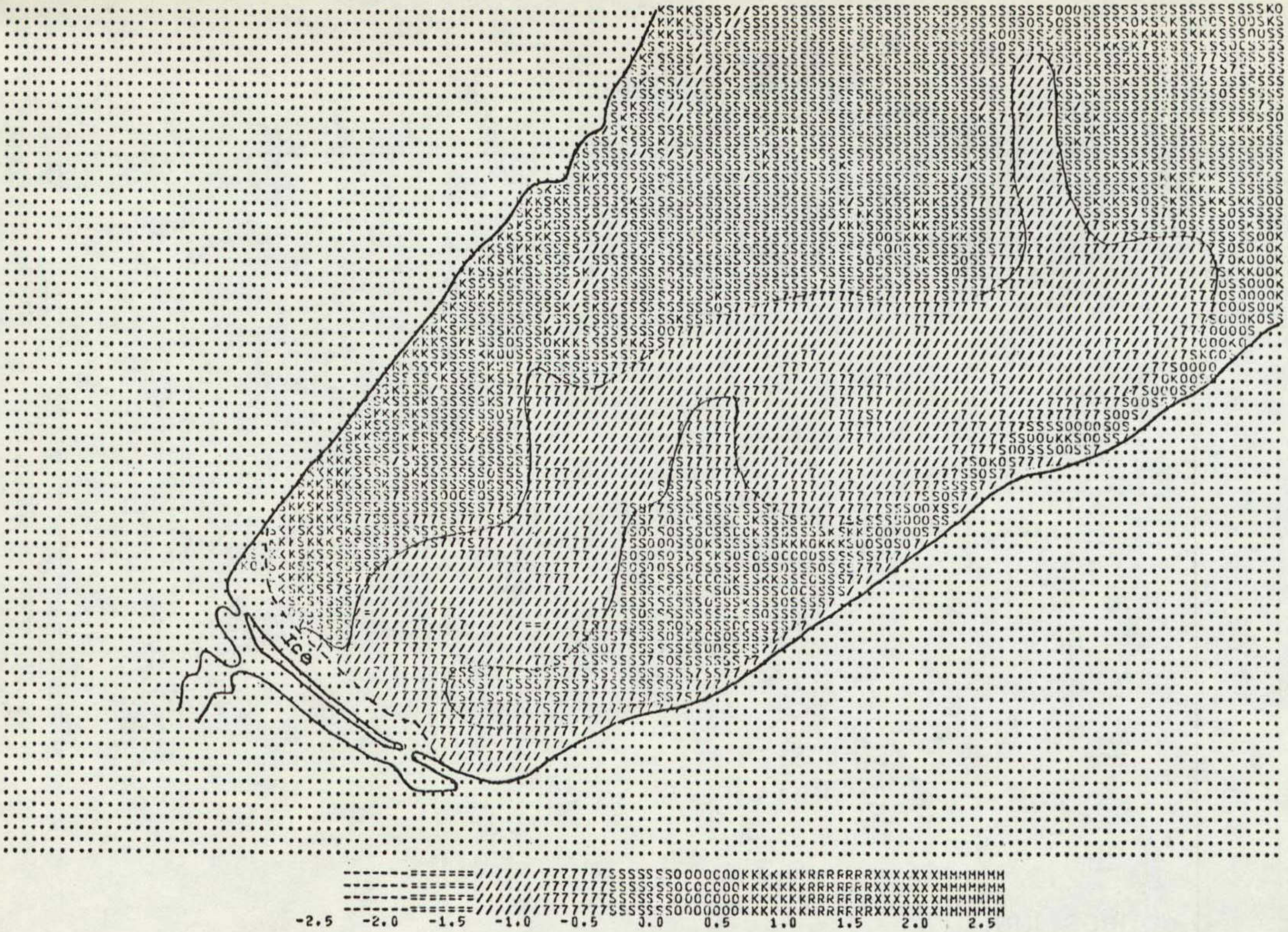

11APR75 (B4C-B5C)/(B5C-B6C)

Figure 6.

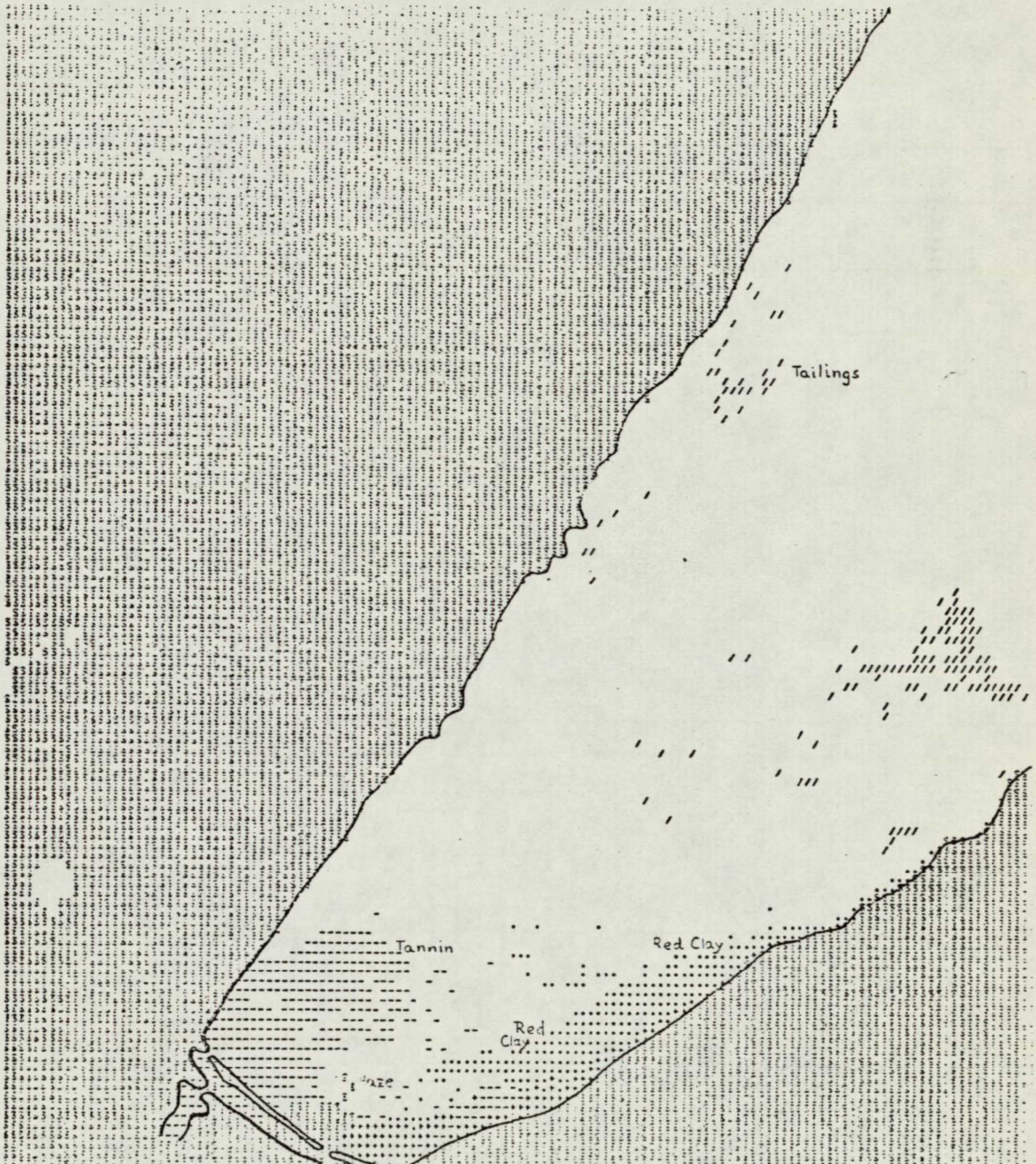

14JUN75

RED CLAY	(B4C-B5C)<3.	(B5C-B6C)>1.	(B4C-B6C)/(B5C-B6C)<1.0
TAILINGS	(B4C-B5C)>6.	(B4C/B5C)≥1.5	(B4C-B5C)/(B5C-B6C)≥1.5
TANNIN	(B4C-B5C)≤-2.	(B4C-B6C)≤-2.	(B4C/B5C)≤0.6

(.)=RED CLAY (/)=TAILINGS (-)=TANNIN (+)=MIXED RED CLAY AND TANNIN

Figure 7.

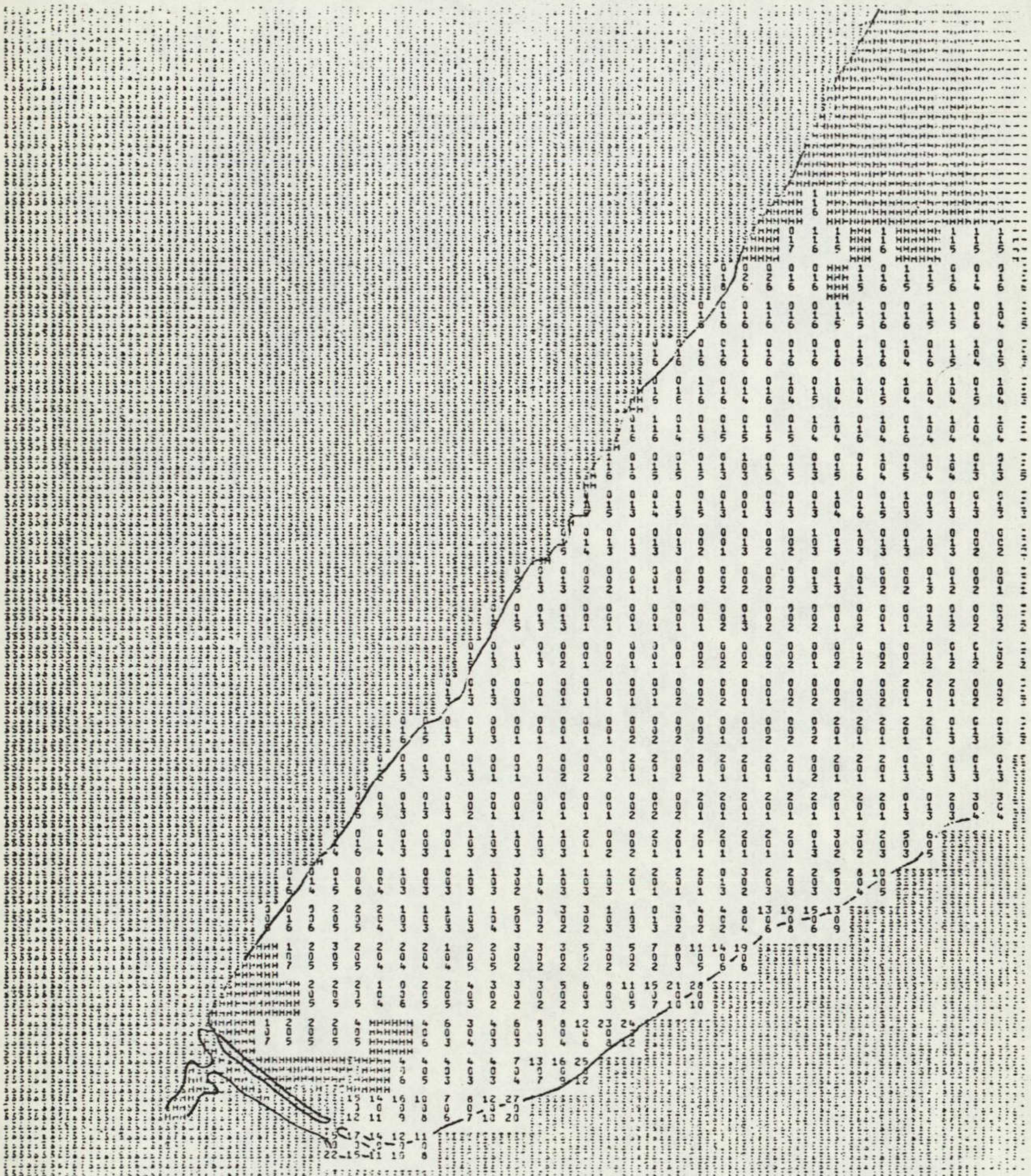

14JUN75

CONTAMINANT CONCENTRATION (MG/L)

($) = LAND OR THICK CLOUDS. (H) = HAZE OR LIGHT CLOUDS.

Red Clay
Tailings
Tannin

Figure 8.

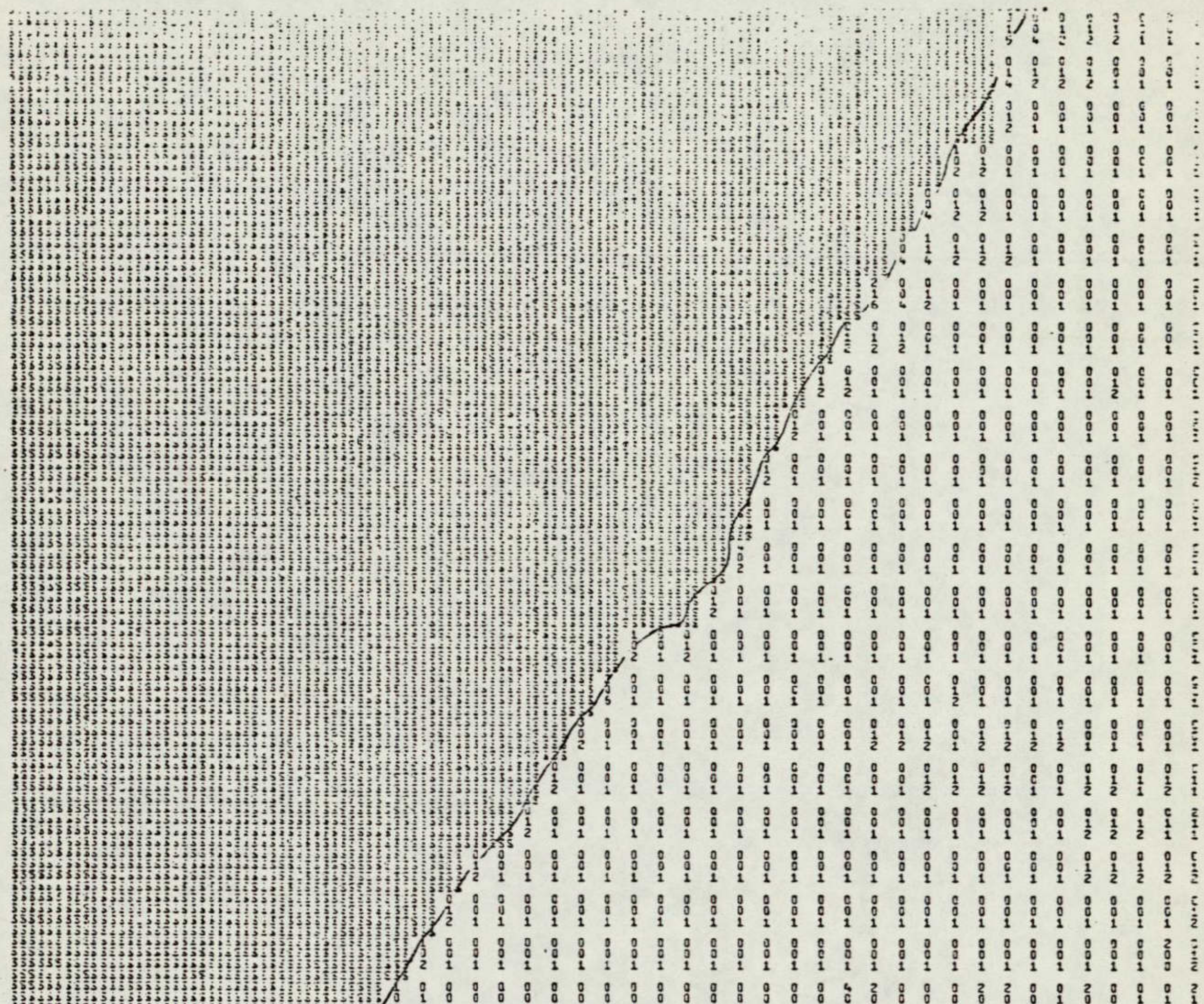

Figure 9.

Appendix A

USE OF REMOTE SENSING IN DETERMINATION OF CHEMICAL LOADING OF LAKE SUPERIOR DUE TO SPRING RUNOFF

G. J. Oman and M. Sydor

USE OF REMOTE SENSING IN DETERMINATION OF CHEMICAL LOADING OF LAKE SUPERIOR DUE TO SPRING RUNOFF*

G. J. Oman and M. Sydor

Department of Physics

University of Minnesota, Duluth

Duluth, Minnesota 55812

Submitted to Canadian Journal of Spectroscopy

January 31, 1978

*Work done for PLUARG Task D Program of the International Joint Commission Studies on Chemical Loading of Great Lakes due to Spring Runoff. Supported by EPA Grant R005286011.

Abstract

Use of remote sensing data in identification of various sections of a complex spring runoff plume in Lake Superior allowed for a grouping of sampling stations according to particulate contaminant type. The grouping provided for a good cross-correlation of the optically detectable parameters with the chemical parameters. The results were used in determination of the total phosphorous and total organic nitrogen loading of the lake due to spring runoff. The results were also helpful in numerical simulation of the long term dispersion of runoff pollutants.

Introduction

In environmental studies of chemical loading of lakes it is necessary to determine the concentrations of pollutants over large areas. This is often cost prohibitive from the standpoint of sampling. However, multispectral remote sensing data provide information useful in extending the sampling data taken at few points to wide areas of the lake provided the optically sensitive parameters can be correlated with chemical parameters over a period of several days. The remote sensing data are also useful in testing of numerical models for simulation of contaminant dispersion in lakes. The aerial multispectral data provide sequential instantaneous information on the large scale phenomena which reflect both the transport and the dispersion processes taking place in the lake. In a sense the remote sensing data provide a good substitute for current measurements, at least for the surface layer of the lake.

To consider how Landsat data can be used in studies of contaminant dispersion and in determination of chemical loading of lakes we will consider as an example the results from an investigation of the effects of 1976 spring runoff from the Nemadji River on western Lake Superior.

Results

During the spring runoff one observes typically a large red clay plume in the extreme western Lake Superior. The plume consists primarily of micron sized particles of red clay from Nemadji River runoff and from erosion of a Lacustrine red clay bank along the Wisconsin shore, Figure 1. A typical red clay plume due to runoff, erosion, and resuspension is shown in Figure 2. To determine the chemical loading of the lake due to runoff for any given plume, it is first necessary to identify the areas of the observed turbidity which are attributable to runoff. This can be done using the optical signatures for particulates characteristic of erosion and runoff, Table I. The

Table I.

Contaminant	Band Combinations
Red Clay	$(B_4-B_5) < 0$ $(B_5-B_6) > 1$ $(B_4-B_6)/(B_5-B_6) < 1$
Tannin	$(B_4-B_5) \leq -2$ $(B_4-B_6) \leq -2$ $(B_4/B_5) \leq 0{\cdot}6$

signatures in Table I were developed from the correlation of the spectral characteristics of the volume reflectance for various particulates in Lake Superior with Landsat 1 multispectral data. It was possible to differentiate the runoff sections of the plume from the turbidity due to erosion because the river runoff contains humic or tannin water rich in organic particulates as well as the red clay particulates which predominate the suspended solids in erosion plumes. Application of the tannin criterion to the Landsat computer tape data for the 1976 spring runoff in western Lake Superior yields the results shown in Figure 3. Figure 3 shows the dense portions of the Nemadji runoff plume. A check on the results in Figure 3 can be obtained from the insitu measurements of the specific conductance. The conductance is two times higher for the tannin water than it is for the lake water. The insitu values for specific conductance in micro mhos/cm are shown by the numbers in Figure 3 at the station locations where samples for chemical analysis were taken. It can be seen that the high conductance values correspond to the runoff section of the turbidity plume. By grouping the sampling stations according to signatures listed in Table I we were able to correlate some chemical parameters with Landsat multispectral data. The correlation of the optically sensitive parameters, turbidity, transmission coefficient, and the suspended solids with all the measured chemical parameters is shown in Table II.

Sufficient statistical data were available in our measurements for cross-correlation of turbidity with total phosphorus, total organic nitrogen, SiO_2, and SO_4. The data from high altitude manned overflights provided by NASA Lewis Research Center (R. Gedney and J. Salzman) showed comparable results. Using the relationship in Figure 4 between the total phosphorus, turbidity, and Landsat Band 5 intensity, we obtain the distribution of total phosphorus in Figure 5 for the spring runoff in western Lake Superior. Table III shows the estimated total phosphorus and total organic nitrogen loading of Lake Superior due to various turbidity sources. Substantial amount of the total phosphorus is directly attributable to the red clay particulates either as a leachate or adsorbed material.

Although the major chemical burden in the Nemadji runoff and the St. Louis River runoff is due to natural turbidity and dissolved material typified by the red clay and the tannin water, the runoff from the two rivers is also associated with man-made contaminants entering the rivers from municipal and industrial discharges of the cities of Duluth, Superior, and Cloquet. It is thus interesting to examine how the runoff plumes disperse in the lake under various wind conditions in relation to the location of the municipal water intakes to assess how the overflow of municipal sewer systems and snow

ALL DATA EXCEPT 11MAY76.
CASE 5: NEHADJI 2.
LINEAR FIT, Y=A+B*X.

Table II.

NUMBER OF DATA PAIRS

		SEC	CON	TMP	TB	SS	%VL	DO	PH	CA	HG	ALK	CL	SO4	SIL	TPH	OPH	NO3	NH3	PON	TON	CLA	CLB	CLC	CAR	PPG	ODR
	SEC		11	11	11	11	11	11	11	11	11	11	11	11	11	11	11	11	11	11	11	10	10	10	10	10	10
	CON	.33		24	21	24	24	24	24	24	24	24	24	24	24	24	24	24	24	24	24	12	12	12	12	12	12
C	TMP	.66	.70		21	24	24	24	24	24	24	24	24	24	24	24	24	24	24	24	24	12	12	12	12	12	12
O	TB	.71	.16	.61		21	21	21	21	21	21	21	21	21	21	21	21	21	21	21	21	12	12	12	12	12	12
R	SS	.64	.19	.50	.92		24	24	24	24	24	24	24	24	24	24	24	24	24	24	24	12	12	12	12	12	12
R	%VL	.34	.35	.11	.35	.20		24	24	24	24	24	24	24	24	24	24	24	24	24	24	12	12	12	12	12	12
E	DO	.56	.66	.75	.72	.57	.00		24	24	24	24	24	24	24	24	24	24	24	24	24	12	12	12	12	12	12
L	PH	.36	.31	.42	.42	.49	.11	.73		24	24	24	24	24	24	24	24	24	24	24	24	12	12	12	12	12	12
A	CA	.33	.50	.53	.40	.43	.17	.68	.25		24	24	24	24	24	24	24	24	24	24	24	12	12	12	12	12	12
T	HG	.57	.76	.76	.63	.56	.09	.87	.55	.72		24	24	24	24	24	24	24	24	24	24	12	12	12	12	12	12
I	ALK	.20	.83	.59	.21	.28	.30	.79	.41	.77	.85		24	24	24	24	24	24	24	24	24	12	12	12	12	12	12
O	CL	.46	.78	.71	.63	.55	.00	.88	.48	.71	.94	.83		24	24	24	24	24	24	24	24	12	12	12	12	12	12
N	SO4	.57	.45	.64	.82	.73	.15	.75	.47	.63	.88	.59	.85		24	24	24	24	24	24	24	12	12	12	12	12	12
	SIL	.65	.56	.71	.80	.68	.15	.82	.47	.65	.88	.64	.91	.94		24	24	24	24	24	24	12	12	12	12	12	12
C	TPH	.67	.36	.64	.88	.76	.22	.74	.54	.54	.79	.43	.77	.93	.91		24	24	24	24	24	12	12	12	12	12	12
O	OPH	.63	.57	.74	.85	.70	.14	.88	.57	.63	.90	.64	.91	.92	.96	.92		24	24	24	24	12	12	12	12	12	12
E	NO3	.13	.80	.50	.08	.09	.11	.62	.35	.53	.65	.76	.64	.34	.40	.25	.49		24	24	24	12	12	12	12	12	12
F	NH3	.62	.52	.67	.72	.64	.04	.73	.42	.60	.86	.61	.81	.90	.93	.87	.88	.37		24	24	12	12	12	12	12	12
I	PON	.52	.12	.43	.69	.47	.18	.31	.43	.14	.47	.08	.29	.60	.41	.60	.53	.16	.46		24	12	12	12	12	12	12
C	TON	.70	.34	.69	.87	.73	.25	.67	.57	.44	.77	.37	.67	.89	.81	.89	.87	.27	.80	.84		12	12	12	12	12	12
I	CLA	.36	.09	.16	.32	.32	.07	.11	.21	.09	.08	.07	.22	.29	.39	.33	.18	.28	.35	.07	.10		12	12	12	12	12
E	CLB	.03	.23	.32	.37	.44	.07	.48	.30	.63	.45	.79	.55	.50	.44	.30	.46	.35	.40	.14	.28	.01		12	12	12	12
N	CLC	.27	.00	.01	.46	.43	.08	.09	.09	.06	.25	.22	.19	.36	.37	.51	.30	.37	.39	.35	.42	.34	.33		12	12	12
T	CAR	.25	.66	.38	.25	.21	.40	.26	.07	.07	.21	.50	.23	.12	.14	.22	.02	.72	.11	.02	.09	.62	.17	.33		12	12
	PPG	.53	.44	.46	.73	.72	.20	.26	.32	.29	.58	.37	.68	.70	.73	.72	.63	.12	.69	.27	.50	.72	.28	.47	.24		12
	ODR	.54	.49	.51	.73	.74	.14	.35	.25	.29	.63	.44	.72	.74	.78	.74	.68	.20	.75	.29	.52	.76	.33	.39	.24	.98	

ORIGINAL PAGE IS OF POOR QUALITY

Parameter Definition for Table II.

SEC = Secchi Disk Transparency in Meters

CON = Specific Conductance in μmhos/cm

TMP = Temperature in Degrees Celcius

TB = Turbidity in NTU

SS = Suspended Solids in mg/ℓ

%VL = Percent Volatiles

DO = Dissolved Oxygen in mg/ℓ

PH = PH

CA = Calcium in mg/ℓ

MG = Magnesium in mg/ℓ

ALK = Alkalinity as mg/ℓ CACO3

CL = Chloride in mg/ℓ

SO4 = Sulphate in mg/ℓ

SIL = Silicate in mg/ℓ

TPH = Total Phosphorus in μg/ℓ

OPH = Ortho Phosphate in μg/ℓ

NO3 = Nitrate Nitrogen mg/ℓ

NH3 = Ammonia Nitrogen in mg/ℓ

PON = Particulate Organic Nitrogen in mg/ℓ

TON = Total Organic Nitrogen in mg/ℓ

CLA = Chlorophyll A in μg/ℓ

CLB = Chlorophyll B in μg/ℓ

CLC = Chlorophyll C in μg/ℓ

CAR = Carotenoids in μg/ℓ

PPG = Phaeophytin Pigments in μg/ℓ

ODR = Optical Density

Table III.

Estimates of Chemical Loads from Various Sources

	Total P Metric Tons			Total Organic N Metric Tons		
	Nemadji	Douglas County Streams	Erosion Resuspension	Nemadji	Douglas County Streams	Erosion Resuspension
April 5	12	6	12	102	70	∿ 30
April 6	15	5	10	120	68	∿ 25

melt runoff may affect the drinking water. Basically one would be interested in determining the dispersion of the runoff water to low concentrations, commensurate with the dilution of pollutants in lake to the levels which would still result in hazardous concentrations of toxic materials at the water intakes. Remote sensing data are available only for a few days. Furthermore, the data are useful in identifying only the relatively high concentration of tracer contaminants. To determine how toxic contaminants from the harbor could disperse with runoff to low concentrations, it is necessary to examine the transports and dispersion of the plumes as a function of winds over long duration. This can be done through use of numerical modeling. To test whether the numerical model results are realistic the simulated high concentration plumes can be compared to the remote sensing data over times long enough to assure credibility. The dissipation of the Nemadji runoff for 1976 was simulated with the aid of a depth integrated model of Lake Superior (Diehl et al.[1]). The transports were calculated using the actual wind conditions over the entire lake from March 31, 1976 to April 7, 1976. The dispersion of the runoff plume was calculated using a particle in cell technique based on Lagrangian formulation of dispersion processes. Since Landsat data were available for April 5 and April 6, and the observed turbidity plumes showed identifiable structures for both days, it was possible to compare the average currents at three points of the lake for the consecutive overflights and to determine the spreading rate of plumes. The details of the numerical model are discussed elsewhere by Oman and Sydor[2]. The Lagrangian marker technique followed the numerical schemes presented in technical reports by Sklarew[3] and Spaulding[4]. The model for plume development produced results quite comparable to the observed runoff plume from the Nemadji River and the

Amnicon River in terms of the distribution of suspended solids and the total suspended load in the lake, Figure 5. The source functions for suspended solids were based on the measured suspended load output from the rivers. Effects of resuspension were included for a period of high turbulence on April 3. The modeled results agreed well with the observed plume dynamics and showed many of the structural features displayed in the observed plume. Since the model results were realistic for the runoff period from March 30 - April 6, calculation of dispersion was extended over a period of one month for two types of winds.

First, variable wind conditions were simulated for a month by recycling the transport patterns produced by the variable winds during the peak Namadji runoff from March 31 to April 6, 1976. The result for the dispersion of runoff for variable winds is shown in Figure 7. The runoff is entrapped in the arm of Lake Superior west of Brule River, Wisconsin and appears to remain in the proximity of the water intakes for prolonged times as long as the variable winds persist. Simulation of runoff dispersion for the westerly winds shows in Figure 7 that the water intake areas would be purged free of the contaminants and that the runoff material would be transported along the Wisconsin shore towards the Apostle Islands. The results for variable winds and the westerly winds are confirmed by numerous Landsat images. Similarly, biological experiments, Rushmeyer et al.[5], show increased abundance of aquatic organisms west of Brule River, apparently due to chemical loading of the lake during runoff and the subsequent entrapment of contaminants for variable wind conditions.

In summary it can be said that the multispectral data for lakes taken over broad spectral bands provides information sufficient for differentiation of broad categories of lake contaminants. The data is useful in studies of the dispersion processes, and in sampling site categorization necessary for cross-correlation of optical and chemical parameters, and the determination of chemical loading of the lake. Projected numerical results verified by remote sensing data indicate that contaminant concentration of 1 mg/ℓ in the harbor would produce a concentration of contaminant in excess of 10^{-8} g/ℓ at the Cloquet water intake. Similarly the Duluth water intake could show for variable wind conditions on the order of 10^{-9} g/ℓ concentration of the contaminant if the contaminant was conservative.

Acknowledgments

We express our gratitude to our co-worker Kirby Stortz and to Robert Bukata of Canada Center for Inland Waters for many helpful discussions. Our sincere thanks to Jack Salzman, Charles Raquet, Richard Gedney, and Donald Shook of NASA Lewis Research Center for their aid in obtaining optical data and for helpful discussions. Their results from the manned overflights were very useful in verification of our calculations of the dynamics of the plume.

References

1. S. R. Diehl, W. E. Maanum, T. F. Jordan and M. Sydor, *J. Geophys. Research, 82,* 977 (1977).
2. G. J. Oman and M. Sydor, submitted to *J. Am. Soc. Civ. Engrs.*
3. R. C. Sklarew, A. J. Fabrik and J. E. Prager, *Systems, Science and Software Report No, 35R-884,* La Jolla, California (1971).
4. M. Spaulding, *NASA Technical Memorandum TMX-73930,* Langley Research Center, Hampton, Virginia (1976).
5. O. R. Ruschmeyer, T. A. Olson and H. M. Bosch, Lake Superior Studies, Minnesota Public School of Health, Univ. of Minn., Duluth, (1956-61).

Figure Captions

Fig. 1. Western Lake Superior - study area.

Fig. 2. Turbidity plume in western Lake Superior at the peak of the 1976 spring runoff. The plume consists primarily of red clay particulates.

Fig. 3. Portions of the turbidity plume attributable to spring runoff. The numbers printed on the plume represent insitu conductivity measurements in μmhos/cm.

Fig. 4. Band 5 intensity vs. turbidity and total phosphorus for the Nemadji River runoff plume.

Fig. 5. Comparison of the observed and simulated suspended solids plumes at 10 mg/ℓ concentration contour. The observed plume contained a load of 32,000 metric tons. A settling rate of 6% was assumed, based on the observed settling rate for identifiable sections of the plume in consecutive Landsat images.

Fig. 6. Distribution of total phosphorus in western Lake Superior for April 5, 1976 based on Band 5 intensity.

Fig. 7. Simulated distribution of runoff showing contaminant accumulation in the extreme western Lake Superior after 30 days of variable winds. The long fetch westerly winds purge the area of contaminants.

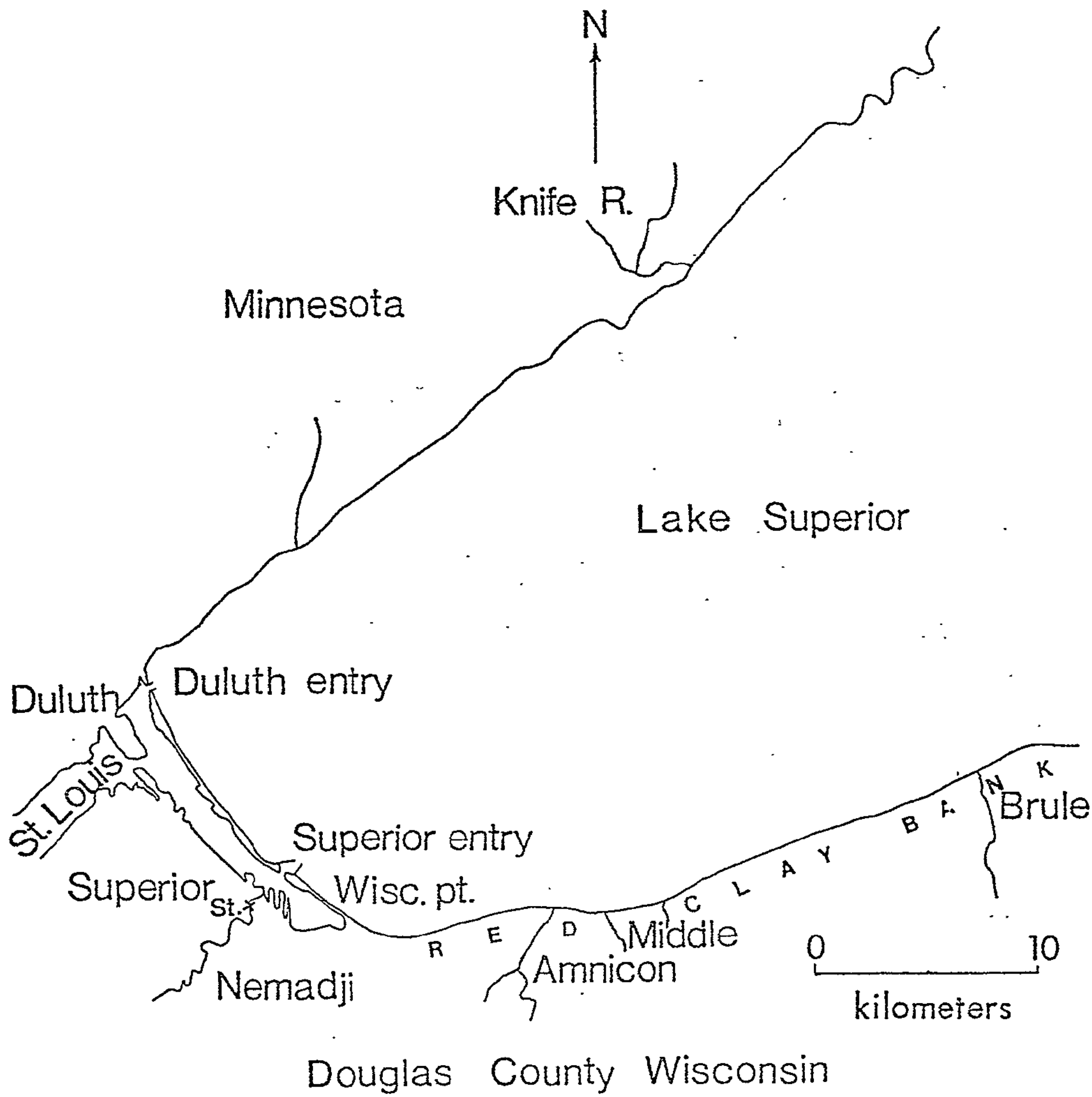
N
Knife R.
Minnesota
Lake Superior
Duluth
Duluth entry
St. Louis
Superior entry
Superior
St.
Wisc. pt.
R E D
C L A Y B A N K
Brule
Middle
Amnicon
Nemadji
0
10
kilometers
Douglas County Wisconsin

Fig. 1.

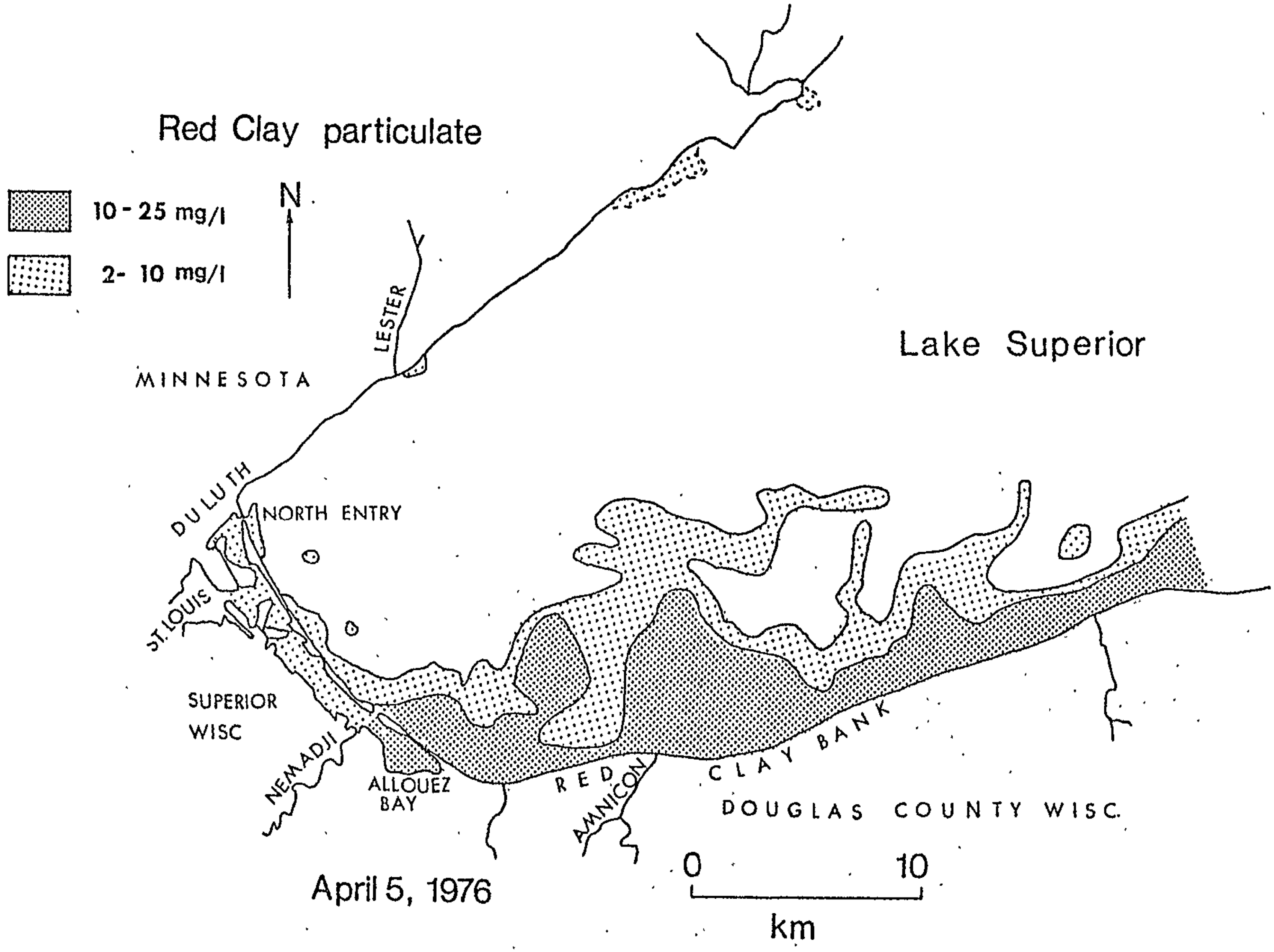
Red Clay particulate
10 - 25 mg/l
2- 10 mg/l
N
LESTER
MINNESOTA
Lake Superior
DULUTH
NORTH ENTRY
ST. LOUIS
SUPERIOR
WISC
NEMADJI
ALLOUEZ
BAY
RED
AMNICON
CLAY BANK
DOUGLAS COUNTY WISC.
0
10
km
April 5, 1976

Fig. 2.

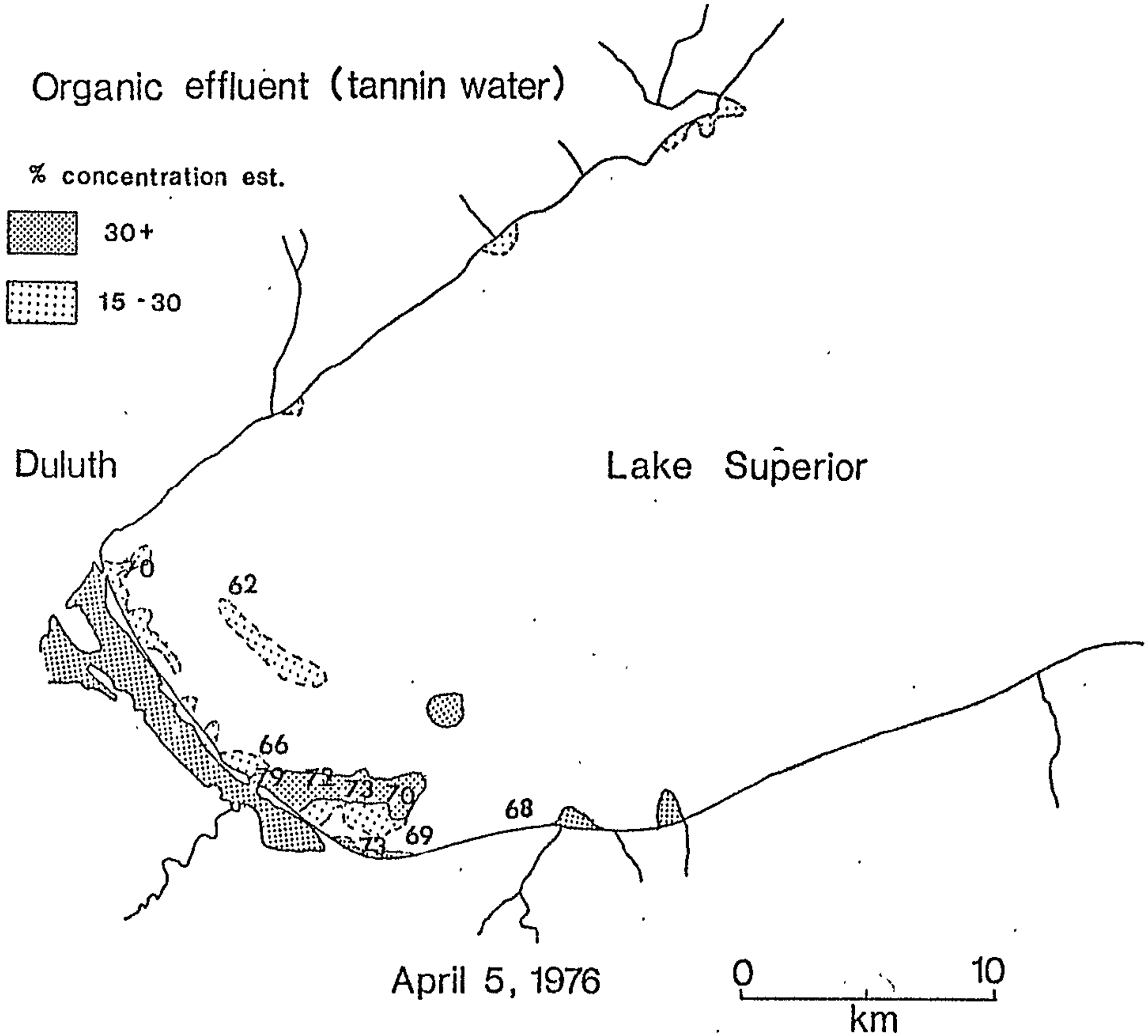
Organic effluent (tannin water)
% concentration est.
30+
15 - 30
Duluth
Lake Superior
70
62
66
79
72
73
70
73
69
68
April 5, 1976
0
10
km

Fig. 3.

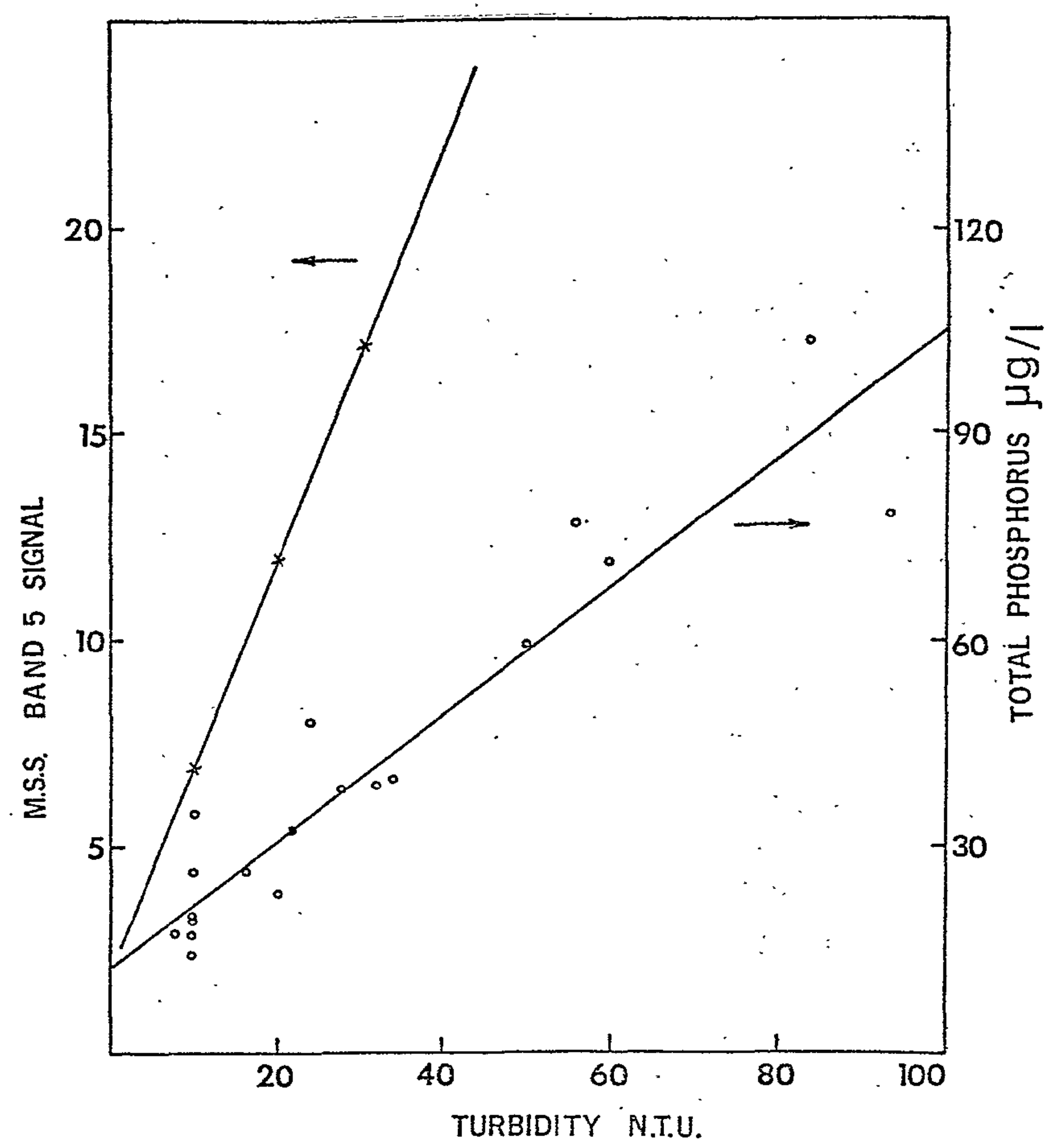
M.S.S. BAND 5 SIGNAL
5
10
15
20
TOTAL PHOSPHORUS μg/l
30
60
90
120
20
40
60
80
100
TURBIDITY N.T.U.

Fig. 4.

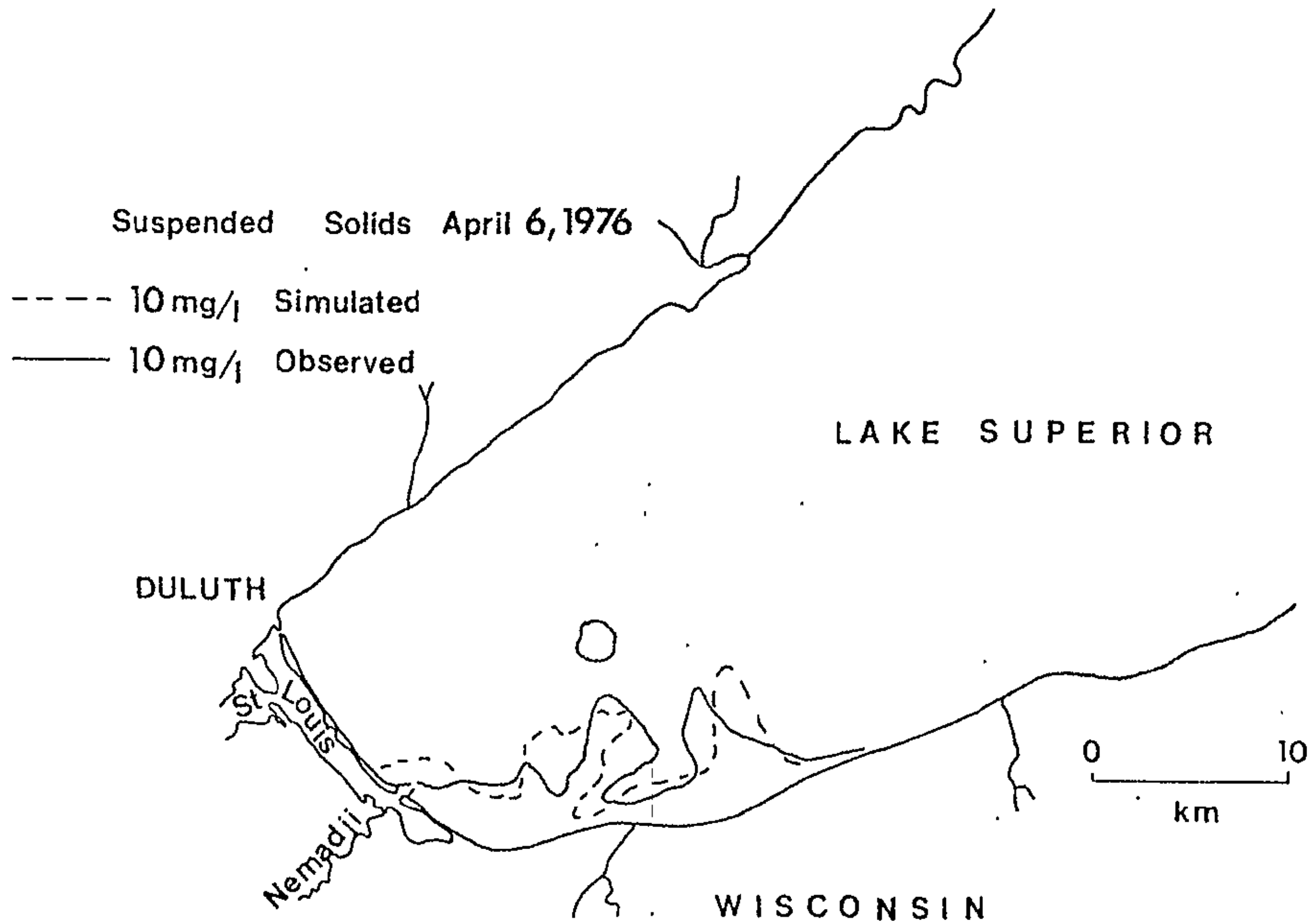
Suspended Solids April 6, 1976
10 mg/l Simulated
10 mg/l Observed
LAKE SUPERIOR
DULUTH
St Louis
Nemadji
WISCONSIN
0
10
km

Fig. 5.

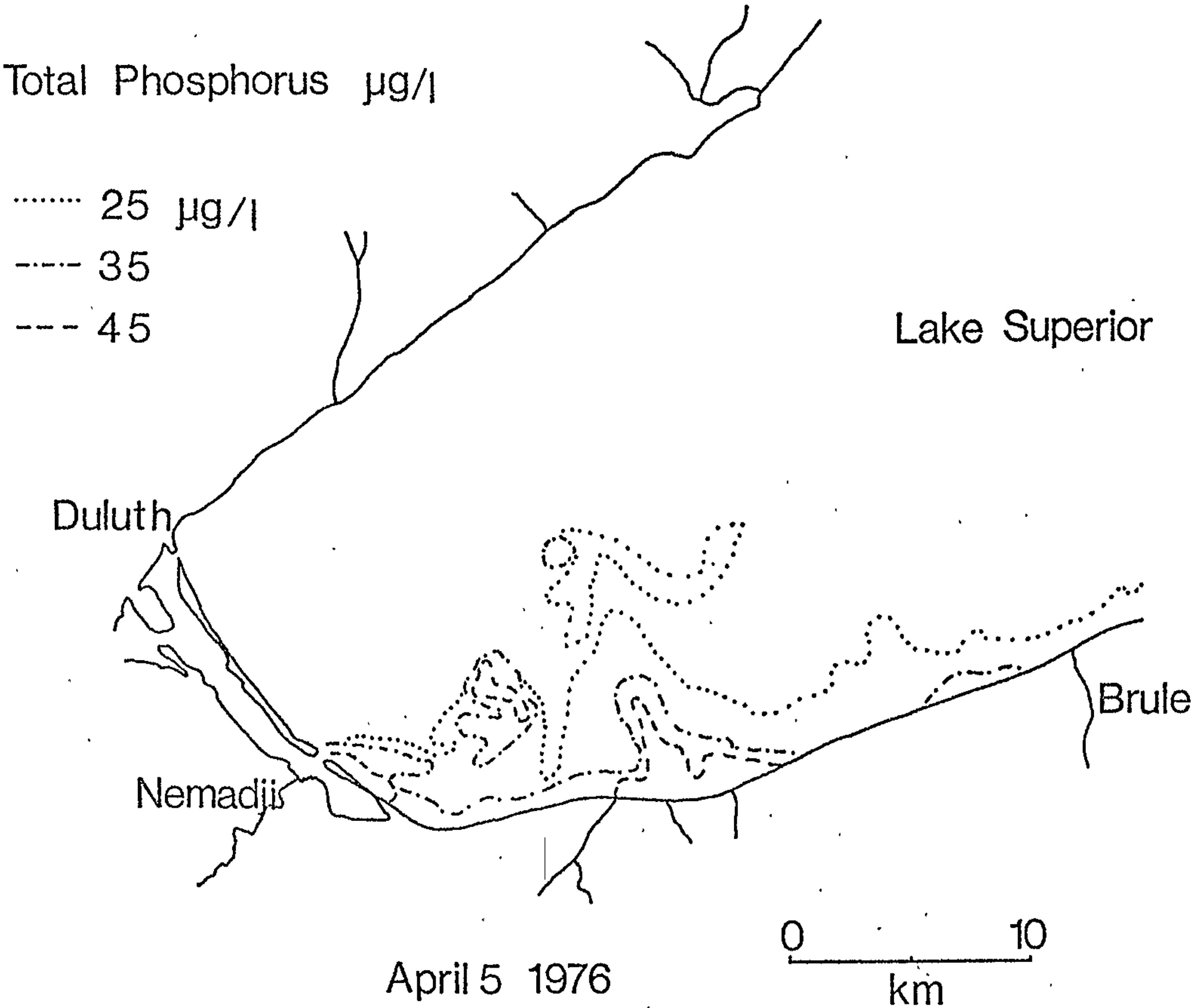
Total Phosphorus µg/l
25 µg/l
35
45
Lake Superior
Duluth
Brule
Nemadji
0
10
km
April 5 1976

Fig. 6.

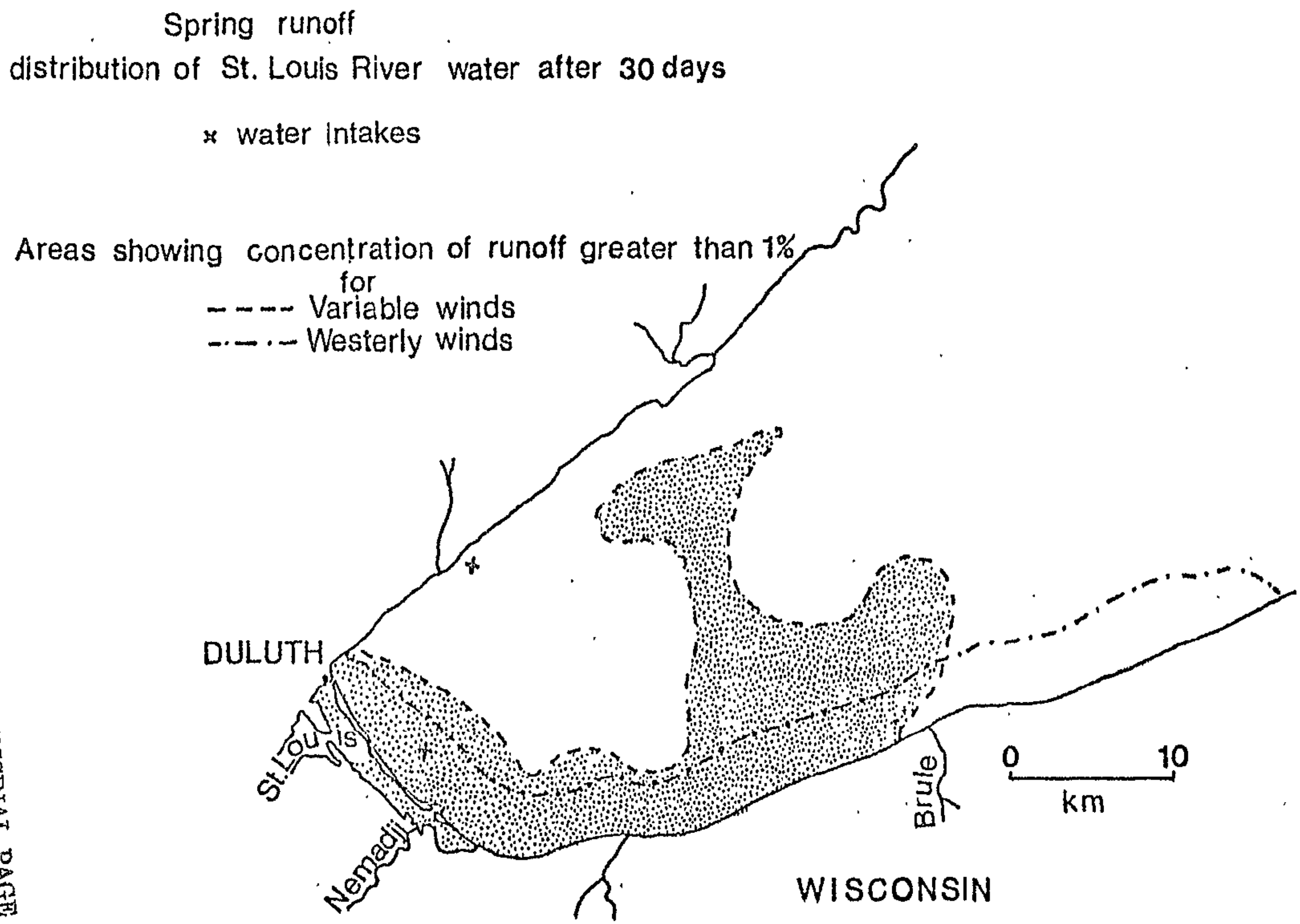
Spring runoff
distribution of St. Louis River water after 30 days
× water intakes
Areas showing concentration of runoff greater than 1%
for
Variable winds
Westerly winds
DULUTH
St. Louis
Nemadji
Brule
0
10
km
WISCONSIN

Fig. 7.

SECTION C

DETECTION OF DUTCH ELM DISEASE

USING OBLIQUE 35MM AERIAL PHOTOGRAPHY

Michael Nash
Drs. Merle Meyer and D.W. French
Institute of Agriculture
University of Minnesota
St. Paul, Minnesota

INDEX

DETECTION OF DUTCH ELM DISEASE
USING OBLIQUE 35MM AERIAL PHOTOGRAPHY

Investigators: Michael R. Nash, Research Assistant
Dr. Merle P. Meyer, Professor of Forestry
Dr. D. W. French, Professor of Plant Pathology
Institute of Agriculture
University of Minnesota
St. Paul, Minnesota

INTRODUCTION

A major difficulty in managing a Dutch Elm Disease control program has been the lack of an efficient low cost system of detecting diseased elms. To date, ground reconnaissance systems are the primary means of locating diseased elms and such systems are slow, costly and often miss trees in an advanced stage of the disease. Elms affected by DED usually start to wilt at or near the top of the tree and early infections are sometimes missed because wilting branches are out of sight of the observer on the ground.

A number of previous trials in Minnesota (Meyer and French 1967, Meyer and French 1968, French 1974) suggested the possibility of vertical stereoscopic color infrared as a reliable disease detection tool. The basic techniques developed by these (and other) studies were evaluated using a major portion of the city of Minneapolis in 1975 by Fairweather, French and Meyer (1976). The entire city was photographed on August 3, 1975, at a scale of 1:9,600 in color infrared with a 9x9-inch format metric camera. A portion of the city also was flown at a scale of 1:6,000. Data obtained on the ground were sufficiently accurate to provide a highly reliable test base.

Interpretation results, using the best available equipment and three qualified interpreters, were disappointing with 47-50% of the diseased elms detected by any one of the interpreters. The percentage of the diseased elms detected was some improvement over the 42% success ratio achieved in a previous study. Detecting only half of the trees is not, however, acceptable for a control program.

Part of the problem in detecting diseased elms has been the confusion of tree crown detail and its condition with the background when photographed vertically (i.e., street surfaces, sidewalks, shrubs, grasses, etc., appearing in the gaps in the tree crowns masked critical details of the crown). The background problems, therefore, could be resolved by photography of the trees at an oblique angle. The infected trees would then be more distinct against a background of healthy trees.

The project reported here was designed to evaluate oblique photography. Because of the cost and difficulty of using a large-format mapping camera at an oblique angle, a small-format (35mm) camera system was selected. The specific objectives of the project were to determine the oblique camera angle which maximizes the amount of tree crown visible to the camera, determine the smallest usable photo scale, determine the optimum time of day (sun angle) for photography, ascertain the camera focal length providing maximum <u>average</u> photo scale without hindering the pilot's ability to navigate accurately, evaluate the relative merits of color infrared (CIR) film photography, and evaluate the time/cost-effectiveness of the system.

EQUIPMENT AND METHODS

The 35mm photography was exposed with the long axis of the frame parallel to the horizon so as to provide the widest possible swath of coverage. As a consequence of the oblique camera angle, the scale of the photographs varied across the narrow width of the format (largest scale on the lower edge nearest the aircraft, smallest scale in the upper edge of view). The average scale of the oblique photograph occurred across the center of each frame parallel to the horizon. For a given scale of photography, the variation in scale across the short axis of the frame varied inversely with the focal length of the lens employed - i.e., the shorter the focal length, the greater the variation in the scale across the frame.

Since it was desirable to maintain the most constant possible scale over the frame, a relatively long focal length was determined to be the most useful. An additional feature of a long focal length was the ability to obtain relatively large photo scales at a safe flying altitude. Consequently, a 135mm focal length was selected as the most desirable. Exposures with this focal length lens at an oblique angle of 45° from a vertical flight altitude of 2,260' produced a photograph with an average scale of 1:7,200 whose scale varied from 1:6,070 at the lower edge, to 1:7,920 at the upper edge. By comparison, employing a 50mm lens to obtain the same average photo scale of 1:7,200, a prohibitively low flight altitude above ground of 835' would be required, and the resulting photo scale range would vary from 1:5,840 on the lower edge to 1:9,880 on the upper edge.

To photograph the sun side of the tree crown for best possible color rendition, the film was exposed with the sun as much behind the camera as possible. Also, the film was exposed with the sun angle greater than the oblique angle of photography (i.e., over 45°) to reduce shadows on the tree crowns as much as possible. During the summer months, these conditions will normally occur between 9:00 A.M. and 3:00 P.M. local sun time for the Minneapolis-St. Paul Area (Table 1).

The photography was accomplished with systematic (pre-planned) parallel flight lines spaced to assure some overlap in coverage between adjacent lines. Also, each exposure in the line of flight was made at an interval which provided some overlap between previous and subsequent exposures (Figure 1). Since a 1:7,200 average scale exposure with a 135mm lens at a 45° angle produces an area of coverage approximately 550 feet parallel to the line of flight by 710 feet across the line of flight, the in-line exposure interval was calculated on the basis of the center of each frame being less than 550' from the preceding, and following, photo centers. Further, initial exposure on a planned line was made (circa) 2,000' before the aircraft was vertically over the line coverage starting point.

A sequence of photographic interval and line spacing to give an overlap of about 15% on all sides of each frame was considered desirable. With a scale of 1:7,200, for example, a line spacing of about 600' (85% of 710') would be required - the number of per-line exposures being calculated on the basis of: Line Length/470' = No. Exposures.

Table 1. Approximate solar altitudes at 45° N. Latitude (Mpls.-St. Paul)

	Time							
	8:30AM &3:30PM	9:00AM &3:00AM	9:30AM &2:30PM	10:00AM &2:00PM	10:30AM &1:30PM	11:00AM &1:00PM	11:30AM &12:30PM	12:00PM noon
June 6	42°	46.5°	51.5°	56.6°	60.5°	64°	66°	67.5°
June 21	43°	47.5°	52.5°	57.5°	61.5°	65°	67°	68.5°
July 6	42°	46.5°	51.5°	56.6°	60.5°	64°	66°	67.5°
July 21	40°	45.5°	50°	55°	58.5°	62.5°	63.5°	65°
Aug. 5	37.5°	43°	47.5°	52°	55°	58.5°	60.5°	62°
Aug. 20	34.5°	39.5°	44°	48°	51°	54.4°	56°	57°

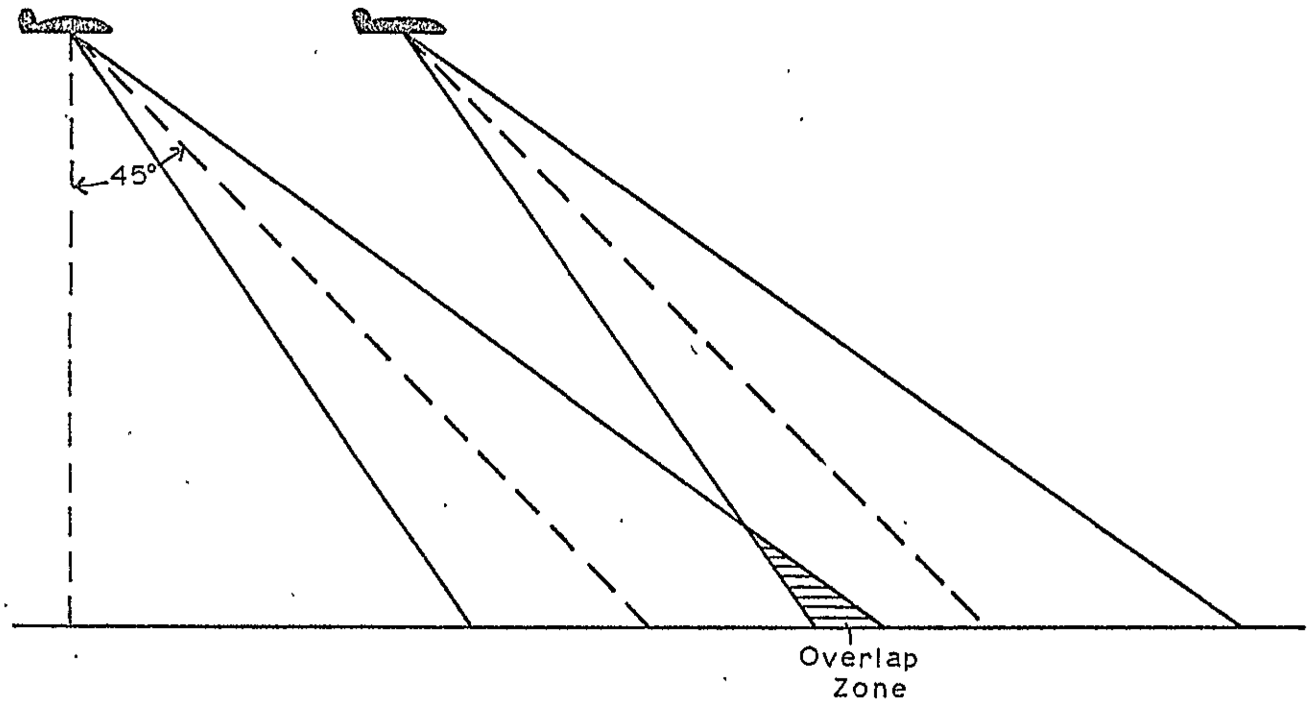

Figure 1. Cross-sectional diagram of camera coverage scheme in the line of flight.

Table 2. Overflight Descriptions

Date	Location	Camera	Type A/C	Film/Filter	Lens	Average Scale	Angle	Purpose
6/30/76	N.W. Mpls.	Nikon F2 Motordrive 35mm	Fixed-wing	Ektachrome-X/HF2 Aerochrome IR Type 2443/W.12	50mm & 135mm	1:7,200 & 1:9,600	25°,40° and 55°	TRAINING & TECHNIQUE DEVELOPMENT FLIGHTS
7/12/76	Lauderdale	Nikon F2 Motordrive 35mm	Fixed-wing	Ektachrome-X/HF2 Aerochrome IR Type 2443/W/12	135mm	1:7,200	45°	
7/22/76	Lauderdale	Nikon F2 Motordrive 35mm	Fixed-wing	Ektachrome-X/HF2 Aerochrome IR Type 2443/W.12	135mm	1:7,200	45°	
8/11/76	E. Mpls.& Lauderdale	Nikon F2 Motordrive 35mm	Fixed-wing	Ektachrome-X/HF2 Aerochrome IR Type 2443/W.12	135mm	1:7,200	45°	
8/3/76	St. Anthony	Nikon F2 Motordrive 35mm	Fixed-wing	Ektachrome-X/HF2 Aerochrome IR Type 2443/W.12	135mm	1:7,200 & 1:8,400	45°	APPLICATIONS TEST FLIGHTS
8/24/76	Como Park	Nikon F2 Motordrive 35mm	Helicopter	Ektachrome-X/HF2	28mm	1:4,200	45°	

AERIAL PHOTOGRAPHY

Four flights starting June 30, 1976, served for developing techniques and two flights in August, 1976, were for evaluating the system (Table 2). The fixed-wing aircraft involved was equipped with a conventional 16-inch diameter camera port in the bottom of the fuselage. A camera tripod mount was devised which placed the camera at the rear edge of the port. The camera could be locked at the selected oblique angle and exposed on a time interval which took aircraft ground speed into account.

GROUND DATA COLLECTION

Ground data were collected by trained, experienced teams directed by the junior author. Locations and descriptions of infected trees were provided in the following form for each area photographed:

<u>Lauderdale</u> - data in narrative form, infected trees identified by address, street, and location in the lot; later transferred to a medium scale photo mosaic overlay.

<u>Minneapolis</u> - data in narrative form as with Lauderdale; later transferred to a medium scale photo mosaic overlay.

<u>North St. Anthony Park section of St. Paul</u> - infected trees located on a large scale, very detailed, city map; later transferred to a photo mosaic overlay.

<u>Como Park in St. Paul</u> - infected trees located on a medium scale photo mosaic overlay.

PHOTO INTERPRETATION SYSTEMS, INTERPRETERS

Three photo interpretation systems were used. The first utilized a

14X binocular microscope to read the individual 35mm slides over a good quality light table. With this viewing unit, the average scale of 1:7,200 was magnified to an approximate scale of 1:500. The 2x2 slides were placed and viewed in the sequence flown along the flight line and match lines between frames in line were easily identified visually and noted from slide-to-slide. A recent photo mosaic (in preference to a planimetric map) was placed alongside the viewing table and suspected trees were noted on an acetate overlay over the mosaic. No particular difficulty was encountered in matching the locations on the 2x2 slides with their locations on the mosaic.

The second viewing system utilized an EK Carousel projector. The 2x2 slides were arranged in the sequence flown and projected onto a 16x24-inch white matte screen in a darkened room. Slide match lines were identified by alternate advance and reversal of adjacent slides. The projected image scale on the screen was approximately 1:400. The interpreter viewing the scene at a comfortable distance viewed the projected image at a somewhat smaller scale than 1:400. The mosaic (with overlay) of the area being surveyed was in a lighted, shielded, position in front of the interpreter where suggested trees could be accurately and conveniently located. In most cases, however, the reflected light from the projection screen was adequate for annotation of the mosaic overlay.

The third viewing system employed a special 6X monocular magnifying viewer - which could be used either with a light table or with skylight illumination (via a special mirror system). It was only used in the analysis of the 1:4,200 scale coverage flown by helicopter on August 24, 1977 of Como Park. As with the other methods, possible diseased elms noted on the individual slides were located in their respective position on the photo mosaic overlay.

Final evaluation of the accuracy of interpretation was acccomplished by comparing the trees detected in the photography with those found on the ground in St. Anthony Park and Como Park.

All four interpreters (one of whom was senior author) were Forestry students (three graduates, one undergraduate) who had had formal training courses in photo interpretation. In addition, all were provided specialized instruction in the three photo interpretation techniques tested in this study. Previously selected and verified cases of DED from portions of the various areas not used in the test were used as aids in DED identification.

In terms of comparative levels of practical photo interpretation experience, the four intepreters were ranked as follows:

Most experienced - Interpreter II (senior author)
- Interpreter I
- Interpreter III
Least experienced - Interpreter IV

In no case were any of the interpreters, including the senior author (Interpreter II), exposed to the ground data prior to, or during, the interpretation process. Every attempt was made, therefore, to assure that the interpretation was as unbiased as possible.

The total area in the study and the number of infected trees in the St. Anthony Park test area were sufficiently large to reduce the interpreter's ability to utilize his memory when involved with more than one interpretation method.

When comparing the color and CIR photography some of the same infected trees were used as test trees. Even so, the chances of recalling individual trees on the color photographs which were previously seen on CIR (or vice-versa) were negligible for the following reasons: (a) although flown on the same day, the color and CIR varied tremendously due to the totally different color rendition, different aspect and frame locations, and variation in sun angle and shadows; and (b) the fact that the interpretation process took place over a considerable period of time.

RESULTS

The percentage of correctly identified cases of Dutch elm disease in the St. Anthony Park test area (scale of 1:7,200) using the binocular microscope system and interpreted by I, II and III ranged from 26-64% with color and from 34-71% with CIR film (Table 3). As expected, the interpreter with the most experience (II) found the highest percentage of diseased trees on both kinds of film. Errors of omission ranged from 36 to 74% with color and from 29 to 66% with CIR film. Errors of commission in relation to total number of deseased trees ranged from 18 to 47% with color and from 16 to 98% on CIR film.

Using the same binocular microscope system and the 1:8,400 scale photography of St. Anthony Park, Interpreter II correctly identified 67% (color) and 74% (CIR) for the total diseased elms known to be present (Table 4). The diseased trees involved here are not the same as those used in the above study (Table 3).

When the 2x2 slides of 1:7,200 scale photography of St. Anthony Park were projected and interpreted by II and III, the most experienced

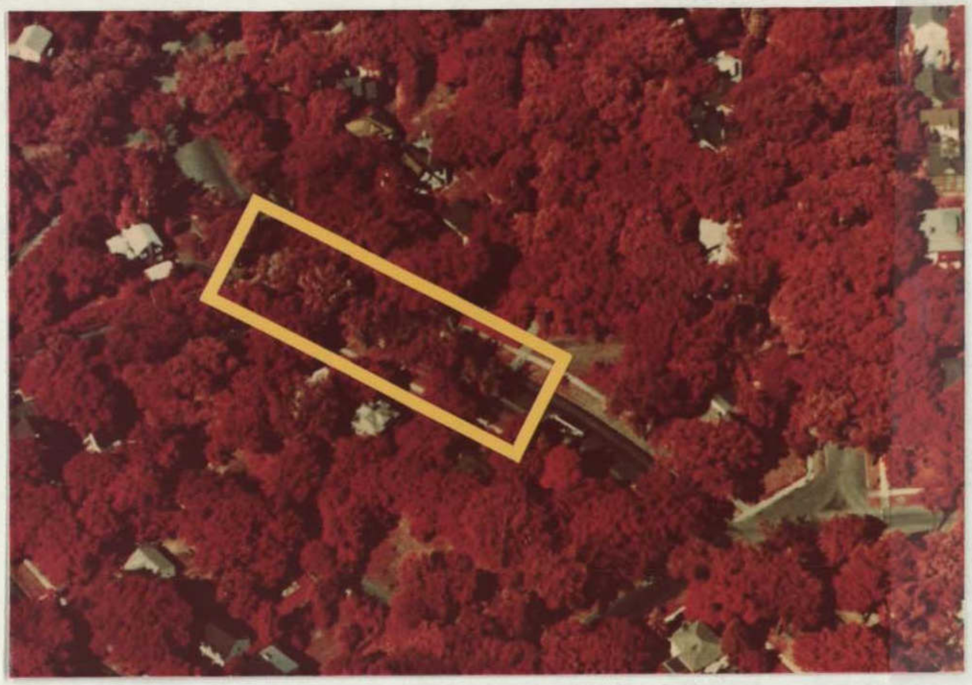

Figure 2. CIR 45° oblique showing diseased trees along street in center of frame. Tree removal crews and equipment are in the location. Flown at a scale of 1:7,200 in August, 1976; flown east-to-west (sun is behine the camera).

Figure 3. Color view of same scene as Figure 2 (above).

Table 3. Number and percentages of diseased elms correctly identified in relation to totals of diseased trees using the Binocular Microsocpe System on 1:7,200 scale St. Anthony Park photography.

	Interpreter					
	I		II[1/]		III[2/]	
	CIR	Color	CIR	Color	CIR	Color
No. diseased trees	120	190	296	273	244	170
No. correctly identified	65	105	210	176	83	45
No. omitted (errors of ommision)	55	85	86	97	101	125
No. incorrect (errors of Commission)	177	82	175	127	38	30
Correctly identified	54%	56%	71%	64%	34%	26%
Errors of Omission	56%	44%	29%	46%	66%	74%
Errors of Commission	98%	43%	59%	47%	16%	18%

1/ Most experienced interpreter

2/ Least experienced interpreter

Table 4. Number and percentages of diseased elms correctly identified in relation to totals of diseased trees using the Binocular Microscope System on 1:8,400 scale St. Anthony Park photography.

	Interpreter II[1/]	
	CIR	Color
No. diseased trees	42	96
No. correctly identified	31	64
No. omitted	11	32
No. incorrect	24	36
Correctly identified	74%	67%
Errors of Omission	26%	33%
Errors of Commission	57%	38%

[1/] The senior author.

interpreter (II) was only slightly more successful than the less experienced person (Table 5). The percentage of correctly identified diseased trees ranged from 54 to 61% with color and from 57 to 64% for CIR - the CIR having provided the best results as was the case when the binocular microscope was used.

With the 6X monocular system, the percentage of correctly identified diseased elms in Como Park (scale of 1:4,200) ranged from 68 to 78% (Table 6). Errors of commission were similar to what had been obtained with the projected 2x2 slide and the binocular microscope. In this study, the most experienced interpreter found the largest number of diseased trees, but the difference between interpreters was not great.

CONCLUSIONS

Although not all of the diseased elms were detected, it was possible with a somewhat experienced photo interpreter to locate up to 78% of diseased elms using color photography at a scale of 1:4,200. The success ratio was 74% with CIR photography at a scale 1:8,400. The errors of commission of 45 and 57%, respectively, in these two studies is not a serious problem - although it would be desirable to reduce these errors so as to eliminate unnecessary ground checking. Experience has shown, however, that some of these so-called errors of commission are actually positive cases of Dutch elm disease and are simply trees which have symptoms only in the very top of their crowns.

Less experienced interpreters had somewhat lower success ratios than experienced interpreters, but even the experienced interpreter with more time with Dutch elm disease would increase his efficiency. With some systems of interpretation, the difference in interpreters was not great.

Table 5. Number and percentages of diseased elms correctly identified in relation to totals of diseased trees using the Projection System on 1:7,200 scale St. Anthony Park photography.

	Interpreter			
	II[1/]		III[2/]	
	CIR	Color	CIR	Color
No. diseased trees	180	195	179	205
No. correctly identified	115	121	102	110
No. omitted	65	74	77	95
No. incorrect	82	72	70	85
Correctly identified	64%	61%	57%	54%
Errors of Omission	36%	39%	43%	46%
Errors of Commission	46%	37%	39%	41%

[1/] Most experienced

[2/] Least experienced

Table 6. Number and percentages of diseased elms correctly identified in relation to totals of diseased trees using the Monocular Viewing System on 1:4,200 scale Como Park color photography.

	Interpreter	
	II[1]	IV
No. diseased trees	56	56
No. correctly identified	42	38
No. omitted	12	18
No. incorrect	25	29
Correctly identified	78%	68%
Errors of omission	22%	32%
Errors of commission	45%	52%

[1]/The senior author.

On the basis of this study, it is difficult to suggest that one system of interpreting the photography is any better than another and the best results will be obtained by experience with any one system. The false color film (CIR) resulted in higher percentages of success than the true color film. At the larger scale of 1:4,200, the success ratio was high but CIR was not involved and, therefore, not compared. Certainly at the smaller scales the CIR film is superior.

Comparing oblique 35mm photography and large scale vertical stereoscopic photography indicates that the 35mm oblique system compares very favorably. With larger scales the oblique photography may provide even higher success ratios than obtained here. As the scale is increased, the cost increases and thus there is a limit to what is a reasonable scale to use for DED detection.

Normally, a new method requires experience and with experience comes refinement and, ultimately, a far better system emerges. In spite of the less than satisfactory success in detecting DED using aerial photography and, in particular, oblique 35mm photography, it does offer promise of a speedy, reasonably efficient technique for locating diseased trees so that they can be dealt with in a prompt manner. This promptness especially early in the season is the essential key to the success of any control program for this and similar diseases.

ACKNOWLEDGEMENTS

Particular thanks go to the forest photo interpreters whose interest and volunteered time made this project possible: Dixon Shelstad, Beth Lutze and Syd Williamson. The assistance of the following IAFHE Remote Sensing Laboratory Personnel with regard to the aerial photography and interpretation is much appreciated: James Marshall, Phillip Grumstrup, Steve Fairweather and Robert Scheierl.

LITERATURE CITED

Meyer, M. and D. French, 1967, Tree disease detection with IR aerial photographs: Proc., Workshop on Aerial Color Photog. in the Plant Sciences, Fla. Dept. Agr., Winter Haven.

Meyer, M. and D. French, 1967, Detection of diseased trees: Photogramm. Engng. 33(4): 1035-1040.

French, D. and M. Meyer, 1968, Aerial survey for oak wilt and DED in Bloomington, MN: Proc., 2nd Biennial Workshop in Aerial Color Photog. in the Plant Sciences, Univ. Fla., Gainesville.

French, D. W., 1974, Forest disease detection and control: IARSL Res. Report 74-2, Univ. of Minn. College of Forestry, St. Paul.

Fairweather, S., D. French and M. Meyer, 1976, Utilization of CIR aerial photography for detection of DED: Ann. Rep. to U. Minn. Space Science Center NASA Proj. NGL 24-005-2631.

APPENDIX

FIELD EVALUATION OF SMALL-SCALE FOREST RESOURCE AERIAL PHOTOGRAPHY

By

J.R. Marshall and M.P. Meyer

J. R. MARSHALL
M. P. MEYER
University of Minnesota College of Forestry
St. Paul, MN 55108

Field Evaluation of Small-Scale Forest Resource Aerial Photography*

Experienced professional field forest resource managers considered scales smaller than 1:24,000 unacceptable for standard data collection.

ABSTRACT: *Economic considerations prevent most forest land managers from obtaining conventional black-and-white medium-scale (circa 1:15,000-1:20,000) forest aerial photography at adequate intervals. Were smaller-scale photos comparably useful, the savings in procurement and interpretation costs could be used for more frequent overflights.*

Forested portions of Minnesota were flown with black-and-white infrared at scales of 1:15,840; 1:24,000; and 1:31,680 and with color infrared at scales of 1:31,680 and 1:80,000. Trained cooperators who analyzed the photographs under field-use conditions with high quality viewing equipment considered black-and-white forest photography at a scale of 1:24,000 marginally acceptable at best, and judged scales smaller than 1:24,000 unacceptable for the resource management applications involved. Overall, good quality summer black-and-white infrared 1:15,840 scale photography was preferred, but many user-cooperators were enthused about the potential of small-scale coverage as a supplement to, not a replacement for, conventional medium-scale photography.

Color infrared transparencies provided more information than black-and-white prints of equivalent scale, but were considered overly cumbersome for day-to-day use under existing field office conditions.

INTRODUCTION

A GROWING PROBLEM in aerial photography applications to forest management in many parts of the U.S. is the lack of funds for obtaining the proper type(s) of photo coverage at adequate intervals in time. A frequently suggested approach to reduced forest photo procurement cost is the use of smaller photo scales (Latham and McCarty, 1972; Lauer and Benson, 1973; Ulliman, 1975). As a case in point, 1:31,680 scale photo coverage in lieu of 1:15,840 scale over a given area would require about 75 percent fewer prints. Such a print number reduction would be reflected in substantially lower costs of acquisition, purchase, storage, handling, and interpretation. However, this would not be a logical substitution if it were

* Presented at the Annual Convention, American Society of Photogrammetry, March 1977, Washington, D.C. Authorized for publication as Sci. Jour. Series Article 9780 by the Univ. of Minn. Agr. Expt Sta., St. Paul.

accompanied by any significant reduction in interpretable information quantity and quality (Nash, 1963). A preliminary study by Ulliman and Meyer (1971) under laboratory conditions suggested the possibility of using smaller scales of summer infrared black-and-white forest photography without serious information loss. This investigation subjected their idea to a field test by experienced cooperators.

Study Area Locations

In order to provide results useful to a large number of forest photography users in the Lake States, a study area with a wide diversity of typical vegetation types—Itasca County, Minnesota—was selected (Figure 1). Secondary sites were chosen in Becker and Mahnomen counties in order to sample slightly different types of areas. Whereas Itasca County typifies the sub-boreal forest of northeastern Minnesota, Becker and Mahnomen are representative of the drier western prairie border counties.

Aerial Photography

The principle objective of this study was to determine the degree of acceptability, to field practitioners, of summer infrared black-and-white infrared photography at a scale, or scales, smaller than the conventional 1:15,840. As Figure 1 and Table 1 indicate, recent 1:15,840; 1:24,000; and 1:31,680 scale coverage was obtained over the study areas. Although all of the 1:24,000 and 1:31,680 scale black-and-white photography was flown in the period 1972-74, only the 1:15,840 over Becker and Mahnomen counties was flown during the same period. In Itasca County, due to problems of weather and flight scheduling, the 1:15,840 scale was not flown in the 1972-74 period and existing 1966-69 coverage had to be utilized as a basis for comparison. This posed no problem insofar as the field cooperators were concerned because of their familiarity with the area and their ability to select representative locations and cover types which had undergone negligible change since photography.

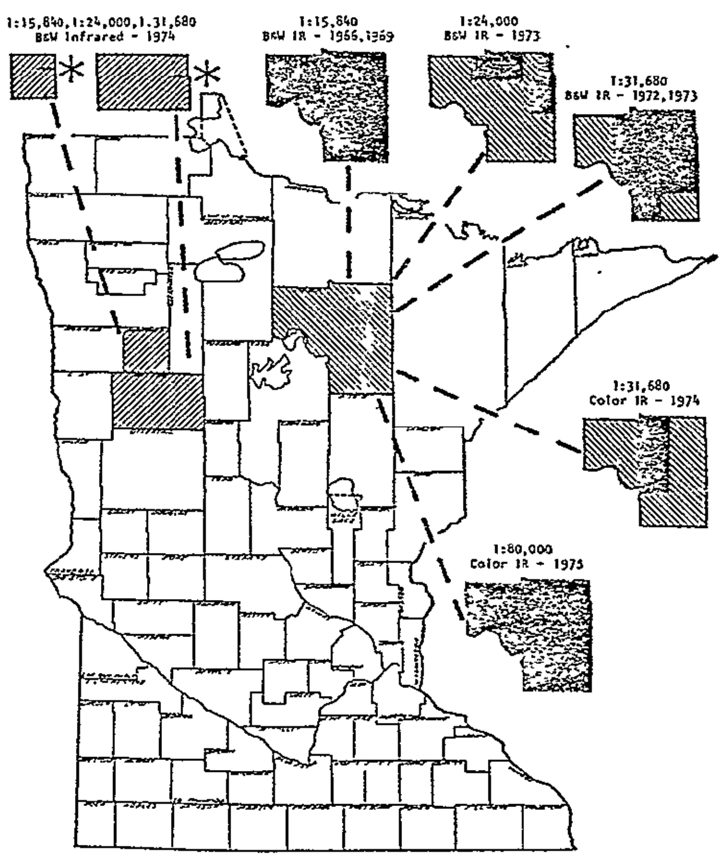

FIG 1. Aerial photography employed in the study.

TABLE 1. CHARACTERISTICS OF PHOTOGRAPHY TESTED

County	Dates	Film & Filter[1]	Scale	Contracting Agency	Field Cooperators Agency	Field Cooperators Individual
BECKER	Sept 1974	Aero IR 2424 Wratten 12	1:15,840 1:24,000 1.31,680	MinnDNR UMinnCollFor UMinnCollFor	MinnDNR	Baumgartner & Rupert
MAHNOMEN	Sept 1974	Aero IR 2424 Wratten 12	1:15,840 1:24,000 1:31,680	MinnDNR UMinnCollFor UMinnCollFor	MinnDNR	Rodewald & Kresien
ITASCA						
· Entire County	Jul-Aug-Sept 1966 July 1969	Aero IR 2424 Wratten 12	1:15,840 1:15,840	ItascaCy USFS	USForServ MinnDNR	Goldie & Goltz[2] Tarbell, Licke, Nixon, Tornes, Mooty, Pierce, & Stenlund[3]
· North Central	Aug-Sept 1972 Jul-Aug 1973	Aero IR 2424 Wratten 12	1:31,680	UMinnCollFor	ItascaCy IRRRB BlandinPapCo	Marshall Kobs, Lauber, Johnson & Olson Peterson, Morrow & Hanson
· North Central and Northeast	Aug-Sept 1973	Aero IR 2424 Wratten 12	1:24,000	UMinnCollFor	RajalatimbCo BoiseCascadeCorp SoilConsServ	Ringold Hubbard, Olson & Cutler Nyberg & Sharp
· North Central	Sept 1974	Aero Ektachrome IR, Wratten 12	1:31,680	UMinnCollFor	USForServ MinnDNR ItascaCy IRRRB	Goldie & Johnson Tarbell, Cass, Nixon & Tornes Marshall Lauber
· Entire County	Aug-Sept 1975	Aero Ektachrome IR, Wratten 12	1:80,000	UMinnCollFor	BlandinPapCo	Peterson, Morrow Hanson

[1] Wratten 12 equivalent used
[2] Both forest management and forest soils specialists involved.
[3] Both forest and wildlife management specialists involved

A secondary purpose of the study was to expose as many cooperators as possible to training and applications experience in the use of color infrared photography and, subsequently, solicit their reactions to it. To this end, a sizable portion of Itasca County was flown with color infrared at a scale of 1:31,680 in 1974 and the entire county was flown at a scale of 1:80,000 (i.e., "quad-centered") in 1975.

STUDY DESIGN, PROCEDURES

USER-COOPERATOR SELECTION AND TRAINING

Because of the intense interest and degree of use of forest aerial photography, a large number of capable cooperators volunteered their services, including users in forestry, wildlife management, and soil science in both public and private sectors of forest land management.

Despite their experience in photo interpretation, additional training in preparation, handling, and viewing and use of the various types of photography was essential. This was accomplished at each cooperator's home station on an individual basis to the degree necessary. Additionally, periodic visits to cooperators served to answer questions and maintain the quality and scope of the evaluations.

PHOTO INTERPRETATION EQUIPMENT, INTERPRETATION AIDS

Although most of the cooperators use aerial photography on a near-daily basis, viewing equipment usually consists of a pocket stereoscope and marginal office working conditions (Figure 2). In order to assure the best possible viewing conditions and consistency, each cooperator was provided with suitable viewing equipment and lighting (Figure 3). For the cooperators involved in viewing the 9×9-inch CIR transparencies, a specially equipped light table was also provided.

In addition to vegetation cover type and condition class delineation, most users frequently perform distance measurements and calculate areas. To provide comparative tests of these functions between photo scales, area dot grids and aerial photo rulers designed for all scales to be tested were furnished.

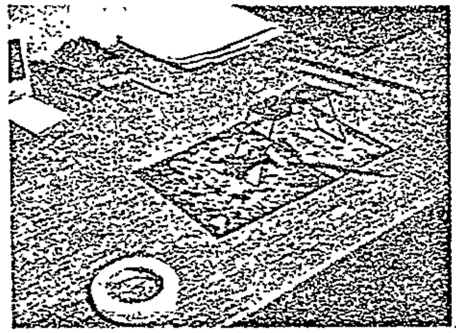

FIG 2. Typical viewing station encountered in the field offices of project cooperators—often crowded, noisy, and poorly lit.

FORMS OF AERIAL PHOTOGRAPHY TESTED

The 9×9-inch prints were printed to the same contrast level on double weight semi-matte paper. Glossy prints also were provided but rejected as unsuitable, primarily because pencil annotations could not be made on the glossy surface.

The color infrared 9×9-inch transparencies were cut, sleeved, and labelled before delivery to the cooperators. All cooperators involved in this portion of the study were given thorough instruction and assistance in handling, viewing, and detail delineation.

To the extent appropriate to their particular work, each cooperator performed specific tasks on the different scales of photo coverage:

- Vegetation cover type and condition class mapping.
- Area measurement
- Distance measurement.
- Planning (e.g., road layout, timber sale design, fire planning).

DESIGN OF TEST QUESTIONNAIRE

All too often, photo interpretation tests are conducted under laboratory or pseudo-field conditions with interpreters who lack the experience and on-the-ground management application's knowledge, typical of the average professional field user. Although such tests lend themselves to various experimental designs capable of producing quantitative results bearing a high degree of statistical credibility, the final results often may not be meaningful in real world terms.

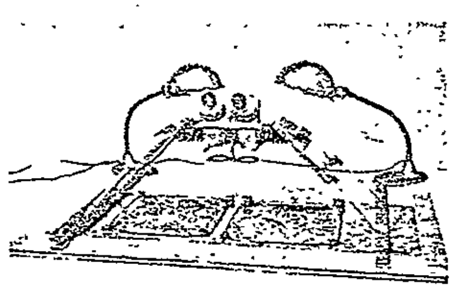

FIG 3 Equipment provided each cooperator for photo evaluation: mirror stereoscope with 3× binoculars, railtype viewing table, metal viewing board with magnets, and individually adjustable lamps.

Because of the diverse biological nature of the scene subjects under analysis by the skilled forest resource photo interpreter, individual subjective judgment based upon experience is his (the interpreter's) most powerful tool in the information extraction and management decision process. As a consequence, this study was designed from the outset to ascribe ratings to the various photo types under evaluation on the basis of the professional judgment of experienced, skilled forest cooperators. A highly structured, quantitatively based assessment was a logistic impossibility under the circumstances and, even if it were, there was no known reliable way in which it could adequately reflect the most useful photo quality evaluator (i.e., individual experience). Consequently, completion of a narrative evaluation based upon the following items was requested from each cooperator at the termination of his work:

Background information.

- Agency/firm, location, management objectives.
- Types, source, and adequacy of photography used.
- Interpretation equipment and facilities.
- Interpreter background.

Test photography evaluation.

- Attitude toward test photography—before and after.
- Comparison of tonal contrast and image qualities.
- Effect of viewing equipment and light quality.
- Summary of reaction to black-and-white photography scale variations.
- Impact of mandatory small-scale photography use.
- Color infrared transparencies.

RESULTS

USER-COOPERATOR PROFILE

On the average, the cooperators use 1:15,840 scale summer black-and-white infrared photography primarily for the purpose of forest resource inventory and management planning.

The typical user has a professional resource management background, including two college-level courses in aerial photo interpretation and eight to ten years of on-the-job interpretation experience.

All cooperators felt the need for more frequent photo coverage, and considered the tonal contrast and image detail quality of black-and-white forest aerial photography to have declined significantly in recent years. Additional research in aerial photography and photo interpretation was deemed desirable, along with additional training sessions, in order to improve the interpreter's ability to identify and classify forest vegetation.

TEST PHOTO EVALUATIONS

It was intended that each cooperator perform sufficient operations with the test photography to arrive at a sound judgment of preference supported by specific reasons. A summary of average cooperator reactions follows:

(1) *Attitude toward smaller scales of black-and-white photography.* Quite negative at first, but became more positive as they grew accustomed to it and began to visualize possible applications.

(2) *Tonal contrast and image quality of smaller-scale black-and-white photography.* Considered much superior to the 1:15,840 scale control photography. Apparently, although the test photography was acquired under typical commercial job conditions and standard contract specifications, the close supervision afforded its procurement apparently resulted in better quality photography than had been accomplished on the previously flown control photography.

(3) *Stereo perception, vegetation and soils classification, and measurement tasks.* (a) although the cooperators generally found more vegetation and/or soil detail visible on the smaller scales than anticipated, there were problems in delineating and labelling small features; (b) distance and area measurement accuracy declined with scale decrease; (c) useful, relative relief perception was attainable with all scales, some feeling they could visualize relief better with the smaller scales; (d) adequate navigation and location accuracy could be accomplished down to a scale of 1:31,680, but at 1:80,000 it became difficult or impossible to achieve; (e) timber volume estimate accuracy declined significantly with photo-scale decrease; (f) timber sale boundaries could be outlined fairly well but area estimates of adequate accuracy were impossible with scales smaller than 1:24,000; and (g) fire planning operations and preliminary road and trail location favored small-scale photography because minute detail was unnecessary and it was helpful to view large areas.

(4) *Time required.* An average of three to four mandays per cooperator. In general, for equivalent tasks, interpretation time increased as the scale decreased.

(5) *Improved viewing equipment and lighting systems.* Readily accepted by all users, who agreed that a mirror stereoscope was essential for viewing smaller-scale photography (greater magnification, wider field of view). It was also agreed that proper lighting was more important than had been generally realized.

(6) *Reaction to smaller scales of black-and-white photography. Favorable.* (a) the larger ground area covered by fewer photographs resulted in better large-area perspective and fewer photos to prepare, view, and carry; (b) less problem in matching detail from photo-to-photo; especially good for road and trail layout; (c) less expensive to procure; (d) broad cover types were more easily and quickly delineated; (e) general patterns of relief were more evident over large areas; and (f) broad soil patterns often were easier to discern. *Unfavorable.* (a) field use limited by inability to study small (important) features without sophisticated viewing equipment; (b) sufficiently accurate measurements not achievable; (c) adequate resource detail often lacking, even with great magnification; (d) necessary detail sometimes visible, but could not be delineated due to space limitations; and (e) one out of four experienced more eyestrain.

(7) *Impact of mandatory use of small-scale photography.* Availability of a sophisticated viewing and lighting system would be an absolute requirement. Additionally, the following undesirable adjustments in interpretation methods and procedures would be necessary: (a) the current minimum type area of 1-2 acres would have to increase to 5-10 acres for 1:24,000-1:31,680 scale photographs, and to 10-30 acres for 1:80,000, depending upon the cover type; (b) minimum linear measurements would increase from the current 0.5 chain on 1:15,840 scale photographs to 1 chain for 1:24,000-1:31,680 scale photographs, and to 5 chains for 1:80,000 scale; (c) ability to discriminate cover type species mixtures, size classes, and stocking would decrease significantly with scale decrease; (d) ground navigation, spot location, and area measurement accuracies would decrease significantly with scale decrease; (e) some system of enlarging the small-scale-generated cover type maps

would be required for field use; and (f) the amount of field checking would increase as the photo scale decreased, at least for the important vegetation and/or habitat types.

(8) *Color infrared transparencies vs. black-and-white prints.* Color infrared transparencies at scales of 1:31,680 and 1:80,000 subjected to various applications tests by a number of cooperators resulted in the following reactions: (a) initially, some found the unnautral colors an obstacle to interpretation, but less a problem as they worked with the film; (b) although, to them, a surprising amount of information was available even on the smaller-scale color infrared, it was difficult to capitalize upon it due to problems of delineation and field checking; (c) eyestrain was not greater than normal, except for one interpreter; (d) mental fatigue was a serious problem for several users; (e) considerable effort with undisturbed concentration was necessary to interpret the smallest scale, a condition hard to achieve in many field offices; and (f) in lieu of matte acetate and pencils used with black-and-white contact prints, clear film overlays and inking pens are necessary for interpretation of film transparencies, a situation found to be difficult and inconvenient and which produced a product difficult to transfer with available mapping equipment and facilities.

In summary, most of the cooperators unreservedly preferred conventional black-and-white photography. Although they could clearly see more detail with color infrared transparencies of equivalent scales, they indicated color infrared would be more palatable if available in the form of color prints which retained the high information level noted on the color infrared transparencies. The substantially higher cost of procurement of the color infrared also posed a deterrent to its favorable consideration.

Summary

The overwhelming preference for a photography type/scale combination was 1:15,840 scale summer black-and-white infrared. A scale of 1:24,000 was determined to be less desirable than 1:15,840, but might be substituted as a matter of necessity providing the overall quality was exceptionally good. A few photo interpretation tasks can be accomplished equally well (or better) with a scale of 1:31,680 as with 1:15,840, but a scale of 1:80,000 is much too small for the majority of required resource management applications.

Color infrared transparencies had the advantage of greater clarity and increased information than was noted on equivalent scales of summer infrared black-and-white photography. However, since aerial photo use is essentially a day-to-day operational function for most field resource management personnel, color infrared transparencies were considered difficult to employ due to the need for specialized facilities and equipment in viewing, interpretation, detail delineation and mapping, and related difficulties in field checking. To this must be added the cost differentials in procurement and use of color infrared photography.

Acknowledgments

This project was funded principally by the McIntire-Stennis Cooperative Forestry Research Program and the University of Minnesota Agricultural Experiment Station. Additional funding from the University of Minnesota Graduate School and NASA's Office of University Relations provided the 1972-74 photography of portions of Itasca County and of Becker and Mahnomen Counties, respectively. Special thanks go to the user-cooperators who gave so generously of their time and skills and without whom accomplishment of the project would have been impossible: District Ranger Melvin Goldie and Soil Scientist Grant Goltz, USDA, Forest Service; Soil Scientist Paul Nyberg, USDA, Soil Conservation Service; Area Staff Forester Roy Tarbell, Game Biologist Jack Mooty, Area Forest Manager Kenneth Baumgartner, and Regional Forest Manager John Rodewald, all of the Minnesota Department of Natural Resources; Land Commissioner William Marshall, Itasca County; Forester L. Chris Peterson, Blandin Paper Company; Forester Stanley Ringold, Rajala Timber Company; Chief Forester John Hubbard, Boise Cascade Corporation; and Staff Forester Orlyn Olson, IRRRB Forestry Division.

References

Latham, R., and T. McCarty, 1972, Recent developments in remote sensing for forestry: *Journal of Forestry*, v. 70(7), p. 398-402.

Lauer, D., and A. Benson, 1973, Classification of forest lands with ultra-high altitude, small-scale, false-color infrared photography: IUFRO S6.05 *Symp.*, p. 143-162.

Nash, A., 1963, Futuristic photo interpretation: *Photogram. Eng.*, v. 29(2), p. 340-342.

Ulliman, J., and M. Meyer, 1971, The feasibility of forest cover type interpretation using small-scale aerial photographs: *Proc.* 7th Symposium on Remote Sensing of Environment, p. 1219-1230.

Ulliman, J., 1975, Cost of aerial photography: *Photogram. Eng.*, v. 41(4), p. 491-497.

SECTION D

USE OF LANDSAT IMAGERY FOR THE STATEWIDE MAPPING AND CLASSIFICATION OF PEAT RESOURCES

Drs. J.E. Goebel, and M. Walton
Minnesota Geological Survey

INDEX

USE OF LANDSAT IMAGERY FOR THE STATEWIDE MAPPING AND CLASSIFICATION OF PEAT RESOURCES

Investigators: Dr. Joseph E. Goebel
Dr. Matt Walton
Minnesota Geological Survey

CURRENT USES OF LANDSAT IMAGERY

LANDSAT imagery is becoming an increasingly useful tool for investigating the geology of Minnesota. The Minnesota Geological Survey is currently applying LANDSAT imagery to the problem of evaluating peat resources.

Peat is Minnesota's newest mineral resource, both in terms of current interest and geologic age. Over wide areas it is still growing and may, to some degree, be a renewable resource, bridging the gap between fossil fuels and living biomass. Most of the peat in the contiguous United States is in Minnesota, covering about 7 million acres or about 13% of the area of the state. This area is estimated to contain about 13 billion tons, dry weight, of peat, equivalent in heat to about 7 billion tons of bituminous coal (Soper, 1919). Peat is very low in sulfur and readily gasified. It is now exploited on a large scale in northern Europe for conversion to electrical power. In 1975, Minnegasco (Minnesota Gas Company) applied to the Minnesota Department of Natural Resources for a lease on 200,000 acres of peatlands north of the Red Lakes with a view toward development for gasification.

The attractions of peat are obvious in a state otherwise lacking energy resources. Peat is valuable as an organic soil conditioner.

Peatlands can be highly productive for protein-rich plants, as well as for that distinctive gourmet delicacy of the state, wild rice. The ecology of peat is fragile and it plays an important role in the hydrology of large areas. The great blanket bog north of Red Lakes and other bogs are of unique scientific interest and value.

The environmental consequences of mining peat of various kinds and the problems of either restoring mined peatlands or reclaiming them for alternative uses need study. European experience is not entirely applicable because our continental climate is significantly different from the more maritime climate of northern Europe. There are many questions that cannot be answered until our peatlands are adequately mapped, classified and studied. The question of the proper use of peat resources is bound to be controversial. Further research on peat is essential.

Three related studies are discussed in this report. Briefly, these are: (1) 1:1,000,000 scale map identifying peat in its geologic environs, (2) a study of techniques for selecting suitable LANDSAT products for identification of artificial drainageways in peatlands and (3) a study of techniques for selecting suitable LANDSAT products for identification of artifically disturbed areas in peatlands.

The single most important objective of all the studies was to determine the optimum synergistic combinations of LANDSAT products for monitoring artificial disturbances of all kinds in peatlands.

PROJECTED USES OF LANDSAT IMAGERY

Pending are two other studies involving LANDSAT products. The first of these involves determination of the synergistic relationships between LANDSAT imagery products and other remote sensing materials useful in geologic investigations. We hope that by systematically studying combinations of remote sensing data we can identify geologic information not readily apparent from examination of each type of datum separately. Hence the use of the term "synergistic" to describe the study.

The other study is an inventory study of the quality and quantity of peatlands. We plan to acquire analytic ground truth from reported field studies, including data such as thickness, bulk density and type of peat as well as pH and water table conditions. By performing a stepwise multiple regression analysis, we hope to clarify the relationships between these peatland characteristics and the environment surrounding the deposits. Our ultimate goal is to identify the quantity and quality of peatlands in Minnesota.

PEAT ENVIRONS OF MINNESOTA

Thomas Malterer's 1976 map, General Map of Peat Deposits of Minnesota, was registered to LANDSAT imagery which confirmed the location of peat as shown on the map. Therefore, Malterer's identification of the extent of peatlands was used as a basis for distinguishing peatlands in our studies.

The following classification scheme which indicates the relationship of peat to its geologic environment was used to prepare a map of peat environs of Minnesota (Plate 1). We first divided peatlands into bogs and fens. Bogs consist dominantly of sphagnum moss and woody peat underlain by decomposed reed sedge peat. There are two types of fens, those located in basins or topographic lows and those restricted to valleys or channels. Fens in basins consist dominantly of woody or reed sedge peat and may overlie gyttja. Fens along channels consist dominantly of reed sedge peat. We drew boundaries to indicate peatlands that occur on glacial lake plains. Boundaries also indicate peatlands associated with glacial outwash as well as those associated with the Des Moines lobe, a shaly, calcareous, clayey till.

ARTIFICIAL DRAINAGEWAYS AND DISTURBANCES

The primary focus of these two studies was to develop a method for identifying artificial drainageways and disturbances in peatlands using LANDSAT imagery. Since the materials and the methods used in the study of drainageways were the same as for the study on artificial disturbances, the procedures discussed below apply to both studies.

We selected a region near the Red Lakes and subdivided this into six smaller subregions. Figure 1 shows the location of the study region. We defined areas as artificially disturbed if they were of sufficient size, tonal contrast and shape to indicate modern intervention by man for purposes of agriculture, livestock or forestry. Artificial drainageways were defined to be agricultural and forestry drainage canals, road ditches and railroad ditches.

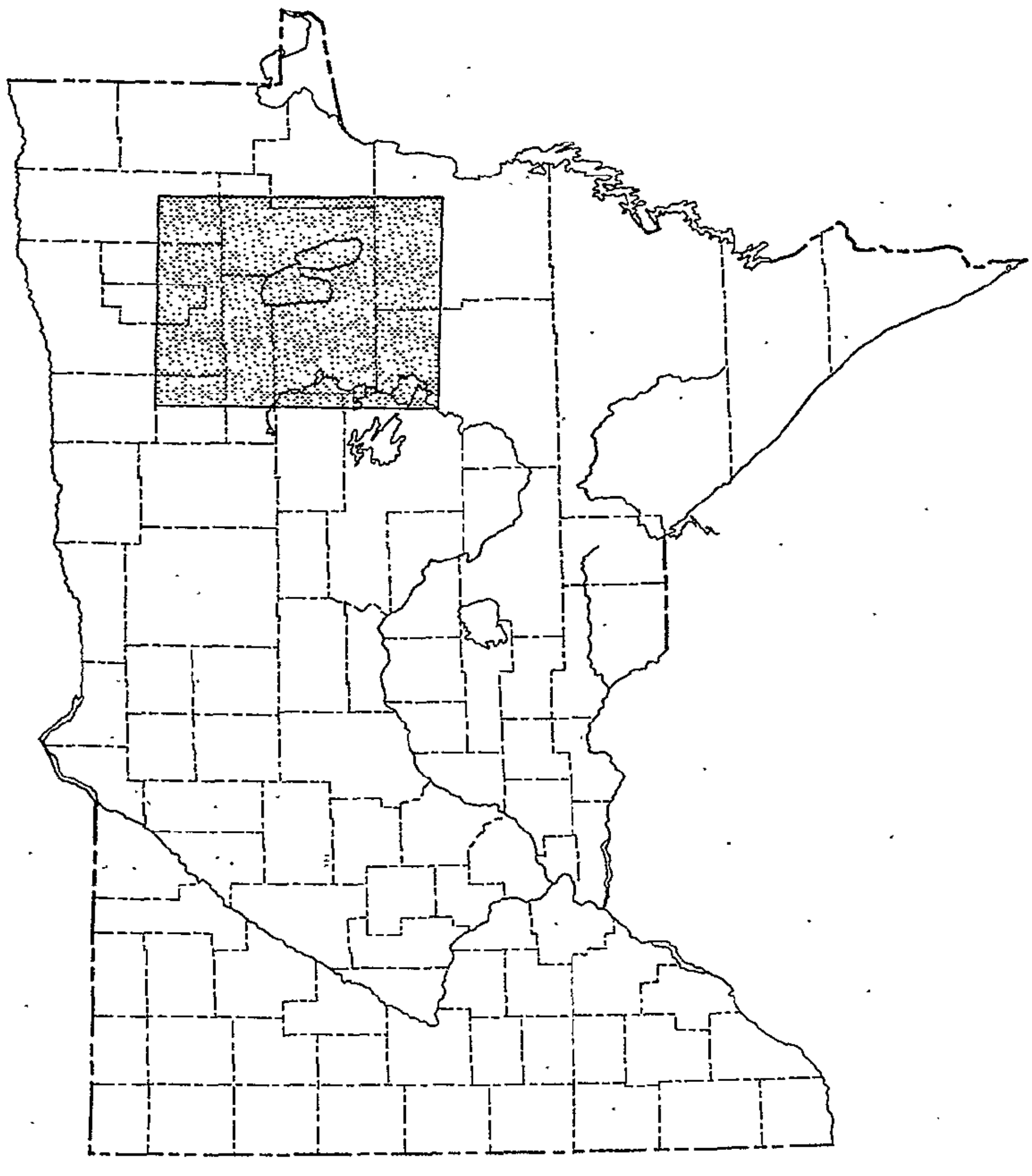

Figure 1. Location of the Study Region

PLATE 1

PEAT ENVIRONS OF MINNESOTA

By

Joseph E. Goebel

1978

The images used were standard LANDSAT composite products at a scale of 1:1,000,000, measuring 7.5 inches on a side with the following characteristics:

Spring: snow off, leaf off, standard LANDSAT product, false color composite, film transparency.

Summer: leaf on, late season, standard LANDSAT product, false color composite, film transparency.

Winter: snow covered, band 7, black and white film transparency.

Band 5: summer, black and white film transparency.

Band 6: summer, black and white film transparency.

Band 7: summer, black and white film transparency.

The term "scene" refers to the specific study region. The term "image" refers to the LANDSAT products. We used six images to study each scene. We looked at LANDSAT images for summer, winter and spring. We also looked at bands 5, 6 and 7 for summer imagery. Areas of artificial drainage and/or artificial disturbances were identified and recorded on overlays. We considered features visible on each season's imagery, each band of summer imagery and on pairs of images, (i.e., season to season, band to band and band to season combinations). We noted whether the features were common on both images in each pair or unique to only one image. Characteristics common to a pair of images were assessed as a single occurrence in tabulating the data.

We determined the total area for each of the six subregions of the study and the total peatland in each and computed the ratio of peatland to total area of the subregions and the entire region. We measured the extent of disturbed areas and artificial drainage in each subregion and computed the ratios of artificially drained or disturbed peatland to peatland of each subregion.

We used the ratios from the six subregions to compute the standard deviation, the mean and the standard score for the entire study region for each season, band and combination of image pair.

These data are summarized in Tables 1 through 11. Finally we evaluated all the combinations of image pairs in terms of their utility as peat use indicators and determined which combinations provided the most useful information.

The following section summarizes a general LANDSAT product selection procedure which we found useful. The procedure was designed to enable users to identify any particular feature in question and prepare efficient training sets for a wide variety of inventory purposes. It permits regional and temporal control of features and can be applied to other problems beside peatland monitoring.

1. Select a test site.

2. Isolate the areal extent of the environment or conditions where the feature under study is most likely to be found, i.e., identify peatlands before attempting to monitor their use.

3. Using a standard light table and standard LANDSAT photographic products, compare bands within seasons and seasons with each other for one scene to determine the most useful combinations. Images from years with drastically different conditions may also be compared.

4. Systematically identify the feature under study on each image independently to maintain objectivity.

5. Calculate the frequency of occurrence of the feature being investigated. Establish the reliability of its occurence

Table 1 Sample Sizes

For this study an area of 24,200 sq. Km. containing 4330 sq. Km of peatland was subdivided into six sample areas which have the following surface areas of which the indicated part is peatland:

Sample Area No.	Surface Area Km^2	Peatland Km^2	Proportion as Peatland
I	4700	880	.187
II	3800	1230	.324
III	4000	1440	.360
IV	3900	100	.026
V	4200	190	.045
VI	3600	490	.136
Whole Area	24200	4330	.179

Table 2 Ratios in Km/Km^2 of artificial drainageways to peatland for each image and for the entire region.

	SUBREGIONS							MEAN	SD	Z
Season	I	II	III	IV	V	VI	Entire Region			
Spring Bands 4-5-7	.014	.017	.005	----	----	.006	.010	.007	.007	4.6
Summer Bands 4-5-7	.016	.015	.009	.010	.011	.004	.012	.011	.004	2.4
Winter Band 7	.018	.013	.009	.020	.005	----	.011	.011	.006	4.6
Summer Band 5	.007	.006	.002	.010	.005	.002	.004	.005	.003	2.5
Summer Band 6	.006	.007	.001	----	----	.004	.004	.005	.003	3.8
Summer Band 7	.014	.011	.008	----	----	.002	.009	.009	.008	5.3

Table 3 Sum in Km/Km^2 of the ratio of the total artificial drainageways to peatland observed on pairs of images. If the drainageways ratios are common to both images, they are counted only once. (Net ratios)

	SUBREGIONS							MEAN	SD	Z
Season	I	II	III	IV	V	VI	Entire Region			
Spring & Winter	.024	.021	.015	----	----	.012	.017	.012	.010	5.7
Spring & Summer	.022	.028	.014	.010	.011	.008	.019	.014	.009	5.3
Winter & Summer	.019	.020	.017	.010	.011	.006	.017	.014	.008	3.2
Summer Bands 5 & 6	.011	.011	.001	.010	.005	.006	.007	.007	.004	3.1
Summer Bands 5 & 7	.016	.014	.007	----	.005	.004	.010	.008	.006	4.1
Summer Bands 6 & 7	.015	.013	.007	----	----	.004	.009	.007	.006	5.0

Table 4 Sum of Ratios in Km/Km^2 of artificial drainageways to peatland common to two images.

	SUBREGION							MEAN	SD	Z
Season	I	II	III	IV	V	VI	Entire Region			
Spring & Winter	.003	.010	.005	----	----	.004	.006	.007	.006	3.0
Spring & Summer	.008	.004	.008	----	----	.004	.006	.006	.005	3.3
Winter & Summer	.009	.009	.006	----	----	.006	.007	.006	.005	3.3
Summer Bands 5 & 6	.001	.002	.001	----	----	----	.001	.001	.001	2.0
Summer Bands 5 & 7	.003	.004	.001	----	----	----	.002	.001	.001	2.8
Summer Bands 6 & 7	.005	.007	.001	----	----	.002	.003	.003	.003	2.8

Table 5 Sum of Ratios in Km/Km^2 of artificial drainage to peatland for drainageways not common to a pair of images.

Season	SUBREGION I	II	III	IV	V	VI	Entire Region	MEAN	SD	Z
Spring & Winter	.020	.011	.010	----	----	.008	.012	.008	.007	4.7
Spring & Summer	.014	.024	.006	.010	.011	.004	.013	.012	.007	2.3
Winter & Summer	.010	.012	.011	----	.011	----	.010	.007	.006	3.3
Summer Bands 5 & 6	.010	.008	.001	----	.005	.006	.006	.005	.004	1.5
Summer Bands 5 & 7	.013	.010	.006	----	.005	.004	.008	.006	.005	3.2
Summer Bands 6 & 7	.010	.007	.006	----	----	.002	.006	.004	.004	4.2

Table 6 Comparison of image pairs with respect to the ratio in Km/Km^2 of Artificial drainageways to peatland to determine data not common to both images.

Image Comparison	Ratio for this image by subregion						
	I	II	III	IV	V	VI	Entire Region
Spring to Winter	.010	.006	.001	----	----	.002	.004
Winter to Spring	.010	.005	.011	----	----	.005	.007
Summer to Winter	.005	.004	.003	----	.011	.001	.004
Winter to Spring	.005	.008	.010	----	----	.007	.007
Summer to Winter	.008	.003	.005	----	.011	.001	.005
Spring to Spring	.007	.011	.001	----	----	.003	.005
Band 5 to Winter	.003	.001	----	----	.003	.002	.001
Band 7 to Spring	.010	.008	----	----	----	.003	.007
Band 7 to Winter	.009	.005	----	----	----	.001	.005
Band 6 to Spring	.001	.001	.002	----	----	.001	.001
Band 6 to Winter	.005	.005	----	----	----	.004	.003
Band 5 to Spring	.005	.003	.001	----	.003	.002	.003

Table 7 Ratios in Km^2/Km^2 of artificially disturbed peatland to peatland for each image.

Season	SUBREGION I	II	III	IV	V	VI	Entire Region	MEAN	SD	Z
Spring Bands 4-5-7	.075	.045	.026	.202	.116	.076	.055	.090	.063	10.7
Summer Bands 4-5-7	.067	.013	.010	.212	.063	.016	.030	.063	.077	10.3
Winter Band 7	.024	.016	.011	.030	.011	----	.014	.015	.011	1.0
Summer Band 5	.022	.005	.003	.061	.016	.002	.009	.018	.022	4.7
Summer Band 6	.028	.011	.003	.010	.011	.004	.011	.011	.009	2.1
Summer Band 7	.049	.021	.011	----	.005	.010	.021	.016	.018	6.7

Table 8 The ratios in Km^2/Km^2 of the sum of the total artificially disturbed peatland observed on superimposed pairs of images to peatland observed for each image.

	SUBREGION							MEAN	SD	Z
Seasons	I	II	III	IV	V	VI	Entire Region			
Spring & Winter	.089	.039	.031	.172	.116	.071	.056	.086	.101	8.8
Spring & Summer	.098	.043	.026	.243	.116	.071	.060	.100	.078	10.8
Winter & Summer	.077	.022	.017	.192	.063	.016	.036	.065	.068	7.9
Summer Bands 5 & 6	.038	.011	.006	.051	.021	.004	.015	.022	.019	1.8
Summer Bands 5 & 7	.050	.023	.012	.051	.021	.008	.024	.027	.019	0.4
Summer Bands 6 & 7	.056	.022	.009	.010	.016	.010	.023	.021	.018	4.7

Table 9 Ratios in Km^2/Km^2 of artificially disturbed peatland common to both images to total peatland common to both images.

	SUBREGION							MEAN	SD	Z
Season	I	II	III	IV	V	VI	Entire Region			
Spring & Winter	.028	.022	.007	.051	.011	.006	.017	.021	.017	1.0
Spring & Summer	.044	.015	.010	.172	.063	.020	.026	.054	.061	10.3
Winter & Summer	.013	.007	.006	.040	.011	----	.008	.013	.014	2.8
Summer Bands 5 & 6	.013	.005	.001	.010	.005	----	.005	.006	.005	0.5
Summer Bands 5 & 7	.020	.003	.002	----	.005	.002	.006	.005	.007	3.2
Summer Bands 6 & 7	.020	.011	.005	----	----	.002	.009	.006	.008	5.5

Table 10 Ratio in Km^2/Km^2 of the sum of the artificially disturbed peatland areas which are not common for the two images to the peatland for each region.

	SUBREGION							MEAN	SD	Z
Season	I	II	III	IV	V	VI	Entire Region			
Spring & Winter	.060	.017	.024	.121	.105	.065	.040	.065	.042	9.6
Spring & Summer	.052	.028	.017	.071	.053	.051	.034	.045	.020	4.7
Winter & Summer	.065	.015	.011	.152	.053	.016	.029	.052	.054	7.4
Summer Bands 5 & 6	.025	.007	.005	.040	.016	.004	.011	.016	.014	2.3
Summer Bands 5 & 7	.030	.020	.010	.051	.016	.006	.017	.022	.016	1.1
Summer Bands 6 & 7	.036	.011	.005	.010	.016	.008	.014	.014	.011	1.9

Table 11 Comparison of image pairs with respect the ratio in Km^2/Km^2 of artificially disturbed peatland to peatland for each region for determining data not common to both images.

Ratio for this image by SUBREGION

Season	I	II	III	IV	V	VI	Entire Region
Spring to Winter	.042	.014	.016	.112	.096	.064	.032
Winter to Spring	.017	.003	.008	.008	.005	.001	.007
Summer to Winter	.050	.008	.006	.150	.051	.017	.022
Winter to Spring	.015	.008	.005	.002	.003	.001	.007
Summer to Winter	.009	.005	.005	.010	.011	.009	.008
Spring to Spring	.044	.024	.011	.014	.040	.010	.026
Band 5 to Winter	.009	.004	.002	.046	.010	.001	.005
Band 7 to Spring	.020	.016	.009	----	.003	.005	.012
Band 7 to Winter	.038	.007	.004	.002	.005	.005	.010
Band 6 to Spring	.007	.004	----	.008	.008	.003	.004
Band 6 to Winter	.015	.006	.003	.005	.001	.002	.006
Band 5 to Spring	.011	.001	.002	.030	.017	.002	.005

with suitable statistical methods. For our study a portable hand calculator sufficed.

6. Deduce the "contributors," i.e., the best kinds of images and combinations for identifying and/or monitoring the feature under study.

RESULTS

PEAT ENVIRONS OF MINNESOTA

The following information about peat and its geologic and geographic settings was deduced from the map, "Peat Environs of Minnesota" (Plate I).

1) Peat is found more often in the cool, poorly drained portions of Minnesota. As a result, peat is concentrated in the northern two-thirds of the state.

2) Most peat is associated with the calcareous, shaly, clayey glacial drift deposited by the ice of the Des Moines lobe.

3) Large peat bogs are associated with major glacial lake plains, such as Glacial Lake Agassiz. On the other hand, peat fens are associated predominantly with outwash and smaller glacial lake plains. The Anoka Sand Plain is one typical example. Peat associated with till tends to occur in regions where till from a glacial event was deposited on top of stagnant ice from an earlier glacial event. The eventual melting of the stagnant ice resulted in a collapse of the overlying till to form the basin for the bog.

4) Peat develops an integral part of the post-glacial drainage most commonly occurring as fens in basins or topographic lows

associated with the upper reaches of streams. Other fen deposits are commonly found in glacial meltwater channels.

Peatlands comprise about 13 percent of Minnesota's total surface area. Our study region around the Red Lakes is 18 percent peatland and includes part of the largest peat bog in the country. It represents a reasonable sampling of the types and amounts of peat. The six subregions of the study region contained percentages of peat ranging from 3 to 36 percent. This indicates some geologic and environmental control on the distribution of peat.

IDENTIFICATION OF ARTIFICIAL DRAINAGEWAYS

We attempted to identify the combinations of bands and/or seasons that would maximize the length of drainageways recognized in the study region.

From Table 2 we see that summer band 7 was the single best band for identifying the drainageways. Winter was the single best season. The comparison of band 5 with band 7 provided the highest ratio of drainageways common to peatlands on both images, with statistically significant results. However the most successful interpretation resulted from a comparison of spring with winter images as indicated on Table 3.

Many drainageways were identified on only one of a pair of images especially on seasonal comparisons. This indicates that seasonal comparisons or at least standard false color composites, presented the largest number of canals most effectively.

A customized false color composite can be generated with colors chosen to optimize the contribution of each band to the composite image. It appears from this study that a false color composite of bands 5 and 7 for spring and band 7 for winter should produce reliable and extensive identification of artificial drainage ways. One alternative would be to combine band 7 from spring, summer and winter images. A more elaborate option would be a comparison of a combination of bands 5 and 7 for spring with a combination of bands 5 and 7 for summer plus band 7 for winter.

IDENTIFICATION OF ARTIFICIAL DISTURBANCES

From table 7 we see that spring standard false-color composites were the most useful for identifying the greatest amount of artifically disturbed areas in peatlands. Summer standard false color composites were also helpful. Band 5 and band 7 were the most useful individual bands.

The spring-summer comparison on Table 8 was outstanding when seeking artificially disturbed areas common to both images of a pair. Bands 5 and 7 of the summer imagery identified the same artificially disturbed areas most frequently of band to band comparisons.

By reviewing the significance of the derived data in Table 10 we determined that the greatest interpretational discrepancies occurred with the spring-winter seasonal comparison and with individual band comparisons between bands 5 and 6 (Table 10). That is areas on one image were not recognized on the other image.

In order to distinguish as many different aspects of peatland use as possible, spring, summer and winter images should be combined into a custom false color composite. Band 7 from spring and winter plus band 5 from summer should provide the most successful identification.

Another option which may maximize interpretive capability is to combine one band from 3 different seasons on a single custom false color composite or generate two false color composites using any combination of the following bands: bands 5 and 7 from spring , bands 5 and 7 for summer or band 7 of winter.

CONCLUSIONS

1. LANDSAT imagery was useful in placing peat bogs and fens in their respective geologic settings.
2. Artificial disturbances and drainageways in peatlands can be recognized and classified with the help of LANDSAT imagery and supplemental ground truth.
3. The procedure outlined in this report permits evaluation of LANDSAT or other remote sensing products with respect to combinations which optimize interpretation of the desired conditions or feature. It is an efficient, rapid, economical method for evaluating the utility of remote sensing products for regional inventory.

LITERATURE CITED

Eng, Morris T., 1976. An aerial evaluation of peat resources, fen patterns, and other surficial deposits, Koochiching County, Minnesota: Reconn. Maps no. 1, western half 2nd no. 2, eastern half, Minn. Dept. of Natural Resources, Div. of Minerals, 1:250,000.

Goebel, Joseph E., 1978. Geologic Map of Minnesota Quarternary Geology: Minn. Geol. Survey, Univ. Minn. State map SM-1, 1:500,000.

Malterer, Thomas M., and Grigal, D., 1976, General map of peat deposits of Minnesota: Soil Science Dept., Univ. Minn., unpublished, 1:500,000.

Soper, E.K., 1919, The peat deposits of Minnesota: Minn. Geol. Survey Bull. 16, 261 p., maps, various scales.

SECTION E

ASSESSMENT OF ICE COVERAGE OF SELECTED LAKES AND STREAMS IN MINNESOTA AND RELATIONSHIP TO METEOROLOGICAL, HYDRAULIC, AND MAN-MADE CONDITIONS

Dr. H. Stefan, A. Fu and A. Wood
St. Anthony Falls Hydraulic Laboratory
University of Minnesota
Minneapolis, Minnesota

INDEX

ASSESSMENT OF ICE COVERAGE OF SELECTED LAKES AND STREAMS IN MINNESOTA AND RELATIONSHIP TO METEOROLOGICAL, HYDRAULIC, AND MAN-MADE CONDITIONS

Investigators: Dr. H. Stefan
Alec Fu
Addison Wood
St. Anthony Falls Hydraulic Laboratory
University of Minnesota
Minneapolis, Minnesota

INFORMATION FROM LANDSAT IMAGERY ON FREEZE-OVER

LANDSAT 1 and 2 images have been used to determine onset of ice coverage of lakes in northern, central and southern Minnesota in November and December 1975. The scenes are identified in Fig. 1. They carry the identification numbers Path 29, Row 27 (North), Path 30, Row 28 (Central), and Path 29, Row 29 (South). Dates of available LANDSAT scenes and cloud coverage during the period of interest, i.e. from October 20, 1975 through January 15, 1976, are shown in Table 1. Similar information for the falls of 1972, 1973 and 1974 has been obtained and imagery for those years has been ordered.

Although the percentage cloud cover identified in Table 1 has been high, much information could be extracted form LANDSAT scenes. LANDSAT imagery was acquired in the form of 9 x 9 black and white prints (Band No. 6) and for cloud covers up to 90 percent. Examination of the images under a magnifying glass shows ice covers quite clearly.

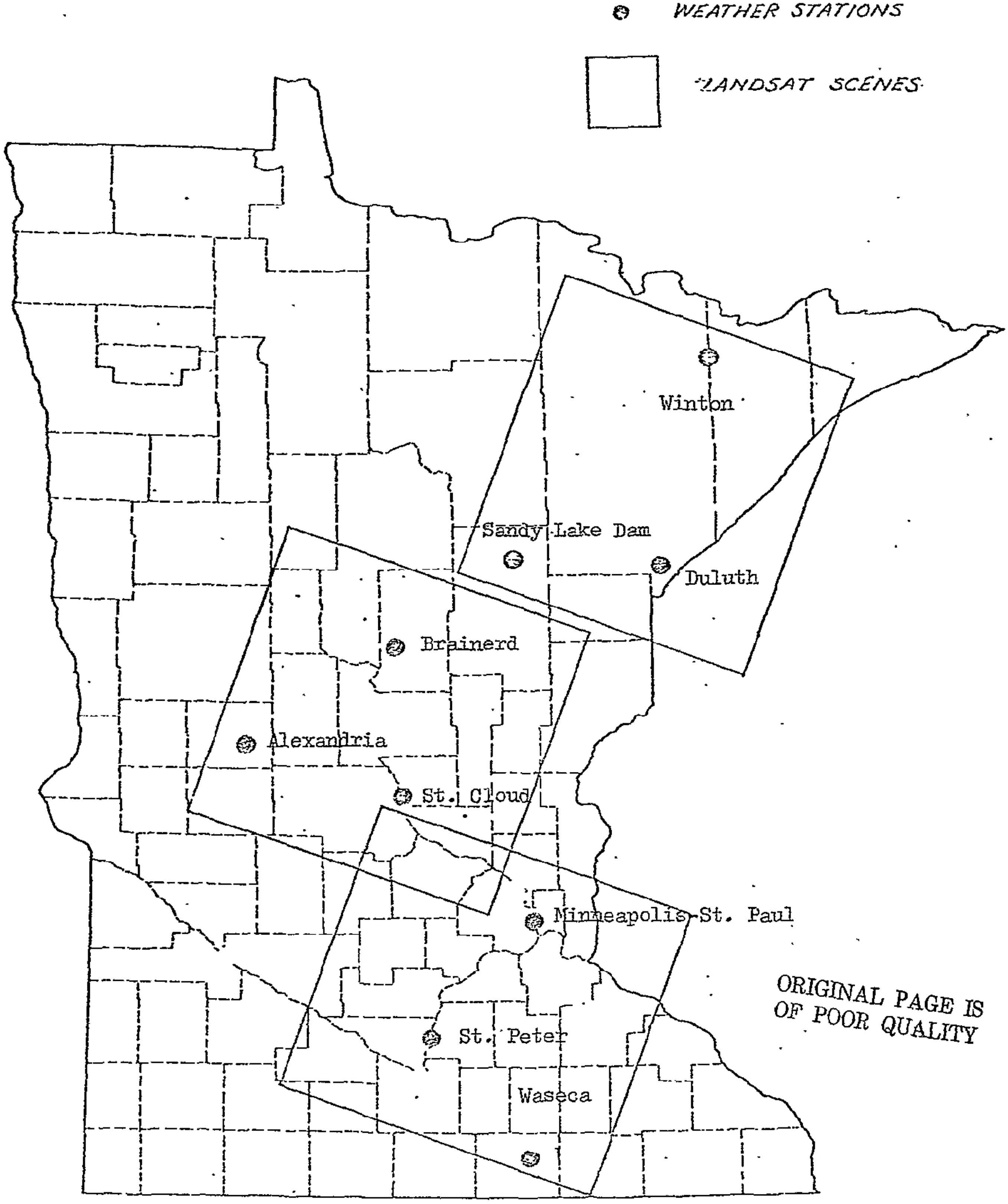

ORIGINAL PAGE IS OF POOR QUALITY

FIG. 1 - Map of Minnesota showing coverage of selected LANDSAT scenes and locations of weather stations.

TABLE 1. Available LANDSAT Scenes, Fall 1975

North

Date	Quality	Cloud Cover (%)
10/27/75	Fair	90
11/05/75	Fair	90
11/14/75	Fair	10
11/23/75	Fair	60
12/02/75	Unavailable	100
12/11/75	Unsatisfactory	70
12/20/75	Unavailable	100
12/29/75	Fair	90
1/07/76	Fair	20
	Average	70

Central

Date	Quality	Cloud Cover (%)
10/28/75	Excellent	80
11/06/75	Excellent	90
11/15/75	Fair	90
11/24/75	Fair	30
12/03/75	Unavailable	100
12/12/75	Excellent	20
12/21/75	Excellent	20
12/30/75	Excellent	40
1/08/76	Unavailable	100
1/17/76	Unavailable	90
	Average	66

South

Date	Quality	Cloud Cover (%)
10/27/75	Excellent	0
11/05/75	Fair	10
11/14/75	Excellent	10
11/23/75	Fair	70
12/02/75	Unavailable	100
12/11/75	Unsatisfactory	90
12/20/75	Unavailable	100
12/29/75	Fair	80
1/07/76	Fair	20
1/16/76	Excellent	10
	Average	49

From 10 to 30 lakes were selected on each LANDSAT scene. The Minnesota Lake Inventory provided the name, the range, township and section, and an identification number for each selected lake. This information was subsequently used to find the median lake depth and the lake surface area from the Clean Lakes Inventory File (CLIF) of the Minnesota Pollution Control Agency.

Ice coverage was classified in 5 categories according to which portion of the lake was ice-covered.

(a) open water

(b) nearly fully open

(c) half open

(d) nearly closed

(e) closed △

Observations on ice coverage were tabulated.

Under clear sky, no difficulty was encountered in the interpretation. Water appeared black and ice greyish white or white on the images. In cases when light to heavy cloud cover prevailed, it was often difficult to distinguish ice and snow from overlying cloud cover on images. In such circumstances, no interpretation was made.

A. O. Lind (1973) in an earlier study already indicated the presence of various ice tones, patterns and arrangements of ice as well as open water in a LANDSAT image of Lake Champlain taken on January 8, 1973. In Lind's opinion, MSS band 5 imagery provided the most useful data. Lind states: "While it was not possible to differentiate open water from one-two day old ice, it was possible to interpret the total signatures of the frozen portion in terms of freezing history or age. The dark gray tones of new smooth ice were found to contrast with the medium gray tones of older ice and the rough texture of wind-jammed bay ice."

During the study of the Minnesota lakes, the presence or absence of ice covers was generally well identified and few instances of ambiguity were encountered.

Occasionally, a lake remained open even after all the surrounding lakes were closed in winter and thawed in early spring before all the other lakes did. These lakes were receiving artificial thermal input and must be treated separately in future analysis. A separate list of such water bodies is attached in the Appendix.

In addition, three weather stations in each LANDSAT frame were identified. They are also shown in Fig. 1. Since the objective is to relate weather to ice coverage, results on ice coverage were plotted separately for lakes located in the vicinity of each weather station.

Figures 2a, 2b, 2c and 2d give examples of ice coverage for four different locations and lakes of different depths. The effect of lake depth on the delay in freeze-over is quite apparent. That delay was also determined theoretically. Not expected was the dependence on lake surface area. A sample graph showing the dependence of ice conditions on lake surface area is given in Fig. 3. The correlation is quite good. Sometimes lake depths and lake sur-

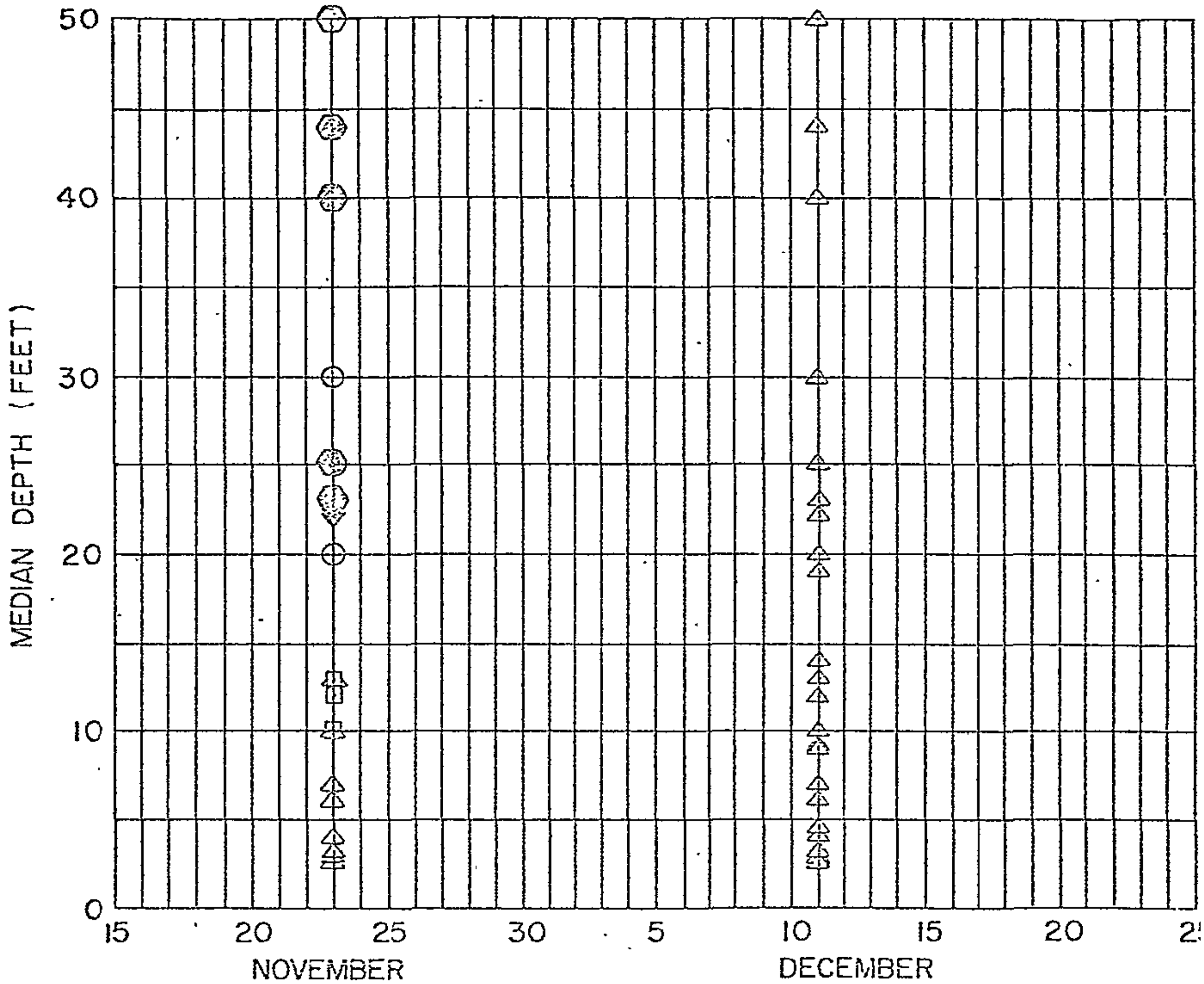

FIG. 2a - Lake ice coverage in fall 1975 as determined from LANDSAT images as a function of lake depth. Lakes near Winton Power Station.

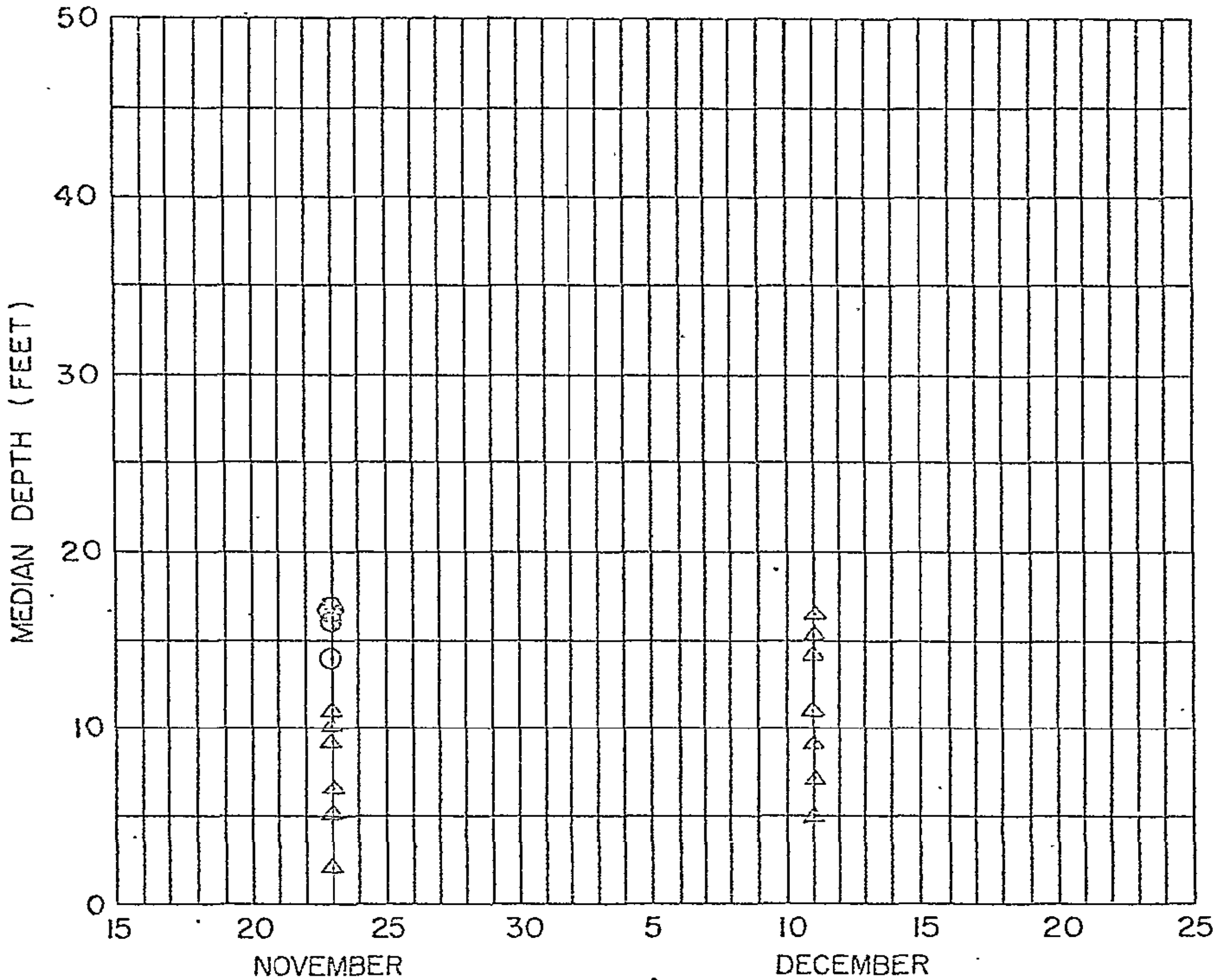

FIG. 2b - Lake ice coverage in fall 1975 as determined from LANDSAT images as a function of lake depth. Lakes near Duluth Airport Weather Station.

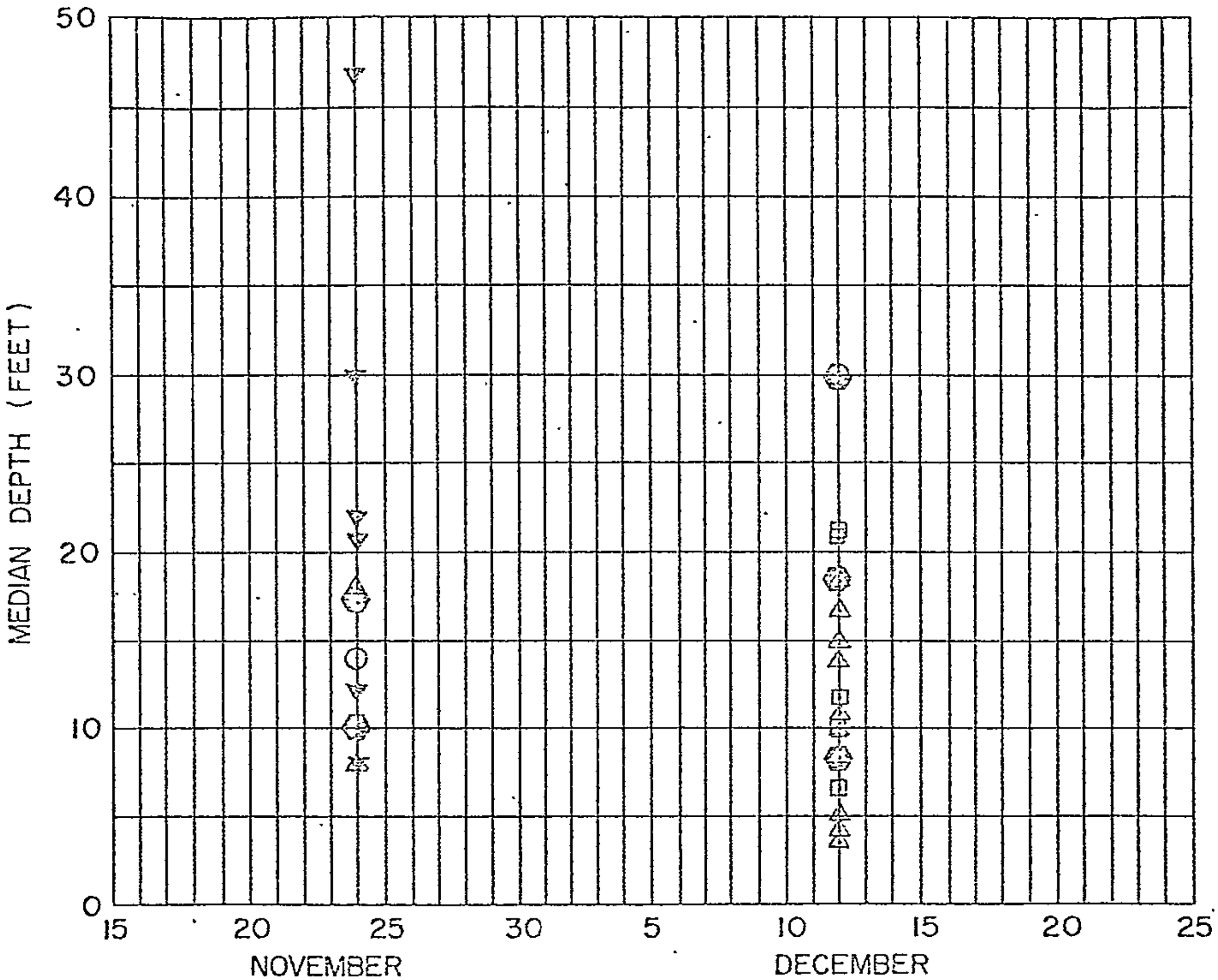

FIG. 2c - Lake ice coverage in fall 1975 as determined from LANDSAT images as a function of lake depth. Lakes near Brainerd Weather Station.

ORIGINAL PAGE IS
OF POOR QUALITY

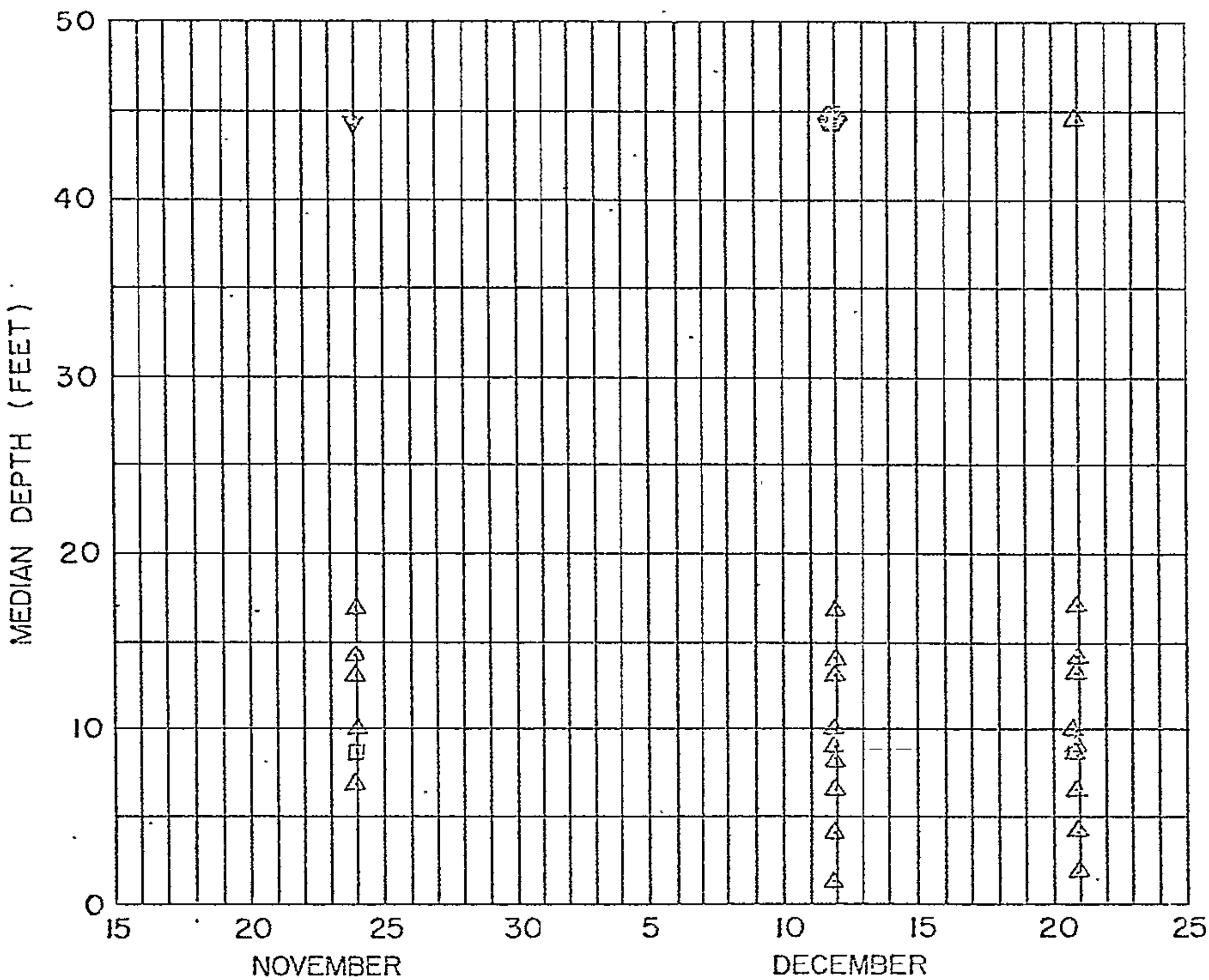

FIG. 2d - Lake ice coverage in fall 1975 as determined from LANDSAT images as a function of lake depth. Lakes near St. Cloud Weather Station.

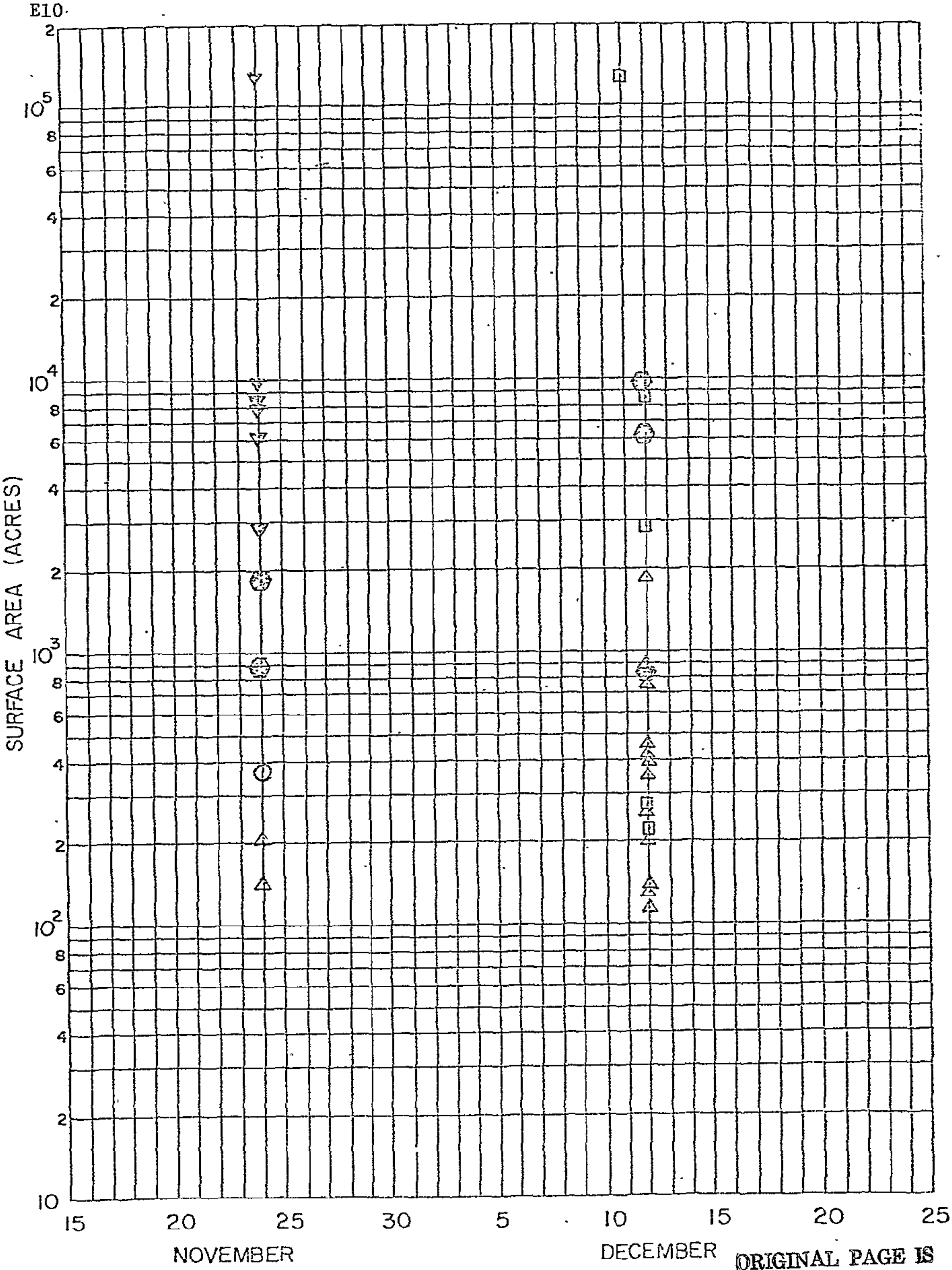

ORIGINAL PAGE IS OF POOR QUALITY

FIG. 3 - Lake ice coverage in fall 1975 as determined from LANDSAT images as a function of lake surface area. Lakes near Brainerd Weather Station.

face areas are related to each other in the sense that larger lakes are also deeper. This is, however, not generally true. It may be that wind effects also have an important role. Wind can prevent formation of a coherent ice cover and wind effects are stronger on lakes with larger fetch (surface area). Ice movement by wind is readily observed in large lakes and has been described e.g. by Tsang (1974).

A graph in which the product of lake median depth and surface area has been used is given in Fig. 4. This may turn out to be the most appropriate representation.

THEORY ON FREEZE-OVER

A mean seasonal water temperature cycle of a lake can be approximated by the relationship

$$T = E_m + \frac{I}{m} + \Delta E \left[1 + \left(\frac{w}{m}\right)^2\right]^{-1/2} \sin(wt - \delta) \qquad (1)$$

Equation (1) is valid only for water temperatures $T \geq 32°F = 0°C$.

The foregoing equation is derived from the mean annual equilibrium temperature cycle

$$E = E_m + \Delta E \sin(wt) \qquad (2)$$

Equations (1) and (2) have been plotted in Fig. 5. Equilibrium temperature E is by definition that water temperature at which the net heat transfer through the water surface is zero. Equilibrium temperature can be computed from weather data, specifically air temperature, solar radiation, dew point temperature, wind velocity and cloudiness ratio. Some actual data from an Environmental

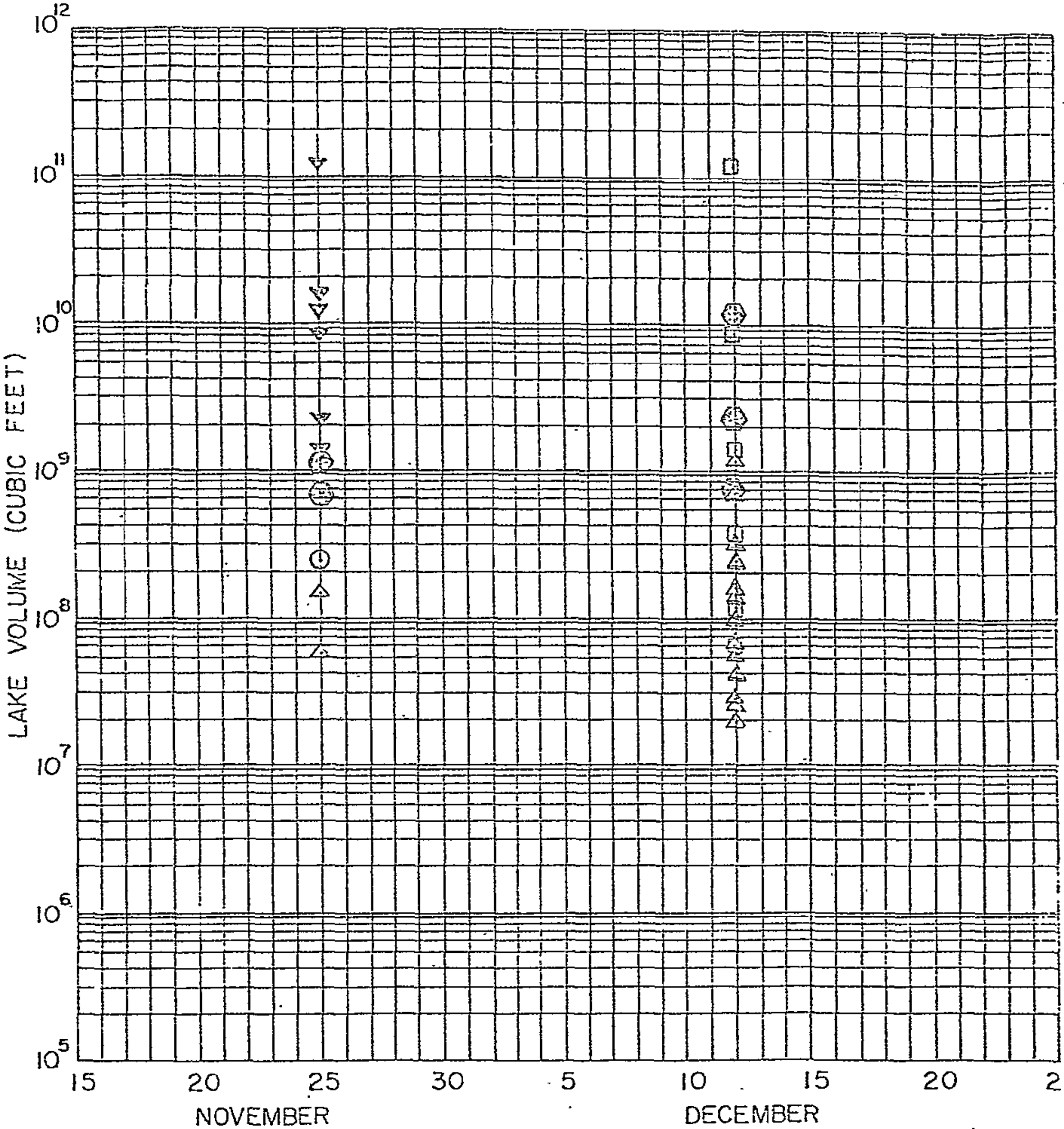

FIG. 4 - Lake ice coverage in fall 1975 as determined from LANDSAT images as a function of lake volume. Lakes near Brainerd Weather Station.

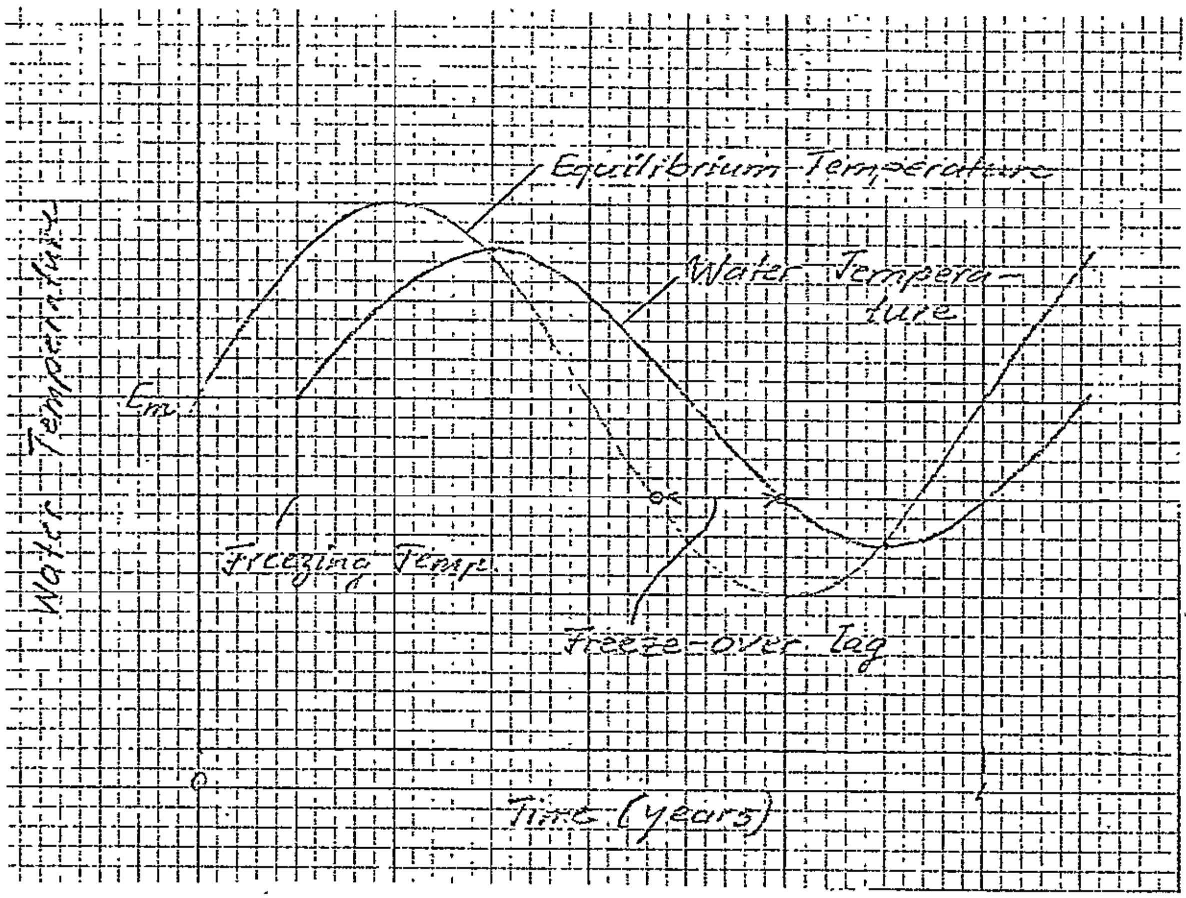

FIG. 5 - Schematic mean annual water temperature and equilibrium temperature cycles.

Protection Agency report (1971) are given in Fig. 6.

In Eq. (1) t = time in days, $w = 2\pi/365$, $m = K/\rho ch$, where K = an annual bulk surface conductance, ρc = specific heat per unit volume, h = mean depth of water body, I is the daily rate of artificial heat input, if any and $\delta = \arctan(\frac{w}{m})$. Typical values for central Minnesota conditions are $E = 49°F$, $\Delta E = 28°F$, $K = 80$ BTU ft^{-2} $day^{-1}°F$, $\rho c = 62.4$ BTU $ft^{-3}°F^{-1}$ and $I = \theta$.

A lake will freeze over, when $T = 32°$ is reached during the cycle of decreasing water temperature (3rd quadrant of the sinusoidal temperature cycle). If Eq. (1) is solved for t at $T = 32°$ F, the result is

$$t = \frac{1}{w} \text{ arc sin } \left[\left\{ \frac{32 - E_m - I_m}{\Delta E} \right\} \left\{ 1 + (\frac{w}{m})^2 \right\}^{1/2} \right] + \delta \qquad (3)$$

The right-hand side of Eq. (3) depends on lake depth h. A lake of depth $h=0$ freezes over when equilibrium temperature reaches zero or when

$$t = \frac{1}{w} \text{ arc sin } \left\{ \frac{32 - E_m - I_m}{\Delta E} \right\} . \qquad (4)$$

Lake depth produces a lag in the freeze-over date. The lag is

$$\text{lag} = \text{arc tan } (\frac{w}{m}) + \frac{1}{w} \left[\text{arc sin } \left\{ \frac{32 - E_m - I_m}{\Delta E} \right\} \left\{ 1 + (\frac{w}{m})^2 \right\}^{1/2} \right]$$
$$- \frac{1}{w} \left[\text{arc sin } \left\{ \frac{32 - E_m - I_m}{\Delta E} \right\} \right] . \qquad (5)$$

Function (5) has been plotted in Fig. 7.

The relationship shown in Fig. 7 is for specified values of

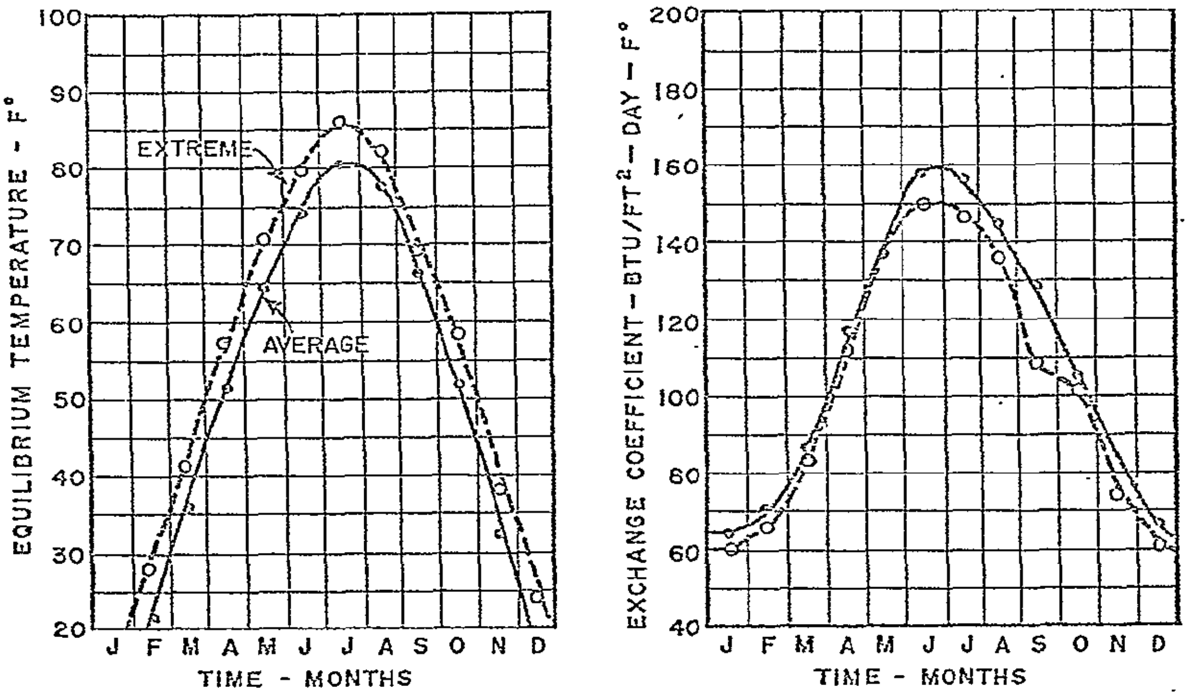

REPRODUCIBILITY OF THE ORIGINAL PAGE IS POOR

DULUTH, MINNESOTA

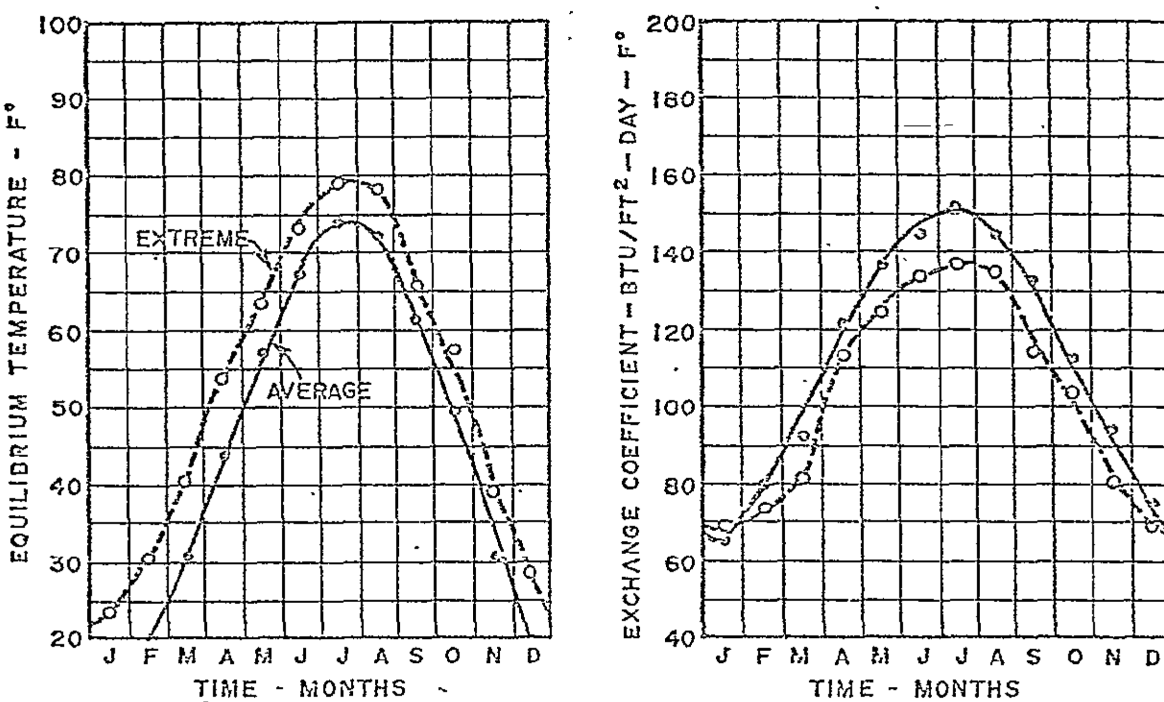

MINNEAPOLIS-ST. PAUL, MINNESOTA

FIG. 6 - Actual mean monthly values of equilibrium temperature and bulk surface heat exchange coefficients.

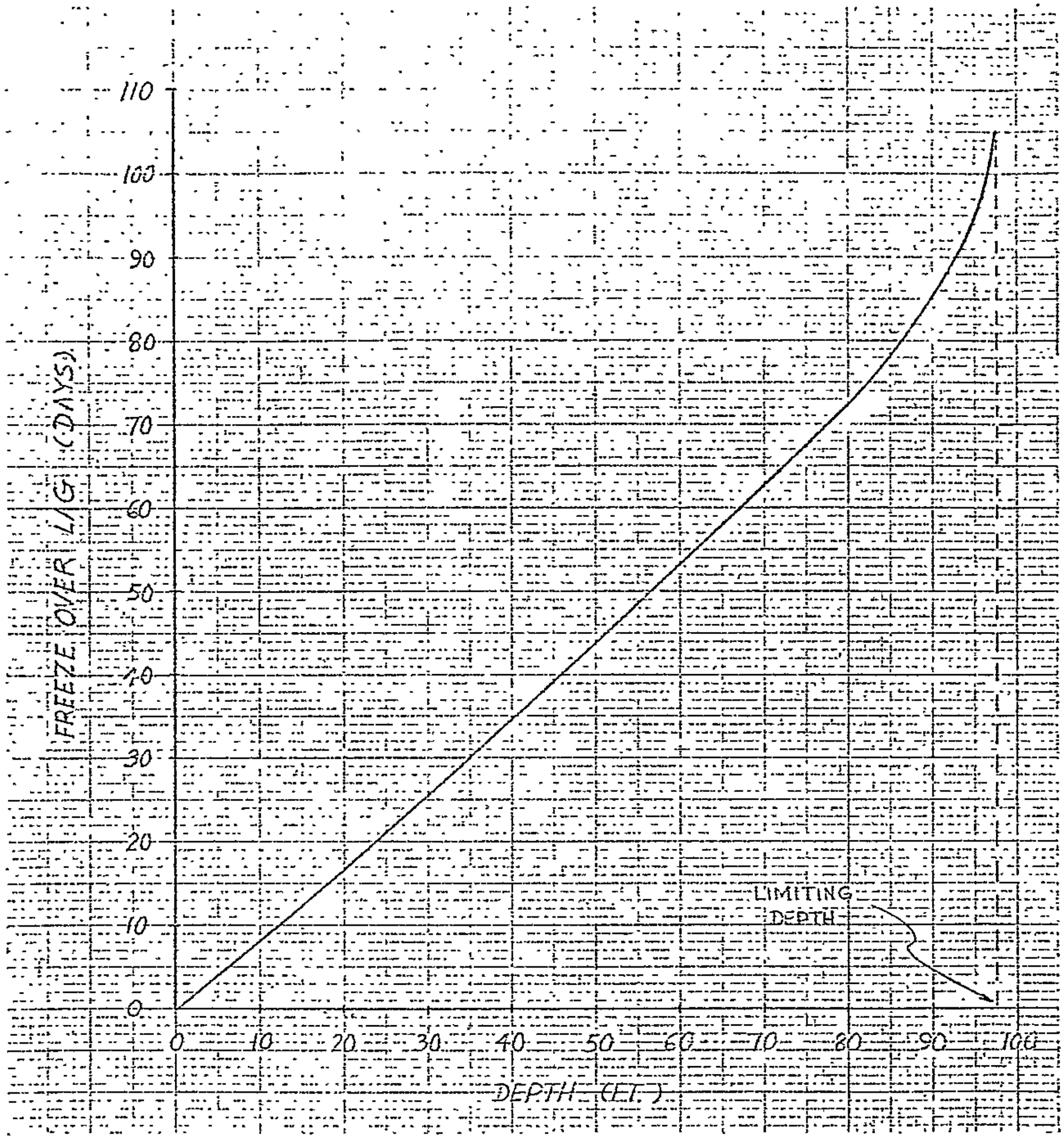

FIG. 7 - Theoretical time lag of freeze-over date as a function of mean lake depth.

$E_m = 49°F, \Delta E = 28°F$ and $K = 80$ BTU ft^{-2} day^{-1}°F^{-1} and $I = 0$, which in essence describe mean climatological conditions in central Minnesota. For other regions and specific years other numerical values would be obtained. Figure 7 does specify an order of magnitude for the lag time. Since it reflects a nearly linear relationship it may be interpreted to mean that for every foot of median depth the freeze-over date will be delayed by approximately one day. Obviously, the total lag between lakes of different depths can add up to considerable lengths of time in terms of days and weeks. Information from satellite imagery given in Fig. 2 corroborates this information. To make the comparison easier, Fig. 8 has been prepared from Fig. 7. More precise theoretical curves for each year and location are being developed.

The theory indicates that a lake will not freeze over at all if its depth exceeds a value which can be derived from the relationship

$$E_m + I_m - 32°F = \Delta E \left[1 + \left(\frac{w}{m}\right)^2\right]^{-1/2} \tag{6}$$

The critical depth is

$$h_{cr} = \frac{K}{w\,c}\left[\left\{\frac{E}{E_m + I_m - 32}\right\}^2 - 1\right]^{1/2} \tag{7}$$

For the before-given numerical values $h_{cr} = 97.5$ ft. A lake with a larger depth than 97.5 ft would, on an annual mean basis, not reach freezing temperature.

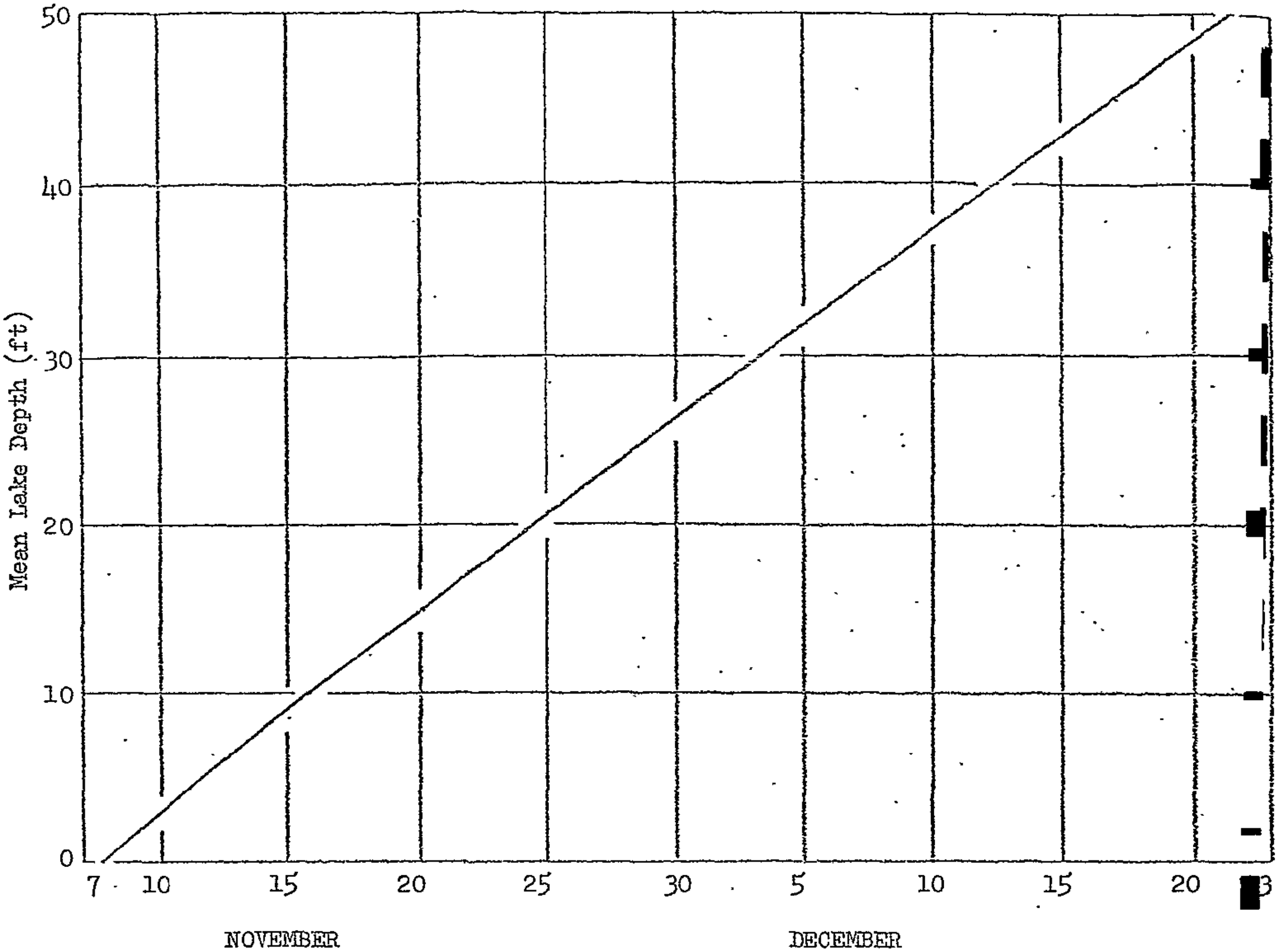

FIG. 8 - Mean annual theoretical freeze-over date for $E_m = 49^oF$, $\Delta E = 28^oF$ and $K = 80$ BTU $ft^{-2} day^{-1}\ {}^oF^{-1}$.

INFORMATION FROM LANDSAT IMAGERY ON SPRING MELTING OF LAKE ICE-COVER

The melting of ice covers on Minnesota lakes in the spring occurs typically between March and May. LANDSAT images for March, April and May 1976 have been used to extract information on ice conditions in spring. Average cloud cover in spring was less than in fall as shown in Table 2. The procedure was similar to that described earlier for fall 1975. Results showing ice conditions as a function of lake depth and date similar to those given in Fig. 2 were plotted. They showed a very poor correlation of ice cover with depth. The reason, of course, is that the melting of the ice cover is only to a minor degree related to the heat budget of the lake water beneath the ice. The radiation balance on the ice as well as along the shorelines, and inflow of water from minor tributaries and overland flow are much more important. Radiation and overland flow, if at all related to lake morphology, would depend on lake surface area. Observations on ice coverage were therefore plotted versus lake surface area in Fig. 9a through 9f. It appears that the spring ice melting is very uniform in time and pretty much independent of lake size.

TABLE 2. Available LANDSAT Scenes, Spring 1976

North

Date	Quality	Cloud Cover (%)
3/01/76	Unavailable	100
3/10/76	Excellent	10
3/19/76	Fair	10
3/28/76	Fair	60
4/06/76	Excellent	20
4/15/76	Fair	70
4/24/76	Unavailable	100
5/03/76	Excellent	10
5/12/76	Excellent	10
5/21/76	Excellent	10
5/30/76	Excellent	60
	Average	42

Central

Date	Quality	Cloud Cover (%)
3/02/76	Unavailable	100
3/11/76	Fair	90
3/20/76	Unavailable	100
3/29/76	Excellent	90
4/07/76	Excellent	0
4/16/76	Fair	70
4/25/76	Excellent	10
5/04/76	Excellent	0
5/13/76	Unavailable	100
5/22/76	Unavailable	10
	Average	57

South

Date	Quality	Cloud Cover (%)
3/01/76	Unavailable	100
3/10/76	Excellent	10
3/19/76	Unavailable	100
3/28/76	Fair	20
4/06/76	Excellent	0
4/15/76	Fair	90
4/24/76	Unavailable	100
5/03/76	Excellent	30
5/12/76	Fair	80
5/21/76	Excellent	30
5/30/76	Excellent	90
	Average	59

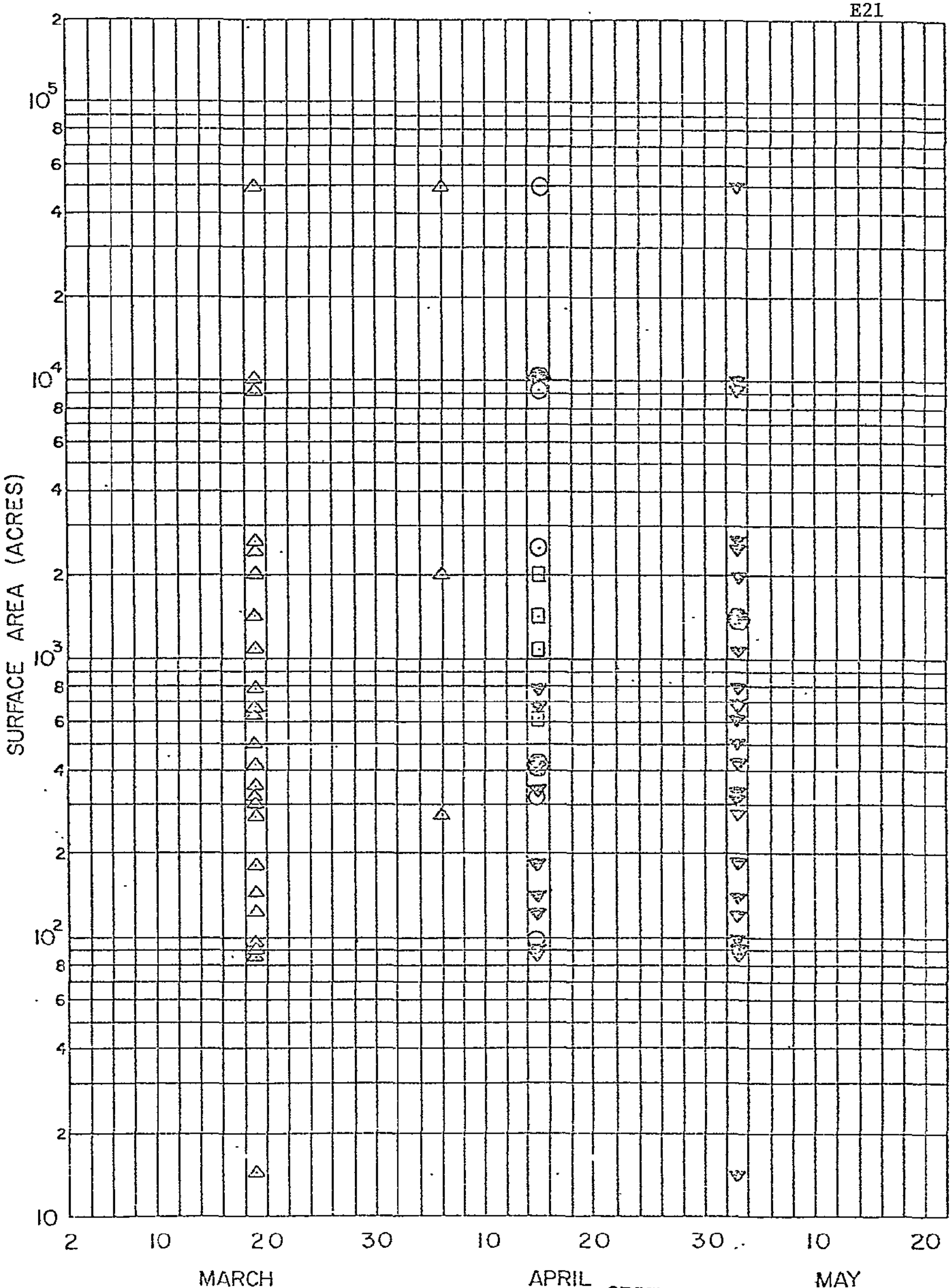

ORIGINAL PAGE IS OF POOR QUALITY

FIG. 9a - Lake ice coverage in spring 1976 as determined from LANDSAT images as a function of lake surface area. Lakes near Winton Power Station.

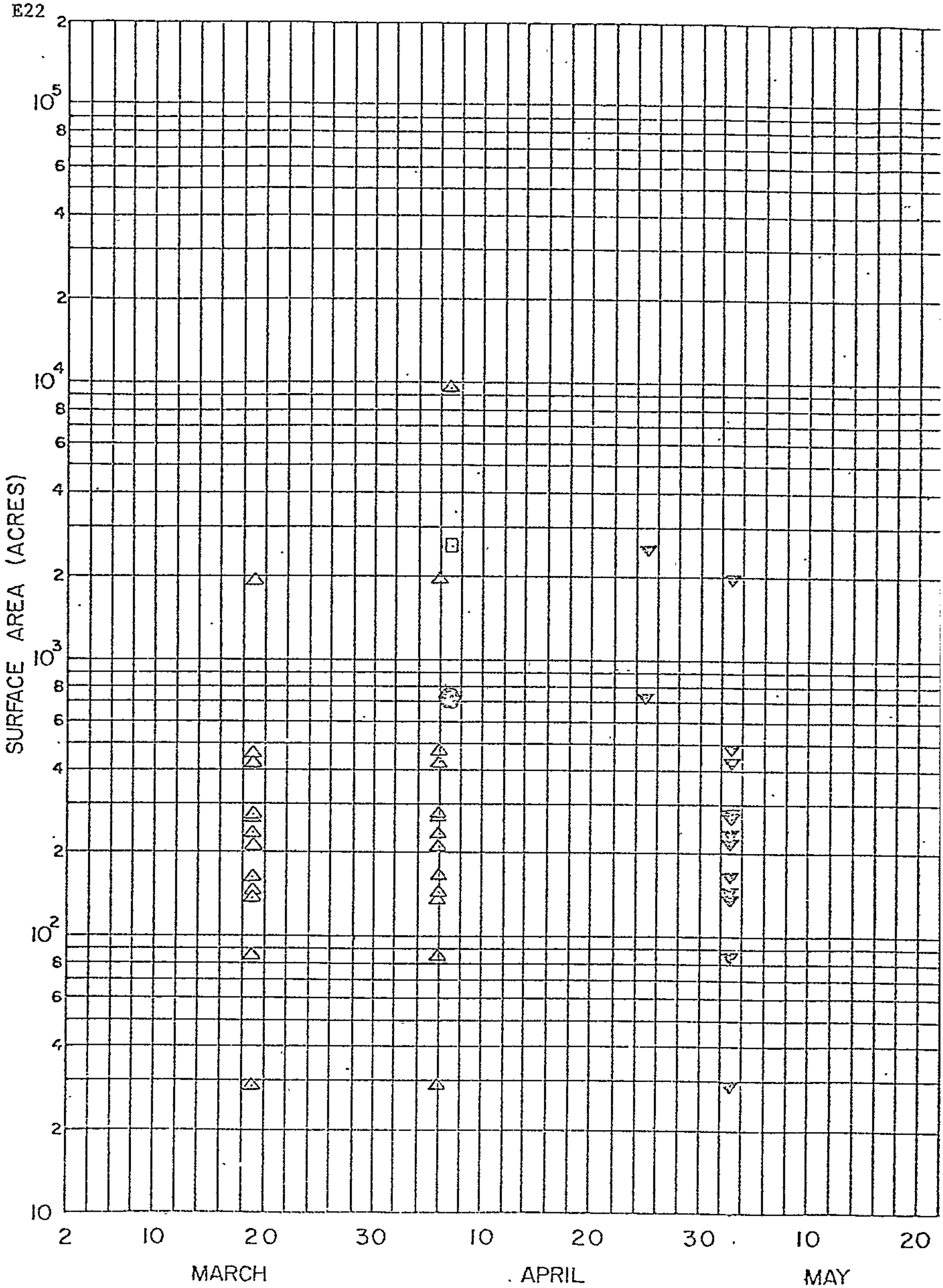

FIG. 9b - Lake ice coverage in spring 1976 as determined from LANDSAT images as a function of lake surface area. Lakes near Sandy Lake Dam Libby Weather Station.

ORIGINAL PAGE IS
OF POOR QUALITY

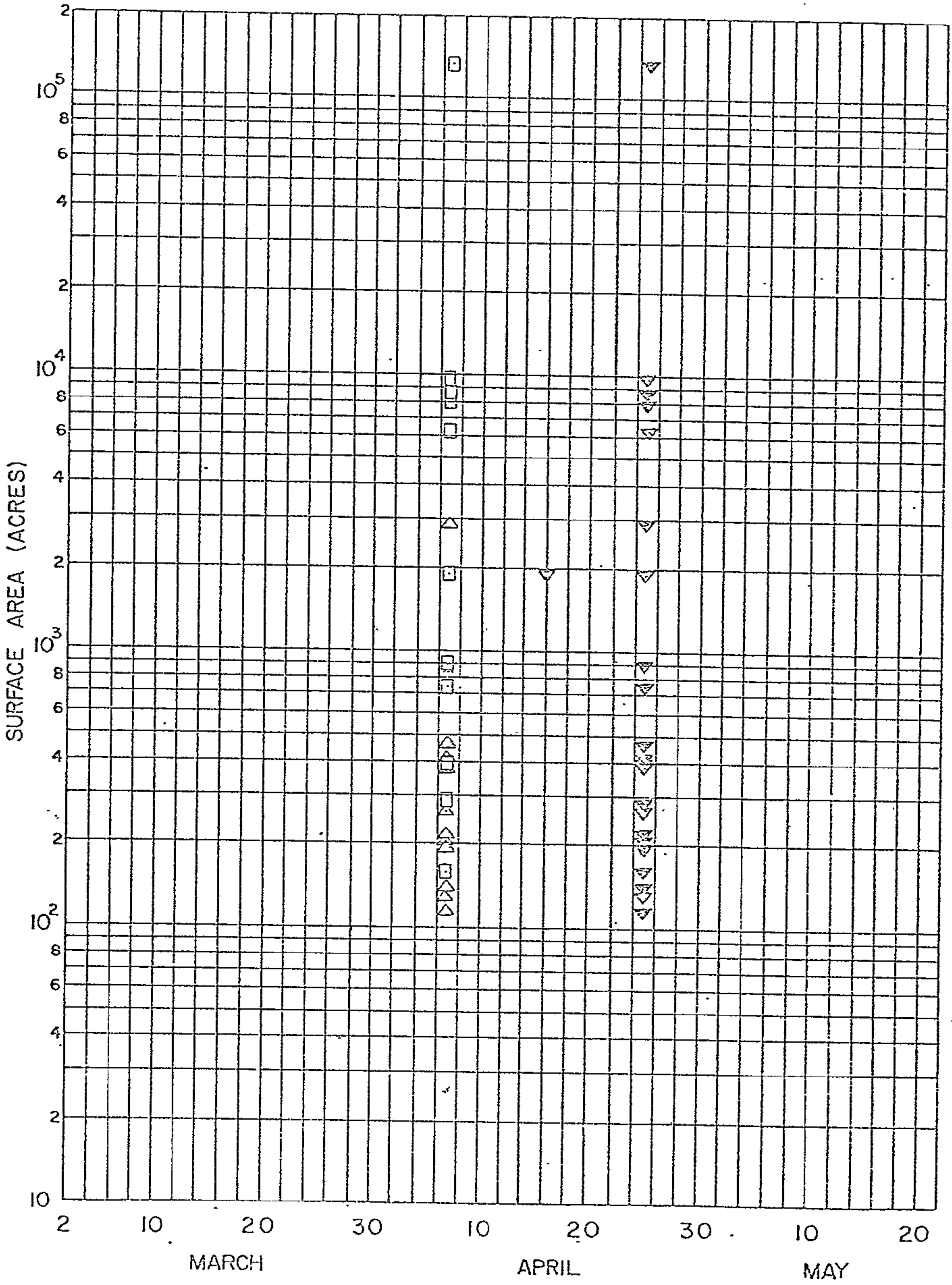

FIG. 9c - Lake ice coverage in spring 1976 as determined from LANDSAT images as a function of lake surface area. Lakes near Brainerd Weather Station.

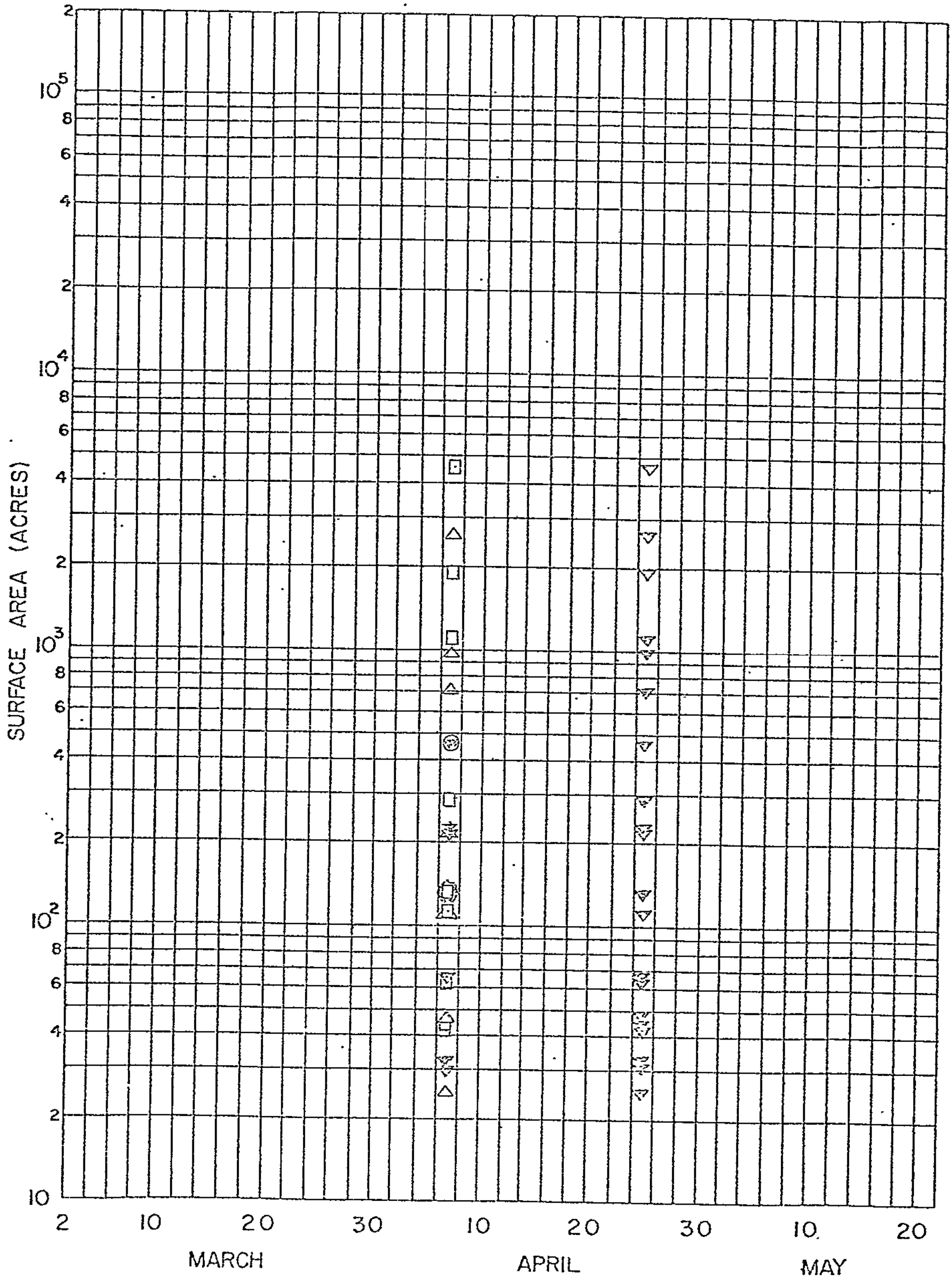

FIG. 9d - Lake ice coverage in spring 1976 as determined from LANDSAT images as a function of lake surface area. Lakes near Alexandria Airport Weather Station.

ORIGINAL PAGE IS
OF POOR QUALITY

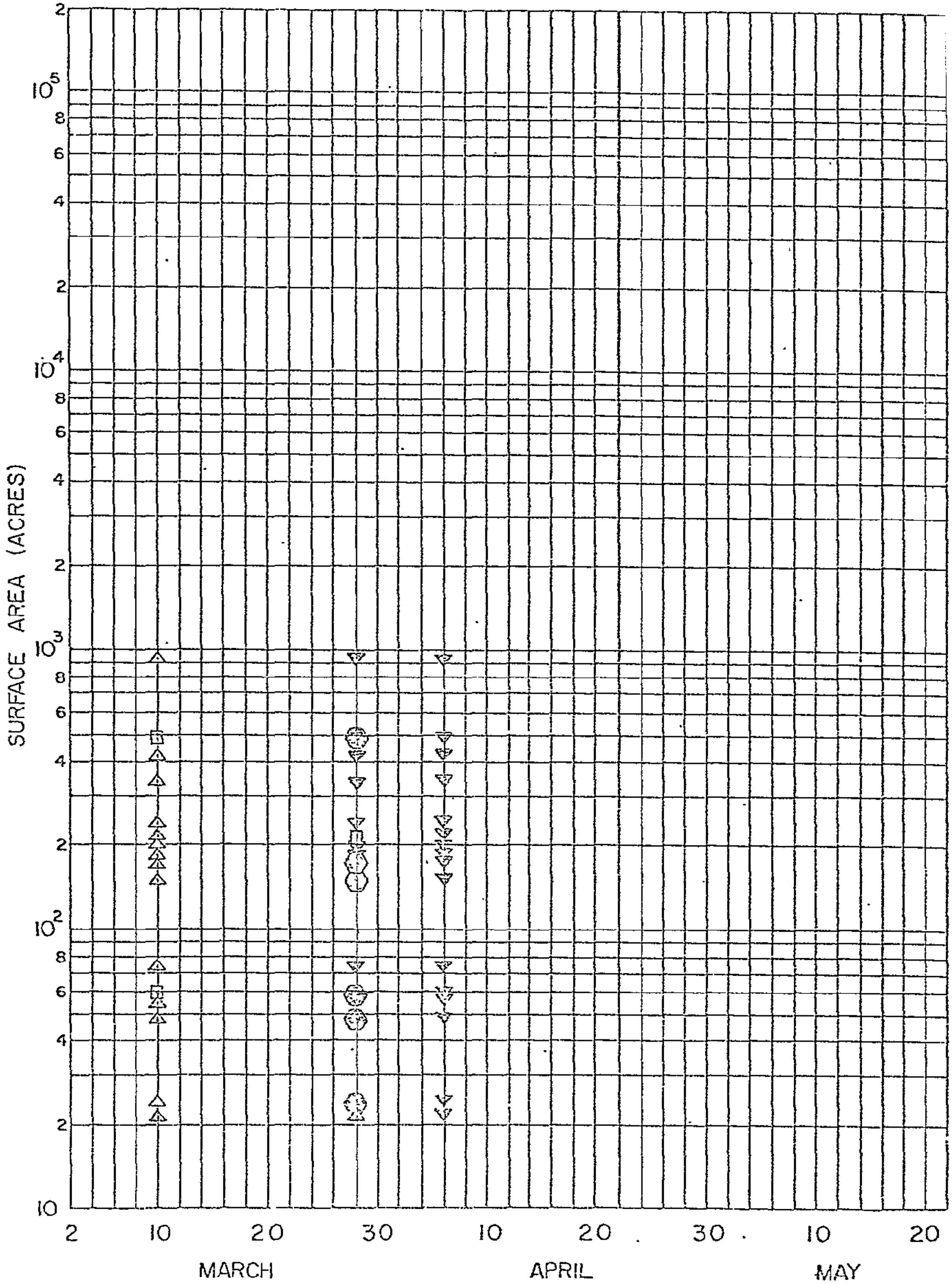

FIG. 9e - Lake ice coverage in spring 1976 as determined from LANDSAT images as a function of lake surface area. Lakes near Minneapolis/St. Paul Airport Weather Station.

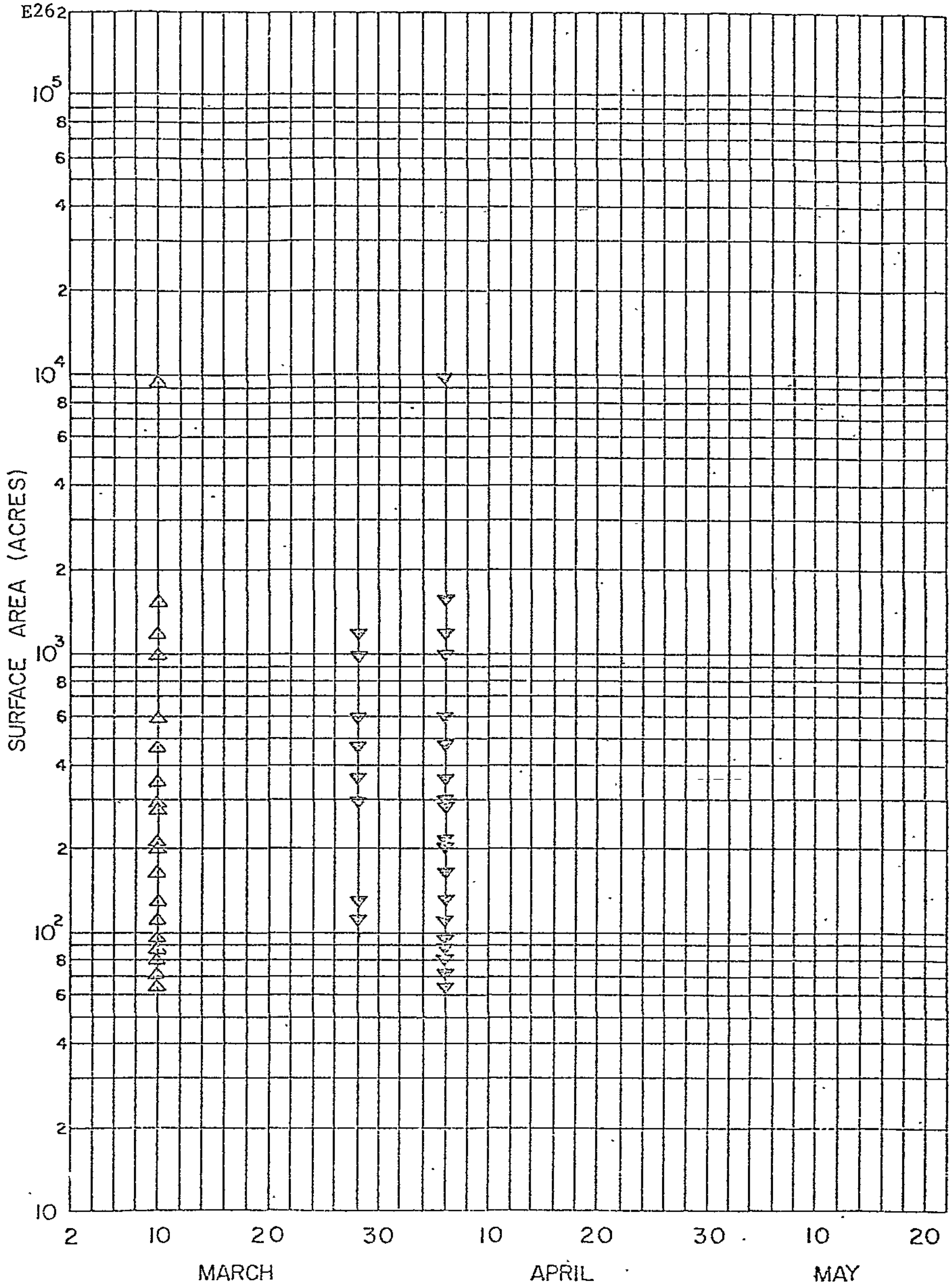

FIG. 9f - Lake ice coverage in spring 1976 as determined from LANDSAT images as a function of lake surface area. Lakes near Minneapolis/St. Paul Airport Weather Station.

FUTURE RESEARCH

Several objectives are identified:

1. Facilitate the method for prediction of freeze-over dates by consideration of air temperature cycles instead of equilibrium temperatures.

2. Refine the method for prediction of freeze-over dates by consideration of air temperature data in each specific year and up to the time (e.g. October 15) at which a prediction is to be made. This can be done e.g. by comparison of the average year with the specific year. LANDSAT imagery for fall 1972, 1973 and 1974 and 1976 will be used for verification.

   Daily air temperatures and degree days above or below freezing temperature will be used. Plots of cumulative degree days below freezing in fall and above freezing in spring are given in the Appendix.

3. Work on a theoretical analysis of spring ice melting to provide a more rational approach to the prediction of the melting date.

4. Explore the usefulness of LANDSAT imagery for a northern location to make predictions for a more southern latitude by introducing a time lag based on latitude in addition to depth. Simultaneous use of air temperature data will be made depending on latitude. A weak dependence of freeze-over on latitude can already be detected in Figs. 2a, 2b, and 2c.

LITERATURE CITED

1. Lind, A.O., "Ice Development on Lake Champlain," Remote Sensing Lab., Vermont University, Burlington, Ontario, July 1973.

2. Minnesota Department of Conservation, Division of Water and Soils, "An Inventory of Minnesota Lakes," Bulletin No. 25, St. Paul, Minn., 1968.

3. Tsang, Gee, "Ice Piling on Lakeshores, with Special Reference to the Occurrences on Lake Simcoe in the Spring of 1973," Scientific Series No. 35, Canada Centre for Inland Water, Burlington, Ontario, 1974.

4. Vanderbilt University, Department of Environmental and Water Resources Engineering, "Effect of Geographical Location on Cooling Pond Requirements and Performance," U.S. Environmental Protection Agency, Water Pollution Control Research Series, 16 130 FQD 03/71.

LIST OF FIGURES

APPENDIX I

MAJOR SOURCES OF HEATED DISCHARGES IN MINNESOTA

Plant	Owner	Receiving Water
Fox Lake	INPD	Fox Lake near Fairmont
Aurora	MNPL	Colby Lake and Partridge River near Hoyt Lakes
Clay Boswell	MNPL	Mississippi River near Grand Rapids
Hibbard	MNPL	St. Louis, Duluth
Black Dog	NSP	Black Dog Lake and Minnesota River near Bloomington
High Birdge	NSP	Mississippi River in St. Paul
A.S. King	NSP	Lake St. Croix near Stillwater
Minnesota Valley	NSP	Minnesota River near Granite Falls
Monticello	NSP	Mississippi River near Monticello
Prairie Island	NSP	Mississippi River Pool No. 3 near Red Wing
Riverside	NSP	Mississippi River in Minneapolis
Hoot Lake	OTTP	Ottertail River and Resevoir near Fergus Falls
Ortonville	OTTP	Cooling Pond near Ortonville and Big Stone Lake

FALL 1975

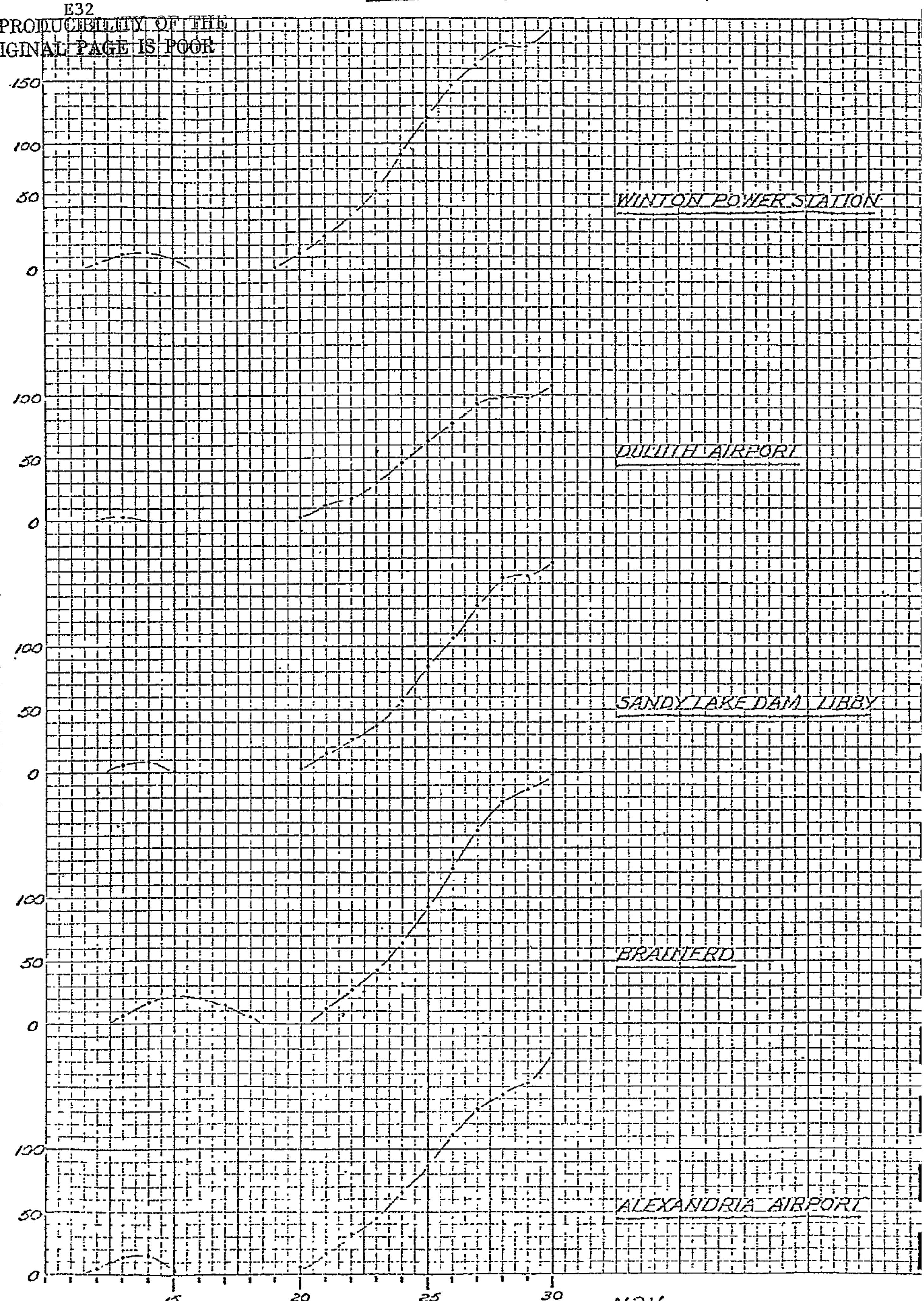
CUMULATIVE DEGREE DAYS < 32°F
WINTON POWER STATION
DULUTH AIRPORT
SANDY LAKE DAM LIBBY
BRAINERD
ALEXANDRIA AIRPORT
150
100
50
0
15
20
25
30
NOV

FALL 1975

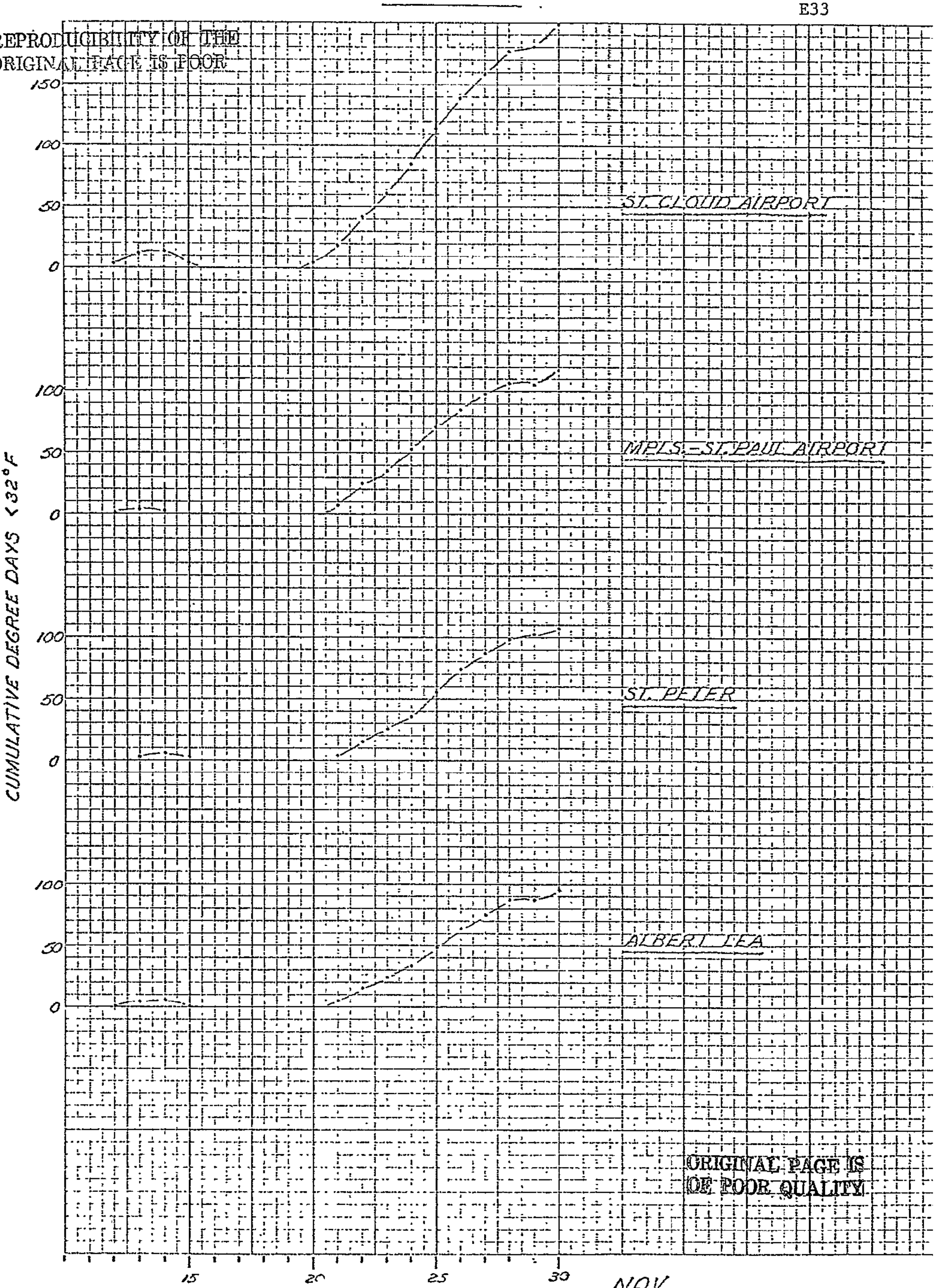
CUMULATIVE DEGREE DAYS < 32°F
150
100
50
0
ST. CLOUD AIRPORT
MPLS.-ST. PAUL AIRPORT
ST. PETER
ALBERT LEA
15
20
25
30
NOV

SPRING 1976

E34

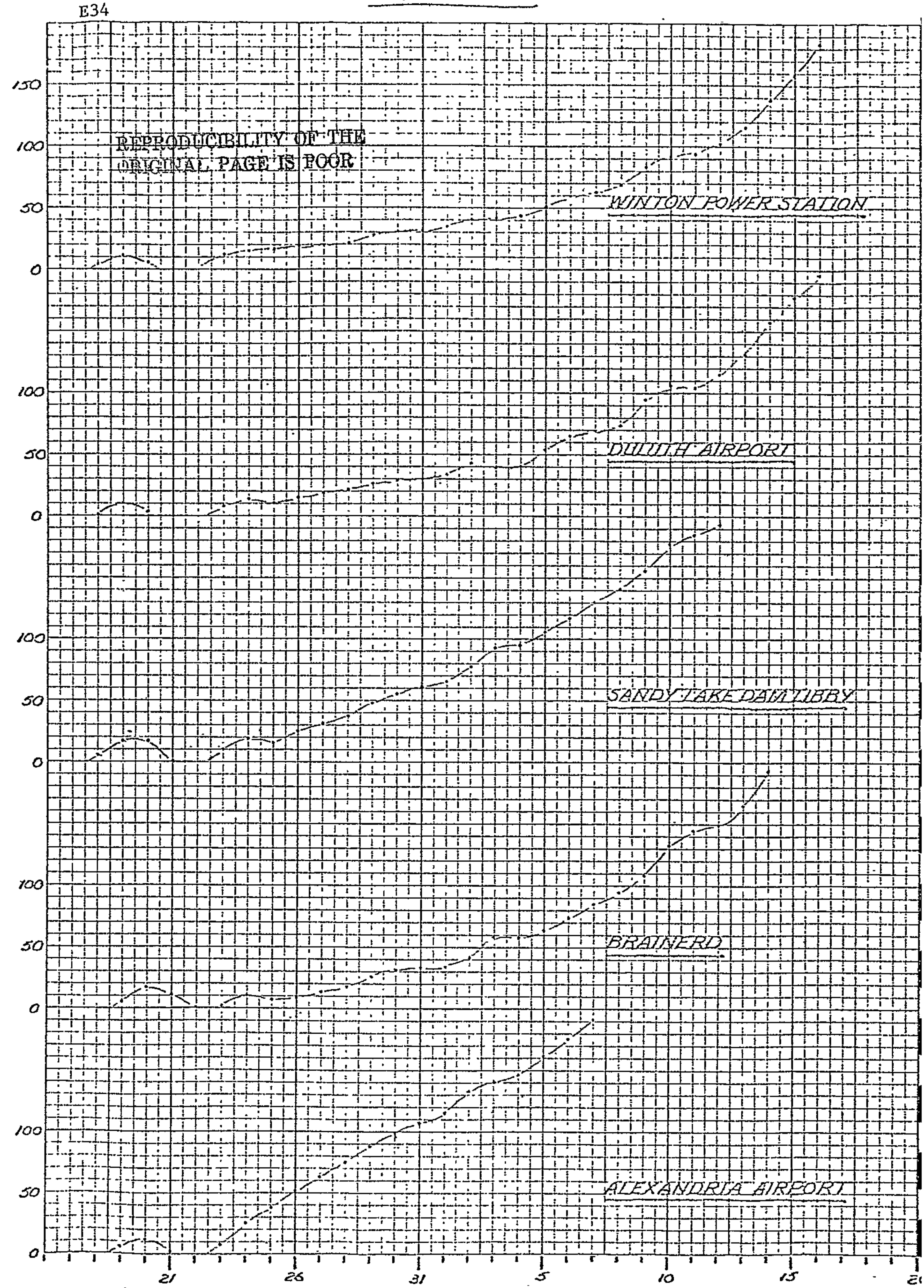

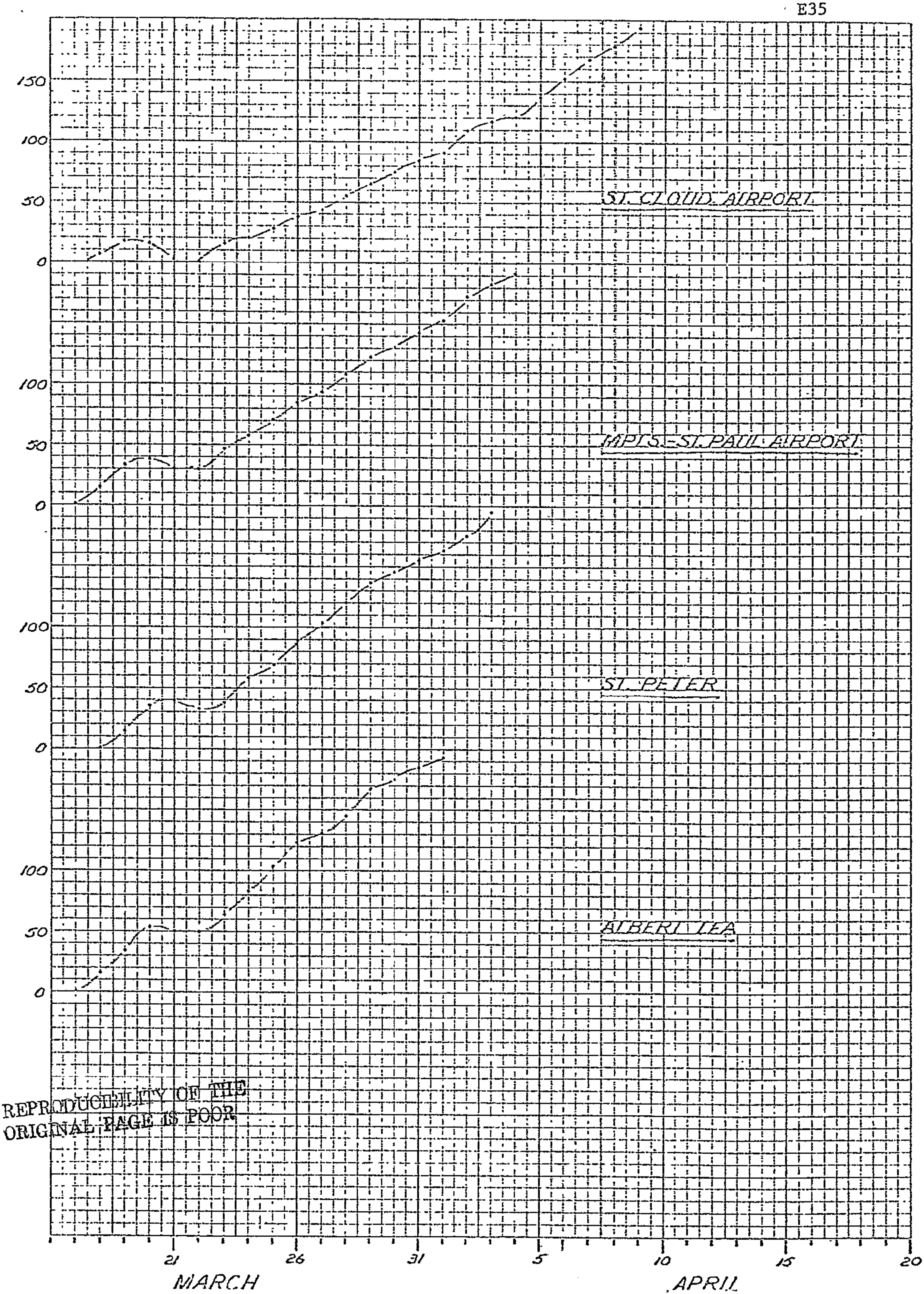

150
100
50
0
ST. CLOUD AIRPORT
100
50
0
MPLS.-ST. PAUL AIRPORT
100
50
0
ST. PETER
100
50
0
ALBERT LEA
21
26
31
5
10
15
20
MARCH
APRIL

SECTION F

EVALUATION OF SOIL MOISTURE STRESS IN WESTERN AND SOUTHWESTERN MINNESOTA

Dr. R.H. Rust and Pierre Robert
Department of Soil Science
University of Minnesota
St. Paul, Minnesota

INDEX

EVALUATION OF SOIL MOISTURE STRESS IN WESTERN AND SOUTHWESTERN MINNESOTA

Investigators: Dr. Richard H. Rust
Dr. Pierre Robert
Department of Soil Science
University of Minnesota
St. Paul, Minnesota

INTRODUCTION

Some areas of Minnesota, particularly in the southwestern and western parts of the state, have been for several successive years under soil moisture stress conditions resulting in variable but important crop yield losses. The ability to follow the spatial distribution or development of moisture stressed areas through crop spectral signature would be valuable for the detection of <u>soil landscapes particularly sensitive to soil moisture stress and also in developing a forecast capability for seasonal crop management</u>.

OBJECTIVES

<u>Principal objectives of the moisture stress project are</u>:

- the detection of moisture stress through crop signature from LANDSAT data and low altitude color infrared photographs;
- the detection of stress as a result of hail, wind, and disease damage;
- the localization of droughty and poorly drained soils;
- the development of forecast ability for seasonal crop management on principal soil landscapes of the region.

Figure 1.

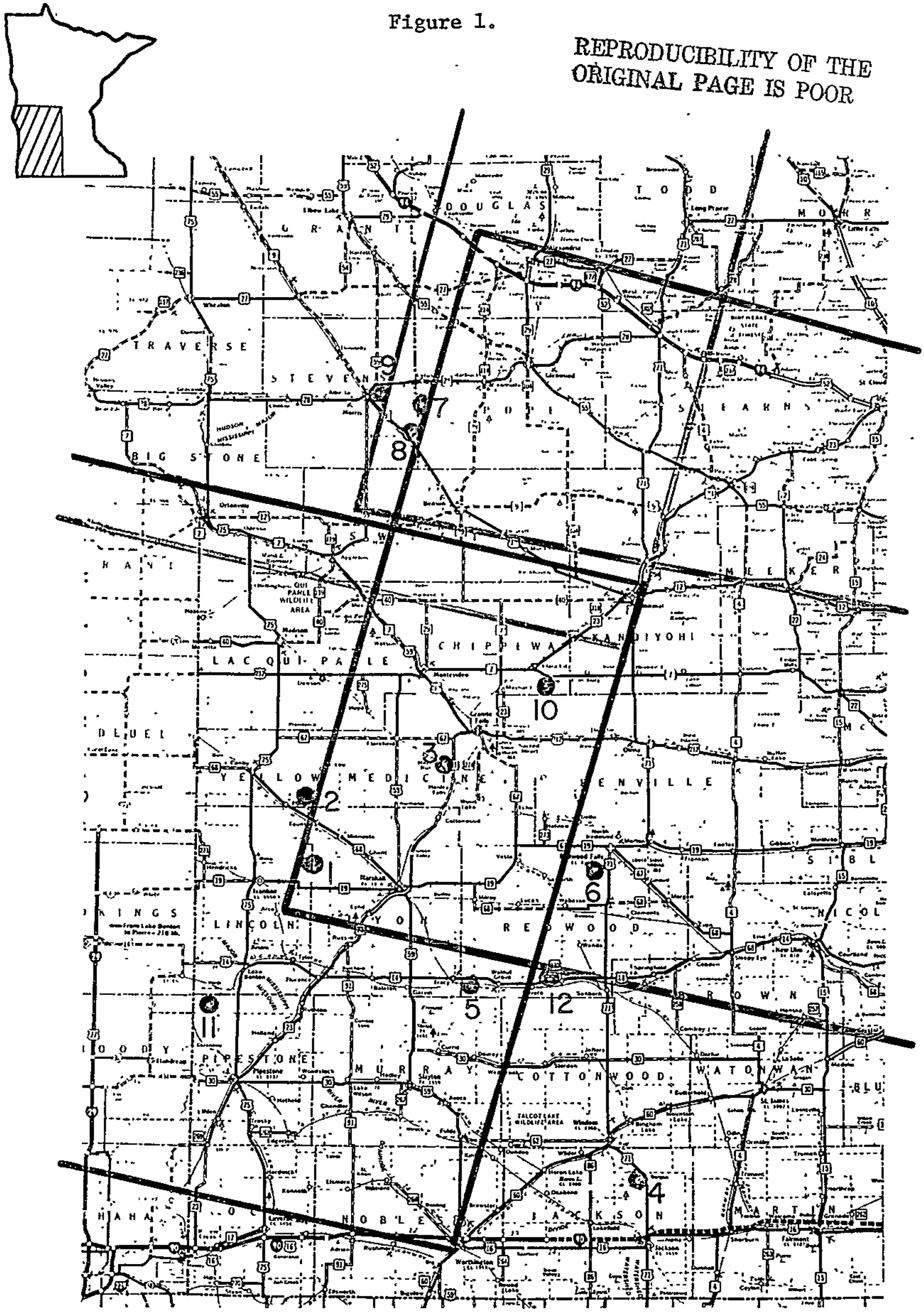

LANDSAT COVERAGE OF SOUTHWESTERN MINNESOTA AND TWELVE GROUND TRUTH SITE LOCATIONS.

PROCEDURES

Twelve sites (figure 1) distributed in various soil landscape situations were selected in southwestern Minnesota. Each site is comprised of 2 homogenous areas, larger than 10 acres, and representative of well-drained (Udolls and Ustolls) and poorly drained (Aquolls) "soilscapes." They were mostly planted in corn with a few in soybeans. Among them, 2 sites feature irrigated and non-irrigated "ground truth" in a same soil landscape situation. Soil moisture was determined from the surface to the depth of rooting zone (figure 2) and the leaf water content at the top and the midheight of the plant.

The sampling was carried out coincident with the LANDSAT overpass (6 and 12 day intervals).

The "ground truth" observations and sampling were provided by field soil scientists of the Soil Conservation Service and cooperators of the West-Central and Southwest Experiment Stations. Precipitation events, farming operations, and crop history were recorded through the season (table 1). Moreover, soil surveys and field crop maps of corresponding sites were gathered or prepared (figure 3).

Aerial color infrared photographs at a 1:72,000 scale were taken over each site in June, July, August, and one flight is scheduled under bare soil surface conditions.

Thermal measurements of fields and leaves were recorded using a Barnes PRT-10L radiometer under various conditions of crop height, field orientation and slope, air temperature, sky and wind velocity.

A greenhouse experiment is underway to determine which stage of plant growth of corn, soybeans, and wheat is more "spectral signature"

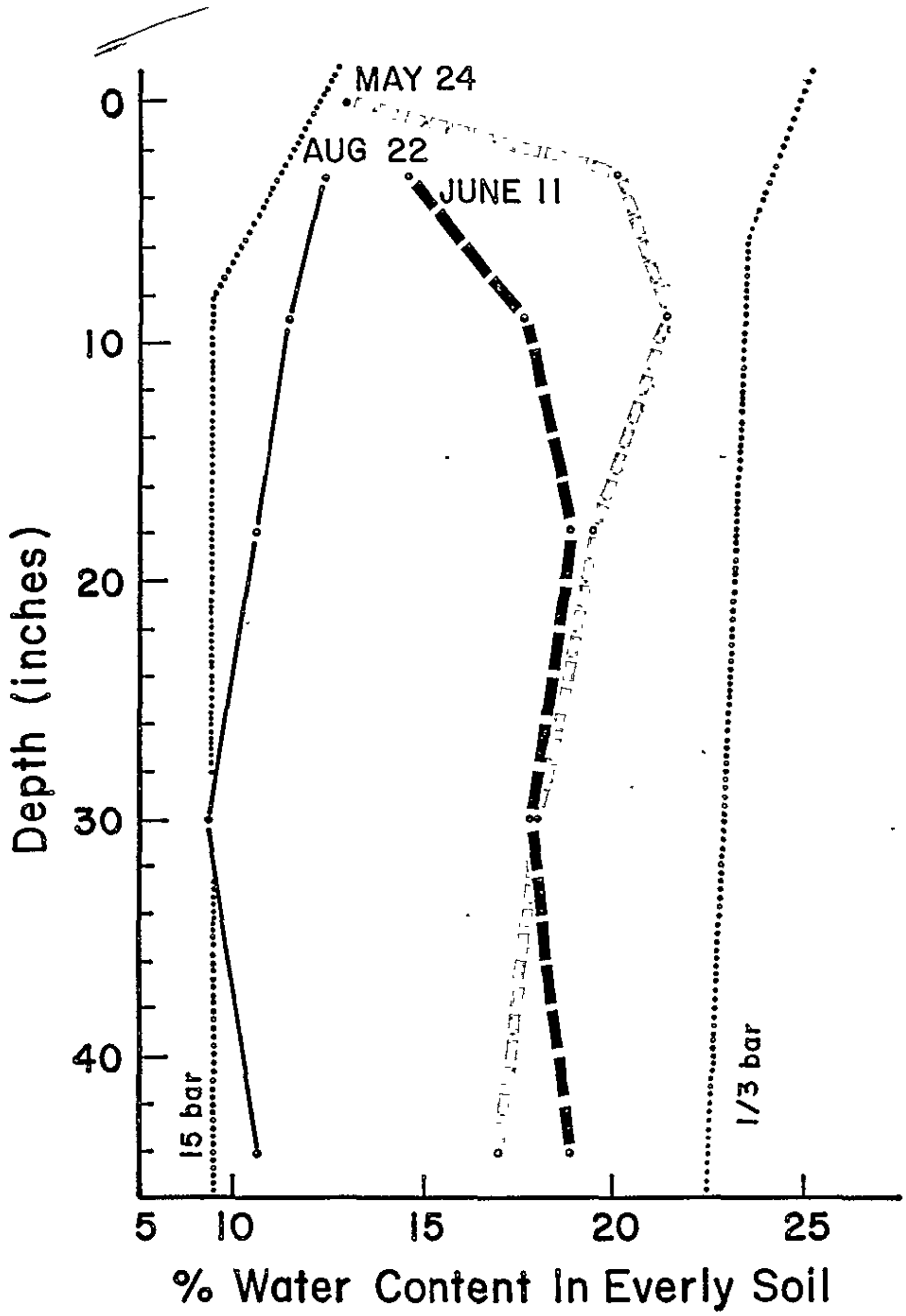

Figure 2. Water-content distribution profiles of selected dates during the growing season. The one-third bar water content represents the maximum amount of water in

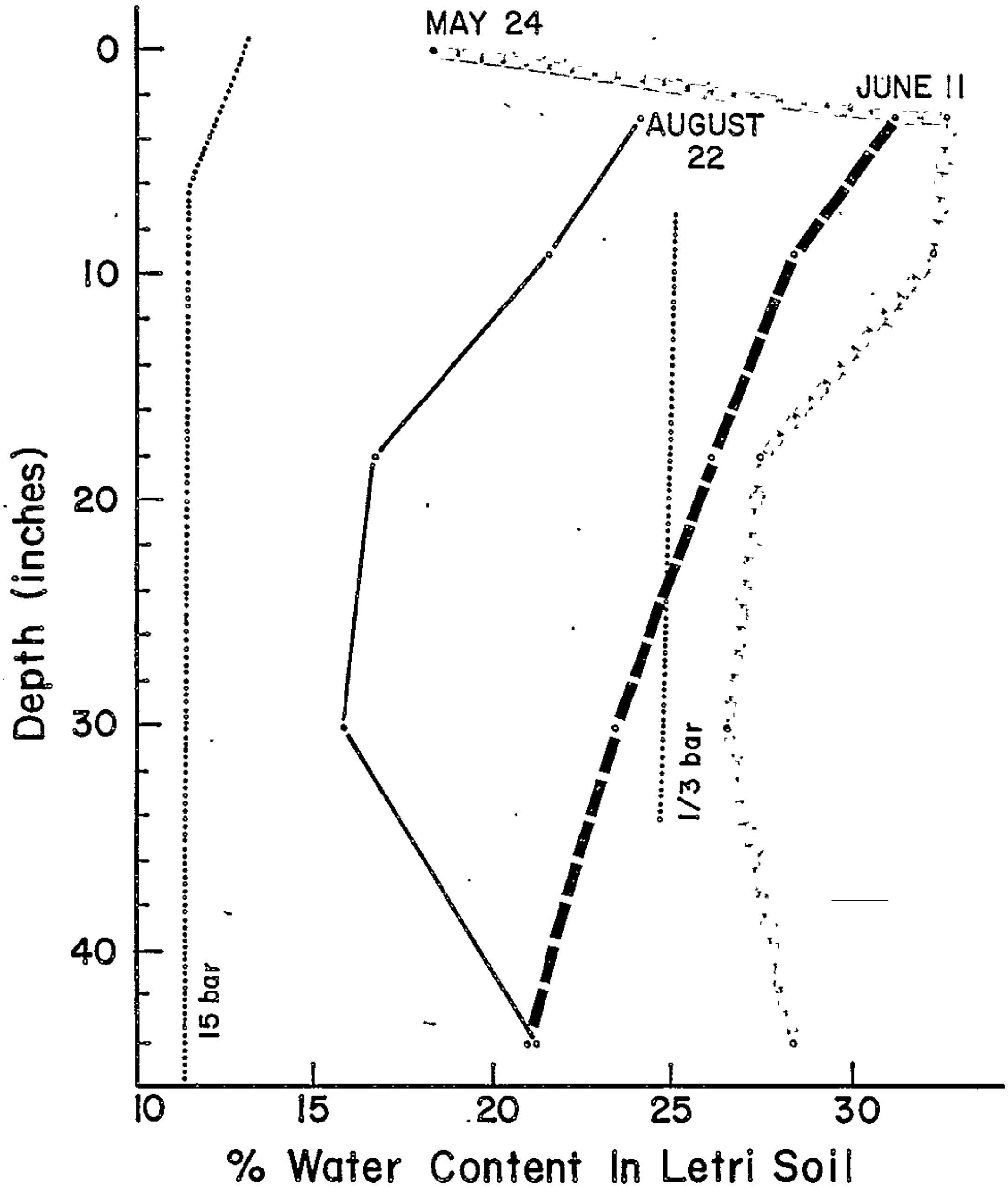

the rooting zone that the soil retains against gravity. The 15-bar water content is the water remaining in the rooting zone at the wilting point of most crops. Water content in excess of 1/3 bar indicates a saturated condition.

Table 1. Example of a field record.

MOISTURE STRESS PROJECT

FIELD INFORMATION

Date: 1977
Field #: 12a, Holmberg
Soil: Ves

Date May-June-July-August.

Month, day hour (1)	Crops (2)	Stage of growth (3)	Height (cm) (4)	Cover (%) (5)	Leaves shape and color (6)	Treatment (7)	Soil Moisture: Rooting Zone (8)	Soil Moisture: Surface (9)	Leaf Moisture (10)	Additional Information (11)
5/6 10:00	Corn	Planting 4/29	0	0	--	NH_4	adequate	good	--	slide $\#12_{a1}$
5/24 10:15	Corn	Emergence	18	5	normal V, turgid, 5G 5/2	-	adequate	very good	--	slide $\#12_{a2}$
6/10 12:00	Corn	Emergence	51	22	slight rolling 5G 5/2	-	adequate	good	--	slide $\#12_{a3}$
6/29 11:00	Corn	Pretassel	145	69	normal V, turgid	-	adequate	good	sample #1	slide $\#12_{a4}$
7/18 11:00	Corn	Tasseled cobs 15 cm	200	88	some stress, curling same color	-	good	fair	sample #2	slide $\#12_{a5}$
7/29 10:15	Corn	cobs 22 cm	235	90	wind damage, curling moderate stress	-	fair	fair	sample #3	-
8/4 10:00	Corn	cobs 22 cm some denting	240	90	damage moderate stress	-	fair	fair	sample #4	-

(1)-(11): See Explanations.

sensitive in relation to water stress; the level of moisture stress detected by plant signature changes; the feasibility of detecting plant moisture stress in the thermal band; and a technique of leaf stress measurement suited to corn and soybeans.

LEGEND

Soil type map

Kr, Br, Sy, Ts: well drained soils
Hd, Tr : poorly drained soils

Crop distribution map

c: corn
s: small grain
+: soil sampling sites

Figure 3. Aerial CIR photograph, soil survey and field crop map of the "Pipestone site (July 18, 1977; 1:72,000 scale).

RESULTS TO DATE

Soil water content

The water-content distribution profile (figure 2, e.g.) of all sites, poorly drained or well drained soils, indicate that the soil water content was always adequate or eventually in excess. There is no evidence of soil water deficiency throughout the 1977 growing season. On the other hand, several poorly drained soils had excess moisture. This can be detected by the tone differences on the color infrared photography of July 18 (figure 3).

When all laboratory results of bulk densities and water retention are completed, a more precise characterization of the available soil water throughout the season will be computed as illustrated in figure 2. A new method of soil water retention measurement on undisturbed soil cores using frozen soil and a special holder mounted on a diamond saw was developed. This arrangement was used to prepare a known volume of soil for density measurement.

Precipitation event records

Nature and amount of precipitation have been recorded at each site and show that precipitation was well-distributed throughout the season. Several sites recorded some hailstorms.

A computerized precipitation map (figure 4) was developed in order to display, for any period of time, cumulative precipitation. The purpose is to study signatures in relation to areas of precipitation, and to delineate well watered or poorly watered areas.

Crop signature

"Ground truth" crop conditions were recorded at the time of sampling for soil moisture (table 1). Color slides were also taken at

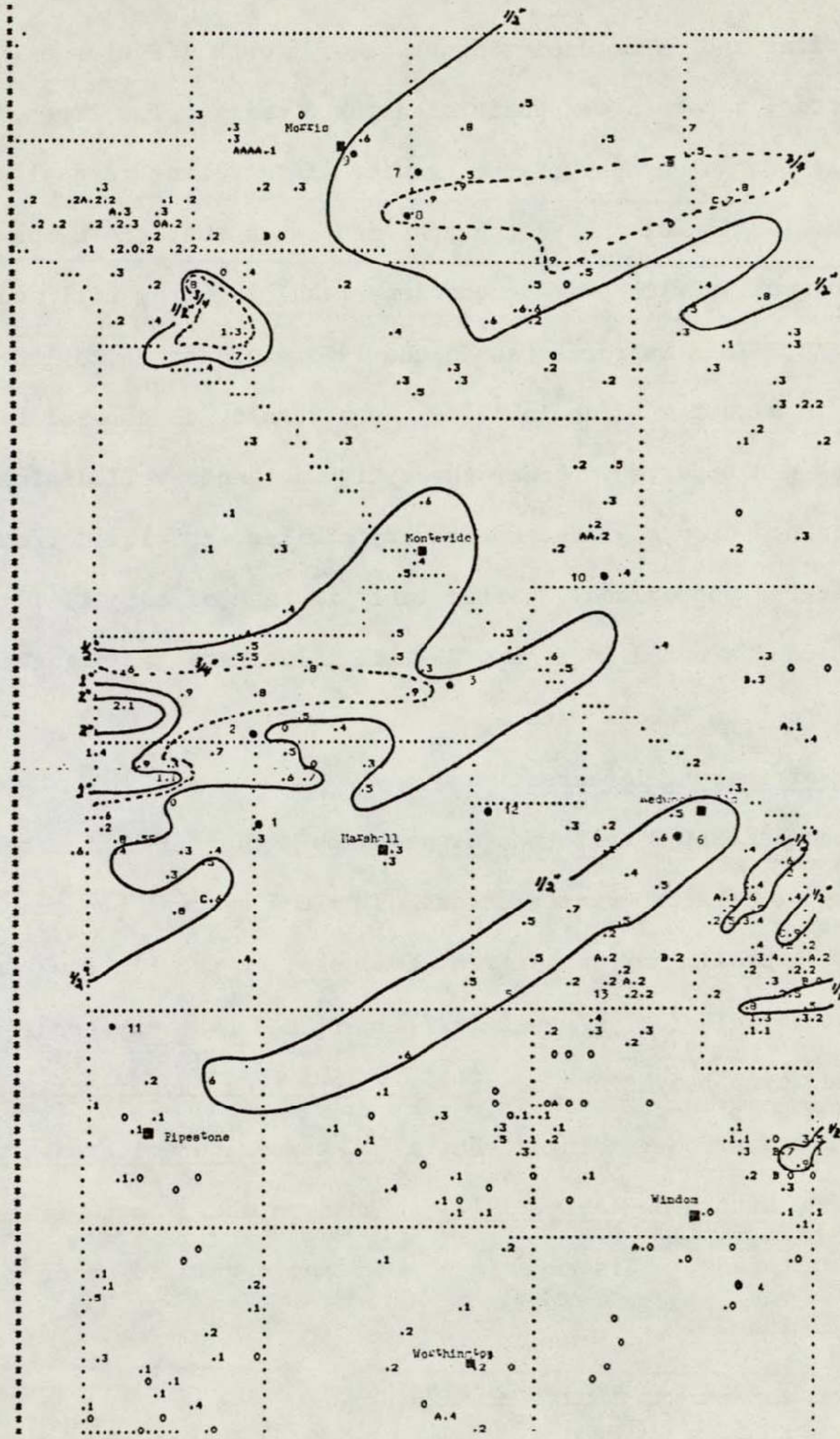

Figure 4. Computerized map of cumulative precipitation in southwest Minnesota for the period June 18-24, 1977. Observation points are supplied by on-farm observers keeping a daily record throughout the season. Isohyetal lines are hand-drawn.

several sites and dates depicting stage of growth (figures 5a, 5b). At Lamberton, a camera was positioned for a daily color image, a kind of time-lapse photography of the growing and maturing corn plant. A general evaluation of the photography indicates that the crops were growing normally, with a few exceptions resulting from hail and/or wind damage. This is reflected in the 1977 yields: 75 to 150 bu/ac compared to almost 0 bu/ac in 1976. As a result, no general "drought signature" was observed. Under these circumstances well drained and poorly drained crop signatures are very similar, as viewed from the color infrared photography, particularly in case of corn fields. An exception can be noted in figure 3 which illustrates a "signature" of damaged corn from excess water.

Use of thermal infrared

Since LANDSAT 3 will be equipped with a thermal radiometer, the capability of detecting water stress using the thermal band may be possible. A preliminary experiment conducted at the St. Paul Campus experimental field (July-August 1977) indicated that sky condition, wind speed, crop height and measurement direction may affect the absolute temperature readings. But a 7°C temperature increase was measured one afternoon (July, 1977) in an area where corn plants were under water stress. This experiment is being continued under greenhouse conditions.

LANDSAT spectral band selection

The 1:1,000,000 scale, bands 5 and 7, less than 10 percent cloud cover imagery available for the 1977 growing season has been acquired. A comparison of band 5 and 7 showed that band 7 is definitely better for our purpose when using the 1:1,000,000 scale imagery.

Figure 5. Corn on the well-drained soils of site (12), Redwood Co.
Upper photo taken June 10; lower photo, August 22.

Mapping of well/poorly drained soils using LANDSAT imagery

The capability of differentiating well and poorly drained soils at a broad scale level was investigated. The "Minnesota Soil Atlas" classes were used. The well drained soils will normally have water table below the rooting zone. The poorly drained soils will commonly have a water table within the rooting zone, unless artificially lowered.

A section of the "New Ulm, Minnesota Soil Atlas" map was used as "ground truth" (figure 6). The analysis of 1976 and 1977 LANDSAT 1:1,000,000 scale, band 5 and 7, imagery was performed with a density slicer (V.P. 8) and a supervised approach (Frazee et al., 1972). As it appears on figure 7, a very satisfactory location of well and poorly drained soils is obtained when using the imagery corresponding to the period of maximum drought development (August 1976).

First greenhouse experiment results

The study of crop signature requires a knowledge of plant water status. Leaf water potential is actually the best evaluation of plant water stress (Kozlowski, 1968). Among several methods, the pressure chamber or pressure bomb seems to be the best field technique (Blum et al., 1972; Boyer, 1970; Frank, 1972; Ritchie and Hinckley, 1975). Since the pressure bombs available were designed for tree leaves, we modified the apparatus to accept corn leaves. Preliminary results suggest that we can measure leaf water potential of corn with reproducibility.

When the computer compatible tapes of summer 1977 will be available, the analysis of the data will include:

- the processing of the LANDSAT CCT using the "Image 100 System" (EROS Data Center) to develop specific spectral signatures corresponding to crop conditions and particularly moisture stress conditions;

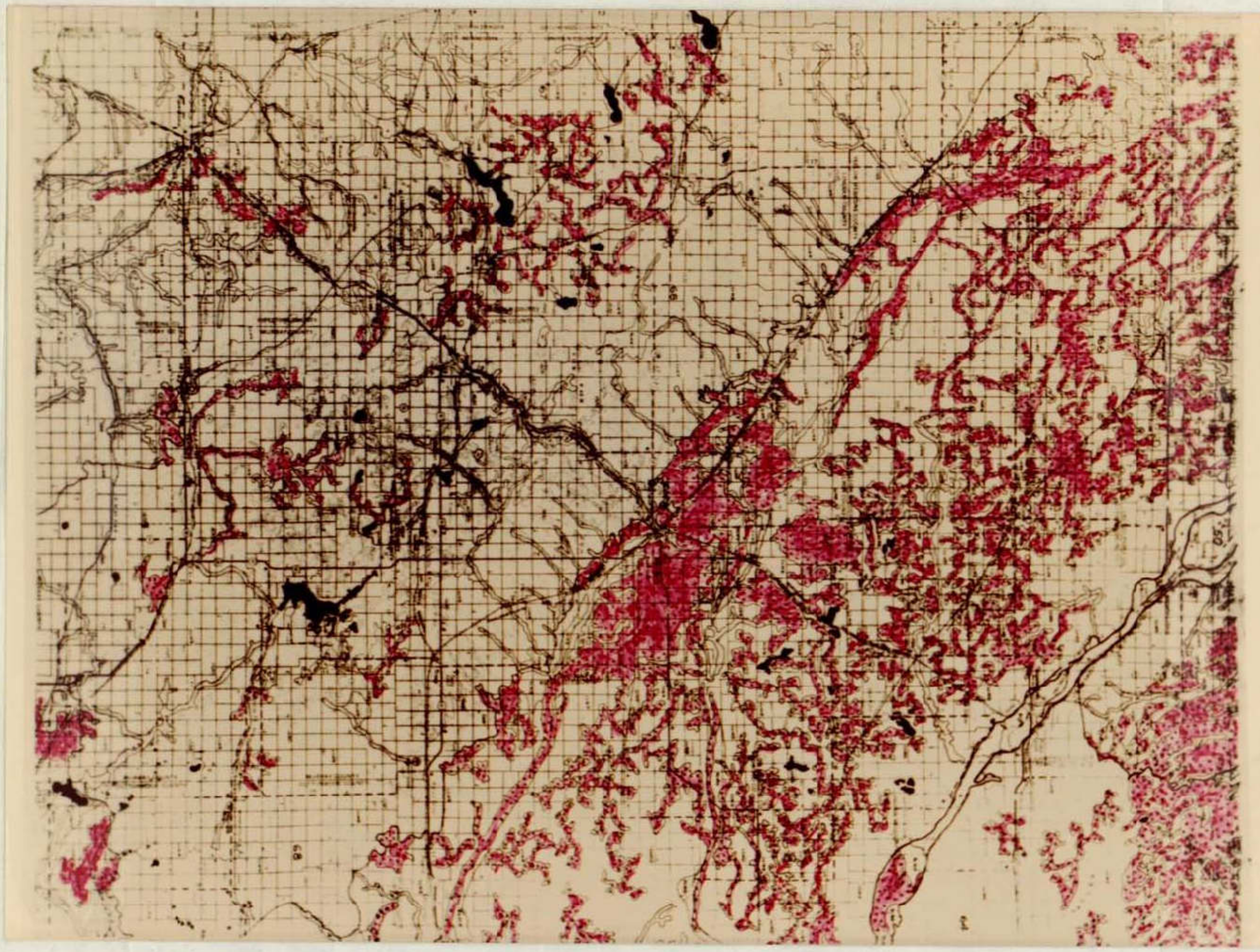

Figure 6. Section of the "New Ulm Minnesota Soil Atlas" map. Original map scale 1:125,000. Section lines are shown. Higher elevations occur in the western and southwestern portions. Areas of poorly drained soils are shown in red. Black areas are lakes. Uncolored areas are mostly well drained soils.

- the use of the EPPL 4 System (Environmental Planning Programming Language, Minnesota Land Management Information System) and the RECOG program (Pattern Recognition Routines for the Automatic Analysis of Remote Sensing Imagery) for the development of an automatic mapping capability through the University Computer Center facilities.

The analysis will include the study of the potentialities of developing drought probability maps during the growing season.

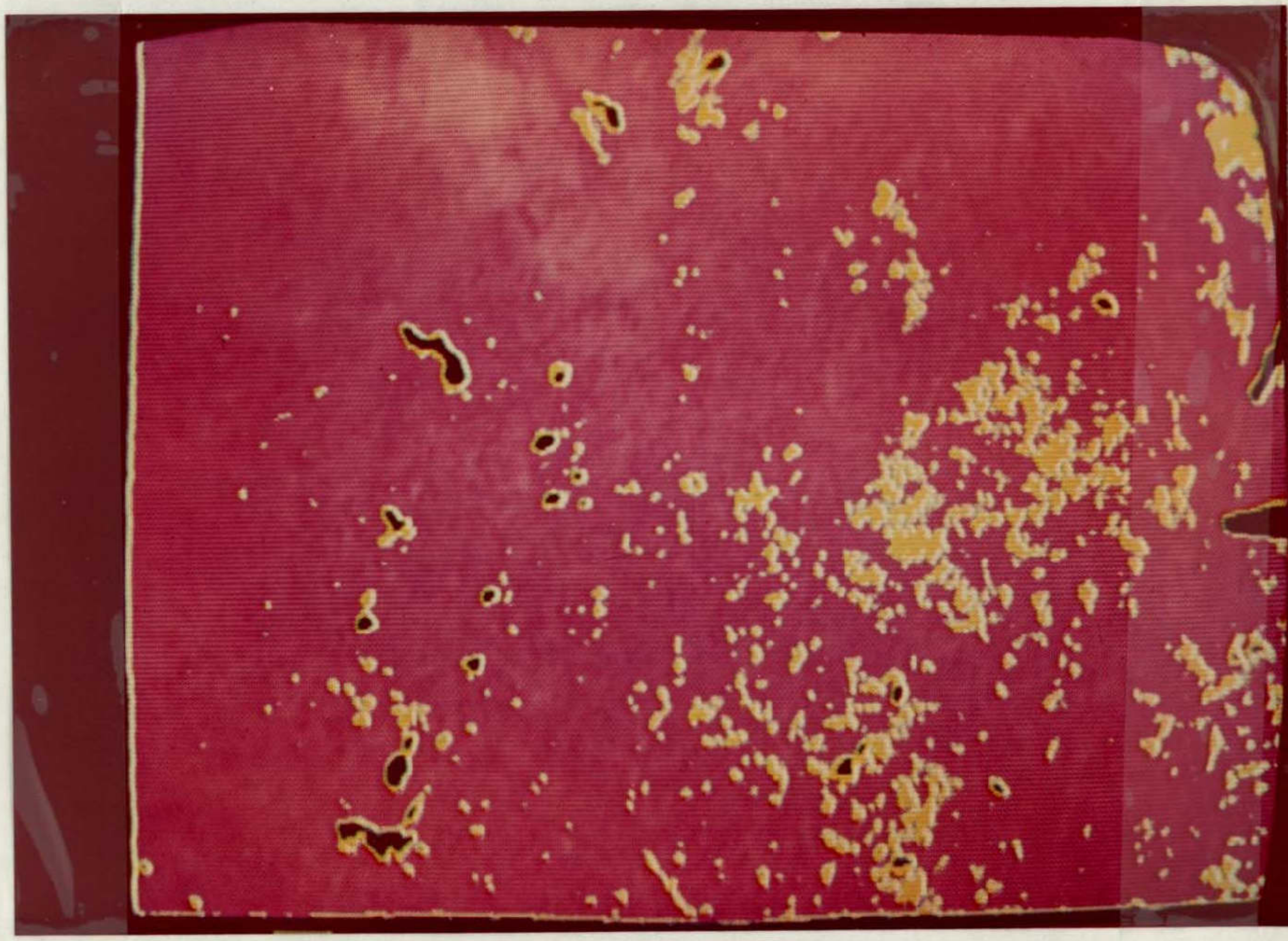

Figure 7. Density sliced photograph of LANDSAT scene, band 7, August 1976 of Figure 6. Black areas are lakes. Yellow areas of poorly drained soils generally correspond to areas outlined in red in Figure 6.

ACKNOWLEDGEMENTS

The cooperation of the following persons and agencies is gratefully acknowledged:

L.D. Hanson, Department of Soil Science

D.G. Baker, Department of Soil Science

W.W. Nelson, Southwest (Lamberton) Experiment Station

S. Evans, West-Central (Morris) Experiment Station

M. Meyer, Institute of Agriculture, Forestry, and Home Economics, Remote Sensing Laboratory

G. Holcomb, O. Gundersen, Agricultural Extension Service

W. Brug, H. Hokansen, J. Murray, C. Neseth, Soil Conservation Service.

LITERATURE CITED

Blum, A., C.Y. Sullivan and J.D. Eastin. 1973. On the pressure chamber technique for estimating leaf water potential in Sorghum. Agron. J. 65:337-338.

Boyer, J.S. and S.R. Ghorashy. 1971. Rapid field measurement of leaf water potential in soybean. Agron. J. 63:344-345.

Frank, A.B. and D.G. Harris. 1973. Measurement of leaf water potential in wheat with a pressure chamber. Agron. J. 65:334-335.

Frazee, C.J., V.I. Myers and F.C. Westin. 1972. Density slicing techniques for soil survey. Soil Sci. Soc. Amer. Proc. 36:693-695.

Ritchie, G.A. and T.M. Hinckley. 1975. The pressure chamber as an instrument for ecological research. Adv. in Ecolog. Research 9:165-254.

Kozlowski, T.T. (ed.). 1968. Water deficits and plant growth, Vol. 1, Academic Press, London and New York.

Rust, R.H., R.A. Erickson, G.A. Harms, and J. Harries. 1978. Minnesota Soil Atlas. New Ulm Sheet. Minn. Agr. Expt. Sta.